THE UNIVERSITY
of EDINBURGH

Adiponectin, Calorie Restriction and Bone Marrow Adipose Tissue: A Triad of Metabolic Influencers

Richard Sulston

Doctor of Philosophy

The University of Edinburgh

2019

I hereby declare that:

a) This thesis has been composed by the below signatory
b) All work presented in this thesis was performed by the below signatory unless where explicitly stated otherwise
c) The work in this thesis has not be submitted for any other degree or professional qualification unless where explicitly stated
d) The work in the enclosed publication was performed by the below signatory unless where explicitly stated

Richard Sulston

Abstract

Adiponectin is well known as an insulin-sensitising hormone secreted exclusively from adipose tissue. Paradoxically, adiponectin is increased during calorie restriction (CR) when typical adipose depots are reduced in volume. Interestingly, bone marrow adipose tissue (BMAT) increases in volume during CR and has been shown to be a major source of circulating adiponectin in this context. CR itself exerts diverse metabolic and skeletal effects: one hypothesis is that increased BMAT contributes to bone loss during CR, whereas many of the metabolic benefits of CR are similar to those ascribed to adiponectin. However, it remains unknown what causes BMAT to increase during CR; if BMAT contributes to circulating adiponectin in other conditions; and if BMAT and/or adiponectin influence skeletal or metabolic adaptations to CR. The goal of my PhD research was to address these critical gaps in knowledge.

My first hypothesis was that BMAT is also a source of adiponectin following treatment with thiazolidinediones, a class of anti-diabetic drugs that increase both BMAT and adiponectin. To address this, mice resistant to BMAT expansion were treated with rosiglitazone, a well-studied thiazolidinedione, to investigate the ability of BMAT to secrete adiponectin in other conditions of BMAT expansion and hyperadiponectinaemia. These mice were less resistant to BMAT expansion in response to rosiglitazone compared to CR, which limited the ability to draw strong conclusions; however, there were some indications that BMAT is an important source of adiponectin in this context, and the data provide other insights about how BMAT compares to other adipose subtypes.

To begin investigating the roles of BMAT and adiponectin during CR, wild-type (WT) male and female mice were placed on varying durations of CR or ad libitum control diet. The increases in BMAT were then assessed and compared to changes in skeletal architecture, adiponectin and glucose tolerance. I found that BMAT expansion depends not only on CR duration, but also varies by skeletal site and between the sexes. BMAT in tibiae and femurs increased with 6-week CR in both sexes, but only female femurs showed increased BMAT after 2-week CR. BMAT expansion generally coincided with bone loss in femurs but occurred after bone loss in tibiae; notably, bone loss occurred in humeri despite a lack of BMAT in these bones. Together, these findings show that BMAT expansion is not required for CR-induced bone loss.

In terms of metabolic and endocrine effects, adiponectin was maximally increased after 3 to 4 weeks of CR, approximately coinciding with the increases in BMAT and adiponectin expression within bone. However, improvements in glucose tolerance occurred after only 1 week of CR, especially in male mice, preceding BMAT expansion and hyperadiponectinaemia. Strikingly, I found that females resist many of the metabolic benefits of CR: unlike males, during CR females did not lose fat mass and had only mild improvements in glucose tolerance. Collectively, it was not clear from these findings if BMAT expansion or adiponectin are playing a role in the metabolic benefits of CR.

For this reason, adiponectin knockout mice (KO) and WT controls were subjected to CR to investigate if adiponectin contributes to CR-induced improvements in glucose homeostasis. Male KO mice performed better in glucose tolerance tests than WT mice, a finding going directly against my hypothesis. This indicates that adiponectin may be playing an unexpected role during CR, in which it impairs glucose tolerance. One possibility is that this relates to adiponectin's role in stimulating fat oxidation; however, further work is required to elucidate the underlying mechanism.

Together, these studies reveal several new discoveries. Firstly, CR-induced BMAT expansion is dependent on CR duration and is both sex- and skeletal-site-specific. Secondly, BMAT expansion is not required for CR-induced bone loss in humeri, but may contribute to bone loss in femurs and tibiae. Thirdly, female mice resist fat loss and improvements in glucose tolerance during CR, an unexpected finding that warrants further study. Fourthly, CR-induced improvements in glucose tolerance precede BMAT expansion and hyperadiponectinaemia, suggesting that the latter are not drivers of the former. Finally, lack of adiponectin is associated with improved glucose tolerance during CR, suggesting that the function of adiponectin during CR is distinct to its reported roles in obesity and insulin-resistant states. The latter indicate that adiponectin may impact the therapeutic benefits of CR and may provide insights toward the evolutionary function of adiponectin during periods of food scarcity.

Lay Summary

Fat tissue was historically thought of as an inert store of energy. Research over the past 4 decades has shown that fat tissue actually releases a wide variety of hormones in the blood and plays an important role in biological processes. One such hormone released from fat is called adiponectin. Adiponectin is secreted exclusively from fat tissue but shows a surprising relationship with fat. As body fat increases, the amount of adiponectin in the blood decreases. Conversely as fat decreases, adiponectin increases. One such time this occurs is during calorie restriction (CR), when daily calorie intake in reduced but malnutrition is avoided. It is known that during CR the majority of fat tissue decreases in mass in order to provide energy but the fat tissue in the bone marrow increases. Additionally, it is known that during CR the fat found in the bones acts as a major secretory source of adiponectin. Therefore, the first hypothesis in this thesis is further examining the role of bone marrow fat in secreting adiponectin during CR and other conditions of simultaneously increased adiponectin and bone marrow fat. We used mice resistant to increased bone marrow fat and treated them with a drug known to increase bone marrow fat and adiponectin. The mice did not sufficiently resist the increases in bone marrow fat and so it was difficult to draw robust conclusions in this regard but there was some evidence that BMAT is an important source of circulating adiponectin in contexts supplementary to CR.

Adiponectin has been shown to improve the response to glucose by limiting the extent to which it increases blood sugar levels. CR has also been shown to exert this effect and so the second hypothesis tested by this thesis is that adiponectin is responsible for some of the metabolic effects of CR. To begin investigating this we exposed male and female mice to varying durations of CR and examined the durational increases in adiponectin and bone marrow fat. I found that the increases in bone marrow fat were highly dependent on the type of bone analysed and the sex of the mouse. Bone loss was not associated with increased bone marrow fat indicating that bone marrow fat increases were not required for bone loss caused by CR. Increases in adiponectin over the different durations of CR roughly coincided with the increases in bone marrow fat and the increase in bone production of adiponectin. However, improvements in response to glucose occurred very rapidly indicating that increased adiponectin nor bone marrow fat is required for this to happen.

Finally, we produced mice that were unable to make adiponectin and gave them a CR diet. If adiponectin is providing some of the benefits of CR we hypothesised that these mice would not respond to CR as well as mice able to produce the hormone. We found the opposite, male mice without adiponectin had a better response to glucose indicating that adiponectin may be playing an unexpected role during CR.

Overall this thesis shows that increased bone marrow fat increases in response to CR are dependent on duration of CR; sex; and the location examined in the skeleton. Secondly, many differences exist between males and females in their response to CR. Thirdly, the role of adiponectin during CR may be more complex than presented in previous research and more research is required to examine the role it is playing during CR.

Contents

1. Introduction

1.1. Adiponectin

1.1.1. The Discovery of the adipocyte-derived hormone adiponectin

Adiponectin is an adipocyte-derived hormone that has been reported to exert beneficial effects on cardiometabolic function, as well as various other health benefits. It was first discovered in 1995 and was initially called adipocyte complement-related protein of 30kDa (Acrp30) given its structural similarity to complement factor C1q[1]. It was identified via an enrichment of adipocyte-specific genes in a subtractive cDNA library[1]. Northern blot analysis showed that this protein was exclusively expressed in adipocytes and expression was increased 100-fold upon adipocyte differentiation[1]. Further experimentation showed that adiponectin was detectable in the extracellular media of cultured adipocytes and in mouse serum, indicating that adipocytes secrete adiponectin into the circulation. In addition, it was found that adiponectin secretion was increased *in vitro* following insulin treatment[1]. Adiponectin was also independently discovered in 1996 by mRNA differential display, whereby the adiponectin cDNA was identified and named *Adipoq*. This study too showed that adiponectin is exclusively expressed in adipocytes, but importantly also observed that adiponectin expression is drastically reduced in the fat pads of obese mice compared to normal weight controls[2]. A human homologue of adiponectin was identified in 1996 using a cDNA library from human adipocytes; it was named adipose most abundant gene transcript 1 (apM1) given the fact it was the most abundant transcript present[3]. More work on human adiponectin using gelatin affinity chromatography revealed that, like mice, human plasma contains high levels of circulating adiponectin[4]. Once adiponectin had been successfully isolated work began to determine the structure of the protein.

1.1.2.Structure and multimerisation of adiponectin

Adiponectin consists of a globular domain and a collagenous domain and is structurally similar to collagen X[2]. This structure is highly conserved with the amino acid sequence sharing 80% homology across all species so far studied[5]. Additionally, many post-translational modifications are present on the collagenous domain including lysine glycosylation sites which have shown to be vitally important in conferring functionality to adiponectin action *in vitro*[5].

Throughout the early work on adiponectin it was repeatedly observed that secreted adiponectin was present at different molecular weights, representing different protein complexes, in both rodents[1] and humans[4]. Further work to classify these complexes showed that adiponectin exists in a variety of multimeric states, the commonest being trimers, hexamers and high-molecular-weight multimers[6,7], in addition to the

proteolytically cleaved globular adiponectin monomer[8,9]. Fluorescent labelling has been used to show that the multimeric state of adiponectin complexes is determined pre-secretion and, once in the circulation, there is no multimer interconversion. Labelled adiponectin concentrations in the circulation decreased over time, indicating degradation in the plasma and the importance of secretion in maintaining and influencing adiponectin concentrations in the blood[10]. Whilst adiponectin has been shown to exhibit a physiological effect, changes in circulating adiponectin concentrations are also associated with a variety of pathologies.

1.1.3. Adiponectin as a biomarker of metabolic dysfunction

The major correlative factor with circulating adiponectin is adiposity. It is well established that hypoadiponectinaemia (<4μg/ml) is associated with high body mass index (BMI) and large adipocyte area in subcutaneous and visceral depots[11-14]. Patients with obesity show an inverse correlation between circulating adiponectin and visceral fat area (measured by computed tomography scans) but not BMI or subcutaneous fat area[15]. Notably, these low concentrations of adiponectin can be reversed by reducing visceral fat area[16,17] indicating an important role for visceral fat in hypoadiponectinaemia. Hypoadiponectinaemia also correlates with the onset of type 2 diabetes and insulin resistance, and circulating adiponectin in is lower in obese type 2 diabetics than age- and BMI-matched non-diabetic obese patients[17]. Higher adiponectin levels are also associated with a reduced risk of developing type 2 diabetes[18].

Adiponectin has also been shown to be associated with various atherosclerotic diseases. Myocardial infarction patients are more likely to display hypoadiponectinaemia[19] and the degree of this can be used to predict the severity of coronary artery atherscerlosis[20]. When looking at cardiac parameters a slightly unexpected pattern exists, with adiponectin concentrations raised in patients with chronic heart failure and further increased as heart failure worsens[21,22]. One hypothesis for this paradoxical relationship is the development of adiponectin resistance, with downregulation of AdipoR1 transcripts downregulated in skeletal muscle biopsies of chronic heart failure paients[23]. Another risk factor in cardiovascular disease development is chronic kidney disease (CKD); in a similar fashion to chronic heart disease, there is some evidence that adiponectin circulates at normal levels in patients with CKD[24]. Additionally, high adiponectin was a predictor for CKD but only in male patients[25]. Despite these associations with CKD, hypertension is negatively correlated with circulating adiponectin, and hypoadiponectinaemia is a risk factor for hypertensive disease[26,27].

Finally, adiponectin has been shown to negatively correlate with bone mineral density[28] which will be discussed further in later sections.

Together, these observations support the conclusion that decreased circulating adiponectin is generally associated with increased cardiometabolic risk, although, as in

the case of CKD in males, increased adiponectin is not always associated with beneficial health outcomes.

1.1.4. Cellular secretion of adiponectin and extracellular adiponectin receptors

As previously mentioned, adiponectin is secreted from adipocytes into the extracellular media *in vitro* and into the circulation *in vivo*. The method of secretion is thought to be via a peri-nuclear compartment related to the Golgi body. This adiponectin-containing membrane compartment is trafficked to the extracellular membrane for release, a process that is distinct to the secretion of leptin, another prominent adipose-tissue-secreted hormone[29].

Once in the circulation, adiponectin is able to bind to two receptors named adiponectin receptor 1 (AdipoR1) and 2 (AdipoR2). Both receptors are structurally analogous, with an intracellular N-terminus and extracellular C-terminus and are located on different chromosomes (AdipoR1 on chromosome 1 in humans and in mice; AdipoR2 on chromosome 12 in humans and chromosome 6 in mice). Double knockout of both AdipoR1 and AdipoR2 in mice has shown that these receptors mediate the majority of adiponectin signalling *in vivo*[30]. Adiponectin has also been shown to associate with T-cadherin receptor in cardiac tissue, with loss of interaction between adiponectin and cardiomyocytes in T-cadherin knockout mice[31]. The downstream effects of activation of these receptors are detailed below.

1.1.5. Multimer-specific signalling of adiponectin

As described above, adiponectin exists in the circulation in a variety of multimeric complexes, typically these are globular adiponectin monomers, low molecular weight trimers (LMW), medium molecular weight hexamers (MMW) and high molecular weight multimers (HMW)[6]. There is evidence that differing molecular weight complexes have distinct signalling effects and may be an important aspect of adiponectin specificity. HMW has been described as a more active form of adiponectin[32] based on findings that the ratio of HMW adiponectin to total adiponectin is a strongly correlated with insulin sensitivity[33], however there is also research to show that total HMW adiponectin is more important than ratio[34]. Regardless, it is known that HMW adiponectin has potent insulin sensitizing effects and these effects are likely mediated through signalling by HMW adiponectin in the liver[35].

Conversely, globular adiponectin has been shown to signal to a large extent on the skeletal muscle to increase activate AMPK resulting in increased fatty acid oxidation and insulin sensitivity[36]. LMW adiponectin is able to cross the blood brain barrier where it can signal via the central nervous system as described below[37].

1.1.6. Action of adiponectin in the central nervous system

Adiponectin signalling in the central nervous system (CNS) is a relatively recent area of study for the signalling effects of the hormone. This may be because the concentration of adiponectin is found in the cerebrospinal fluid (CSF) at a 1000-fold lower concentration compared to the serum[38]. Despite this, adiponectin has been shown to have effects on a multitude of brain parhways with a variety of outcomes.

It has been shown that administration of adiponectin by intracerebroventricular (ICV) injection directly into the CSF causes a reduction in food intake in rats[39]. Additionally, this effect was shown to be specific to AdipoR1 mediated signalling by knockdown of each adiponectin receptor[39]. Furthermore, ICV administration of adiponectin has been shown to decreases body weight in obese mice with an associated increased in energy expenditure[40]. Adiponectin has also been shown to play a role in stroke response, cerebral artery occlusion was performed on adiponectin knockout and wild-type mice. This study showed that adiponectin knockout mice had larger infarct sizes as well as more severe neurological harm[41]. Finally, a potential negative role for adiponectin in the CNS was shown in patients suffering from Alzheimer's disease. Adiponectin concentrations in the plasma were higher in patients with mild cognitive impairment and patients with Alzheimer's disease compared to healthy controls[42]. This correlation was also observed between CSF adiponectin concentrations and mildly cognitively impaired patients but not in patients with Alzheimer's disease[42].

The above studies show a potentially important role for adiponectin in the CNS both in terms of feeding behaviour and metabolism but also in neurological pathologies. Whilst the central effects of adiponectin are not the focus of this thesis and do not appear in the following hypotheses, it is worth staying mindful of the central effects caused by adiponectin signalling.

1.1.7. Action of adiponectin action in skeletal muscle

Studies of adiponectin signalling in the skeletal muscle have been primarily focussed on its insulin-sensitising and anti-diabetic effects, given skeletal muscle's important role in these physiological responses[43]. *In vitro* research has shown that adiponectin is able to increase glucose uptake in cultured rat skeletal myocytes[44] and this was further confirmed in *in vivo* models which also implicated a role for AMPK activation in downstream signalling[36,45]. Further mechanistic research on the insulin-sensitising effects of adiponectin showed that adiponectin signalling induces glucose transporter

type 4 (GLUT4) translocation to the plasma membrane of myocytes[44]. Adiponectin knockout mice have been used to investigate the role of adiponectin in peripheral glucose homeostasis, and whilst these mice have only a mild insulin resistance, when fed a high-fat diet the knockout mice develop more-severe metabolic dysfunction than wild-type controls[46,47].

Adiponectin is also able to influence lipid homeostasis in the muscle, where it has been shown to act, again, through AMPK activation to increase fatty acid oxidation[45,48]. This increase of fatty acid oxidation in the muscle has also been linked with weight loss in response to adiponectin signalling[8]. In addition to fatty acid oxidation, adiponectin has been implicated in mitochondrial biogenesis, with insulin-resistant individuals showing a strong positive correlation between circulating adiponectin and mitochondrial DNA content in the muscle[49]. It was also shown that mice lacking adiponectin have lower mitochondrial number and lower mitochondrial enzymatic activity in their skeletal muscle[49]. *In vitro* experimentation revealed that adiponectin treatment of primary myocytes induces mitochondrial biogenesis and increases fatty acid oxidation[49]. The mechanism of action of adiponectin-mediated increases in mitochondrial biogenesis is through a suppression of Mitogen-Activated Protein Kinase Phosphatase-1 (MAPK1) in skeletal muscle[50].

Peroxisome proliferator-activated receptor γ coactivator 1 alpha (PGC1α) is a further protein linked to both adiponectin signalling and mitochondrial biogenesis. PGC1α is commonly regarded as a master inducer of mitochondrial biogenesis and respiration[51]. A link between adiponectin signalling has been shown by suppression of adipoqR1 causing a decrease in PGC1α expression, further resulting in a decrease in mitochondrial content of primary cultured myocytes[52].

1.1.8. Action of adiponectin in the liver

Hepatocytes have been shown to express both adipoR1 and adipoR2 on their plasma membranes[53] and treatment of cultured hepatocytes with adiponectin causes them to be more sensitive to insulin-mediated reductions in glucose production, even at sub-physiological concentrations of insulin[54]. When adiponectin is injected intraperitoneally it is able to lower the blood glucose concentrations in both healthy and diabetic mice[54]. Despite this action, supra-physiological levels of injected adiponectin do not cause hypoglycaemia [54]. When compared to the effects of insulin injection, adiponectin is able to lower blood glucose even when the ability of insulin to stimulate glucose uptake is removed[55]. Therefore, it could be suggested that adiponectin acts in the liver to inhibit glucose production, rather than increasing glucose uptake[56]. This was confirmed by combining adiponectin infusion with hyperinsulinaemic euglycaemic clamps: adiponectin caused a 65% reduction in glucose production and a down regulation of hepatic gluconeogenic enzymes, indicating that adiponectin reduces hepatic glucose

production[57]. Additionally, cultured hepatocytes treated with adiponectin show greatly reduced glucose production and secretion into the culture medium[58].

Presently, the majority of research regarding adiponectin has focus on states of obesity or insulin resistance. Yet little research has been performed on adiponectin in organisms of relatively improved metabolic health such as calorie restriction where the role of adiponectin is largely unknown.

1.2. Caloric restriction

1.2.1. Human examples of calorie restriction

The above findings demonstrate the extensive study of adiponectin, particularly in the context of diabetes and obesity. Yet adiponectin is greatly increased in conditions of caloric restriction (CR). CR is the dietary regimen of reducing daily calories and, when used as a method for improving health, also involves avoiding any form of associated malnutrition. Historical examples of this occurring in the human population are rare given the high likelihood of malnutrition occurring during calorie scarcity; however, some examples do exist. For example, Okinawa is a small cluster of Japanese Islands in the East China Sea whose occupants historically have eaten a low-calorie but nutrient-rich diet. The dietary calorie intake of the Okinawan population compared to the mainland Japanese is reported to be 83%[59]. Studies on the Okinawans have shown that they have increases in both their maximal and average life span, and a lower incidence of coronary heart disease as well as a variety of cancers including colon, breast and prostate[60]. It is important to note that this effect was only observed in Okinawans born before World War Two, because after this the diet of the islanders changed dramatically to more closely resemble that of mainland Japan. This also caused a convergence in life expectancy between Okinawa and mainland Japan, with the latter even overtaking Okinawa in life expectancy[61]. Together, this supports this concept that CR in humans can increase life expectancy and decrease the incidence of chronic diseases.

An example of a smaller but more controlled human CR is the Biosphere 2 simulation. Biosphere 2 did not begin as a calorie restriction experiment but was an attempt to simulate conditions of extra-terrestrial habitation. A 3.15 acre closed system biosphere was constructed in Arizona with 8 participants living inside without external influence for 2 years[62,63]. The participants were solely responsible for growing enough food to sustain themselves over the 2-year experiment and, prior to commencement, daily calorie intake was predicted to be ~2500kcal per person per day. Due to crop cultivation issues actual calorie intake during the first 6 months of the experiment was 1784kcal per person per day, rising to ~2000 kcal for the remainder of the study[64]. Whilst this represented a large decrease in calorie intake, the food that was grown was high in

nutrients, preventing any form of malnutrition. All participants displayed weight loss over this period, with males and females displaying a 21% and 14% reduction in body weight, respectively[64], which was caused by a decrease in body fat[65]. In addition to the weight loss, many physiological and biochemical changes were observed in the participants, including significant decreases in cholesterol (both LDL and HDL) and triglycerides. Upon exit of Biosphere 2 and resumption of a normal diet these parameters generally returned to pre-experiment levels, indicating these changes are a result of the Biosphere 2 environment and likely due to the calorie restriction[66].

Whilst suggestive, the Biosphere 2 study was not designed to directly test the effects of CR in humans and there was a pressing need for a clinically control trial into the effects of CR in humans. The CALERIE (Comprehensive Assessment of Long-term Effects of Reducing Intake of Energy) study is a cross-centre study aimed at examining the effects of caloric restriction on humans in a controlled manner. The experiment commenced in May 2007 with the recruitment of 220 healthy volunteers across three sites in the USA. Participants were randomly assigned to either a calorie restriction or ad-libitum diet in a 2:1 ratio. Volunteers on the calorie restriction diet underwent a 25% reduction in daily calories, with behavioural and dietary modifications in order to maximise adherence to the long-term diet[67]. Large effects were observed by this 2 year calorie restriction: participants in the calorie-restricted group were significantly lighter than the ad-lib diet group, with loss of both fat-free mass and fat mass[68]. Subcutaneous and visceral adipose depots were each reduced, along with a reduction in ectopic lipid in the liver and soleus muscle[68]. Blood biochemistry was also significantly altered: circulating fatty acids were increased by calorie restriction whilst insulin sensitivity was increased and fasting blood glucose reduced[69].

These examples show CR as a powerful tool for improving human health and potentially longevity. Large changes are observed in body weight, particularly accounted for by fat mass, as well as a wide variety of metabolic benefits including improvements in insulin and glucose tolerance and reductions in hepatic lipid accumulation.

1.2.2. Suitability of animal models of calorie restriction

The recent interest in the health benefits of CR in humans is based largely on studies in animal models. Much of the early caloric restriction experimentation on animals focussed on the ability of caloric restriction to extend lifespan. This is now a well-established effect in a diverse range of organisms from single celled species such as yeast[70], through simple multicellular organisms such as nematode worms and flies and onto rodents[71,72] and, potentially, primates[73,74]. Some ambiguity remains around the effects of calorie restriction on primates given the time taken to perform these experiments and the difficulty at the time in sourcing primates resulting in animals that had previously been used in other experiments. Despite these potentially confounding

issues, there is now evidence that calorie restriction has caused a decrease in all-cause mortality in rhesus monkeys[75]. Additionally there were substantial reductions in the incidence of cancer, insulin resistance and diabetes[75].

Currently, mice and rats are some of the most widely used organisms to examine the effects of caloric restriction. They appear to be a good model of mimicking the effects of caloric restriction in humans. This is evidenced by the analogous effects of calorie restriction in both humans and rodents.

1.2.3. Mechanism of metabolic effects

The metabolic adaption to calorie restriction is well established. In the fed state ingested glucose is absorbed by the liver and skeletal muscle; the latter occurs in direct response to increased concentrations of blood insulin. In the liver and muscle, glucose is readily converted to glycogen, gluconeogenesis is also supressed in the liver[76]. This acts to remove excess glucose from the blood and store it as glycogen for use in times of energy scarcity[76]. In the following hours post-feed, the concentrations of blood glucose start to decrease as does the concentration of insulin, concurrently the concentration of glucagon rises[76]. Glucagon acts to stimulate the breakdown of glycogen in the liver to glucose and inhibits hepatic glycogen and fatty acid synthesis resulting in a large increase in the glucose secretion from the liver[76]. As glucose scarcity continues, the skeletal muscle becomes more reliant on fatty acids for their energy requirements whilst the resulting glycerol is transported to the liver, further driving gluconeogenesis[76]. Proteolysis is also utilised to provide more products for use in gluconeogenesis. During prolonged starvation, ketone bodies synthesised from fatty acids become a major energy source, able to pass the blood brain barrier, they alleviate the need for glucose in the brain and help reduce the amount of proteolysis occurring, preserving essential muscle required for survival[76]. Once these fatty acids reserves are exhausted only protein remains for energy eventually leading to heart, liver or kidney failure and death[76,77].

One of the earliest hypotheses for how CR imparts its effects focused on the body size of rats following calorie restriction, showing that reduction in growth corresponded to an increase in life span[72,78]. Further work to better characterise this effect showed that loss of fat was an important factor in the beneficial effects of caloric restriction[79]. A reduction in energy expenditure could explain these effects on body morphometry and has also been proposed as a mechanism of caloric restriction's effects[80]. However, the research has shown mixed results with some showing that chronic calorie restriction does not influence relative metabolic rate and therefore is not a causal factor in the effects of calorie restriction[81,82]. Interestingly, others show that metabolic rate is decreased by CR[83].

It has been suggested that the effects of caloric restriction occur in two phases: first the animal adapts to the reduction in calories, followed by a second phase that lasts the

remainder of the animal's lifespan. The metabolic rate of rats is decreased by transient calorie restriction and the metabolic rate returns to basal levels within a few weeks as the rats adapt to the diet[82]. During this adaptive period animals exhibit rapid weight loss, specifically for fat mass[84]. This follows the reduction in blood glucose stimulating the breakdown of glycogen by the release of glucagon from the pancreas[85]. Glycogen supplies are rapidly depleted and so the animal resorts to fat oxidation to provide energy, including the synthesis of ketone bodies to help meet the organism's energy needs. This pattern of adaption results in a large decrease in blood glucose initially, followed by a rise to maintain a steady concentration, albeit lower than ad-libitum fed levels[86]. These chronically reduced blood glucose concentrations cause less insulin to be released by the β cells in the pancreas which in turn increases insulin sensitivity of the animals[87].

The neuroendocrinology of animals during caloric restriction is greatly altered and has been proposed as a mechanism of action for some of the effects of this dietary intervention. Glucocorticoids have been shown to be largely elevated during calorie restriction[88,89] but neuronal adaptation has also been shown to occur during chronic calorie restriction with reductions in glucocorticoid receptors acting as negative feedback to limit excessive glucocorticoid activity[90].Therefore, this may not represent a mechanism of action through which calorie restriction greatly acts.

Insulin-like growth factor 1 (IGF-1) is a liver-derived hormone downstream of growth hormone (GH) signalling. It acts in a multitude of tissues to stimulate growth and proliferation whilst also inhibiting cell death[91]. During calorie restriction IGF-1 is greatly reduced[92] in the circulation and this reduction has been shown to influence longevity[93-95]. In addition, IGF-1 has been shown to induce hypoglycaemia when infused into rats[96] and to recover growth rate of diabetic rats[97]. For these reasons, IGF-1 has also been suggested to be an important regulator of the effects of caloric restriction. Yet despite these findings, data in humans have shown that protein restriction may be a more important determinant on plasma IGF-1 concentrations than more general calorie restriction, especially considering it has been shown that CR does not reduce IGF-1 in humans[98].

1.2.4.Adiponectin and caloric restriction

Given that adiponectin is exclusively secreted from adipocytes, and that calorie restriction causes a decrease in body mass caused by a decrease in fat mass, it would seem likely that during calorie restriction concentrations of circulating adiponectin would be reduced; however, this is not the case. During caloric restriction concentrations of adiponectin greatly increase[99-101] and, conversely, during obesity, adiponectin concentrations are reduced[3,102,103]. Many of the metabolic effects of adiponectin (discussed above) are similar to effects of caloric restriction, yet little work

has been done to investigate if adiponectin contributes to the benefits of caloric restriction.

The role of adiponectin as a hormone acting in starvation in opposition to insulin has also been widely discussed. Briefly, adiponectin's ability to increase fatty acid oxidation and insulin sensitivity while also decreasing energy expenditure and gluconeogenesis and this is postulated to act to minimise the anabolic effects of insulin signalling during CR. This is compounded by the evolutionary basis for adiponectin being unlikely due to a need for reacting to obesity, type 2 diabetes and other outcomes of our sedentary western lifestyles, but more likely as a method of surviving starvation, a far more likely encountered pathology during human evolution[104-106]. Independently it has been shown that adiponectin plays a role in energy expenditure with adiponectin deficient mice showing decreased food intake and increased energy expenditure[37].

Direct evidence for adiponectin's beneficial role in calorie restriction come from studies of myocardial infarction. Caloric restriction has been shown to provide a cardioprotective effect when rats are injured by cardiac reperfusion injury[107] and this effect is abrogated in transgenic mice with reduced circulating adiponectin[108]. Also a CR study in Adipoq KO mice, showing that the KOs have impaired response to CR-mediated improvement in hind limb ischaemia[109]. So, there seems to be a role for adiponectin in the cardiovascular benefits of CR.

In obesity, decreased circulating adiponectin is mirrored by decreased expression and secretion from WAT, yet in CR, increased circulating adiponectin can occur despite no increase in adiponectin expression in WAT[110]. Other secretory sites of adiponectin aside from the traditional WAT have therefore been investigated and the influence of bone marrow adipose tissue on circulating adiponectin is introduced below.

1.3. Bone marrow adipose tissue

1.3.1. Basic physiology

The presence of adipose tissue within the bone marrow cavity has been known scientifically since the late 19th century[111]. Yet, the physiological and clinical significance of this adipose depot has been relatively ignored until recently. An important early observation in bone marrow adipose tissue (BMAT) research was histogenic differences between the BMAT and the haematopoetic red marrow cells[112]. Further ultrastructural analyses suggested that BMAT and white adipose tissue (WAT) do not share a common progenitor cell type[113]. BMAT is typically found at the periphery of the skeleton[114] and begins to increase from distal regions, such as the toes, after birth[115]. BMAT continues to accumulate through life, first increasing in distal sites and moving into the proximal skeleton[116]. This pattern is apparent in rodents, with the tail representing the most distal skeletal site and location of earliest BMAT development[117]. As BMAT develops, two

distinct types of adipocytes can be observed histologically: in the distal regions of the bones BMAT adipocytes appear tightly packed and resemble WAT. This depot of adipocytes is termed constitutive BMAT (cBMAT) given that it is present in the skeleton from shortly after birth[116,118]. On the other hand, BMAT adipocytes present in the proximal regions of long bones and in the axial skeleton present in a more heterogeneous environment. These are single adipocytes interspersed within the haematopoietic red marrow cells; they possess a far greater plasticity in response to exogenous stimuli and so are referred to as regulated BMAT (rBMAT)[118]. Variation between cBMAT and rBMAT is not limited to the microenvironment of these cells. For example, cBMAT adipocytes have been shown to be larger than rBMAT cells in diameter and therefore volume[118]. In addition, differences in fatty acid composition also exist with distal regions of bones containing higher levels of unsaturated fatty acids compared to more central or proximal regions[118,119]. The mass of BMAT in adults is approximated to be 2.48kg in males and 1.8kg in females[120], therefore, for an average 73kg male BMAT represents approximately 3.4% of total body mass and 3% in a 60kg female[120]. This relateees to around 8 – 10% of the total fat mass of an individual. As discussed below, BMAT *increases* during states of energy deficit, such as CR or anorexia nervosa. Therefore, during these conditions BMAT can comprise an even greater percentage of total fat mass[121].

1.3.2. Clinical and molecular influencers of BMAT volume

One of the most robust indicators for increased BMAT volume is age. It has been shown that BMAT first appears in the toes around birth[115] and continues to grow from the most distal regions to more proximal until 20 to 25 years of age[116]. BMAT accumulation in the axial skeleton then continues with advanced age, accelerating particularly in women post-menopausally[122].

An area underscoring the strong clinical relevance of BMAT is the association between elevated BMAT volume and increased risk of bone loss and osteoporosis[123,124]. BMAT accumulation has been associated with the loss of a wide variety of calcified bone parameters[125-127]. However, whilst this is a well-established correlation, evidence suggests that increased BMAT volume is not always required for reductions in bone integrity[128,129].

Like WAT, the transcription factor PPARgamma is a key regulator of BMAT formation. Thiazolidinediones (TZDs) are a class of pharmacological PPARγ agonists that have been shown to cause large increases in BMAT volume[130] whilst also providing anti-diabetic effects[131]. Despite the strong antidiabetic effects of these drugs their use was widely discontinued given the side effect of increased bone fracture risk[132].

The most important modulator of BMAT, in the context of this thesis, is caloric restriction. Despite the loss of WAT during calorie restriction, as discussed above, BMAT

volume increases in times of energy scarcity. This counter-intuitive phenomenon has been observed in a wide variety of organisms including mice[133], deer[134] and moose[135]. In addition to calorie restriction, BMAT has also been shown to increase in more pathological contexts of energy deficit, such as during anorexia nervosa in humans[136,137].

Several mechanisms have been proposed to contribute to BMAT accumulation during CR. One notable candidate is the adipokine leptin. The ob/ob mouse, lacking leptin, and the db/db mouse, lacking the leptin receptor, both show increased BMAT[138,139], whilst leptin treatment abrogates this effect[140]. However, more recent research has shown that hypoleptinaemia is not required for BMAT expansion and is more associated with increased glucocorticoids[129].

Growth hormone (GH) has been proposed to play an important role in BMAT expansion given that mice with spontaneous mutations in GH signalling have low GH concentrations as well as high BMAT volumes[141]. Additionally, mice with high GH concentrations have relatively little BMAT[142]. However, GH may not be the major determinant, as humans with anorexia nervosa have high concentrations of GH yet large amounts of BMAT. A proposed reason for this is that patients with anorexia have developed a resistance to the signalling of GH as, despite having high GH, they show low levels of IGF-1[143]. As mentioned above, CR is known to decrease IGF-1 in animal models so it may be that decreased IGF-1 contributes to expansion of BMAT during CR, although this remains to be formally tested.

There is not a large amount of research regarding temporal relationship between CR and BMAT expansion. It has recently been shown that short term fasting causes an increase in vertebral BMAT but not femoral BMAT[144]. However, this temporal relationship remains ignored, highlighting the need for further research to help identify potential causes and consequences of BMAT expansion during CR.

1.3.3. BMAT endocrinology and metabolic influence

The ability of WAT to act as an endocrine organ is now well established and specific adipokines are numerous, including the satiety hormone, leptin[145,146]; the antidiabetic hormone, adipsin[147]; and, as previously mentioned, adiponectin. Despite the endocrinology of WAT being well studied, the endocrinology of BMAT is far less well characterised.

In vitro study of adipocytes differentiated from bone marrow mesenchymal stem cells has shown leptin expression and secretion[148-150], however differentiated and cultured bone marrow adipocytes may not faithfully represent the true nature of these cells in vivo. An in vivo example of leptin expression from BMAT comes from a microarray analysis of isolated mouse bone marrow adipocytes showing enriched levels of *Lep*

transcript[151]. In addition to this, *Lep* transcripts have also been detected in the distal BMAT of rabbits where, as in WAT, they are downregulated during CR[129].

Given the above observations, a logical hypothesis was that BMAT may be contributing to the calorie restriction induced hyperadiponectinaemia. Notably, this effect is not solely limited to calorie restriction: BMAT increases and hyperadiponectinaemia are concordant in conditions such as aging[151,152], animal models of type 1 diabetes[153,154], anorexia nervosa[136,155] and TZD treatment[156,157]. However, whether BMAT also contributes to hyperadiponectinaemia in these or other conditions remains unknown. Similarly, it is unclear whether, by producing adiponectin, BMAT contributes to the systemic metabolic effects of CR.

Empirical evidence for BMAT secretion of adiponectin during calorie restriction is based on studies in transgenic Ocn-Wnt10b mice. These mice have increased bone formation resulting from the transgenic expression of the signalling molecule, Wnt10b, from the human osteocalcin promoter; this results in osteoblast-specific Wnt10b overexpression[158]. Wnt10b is known to stimulate osteoblastogenesis and inhibit adipogenesis[159], and therefore they were tested as a model that may be BMAT-deficient. Consistent with this, these Ocn-Wnt10b mice display a higher bone mass and, whilst the volume of BMAT is the same on a normal chow diet, when placed on a CR diet the WT mice show the expected increase in BMAT but this increase is significantly blunted in the Onc-Wnt10b mice[121]. In addition to the effect on BMAT volume, Ocn-Wnt10b mice also have significantly lower concentrations of adiponectin in the circulation, including total levels and the levels of the specific multimers[121]. This occurs despite no changes in adiponectin production from WAT. Together, this indicates that increases in BMAT are required for the hyperadiponectinaemia induced by CR.

1.4. Hypothesises and aims

Given the preceding information, I propose the following hypothesis:

BMAT is an important secretory source of adiponectin during CR as well as other condition of BMAT expansion and hyperadiponectinaemia. Furthermore, this secreted adiponectin is at least partly responsible for the metabolic adaptions induced by CR. I will test this hypothesis through the following sub-hypotheses and aims:

1. BMAT will contribute to hyperadiponectinaemia not only during CR but also in response to TZD treatment, another context in which both BMAT and circulating

adiponectin are increased. I will address this hypothesis by pursuing the following aims:

a. Determine if Ocn-Wnt10b mice also resist TZD-induced BMAT expansion.
b. Determine if Ocn-Wnt10b mice resist TZD-induced hyperadiponectinaemia, compared to wild-type controls.

I hypothesise that mice resistant to BMAT expansion will show blunted hyperadiponectinaemia in response to TZD treatment, compared to wild type controls.

2. CR-induced BMAT expansion is dependent on the duration of CR and is associated with endocrine, skeletal and metabolic effects of CR. I will address this hypothesis by pursuing the following aims:
    a. Determine the time frame over which BMAT expansion occurs in response to CR.
    b. Determine the time frame over which hyperadiponectinaemia occurs in response to CR.
    c. Determine the time frame over which beneficial metabolic adaptions occur in response to CR, including decreased fat mass and improved glucose tolerance.
    d. Compare these time frames to evaluate if changes in BMAT and hyperadiponectinaemia are associated with the metabolic adaptions.

I hypothesise that changes in BMAT will precede or occur simultaneously with the onset of hyperadiponectinaemia, and that hyperadiponectinaemia will precede or occur simultaneously to the metabolic adaptions to caloric restriction.

3. Adiponectin contributes to the metabolic effects of CR. I will address this hypothesis by pursuing the following aims:
    a. Generate a transgenic adiponectin knock-out mouse line and compare how this mouse responds to CR vs wild type mice across a variety of metabolic parameters.

I hypothesise that mice lacking adiponectin will have impaired metabolic adaptions to caloric restriction.

2. Materials and methods

2.1. Animal husbandry

2.1.1. General husbandry

2.1.1.1. Ocn-Wnt10b mice

The study was approved by the University Committee on Use and Care of Animals and mice were cared for by the Unit for Laboratory Animal Medicine at the University of Michigan. These mice were generated, bred and culled prior to commencement of this PhD project. Ocn-Wnt10b mice overexpress the Wnt10b specifically in osteoblasts resulting in increased bone mineral density, bone volume fraction and trabecular number. This effect is caused by an increased number of osteoblasts per bone surface.[158] A consequence of this increase in bone is that there is significantly less BMAT volume in the medullary cavity of the bones making it a useful tool for studying BMAT expansion *in vivo*[121]. At the time these mice were used no other models specifically resistant to BMAT expansion existed. Now, multiple research groups are developing rodent models which lack BMAT and these will be discussed in subsequent chapters.

2.1.1.2. C57BL/6NCrl mice and adiponectin knock-out mice

The studies at The University of Edinburgh were approved by the local named veterinary surgeons in line with establishment, project and personal licences issued by the UK Home Office. Mice were housed in communal housing rooms with a 12-hour light-dark cycle between 7am and 7pm and at an ambient temperature of 25°C.

2.1.2. Transgenic line generation

2.1.2.1. Ocn-Wnt10b mice

Ocn-Wnt10b mice were generated at the University of Michigan prior to commencement of this PhD project as previously reported[158]. In summary, the human osteocalcin promoter from pBS(K-) vector was excised using *HindIII and Xhol*. This DNA was ligated into pCRII vector containing mouse cDNA for *Wnt10b* at the *HindIII/Sal1* site; this was followed by a rabbit β-globin intron/poly A tail sequence. The transgenic construct containing the Ocn-Wnt10b region was digested using *HindIII, XholI,* purified, and microinjected into fertilised C57BL/6J mice eggs. Successful transgene integration was screened for by PCR using transgene specific primers. One founder male was selected for moderately increased BMD and was bred with wild-type C57BL/6J females to generate line designated 488 from which experimental mice were bred.

2.1.2.2. C57BL/6NCrl mice

These mice were acquired from breeding stocks maintained by the Bioresearch and Veterinary Services at The University of Edinburgh.

2.1.2.3. Adiponectin knock-out mice

Transgenic *Adipoq*$^{tm1a(KOMP)Wtsi}$ sperm was purchased from The Knockout Mouse Project KOMP Repository. This sperm was used the fertilise wild-type C57BL/6N (Charles River Laboratory, acquired from local BVS stock) mouse eggs by *in vitro* fertilisation. Recombinant Tet-Cre recombinase was also injected into the egg causing recombination at the LoxP sites thereby excising exon 3 of the *Adipoq* gene at the single-cell stage. This converted the *Adipoq*$^{tm1a(KOMP)Wtsi}$ allele to the *Adipoq*$^{tm1b(KOMP)Wtsi}$ allele (Figure 2.1). Subsequent heterozygous pups were bred with other heterozygotes to generate pups homozygous for the *Adipoq*$^{tm1b(KOMP)Wtsi}$ allele (KO) or control mice homozygous for the wild-type allele (WT); these two genotypes were used as the experimental mice.

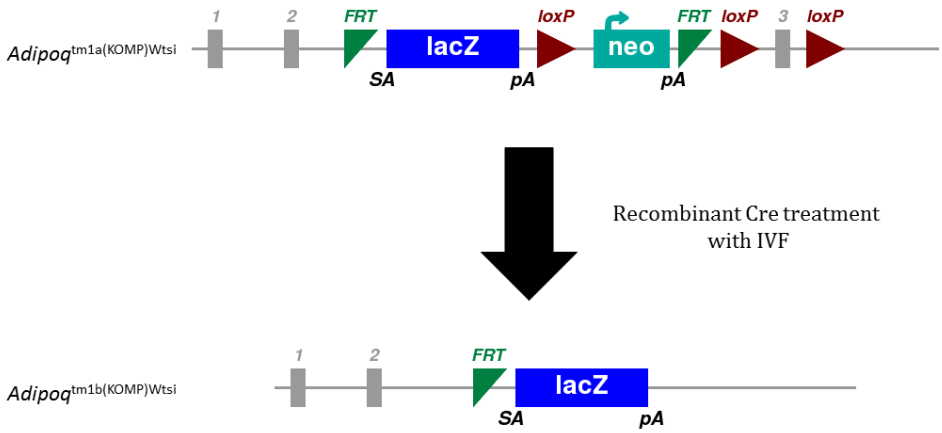

Figure 2.1 – Conversion of tm1a to tm1b allele. Sperm containing the tm1a allele was purchased and used to fertilise wild type eggs. During the IVF process, recombinant Cre recombinase was also injected causing conversion to the tm1b allele by excision of exon 3 of the Adipoq gene. Grey boxes are exons (numbered above); *FRT*, flippase recognition target; *lacZ*, open reading frame for b-galactosidase reporter gene; *loxP,* recombination site for Cre recombinase; *neo,* open reading frame for neomycin resistance gene. Figure from www.komp.org.

2.1.3. Rosiglitazone treatment

The in vivo work in this section was done by researchers at the University of Michigan and not as part of this PhD project.

Male and female wild type or Ocn-Wnt10b mice on a C57BL/6J background were fed a normal chow diet until 10 weeks of age. From 10-22 weeks of age, the mice were fed a western-style diet high in fat and sucrose (Research Diets, D12079B). At 18 weeks of age mice were evenly assigned to 1 of 4 groups: the first group remained on the western diet until 30 weeks of age, the other 3 groups received TZD treatment for 2, 4 or 8 weeks in duration. TZD was administered via the diet with western diet supplemented with

Rosiglitazone at 0.175mg/g of diet (Research Diets, D12112601). Two-week-treated mice received this diet from 28 to 30 weeks of age; four-week mice from 26 to 30 weeks of age; and eight-week mice from 22 to 30 weeks of age. At 29.5 weeks of age, the mice were fasted overnight and blood glucose concentrations measured. At 30 weeks of age, the mice we euthanized and the tissues isolated for downstream analysis.

2.1.4. Caloric restriction

At eight weeks of age C57BL/6NCrl mice were transferred from group housing to single housing in new, clean, cages. The diet was changed from standard chow (Special Diet Services, UK) to Research Diets D12450B. From 8-9 weeks of age, body mass and *ad libitum* (AL) food consumption was measured daily at 9:30am. Mean food intake was calculated over the final 5 days of single housing to allow mice to first adapt to the stress of single housing before assessing food consumption. Mice were randomly assigned to either remain on AL diet or changed to CR diet, ensuring equal numbers of each sex and genotype on each diet. Mice assigned to AL diet continued to have 24-hour access to diet D12450B. Mice assigned to CR diet received 70% mass of calculated AL intake. For the CR time course, this was 2.1 g/day and for the adiponectin knockout experiment was 2.2 g/day. CR mice diet was changed to Research Diets D10012703, a micronutrient enriched diet used to ensure adequate micronutrient intake. The CR diet was administered once daily at 9:30am directly into the cage. For CR timecourses, mice were maintained on CR or AL diet for 1, 2, 4 or 6 weeks. For studies in *Adipoq* KO mice, mice were maintained on CR or AL diet for 4 weeks, a duration sufficient for maximum levels of hyperadiponectinaemia in the WT mice.

Given that we have previously observed large increases in both circulating adiponectin and BMAT after 6 weeks of calorie restriction[121] we used this as the longest time point to ensure that we saw the same effects. Subsequently we chose evenly spaced timepoints from 0 to 6 weeks to maximise the changes of accurately detecting the dynamic changes in these parameters.

For the adiponectin knockout study, 4 weeks was used for the duration of CR because it was by this time point that we observed maximal increases in circulating adiponectin concentration. We also saw large improvements in glucose tolerance by 4 weeks CR indicating that we could accurately test the hypothesis that adiponectin was contributing to CR-induced improvements in glucose tolerance whilst minimising the duration of the experiment. This is beneficial in terms of costs, time and, most importantly, animal welfare.

The CR diet D10012703 contains a higher concentration of micronutrients compared to the AL diet. This is to ensure that the CR mice, which eat a lower mass of diet, receive adequate micronutrients to avoid malnutrition which could confound the results. The

result is that the AL diet and CR diet both result in approximately equal masses of nutrient mix ingested despite the 30% reduction in macronutrients.

Whilst the macronutrient concentrations in table 2.1 show that the diets are approximately the same composition, some more subtle differences are seen in fat source with the CR diet containing proportionally more soy-bean oil and less lard. These differences are relatively small and so are not anticipated to influence the result of the experiments by a large amount.

Diet	D12450B		D10012703	
Food group	grams	% (kcal)	grams	% (kcal)
Protein	19.2	20	18.9	20
Carbohydrate	67.3	70	66	70
Fat	4.3	10	4.2	10
kcal/gram	3.85		3.77	

Table 2.1 – Diet composition by energy source. Grams and percentage contribution by kcal of proteins, carbohydrates and lipids.

Diet	D12450B		D10012703	
Ingredient	grams	kcal	grams	kcal
Casein	189.6	758.3	186.0	744.0
L-Cysteine	2.8	11.4	2.8	10.6
Corn starch	298.6	1194.3	279.0	1116.1
Maltodextrin 10	33.2	132.7	46.5	186.0
Sucrose	331.7	1327.0	321.5	1286.1
Cellulose, BW200	47.4	0.0	46.5	0.0
Soybean oil	23.7	213.3	26.6	239.2
Lard	19.0	170.6	15.3	138.2
Mineral mix S10026	9.5	0.0	13.3	0.0
Dicalcium phosphate	12.3	0.0	17.3	0.0
Calcium carbonate	5.2	0.0	7.3	0.0
Potassium citrate	15.6	0.0	21.9	0.0
Vitamin mix 10001	9.5	37.9	13.3	53.1
Choline bitartrate	1.9	0.0	2.7	0.0
FD&C yellow dye	0.0	0.0	0.0	0.0
FD&C blue dye	0.0	0.0	0.0	0.0
Total	1000.0	3845.3	1000.0	3773.3

Table 2.2 – Diet composition by ingredient. Grams and kcal of each ingredient per 1000g.

2.1.5. Blood sampling

Tail vein blood was acquired from the mice weekly, including prior to commencement of the dietary intervention and prior to cull. Mice were not restrained during blood sampling to limit stress effects. A razor blade was used to make a small incision on the side of the tail and resulting venous blood was collected in EDTA-coated capillary tubes (Sarstedt, 16.444). Blood glucose was also measured using a blood glucose monitoring system (OneTouch Verio® meter or OneTouch Verio® IQ meter). Blood collected in EDTA capillary tube was centrifuged at 2000 rcf for 10 minutes and the upper layer of blood plasma transferred to a fresh tube for storage at -80°C.

2.1.6. Body composition

Body composition was measured fortnightly in the CR time-course mice and weekly in the Adipoq knockout mice. Body composition was measured by time domain nuclear magnetic resonance imaging (TD-NMR) using a Minispec LF50 (Bruker, UK) as per manufacturer's instructions.

2.1.7. Oral glucose tolerance test

The evening (5-6 pm) prior to oral glucose tolerance test (oGTT) CR mice were given a normal daily portion (2.1 g, CR time-course; 2.2 g, Adipoq KO) and AL mice were given an average daily dose of diet (3 g, time-course; 3.1 g, Adipoq knockout); all other diet was removed. The next day at 12pm an oGTT was performed, corresponding to an estimated fasting duration of ~6-12 hours. Mice were administered with 2 mg of D-glucose (Sigma, G8270) per gram of body mass by oral gavage of 25% w/v D-glucose solution. Blood glucose was measured (as above) prior to gavage and 15, 30, 60 and 120 minutes post-gavage. At each timepoint a blood sample was also taken from the tail vein to allow for analysis of plasma insulin concentrations. The oGTT was done 2 days prior to cull to allow recovery of the mice.

2.1.8. Indirect calorimetry

Adiponectin knockout mice underwent the previously described CR protocol; however, at the end of the 4-week dietary intervention, mice were placed in metabolic cages (TSE Phenomaster) for 3 days. Mice were fed as usual: AL mice with free access to food and CR mice fed in the morning daily. A flow rate of $0.35 L min^{-1}$ was used following calibration, with the aim of keeping the respiratory exchange ratio (RER) between 1 and 0.7. Values were expressed relative to lean mass of mice. Data was recorded over the 3-day period but only the final 24 hours were analysed and presented to avoid the period of adaption to the foreign environment.

2.1.9. Cull and necropsy

At 5-6 pm on the day prior to termination CR mice were given 1.1 g CR diet whilst AL mice were given 1.5 g AL diet and remaining food removed in order to ensure both groups of mice were fasted to an equivalent degree. This was done to ensure that any

differences between groups reflect effects of longer-term CR, and not simply differences between fasted (CR) and non-fasted (AL) mice; a similar approach has been recommended by leading experts in animal CR studies[160]. Mice were culled by cervical dislocation followed by decapitation. The following tissues were dissected and frozen and/or fixed in 10% neutral-buffered formalin (Sigma): tail vertebrae; brown adipose tissue (BAT); humeri; ulnae and radii; inguinal WAT (iWAT); gonadal WAT (gWAT); mesenteric WAT (mWAT); tibiae; femurs; gastrocnemius muscle; soleus muscle; kidneys; spleen; pancreas; liver; heart; thymus; lumbar vertebrae; and, in Adipoq mice only, brain. Selected tissues were also weighed prior to freezing/fixing.

2.2. Endocrine factors

2.2.1. Circulating adiponectin

Circulating adiponectin was quantified using Adiponectin ELISA (R&D, MRP300). Plasma was diluted with assay diluent (RD1W) 10,000-fold for mice treated with TZD and 4,000-fold for mice not receiving TZD. The provided adiponectin standard was prepared and serially diluted according to manufacturer's instructions. Assay diluent (50 µL) was added to each well of the provided 96-well anti-adiponectin-antibody-coated plates, followed by 50 µL of sample or standard, and the plate incubated for 3 hours at room temperature. Wells were aspirated and washed 5 times with 400 µL wash buffer. Mouse adiponectin conjugate (100 µL) was added to each well and the plate incubated for 1 hour at room temperature. All wells were aspirated and washed 5 times again. Substrate solution (100 µL) was added to each well and the plate was incubated for 30 minutes at room temperature in the dark. Stop solution (100 µL) was then added to each well and a plate reader (Infinite 200 Pro, Tecan Life Sciences) used to measure the optical density of each well at 450 nm, with a correction against 570 nm. Sample concentrations were interpolated from standard curves and corrected for initial dilution.

2.2.2. Circulating leptin

Circulating leptin was quantified using leptin ELISA (R&D, MOB00). Plasma was diluted 20-fold in calibrator diluent (RD5-3) and the provided standard was prepared according to the manufacturer's instructions. Assay diluent (50µl) was pipetting into each well of anti-leptin-antibody-coated 96 well microplate as well as 50µl of diluted plasma or standard control sample and the plate incubated for 2 hours at room temperature. All wells were aspirated and washed 5 times by sequential additions and aspirations of 400 µl wash buffer. Mouse/rat leptin conjugate (100µl) was added to each well and the plate was incubated for 2 hours at room temperature. The plate was washed a further 5 times and 100 µl substrate added, the plate was incubated at room temperature for 30 minutes in the dark and then 100 µl stop solution added to each well. The optical density of each well measured with an Infinite 200 Pro plate reader at 450 nm with a correction against

570nm. Sample concentrations were interpolated from standard curve and corrected for initial dilution.

2.2.3. Circulating insulin

Mouse insulin ELISA (Crystal Chem, 90080) was used to quantify circulating insulin concentrations from plasma samples taken during glucose tolerance test. The provided mouse insulin standard was diluted to 6.4, 3.2, 1.6, 0.8, 0.4, 0.2, 0.1 and 0 ng/ml. Standard or mouse plasma (5µl) was added to each well of a provided 96 well anti-insulin-antibody-coated plate with 95µl assay diluent. The plate was incubated for 2 hours at 4°C then washed 5 times with 400 µl wash buffer. Conjugate solution (100µl) was added to the plate, incubated for 30 minutes at room temperature and washed as before. Substrate solution (100µl) was added and the plate incubated for 40 minutes at room temperature before 100 µl of stop solution was added. Absorbance of each well was measured with an Infinite 200 Pro plate reader at 450 nm with a correction at 630 nm and the concentration of the plasma samples interpolated vs the absorbance of the standards.

2.2.4. Circulating IGF-1

Mouse IGF1 ELISA Kit (Abcam, ab100695) was used to quantify plasma IGF-1 concentrations. Standards were serially diluted to final concentrations of 2000, 666.7, 222.2, 74.07, 24.69, 8.23, 2.74 and 0 pg/ml. Plasma from the calorie restriction time-course was diluted 807-fold in assay diluent A. Standard or diluted sample (100µl) was added to each well of the supplied 96 well plate and incubated for 2.5 hours at room temperature. The plate was washed by adding 400 µl wash buffer to every well, repeated 4 times. Biotinylated IGF1 detection antibody (100µl) was added to each well and the plate was incubated for 1 hour at room temperature,. Following this, the 4 washes were repeated and 100 µl HRP-streptavidin solution was added to each well and the plate incubated for 45 minutes at room temperature. The 4 washes were repeated again and 100 µl of TMB one-step substrate reagent was added to every well followed by an incubation for 30 minutes at room temperature in the dark; 50 µl stop solution was then added to every well and the absorbance of each well measured with an Infinite 200 Pro plate reader at 450nm. Concentrations of the plasma samples were interpolated from absorbance of the standards and multiplied by the dilution factor.

2.2.5. Circulating corticosterone

Corticosterone ELISA (Enzo, ADI-900-097) was used to quantify circulating corticosterone concentrations in CR time-course mice. Protein-bound corticosterone was displaced into the plasma by adding 3 µl steroid displacement reagent diluted 1:100 (80-0925) to 3 µl of plasma, incubated at room temperature for 5 minutes and then made up to 150 µl with assay diluent (80-0921). Corticosterone standard (200000 pg/ml, 80-0916) was serially diluted to 20000, 4000, 800, 160, 32 and 0 pg/ml. Standard or diluted

plasma (100µl) was added to each well of the plate (80-0045) followed by 50 µl of conjugate (80-0917) and then 50 µl of antibody solution (80-0918). The plate was incubated for 2 hours at room temperature then each well was washed with 400 µl wash buffer (80-1286), pNpp substrate solution (200µl) (80-0075) was added to each well and the plate incubated for 1 hour at room temperature. 50 µl of stop solution (80-0247) was added to each well and the optical density of each well was measured with an Infinite 200 Pro plate reader at 405 nm with a correction at 580 nm. Plasma corticosterone concentrations were calculated from interpolation against absorbance of the standards and correction for initial dilution.

2.3. Bone parameters

2.3.1. Bone isolation

Bones were dissected from mice as described in section 2.1.4. Soft tissue was removed from the bones using scissors, razor blades and abrasive tissue paper in order to limit contamination by extraosseous tissue. Bones were fixed in 10% neutral buffered formalin solution (Sigma, HT501380-9.5L) for 48 hours at 4ºC then transferred to 0.1M Sorensen's buffer (81 mM KH2PO4, 19 mM Na2HPO4, pH 7.4) at 4ºC.

2.3.2. Calcified bone µCT scanning

Bones were embedded in a 30 ml screw top tube in 1% agarose (w/v) in water in 2 layers of 5 bones per layer. The tubes were scanned in Skyscan 1172 (Bruker) at a pixel size of 6.026µm. The camera used was Hamamatsu 10Mp, X-ray voltage used was 54kV and current was 185µA with an exposure time of 1767ms. Two-frame averaging was applied with a 360° rotation in 0.28° steps. Images were reconstructed using NRecon software (Bruker) with a misalignment compensation of 0.5, ring artefact reduction of 5 and beam-hardening correction of 40%.

2.3.3. Decalcification

Bones were decalcified in a solution of 14% EDTA (VWR, cat. no. 20302.260) for 14 days, with the EDTA solution replaced every 3 days. After these 2 weeks, the bones were washed with Sorensen's buffer 3 times to ensure complete removal of the EDTA solution. Decalcification was performed at 4°C.

2.3.4. Osmium tetroxide staining

Bones were stained with 1% osmium tetroxide solution (equal parts 2% osmium tetroxide (Agar Scientific, cat. no. AGR1022) and Sorensen's buffer). The solution was left on the bones for 24 hours then aspirated and the bones washed 3 times with Sorensen's buffer.

2.3.5. Osmium tetroxide stained bone µCT scanning

Bones were embedded in agarose as described above. The tubes were scanned in a Skyscan 1172 (Bruker) at a pixel size of 12.055µm. The camera used was Hamamatsu 10Mp, X-ray voltage used was 54kV and current was 185 µA with an exposure time of 885ms. Four-frame averaging was applied with a 360° rotation in 0.4° steps. Images were reconstructed using NRecon software (Bruker) with a misalignment compensation of 0.5, ring artefact reduction of 10 and beam-hardening correction of 40%.

2.3.6. CTAn analysis

Once bones had been scanned in batches of 5 in each layer it was required to separate each bone into an individual stack of images representing one bone, this was done using CTAn software (Bruker). The individual bones were separated into specific regions of interest, for calcified bones these regions were the trabecular region and cortical region and for osmium-tetroxide-stained bones this was the proximal and distal regions of the bone. Specific slice numbers and intensity thresholds used for each bone can been seen in the table below. Automated region of interest (ROI) drawing was used according to instructions from Bruker[161]. Analysis of these ROIs in calcified bone was achieved using built-in custom processing within CTAn software that covered the most common aspects of bone biology. Osmium-stained femurs and humeri were analysed as a whole bone whilst tibiae were separated into proximal and distal regions with the boundary defined as the junction of the tibia and fibula.

Region	Distance from growth plate (slices)	Length of region (slices)	Pixel intensity threshold used for analysis
Trabecular	60	200	65
Cortex	500	200	70
BMAT	N/A	N/A	80

Table 2.3 – Parameters used for trabecular, cortical and bone marrow adipose analysis of bone.

2.4. Transcript analysis

2.4.1. RNA isolation

Tissues of interest were frozen on dry ice after being dissected. The tissue was then ground to a fine powder using a pestle and mortar whilst continually being submersed in liquid nitrogen. To approximately 200mg of this powdered tissue, 600 µl Ribozol (VWR Chemicals, 1B1304) was added and the tissue homogenised by repeated aspiration and expulsed through a 21G needle attached to a Luer-lock syringe. Following homogenisation, a further 600 µl of Ribozol was added and the process of

homogenisation repeated. The homogenate was stored at room temperature for 10 minutes to allow dissociation of nucleoproteins and other macromolecular complexes. When adipose tissue, or other tissue with high lipid content, was used, the upper lipid layer was removed and replaced with an equivalent volume of Ribozol. Chloroform (200µl) was added to the tissue homogenate and the tube shaken for 20 seconds to ensure thorough mixing of the sample. The sample was incubated at room temperature for 3 minutes then centrifuged at 15,000 rcf for 15 minutes at 4°C. The upper layer was transferred to a new Eppendorf containing 700 µl isopropanol, gently mixed by inversion and incubated at room temperature for 15 minutes. The samples were stored at -20°C overnight then centrifuged at 20,000 rcf for 30 minutes at 4°C in order to pellet the RNA. The supernatant was removed from the pellet and discarded. Ethanol (1.5ml, 75%) was added to the pellet and the sample vortexed to wash the pellet. The sample was centrifuged at 12,000 rcf for 5 minutes at 4°C. Following this, the supernatant was removed and the wash procedure repeated with final removal of the supernatant and subsequent air-drying of the RNA pellet for 5 minutes at room temperature. The pellet was resuspended in 50 µl nuclease-free water (Fisher) and RNA concentration and purity determined by Nanodrop (1000, ThermoFischer).

2.4.2. Reverse transcription

Reverse transcription reactions (50 µl total volume) were performed containing: 1 µg RNA (from 2.4.1); Reverse transcription buffer (Life Technologies, N8080234) at 1X working concentration; 5.5mM $MgCL_2$ (Sigma, M8266); deoxyadenosine triphosphate, deoxyguanosine triphosphate, deoxycytidine triphosphate and deoxythymidine triphosphate all at 0.5mM each (GeneAmp dNTP mix, Life Technologies, 430442); 0.83 µM random hexamers (Life Technologies, SO142); 0.8 U/µL RNase inhibitor (Life Technologies, 10859710); and 1.25 U/µL Multiscribe reverse transcriptase (Life Technologies, 4311235). The samples were incubated in a thermocycler (Techne) at 25°C for 10 minutes, 37°C for 30 minutes then 95°C for 5 minutes, resulting in a cDNA solution.

2.4.3. qPCR

A small aliquot of each set of reverse-transcribed cDNA was pooled to generate a representative pooled cDNA from each set of samples. This pooled sample was serially diluted with RNase-free water to generate a 3, 9, 27, 81 and 243-fold diluted standard series. The individual cDNA samples were diluted 4-fold in RNase-free water to ensure their concentration fell within the range of the standard series.

2.4.3.1. Taqman qPCR

qPCR reactions were run on 384-well plates (Sarstedt, 72.1985.202) as 10 µl reactions each containing: 2 µl diluted cDNA solution; 2.75 µl RNase free water; 5 µl 2x Probe Blue Mix buffer (PCR Biosystems), PB20.27-20); and 0.25 µl relevant probe and primer mix

(listed in section 2.4.4). Plates were incubated in a Lightcycler 480 (Roche) following a program consisting:

Cycle 1 (x1): 95 ºC for 5-10 minutes;
Cycle 2 (x50): 95 ºC for 10 seconds
60 ºC for 30 seconds
Cycle 3 (x1): 37 ºC (hold)

2.4.3.2. SYBR green qPCR

qPCR reactions were run on 384-well plates as 10µl reactions each containing: 2µl diluted cDNA solution; 2µl RNase free water; 5µl 2x SyGreen Blue master mix (PCR Biosystems, PB20.11) and 0.5µl each of forward and reverse primer (CONC) (listed in section 2.4.4). Plate was incubated in a Lightcycler 480 (Roche) following a program consisting:

Cycle 1 (x1): 95 ºC for 10 minutes;
Cycle 2 (x40): 95 ºC for 10 seconds
60 ºC for 30 seconds
Cycle 3 (x1): Melt curve (65 to 95 ºC, at 0.06 ºC/second); 10 acquisitions per ºC
Cycle 4 (x1): 37 ºC (hold)

2.4.3.3. qPCR primers

qPCR primers used are shown in Table 2.4

Gene name	**Detection type**	**Supplier**	**Sequence/Catalogue #**
18S	Sybrgreen	Integrated DNA technologies	F: CGCTTCCTTACCTGGTTGAT R:GAGCGACCAAAGGAACCATA
Acadm	Taqman	ThermoFisher	Mm01323360_g1
Adipoq	Sybrgreen	Integrated DNA technologies	F: AAGAAGGACAAGGCCGTTCTCTT R: GCTATGGGTAGTTGCAGTCAGTT
Bglap	Taqman	ThermoFisher	Mm03413826_mH
Fabp4	Sybrgreen	Integrated DNA technologies	F: TGGAAGCTTGTCTCCAGTGA R: AATCCCCATTTACGCTGATG

Lep	Sybrgreen	Integrated DNA technologies	F: GACACCAAAACCCTCAT R: CAGTGTCTGGTCCATCT
Pgc1a	Taqman	ThermoFisher	Mm01208835_m1
Ppia	Sybrgreen	Integrated DNA technologies	F: CACCGTGTTCTTCGACATCA R:CAGTGCTCAGAGCTCGAAAGT
Tbp	Sybrgreen	Integrated DNA technologies	F: ACCTTATGCTCAGGGCTTGG R: GCCGTAAGGCATCATTGGAC
Tfam	Taqman	ThermoFisher	Mm00447485_m1

Table 2.4 – Primers used for qPCR. Primers used are listed in alphabetical order. Sybrgreen primers were ordered from a custom oligonucleotide company. All primers were tested against a standard curve of cDNA and by melt curve analysis , followed by running products on a gel, to ensure reaction specificity. Primers were ordered from Integrated DNA Technologies (IDT).

2.4.4. Analysis

Cycle threshold (ct) was determined using Lightcycler 480 software (Roche) by second derivative of the amplification curves. The ct values of the serial diluted cDNA pool (described in section 2.4.3) were plotted against their relative concentration to generate a standard curve of ct vs concentration. The relative concentration of the unknown samples was interpolated against the standard curve, this relative concentration was then used as a measure of cDNA transcript quantity in the sample and thus of relative expression of the gene of interest.

2.5. Lipid analysis

2.5.1. Triglyceride quantification

Approximately 100 mg of liver tissue was cut from the frozen liver samples and placed in 1 ml cooled PBS containing 5% v/v IGEPAL CA-630 (Sigma, I8896) on ice. Tissue was homogenised using steel ball bearings and high-frequency shaking and this homogenate was centrifuged at 12,000 rcf for 10 minutes at 4°C in order to pellet cell debris. The supernatant was removed and transferred to a clean Eppendorf and any lipid that had collected on the top was resuspended. Pre-prepared 500 mg/dl triglyceride standard (Sigma, 17811-1AMP) was serially diluted to 250, 125, 62.5, 31.25, 15.625 and 7.8125mg/dl, a solution containing no triglyceride standard was included as a negative control. Either the standards or liver samples (2µl) were pipetted into a 96-well plate in duplicate. Triglyceride concentrations were determined using reagents from Sentinel (Sentinel 17624H). Solution 1 (200µl) was added to each well and the plate incubated at

37°C for 10 minutes. Following this, the absorbance of each well in the plate was measured at both 546nm and 700nm. The 546nm reading was subtracted from the 700nm for each well and then the average absorbance for the blank duplicates was subtracted from the average absorbance of the samples and standards duplicates. Standard absorption was plotted against concentration and the line of best fit calculated using a linear regression model (Graph Pad Prism 7). The concentration of the samples was interpolated from this line of best fit and was normalised against the mass of liver used at the start of the protocol.

2.5.2. Plasma NEFA quantification

Non-esterified fatty acid standard solution (Wako Diagnostics, 276-7649) was serially diluted to concentrations; 1, 0.5, 0.25 and 0.125mM as well as a blank solution. The standard solution or endpoint core plasma (2µl) was pipetted into a 96 well plate in duplicate. Reagent 1 (200µl) (Wako Diagnostics, 999-34691, 995-34791) was added to each well and the plate incubated at 37°C for 5 minutes. Absorbance of each well was measured at 550 and 660nm. Reagent 2 (100µl) (Wako Diagnostics, 991-34891, 993-35191) was added to each well and the plate was incubated again at 37°C for 5 minutes and the absorbance measured at 550 and 660nm. The 660nm reading was subtracted from the 550 reading from both measurements and the mean blank absorbance subtracted from the mean duplicate absorbance from each sample. Absorbance of the standards was plotted against concentration, the line of best fit calculated using a linear regression model (Graph Pad Prism 7), and the concentration of the samples was interpolated from this line of best fit.

2.5.3. Liver ceramide quantification

This work was performed by Ben Thomas (PhD student, Cawthorn Lab) in collaboration with Phil Whitfield at the University of the Highlands and Islands.

Frozen liver tissue (100 mg) was homogenised in ice-cold MeOH using a tissue homogeniser. Fifty µl of each sample was combined with100 µl ceramide 17:0 (1 µM in MeOH) and 25 µl dihydroceramide 12:0 (2 µM in MeOH). MeOH (1.875 ml) and $CHCl_3$ (4 ml) were added and the samples were stored on ice for 1 hour with intermittent vortex mixing. The samples were then centrifuged at 2,000 rpm for 5 minutes at 4°C and the supernatant collected. KCl (0.9%; 1.45 ml per sample) was added to the previously acquired supernatant and the samples were centrifuged again at 2000 rpm for 5 minutes at 4°C. The resulting lower phase was collected and evaporated under nitrogen until completely dry, then reconstituted in 1 ml $CHCl_3$. Solid phase extraction was performed via a 100 mg, 3 ml silica isolute. The column was conditioned with 2 additions of 3 ml $CHCl_3$ then loaded with 1 ml of the sample. The bound sample was washed with 2 washes of 3 ml $CHCl_3$ then eluted with 2 additions of 1:1 ethylacetate $CHCl_3$. The collected eluate was evaporated and dried under vacuum and reconstituted in 200 µl

MeOH. Two µl were injected into the LC-MS/MS for ceramide analysis and 10 µl for dihydroceramide analysis. Liquid chromatography was performed using Phenomenex kinetex C8, particle size: 1.7 µm, pore size 100Å, 100 mm x 2.1 mm (00D-4499-AN). Mobile phase A was 90% H_2O, 9.9% acetonitrile and 0.1% formic acid. Mobile phase B was 99.9% acetonitrile and 0.1% formic acid. The gradient was held at 80% mobile phase B for 1 minute then gradually increased to 100% mobile phase B over 15 minutes. Mobile phase B at 100% was maintained for 1 minute and then equilibrated to storage conditions. The flow rate used was 500 µl per minute at 40°C. This lipid extraction protocol is based on a 1957 paper by Folch et al.[162]

2.6. Protein analysis

2.6.1. Protein extraction

Frozen tissue was ground into a fine powder as described in 2.4.1. Approximately 100 mg of powdered tissue was mixed with 1 ml protein lysis buffer (1% SDS, 12.7mM EDTA, 60mM Tris, pH 6.8, 1mM Na_3VO_4, and 1mM NaF) heated to 90°C. The mixture was passed by and down a syringe through a 21G needle to ensure complete homogenisation. The homogenate was centrifuged at 14,000 rpm for 15 minutes at 4°C to pellet any un-lysed cells or large cell debris and the supernatant was transferred to a new Eppendorf tube. Protein concentrations was calculated using Pierce BCA protein assay kit (Thermo Fischer Scientific, 23225) according to manufacturer's instructions.

2.6.2. Immunoblot assay

From tissue lysates 1 µg, or from plasm a 1.5µl, was mixed with loading buffer with a final concentration of 1% SDS, 10% glycerol, 0.0125% bromophenol blue and 60 mM Tris-HCl pH 6.8. Proteins were separated by molecular weight by SDS gel electrophoresis through either 4-12% or 12% Bis-Tris polyacrylamide gels (BioRad, 3450125/3450119) using Criterion cell running tank and PowerPac power supply (BioRad, 1656019). Gels were run until the loading buffer ran off the bottom of the gel, the protein was then transferred to PVDF blotting membrane (GE Amersham Hybond, 10600023) using a wet transfer using Criterion Blotter (BioRad, 1704070) at 350 mA for 150 minutes at 4°C ambient temperature. If required, LiCor total protein stain (LiCor, P/N 926-11010) was used to quantify the total protein present in each lane according to manufactures instructions. The membrane was then blocked in 5% milk powder (ASDA, 11992) in TBST for 1 hour at room temperature then washed 3 times in TBST for 5 minutes per wash. The membrane was then incubated with the relevant primary antibody (listed below) overnight at 4°C or for 1 hour at room temperature then washed 3 times in TBST. The membrane was incubated in secondary antibody (see below) in 5% milk for 1 hour at room temperature, washed 3 times and then visualised on LiCor Odyssey CLx Fluorescent imaging system. Protein was quantified using Image Studio Lite Ver 5.2 software.

2.6.3. Antibodies used

Protein epitope	Mono/Polyclonal	Supplier	Catalogue number	Species raised in
Adiponectin	Polyclonal	Sigma-Aldrich	A6354-200UL	Rabbit

Table 2.5 – Antibodies used for western blotting.

2.7. Statistical analysis

Statistical analysis was performed using Graph Pad Prism 7. For analyses comparing the interaction of two factors, a 2-way analysis of variance (ANOVA) was used to compare the significance of contribution to variance by each factor. Additionally, multiple comparisons by Sidak's test were performed when a particular factor was shown to be a significant cause of variance. For non-interactive data with more than two variables, a 1-way ANOVA was used to test for significant variance with the data, when this was detected a Tukey's multiple comparisons test was used to compare specific groups. For non-interactive data only containing 2 variables a student's T test was used to detect significant differences between the 2 groups. A significance threshold of 95% was used throughout.

Power calculations were performed prior to commencement of the experiments to determine the preferable number of animals per group. BMAT increase effect size was calculated from previous studies but the results showed that the study would require in excess of 60 mice. This was not in concordance with previous studies and so the decision was made to repeat previously used group sizes which had previously shown statistically significant effects.

3. Increased Circulating Adiponectin in Response to Thiazolidinediones: Investigating the Role of Bone Marrow Adipose Tissue

3.1. Introduction

Thiazolidinediones (TZD) are a class of pharmacological agents that includes the drugs rosiglitazone malate and pioglitazone hydrochloride. These drugs are highly selective agonists of peroxisome proliferator-activated receptor gamma (PPARγ)[163,164] a nuclear hormone receptor that is best known for its effect on adipocyte differentiation and regulation of adipogenic and lipogenic pathways[165-167]. In addition, PPARγ plays an important role in glucose and lipid homeostasis by altering the secretion of various hormones, including decreasing the concentrations of resistin[168], leptin [169] and, importantly, increasing circulating adiponectin[170]. Most of the focus on TZDs relates to the antidiabetic, insulin-sensitising effects of the drugs. Rosiglitazone, used in the present experiment, is a member of the TZD family and was sold under the trade name Avandia[171]. Rosiglitazone was used in diabetic patients to reduce their blood glucose concentrations to near normal levels by increasing sensitivity of muscle, liver and adipose tissue to insulin[172]. Despite these promising effects of rosiglitazone and TZD drugs in general, they were pulled from the market. They were shown to significantly increase the risk of myocardial infarction and heart failure[173]. In addition to these cardiac issues, TZD treatment has also been associated with bone loss, including reduced bone formation rate and increased BMAT volume[174]. Downstream transcriptional targets of PPARγ activation include adiponectin[175], IGF-1[176], TGFβ[177] and fatty acid-binding protein 4 (FABP4) [178].

BMAT volume and adiponectin concentrations increase in response to CR, and BMAT has been established to secrete adiponectin and act as a significant source of this hormone during CR[121]. We hypothesised that when BMAT and adiponectin are both increased in conditions other than CR, that BMAT would also be a significant source of circulating adiponectin. Increases in BMAT volume and hyperadiponectinaemia occur simultaneously in a wide variety of conditions including type 1 diabetes[153,154] and aging[179,180]. Notably, TZD treatment also causes marked BMAT expansion and hyperadiponectinaemia and, like CR, exerts insulin-sensitising effects[130,175]. Thus, we hypothesised that the Ocn-Wnt10b mouse, previously shown to resist CR-induced BMAT

expansion, would also resist TZD-induced BMAT expansion and that this would attenuate or prevent the induction of hyperadiponectinaemia.

The initial work for this study was performed at The University of Michigan, the samples were subsequently brought to The University of Edinburgh for analysis by me. Some of this analysis has been previously submitted for award of an MSc in Cardiovascular Biology. Therefore, the following figures comprise data generated as part of this PhD thesis: Figures 2 – 5 and 8. Data in Figure 1 was generated by researchers at the University of Michigan and data in Figures 6 and 7 was submitted as part of the above mentioned MSc.

frontiers in Endocrinology

ORIGINAL RESEARCH
published: 21 September 2016
doi: 10.3389/fendo.2016.00128

Increased Circulating Adiponectin in Response to Thiazolidinediones: Investigating the Role of Bone Marrow Adipose Tissue

*Richard J. Sulston[1], Brian S. Learman[2], Bofeng Zhang[2], Erica L. Scheller[2], Sebastian D. Parlee[2], Becky R. Simon[3], Hiroyuki Mori[2], Adam J. Bree[2], Robert J. Wallace[4], Venkatesh Krishnan[5], Ormond A. MacDougald[2,3,6] and William P. Cawthorn[1,2,5]**

[1] University/British Heart Foundation Centre for Cardiovascular Science, The Queen's Medical Research Institute, University of Edinburgh, Edinburgh, UK, [2] Department of Molecular & Integrative Physiology, University of Michigan Medical School, Ann Arbor, MI, USA, [3] Program in Cellular and Molecular Biology, University of Michigan Medical School, Ann Arbor, MI, USA, [4] Department of Orthopaedics, University of Edinburgh, Edinburgh, UK, [5] Musculoskeletal Research, Lilly Research Laboratories, Indianapolis, IN, USA, [6] Department of Internal Medicine, University of Michigan Medical School, Ann Arbor, MI, USA

OPEN ACCESS

Edited by:
Basem M. Abdallah, University of Southern Denmark, Denmark

Reviewed by:
Melissa Orlandin Premaor, Universidade Federal de Santa Maria, Brazil
Jan Tuckermann, University of Ulm, Germany

***Correspondence:**
William P. Cawthorn
w.cawthorn@ed.ac.uk

Specialty section:
This article was submitted to Bone Research, a section of the journal Frontiers in Endocrinology

Received: 14 June 2016
Accepted: 05 September 2016
Published: 21 September 2016

Citation:
Sulston RJ, Learman BS, Zhang B, Scheller EL, Parlee SD, Simon BR, Mori H, Bree AJ, Wallace RJ, Krishnan V, MacDougald OA and Cawthorn WP (2016) Increased Circulating Adiponectin in Response to Thiazolidinediones: Investigating the Role of Bone Marrow Adipose Tissue. Front. Endocrinol. 7:128. doi: 10.3389/fendo.2016.00128

Background: Bone marrow adipose tissue (MAT) contributes to increased circulating adiponectin, an insulin-sensitizing hormone, during caloric restriction (CR), but whether this occurs in other contexts remains unknown. The antidiabetic thiazolidinediones (TZDs) also promote MAT expansion and hyperadiponectinemia, even without increasing adiponectin expression in white adipose tissue (WAT).

Objectives: To test the hypothesis that MAT expansion contributes to TZD-associated hyperadiponectinemia, we investigated the effects of rosiglitazone, a prototypical TZD, in wild-type (WT) or *Ocn*-Wnt10b mice. The latter resist MAT expansion during CR, leading us to postulate that they would also resist this effect of rosiglitazone.

Design: Male and female WT or *Ocn*-Wnt10b mice (C57BL/6J) were treated with or without rosiglitazone for 2, 4, or 8 weeks, up to 30 weeks of age. MAT content was assessed by osmium tetroxide staining and adipocyte marker expression. Circulating adiponectin was determined by ELISA.

Results: In WT mice, rosiglitazone caused hyperadiponectinemia and MAT expansion. Compared to WT mice, *Ocn*-Wnt10b mice had significantly less MAT in distal tibiae and sometimes in proximal tibiae; however, interpretation was complicated by the leakage of osmium tetroxide from ruptures in some tibiae, highlighting an important technical consideration for osmium-based MAT analysis. Despite decreased MAT in *Ocn*-Wnt10b mice, circulating adiponectin was generally similar between WT and *Ocn*-Wnt10b mice; however, in females receiving rosiglitazone for 4 weeks, hyperadiponectinemia was significantly blunted in *Ocn*-Wnt10b compared to WT mice. Notably, this was also the only group in which tibial adiponectin expression was lower than in WT mice, suggesting a close association between MAT adiponectin production and circulating adiponectin. However, rosiglitazone significantly increased adiponectin protein expression in WAT,

suggesting that WAT contributes to hyperadiponectinemia in this context. Finally, rosiglitazone upregulated uncoupling protein 1 in brown adipose tissue (BAT), but this protein was undetectable in tibiae, suggesting that MAT is unlikely to share thermogenic properties of BAT.

Conclusion: TZD-induced hyperadiponectinemia is closely associated with increased adiponectin production in MAT but is not prevented by the partial loss of MAT that occurs in *Ocn*-Wnt10b mice. Thus, more robust loss-of-MAT models are required for future studies to better establish MAT's elusive functions, both on an endocrine level and beyond.

Keywords: bone marrow adipose tissue, white adipose tissue, brown adipose tissue, thiazolidinedione, rosiglitazone, adiponectin, beige adipocyte, UCP1

INTRODUCTION

Adipose tissue is typically classified into two broad subtypes, white adipose tissue (WAT) and brown adipose tissue (BAT). WAT is commonly known for its role in energy storage and release and is now established as a major endocrine organ. BAT also mediates some endocrine functions but is more widely known for its ability to mediate adaptive thermogenesis (1). Through these functions, both WAT and BAT impact metabolic homeostasis; hence, the global burden of obesity and metabolic disease has motivated extensive study of these tissues (2).

In addition to WAT and BAT, adipocytes also exist in the bone marrow, and such marrow adipose tissue (MAT) has been estimated to account for over 10% of total adipose tissue mass in lean, healthy humans (3). We recently revealed that MAT characteristics are region-specific, such that MAT can be classified into two broad subtypes: regulated MAT (rMAT), which exists in more proximal skeletal sites and consists of adipocytes interspersed with hematopoietic BM; and constitutive MAT (cMAT), which exists in more distal regions (e.g., distal tibia, caudal vertebrae) and appears histologically similar to WAT, with few visible hematopoietic cells (4). These MAT subtypes also differ in their lipid composition and response to external stimuli (4). Both rMAT and cMAT appear to be developmentally and functionally distinct to WAT and BAT, and therefore MAT may represent a third general class of adipose tissue (5, 6). Despite these advances, knowledge of MAT formation and function remains relatively limited (2). However, research from others and us suggests that, like WAT, MAT is an endocrine organ that can exert local and systemic effects (3, 7).

The appreciation of WAT as an endocrine organ derives largely from the discovery in the mid-1990s of two adipocyte-derived hormones, leptin and adiponectin, each of which impacts metabolic homeostasis (8–10). These two hormones have since been mentioned in over 40,000 publications, reflecting the extensive depth of WAT research. Circulating leptin concentrations correlate directly with body fat percentage and are therefore increased in obesity. In contrast, adiponectin concentrations are decreased in obesity and insulin-resistance; hence, hypoadiponectinemia is now an established biomarker for increased risk of cardiometabolic disease. Conversely, circulating adiponectin is elevated in conditions of leanness and insulin sensitivity, such as during caloric restriction (CR) (2). This counterintuitive observation has been dubbed the "adiponectin paradox": why should circulating adiponectin increase when the amount of WAT, the presumed source of adiponectin, is decreased? Moreover, CR can cause hyperadiponectinemia without increasing expression or secretion of adiponectin from WAT (2), suggesting that other tissues contribute to this effect. Our recent research has highlighted a potential explanation for this paradox, revealing, unexpectedly, that MAT is a source of circulating adiponectin during CR (3).

Our studies into MAT and CR were motivated by the striking observation that, in contrast to WAT and BAT, MAT accumulates during CR (3, 11, 12). The biochemical phenotype of this CR-responsive MAT remains to be elucidated; however, we have since shown that these increases occur predominantly in regions of rMAT rather than cMAT (2). This phenomenon led us to investigate if MAT contributes to increased circulating adiponectin during CR. After confirming that MAT expresses and secretes adiponectin (3), we then tested if MAT accumulation is required for CR-associated hyperadiponectinemia. To do so, we used *Ocn*-Wnt10b mice, a transgenic model in which the secreted ligand, Wnt10b, is expressed in osteoblasts from the *Ocn* promoter (13). Because Wnt10b simulates osteoblastogenesis and inhibits adipogenesis, these mice have increased bone formation and decreased bone marrow volume (3, 13). We found that *Ocn*-Wnt10b mice also resist CR-associated MAT expansion, both in rMAT and cMAT (2, 3). Notably, hyperadiponectinemia during CR is also blunted in these mice, despite no differences in adiponectin expression in WAT (3). Finally, impaired MAT expansion also coincides with blunted hyperadiponectinemia in a separate mouse model of CR (14) and during CR in rabbits (12). Together, these observations suggest that MAT expansion is required for CR-induced hyperadiponectinemia, supporting the conclusion that MAT is a source of circulating adiponectin in this context.

To further investigate this endocrine function, we sought to determine if MAT also influences circulating adiponectin beyond CR. For example, increases in both MAT and circulating adiponectin occur in many other conditions, including aging, estrogen deficiency, type 1 diabetes, cancer treatment, and in response to fibroblast growth factor-21 or glucocorticoid therapy

(2). Notably, these increases also coincide during treatment with thiazolidinediones (TZDs), a class of insulin-sensitizing, antidiabetic drugs that act as agonists for the nuclear hormone receptor, peroxisome proliferator-activated receptor gamma (PPARγ) (15, 16). Binding and subsequent activation of PPARγ causes it to activate the expression of its transcriptional targets, including adiponectin and other lipid-metabolism-associated genes such as fatty acid-binding protein 4 (*Fabp4*) (17). Thus, TZDs, such as rosiglitazone, significantly increase circulating adiponectin in rodent models and human patients (18, 19). Importantly, preclinical studies suggest that such hyperadiponectinemia is required for the full insulin-sensitizing effects of TZDs (20). Despite the beneficial effects of TZDs in improving glucose tolerance, their clinical use has been restricted owing to increased risk of myocardial infarction and bone fractures (21, 22); the latter may relate to the ability of TZDs to drive MAT expansion. If so, MAT expansion may be detrimental to the clinical utility of these drugs. However, it is notable that TZDs can increase circulating adiponectin without increasing adiponectin expression in WAT (23, 24), and that some studies suggest that TZD action is independent of WAT (25). Thus, given the contribution of MAT to increased circulating adiponectin during CR, we hypothesized that MAT also contributes to TZD-induced hyperadiponectinemia. If so, MAT expansion may play a role in the beneficial insulin-sensitizing effects of TZDs.

Herein, we investigated this hypothesis by feeding wild-type (WT) and *Ocn*-Wnt10b mice a Western diet to induce obesity and glucose intolerance, followed by treatment with rosiglitazone, a prototypical TZD. We postulated that, as in CR, these mice would resist TZD-induced MAT expansion. As secondary analyses, we also investigated the contribution of WAT to TZD-mediated hyperadiponectinemia and the possibility, suggested previously (26), that MAT has BAT-like properties. Our results shed light on MAT's characteristics and highlight technical considerations that will be important for future research into MAT formation and function.

MATERIALS AND METHODS

Animals and Animal Care

Ocn-Wnt10b mice (Wnt10b) or non-transgenic controls (WT) were on a C57BL/6J background and were bred in-house, as described previously (13). The University of Michigan Committee on the Use and Care of Animals approved all animal experiments, with daily care of mice and rabbits overseen by the Unit for Laboratory Animal Medicine (ULAM).

Diets and Rosiglitazone (TZD) Treatment

Male WT ($n = 18$), male Wnt10b ($n = 22$), female WT ($n = 20$), and female Wnt10b ($n = 15$) mice were fed a standard laboratory chow diet (Research Diets, D12450B) from weaning until 10 weeks of age. From 10 to 22 weeks of age, all mice were fed a high-fat, high-sucrose Western diet (Research Diets D12079B), with the goal of promoting diet-induced obesity and glucose intolerance. The rationale for this was that, if *Ocn*-Wnt10b mice resisted hyperadiponectinemia, they might also be less responsive to the metabolic effects of TZD treatment. Thus, mice were fed a Western diet prior to TZD treatment, with the aim of allowing detection of metabolic improvements upon TZD administration. At 18 weeks of age, mice were fasted overnight; body mass and fasting glucose were then recorded and body fat, lean mass, and free fluid were measured in conscious mice using an NMR analyzer (Minispec LF90II; Bruker Optics, Billerica, MA, USA). These measurements were then used as a basis to assign mice to four evenly matched groups (with similar body mass, fat mass, and fasting glucose), with each group corresponding to a different duration of rosiglitazone (TZD) treatment. Mice were then treated with or without TZD from 22 to 30 weeks of age. TZD was administered in the diet (Research Diets D12112601) by supplementing diet D12450B with rosiglitazone at 0.175 mg/g diet; based on daily consumption of D12450B, this concentration was estimated to give a final dose per mouse of 15 mg/kg body mass per day. This approach is similar to that used in previous studies investigating rosiglitazone-induced MAT accumulation (26–28). The four experimental groups were as follows: control mice (0 weeks' TZD), which continued to receive Western diet D12079B from 22 to 30 weeks of age; 2 weeks' TZD mice, which received D12079B from 22 to 28 weeks and D12112601 from 28 to 30 weeks; 4 weeks' TZD mice, which received D12079B from 22 to 26 weeks and D12112601 from 26 to 30 weeks; and 8 weeks' TZD mice, which received D12112601 from 22 to 30 weeks. Numbers of mice per group and diet durations are described further in **Table 1**. At 29.5 weeks of age, blood glucose concentrations were recorded after an overnight fast to assess the effects of TZD treatment. At 30 weeks of age, serum was sampled, mice were humanely euthanized, and tissues were isolated for further analysis.

Blood Collection and Serum Adiponectin Analysis

Blood was sampled from the lateral tail vein of mice using Microvette CB 300 capillary collection tubes (Sarstedt, Newton,

TABLE 1 | Summary of groups for control or TZD treatment.

Weeks of TZD	Ages (weeks) fed Western diet (D12450B)	Ages (weeks) fed TZD diet (D12112601)	Group sizes for each sex and genotype
0	22–30	N/A	WT male, 5; *Ocn*-Wnt10b male, 5 WT female, 6; *Ocn*-Wnt10b female, 4
2	22–28	28–30	WT male, 3; *Ocn*-Wnt10b male, 7 WT female, 5; *Ocn*-Wnt10b female, 3
4	22–26	26–30	WT male, 5; *Ocn*-Wnt10b male, 5 WT female, 5; *Ocn*-Wnt10b female, 3
8	N/A	22–30	WT male, 5; *Ocn*-Wnt10b male, 5 WT female, 4; *Ocn*-Wnt10b female, 5

NC, USA). Blood glucose was measured using an Accu-Chek Aviva glucometer. To obtain serum, blood samples were allowed to clot on ice for 2 h before centrifuging at 3,800 RCF for 5 min at 4°C. Serum adiponectin was determined using an ELISA kit (catalog no. MRP300) from R&D Systems (Bio-Techne Ltd., Abingdon, UK) according to the manufacturer's instructions.

Osmium Tetroxide Staining and μCT Analysis

Tibiae were isolated and, after removal of external soft tissue, fixed in formalin at 4°C. Fixed tibiae were decalcified in 14% EDTA for 14 days and then washed in Sorensen's Phosphate buffer (81 mM KH_2PO_4, 19 mM $Na_2HPO_4 \cdot 7H_2O$, pH 7.4). Decalcified tibiae were stored in Sorensen's Phosphate buffer at 4°C until ready to be stained with osmium tetroxide. To do so, osmium tetroxide solution (2% w/v; Agar Scientific, UK) was diluted 1:1 in Sorensen's Phosphate buffer. Tibiae were then stained in this 1% osmium tetroxide solution for 48 h at room temperature, then washed, and stored in Sorensen's Phosphate buffer at 4°C prior to micro computed tomography (μCT) analysis.

Micro Computed Tomography Analysis

Layers of four to five stained tibiae were arranged in parallel in 1% agarose in a 30-mL universal tube and mounted in a Skyscan 1172 desktop micro CT (Bruker, Kontich, Belgium). The samples were then scanned through 360° using a step of 0.40° between exposures. A voxel resolution of 12.05 μm was obtained in the scans using the following control settings: 54 kV source voltage, 185 μA source current with an exposure time of 885 ms. A 0.5-mm aluminum filter and two-frame averaging were used to optimize the scan. After scanning, the data were reconstructed using Skyscan software NRecon v1.6.9.4 (Bruker, Kontich, Belgium). The reconstruction thresholding window was optimized to encapsulate the target image. Volumetric analysis was performed using CT Analyser v1.13.5.1 (Bruker, Kontich, Belgium).

Real-time Quantitative PCR

RNA was extracted from tissue using RNA STAT60 reagent (Tel-Test, Inc.) according to the manufacturer's instructions. Synthesis of cDNA was done using TaqMan reverse transcription reagents (Thermo Fisher Scientific) using 1 μg of RNA template per reaction, as per manufacturer's instructions. Transcript expression was then analyzed by quantitative PCR (qPCR) in 10 μL duplicate reactions using qPCRBIO SyGreen Mix (part number PB20.11; PCR Biosystems, UK) and 1–4 μL of cDNA template. Reactions were loaded into 384-well qPCR plates (part number 72.1985.202; Sarstedt, UK) and run on a Light Cycler 480 (Roche). Transcript expression was calculated based on a cDNA titration loaded on each plate and was presented relative to expression of the housekeeping gene *Ppia*. Primers for *Adipoq* and *Ppia* were described and validated previously (3).

Immunoblot Analysis

Frozen tissue was processed as described previously (12). The resulting protein lysates were separated by size using gradient (4–12%) polyacrylamide gels (BioRad). Protein was then transferred to Immobilon-FL membrane (Millipore) for 150 min at 350 mA, 4°C, using a Criterion wet-transfer system (BioRad). Post-transfer, the membranes were blocked in 5% milk for 1 h at room temperature, then immunoblotted with primary antibody in 5% bovine serum albumin overnight at 4°C. Membranes were then incubated in 1:15,000-diluted fluorescently labeled secondary antibody (LiCor) for 1 h at room temperature. Signal was detected using the LiCor Odyssey system and band intensities quantified using LiCor Image Studio Lite software. The following primary antibodies were used: rabbit anti-adiponectin antibody (Sigma, A6354-200UL) diluted 1:1,000 in 5% BSA; rabbit anti-uncoupling protein 1 (UCP1) antibody (Sigma, U6382) diluted 1:10,000 in 2.5% milk; and rabbit anti-β-actin antibody (Abcam, ab8227) diluted 1:1,000 in 5% BSA.

Data Presentation and Statistical Analysis

Data are presented as box and whisker plots overlaid with individual data points for each animal. Boxes indicate the 25th and 75th percentiles; whiskers display the range; and horizontal lines in each box represent the median. Group sizes are described in **Table 1**. Statistical analysis was done using GraphPad Prism 6 software, with significant differences assessed by two-way ANOVA using a Tukey or Sidak *post hoc* test for multiple comparisons, as appropriate. A P-value <0.05 was considered statistically significant. A significant influence of TZD treatment, across all treatment groups, is indicated by †. For multiple comparisons, asterisks (*) indicate significant differences between genotypes within each TZD group, while hash signs (#) indicate significance between TZD-treated and non-TZD-treated controls within each genotype.

RESULTS

Effects of TZD on WAT Mass and Fasting Glucose Do Not Differ between WT and *Ocn*-Wnt10b Mice

Circulating adiponectin is decreased in states of obesity and glucose intolerance (29), while TZDs modulate both fat mass and glucose homeostasis. Therefore, after treating WT and *Ocn*-Wnt10b mice with or without rosiglitazone for 2, 4, or 8 weeks, we first assessed body mass, fat mass, and fasting glucose, primarily as readouts of TZD action but also as parameters that might influence circulating adiponectin. While body masses of female or male mice did not differ with TZD treatment (**Figures 1A,C**), across both genotypes, TZD was associated with significant loss of gonadal WAT (gWAT), a visceral adipose depot, in both females ($P = 0.027$) and males ($P = 0.006$) (**Figures 1B,D**). Conversely, the mass of inguinal WAT (iWAT), a subcutaneous depot, significantly increased with TZD treatment in males ($P = 0.002$) (**Figure 1D**). Analysis of fasting glucose revealed no effects of TZD in female mice (**Figure 1E**), whereas TZD significantly decreased fasting glucose across WT and *Ocn*-Wnt10b males (**Figure 1F**). These findings are consistent with previous studies demonstrating that rosiglitazone decreases gWAT mass (26, 27), increases subcutaneous WAT (30), and ameliorates hyperglycemia (16);

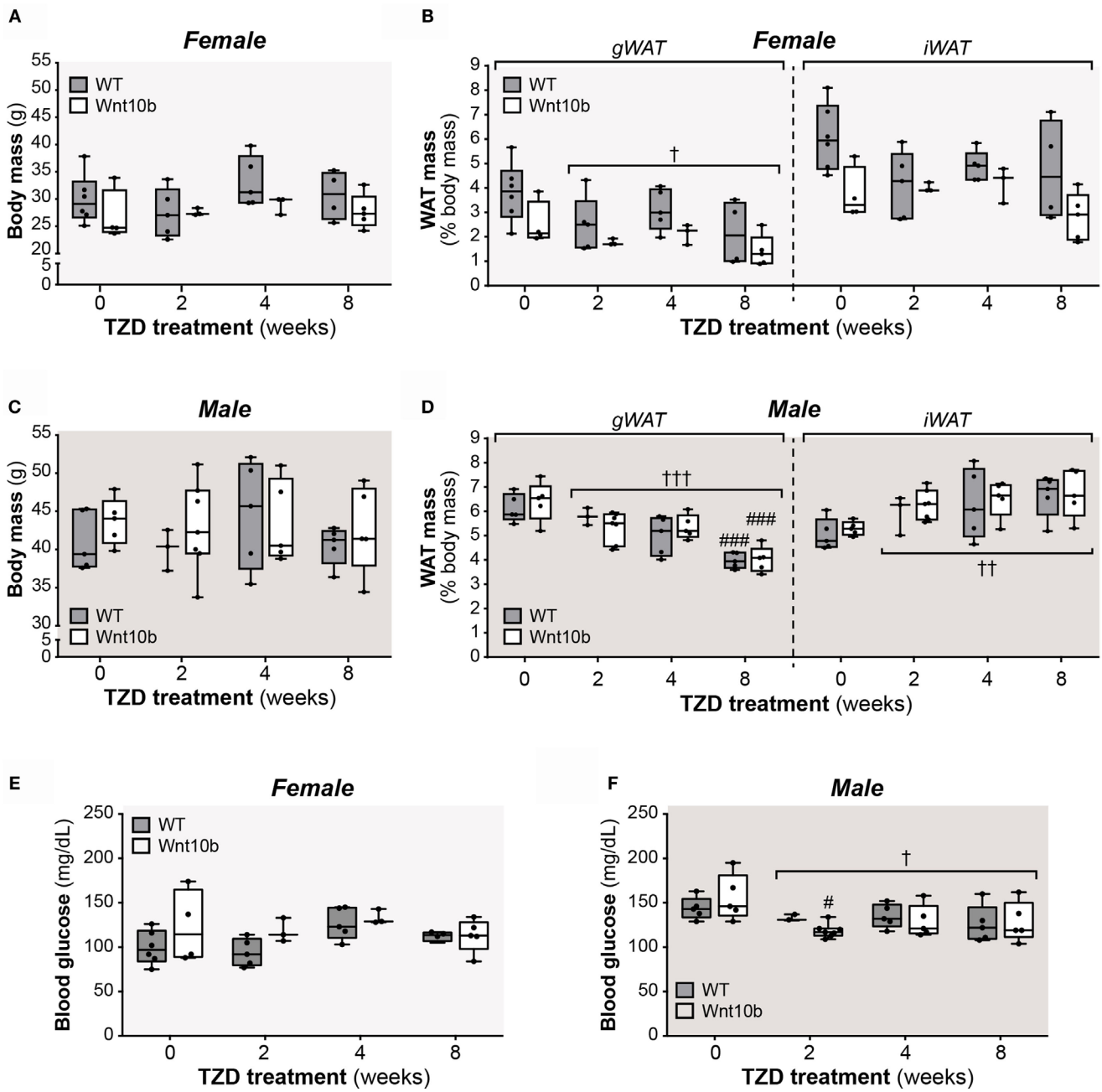

FIGURE 1 | **Effects of rosiglitazone on body mass, fat mass, and fasting glucose**. Male and female mice were fed a control Western diet only or a Western diet supplemented with rosiglitazone for 2, 4, or 8 weeks, as described in Section "Materials and Methods." **(A,C)** Body masses of females **(A)** and males **(C)** were recorded prior to necropsy at 30 weeks of age. **(B,D)** Masses of iWAT and gWAT were recorded at necropsy for female **(B)** and male mice **(D)** and are shown as percentage of total body mass. **(E,F)** Fasting blood glucose, as recorded at 29.5 weeks of age. For **(A–F)**, a significant influence of TZD treatment, across all treatment groups, is indicated by † ($P < 0.05$), †† ($P < 0.01$) or ††† ($P < 0.001$). Within each genotype, significant differences between untreated controls (0-week TZD) and individual durations of TZD treatment are indicated by ### ($P < 0.001$). Within each TZD treatment group (0-, 2-, 4-, or 8-week TZD), there were no statistically significant differences between WT and *Ocn*-Wnt10b mice.

however, it is unclear why rosiglitazone influenced iWAT mass and fasting glucose in males but not in females. In contrast to these effects of rosiglitazone, body mass, WAT mass, or fasting glucose did not differ between WT and *Ocn*-Wnt10b mice within each TZD treatment group (**Figures 1A–F**). Thus, differences in peripheral adiposity or glucose homeostasis, which can influence circulating adiponectin, did not occur between WT and *Ocn*-Wnt10b mice.

TZD Increases rMAT and cMAT Volume in WT Mice, and These Effects Are Partially Blunted in *Ocn*-Wnt10b Mice

Having characterized these peripheral metabolic parameters, we next investigated the impact of TZD on MAT expansion and whether this differs between WT and *Ocn*-Wnt10b mice. To do so, we first used an approach based on staining tibiae with osmium tetroxide, which covalently binds to unsaturated lipids within bone marrow and thereby acts as a strong contrast agent for MAT detection by μCT (31). As shown in **Figure 2A**, osmium staining in the proximal diaphysis, corresponding to rMAT, was markedly increased in females of both genotypes following 4- or 8-week TZD treatment. Statistical analyses confirmed that, across all groups of females, TZD significantly influenced the volume of rMAT, as well as that of cMAT and total MAT ($P < 0.0001$ for each) (**Figures 2B,C**). Multiple comparisons were then made to assess the effect of each duration of TZD treatment in each genotype of mice, relative to untreated controls. This revealed that, in female WT mice, TZD treatment for 4 or 8 weeks significantly increased rMAT volume in proximal tibiae and cMAT volume in distal tibiae (**Figures 2A,B**). Thus, total tibial MAT volume was also significantly increased by 4- or 8-week TZD in WT females (**Figure 2C**). Similar effects of TZD were also observed in *Ocn*-Wnt10b females (**Figures 2A–C**), and rMAT volume did not significantly differ between genotypes (**Figure 2B**). However, cMAT volume was markedly lower in *Ocn*-Wnt10b females within each TZD treatment group (**Figure 2B**). Total tibial MAT volume was also significantly decreased in *Ocn*-Wnt10b compared to WT females following 8 weeks' TZD (**Figure 2C**).

Compared to the female mice, osmium staining was less pronounced in the rMAT of TZD-treated males (**Figure 2D**). Nevertheless, statistical analysis across all groups of males revealed a significant influence of TZD on the volumes of rMAT ($P = 0.0015$), cMAT ($P = 0.0006$), and total MAT ($P = 0.0003$) (**Figures 2E,F**). Multiple comparisons further revealed that, in WT males, treatment with TZD for 8 weeks, but not shorter durations, significantly increased volumes of rMAT, cMAT, and total MAT (**Figures 2E,F**). This also occurred for cMAT and total MAT, but not rMAT, in *Ocn*-Wnt10b males (**Figures 2E,F**). As found for female mice, male *Ocn*-Wnt10b mice had significantly decreased cMAT volume compared to their WT counterparts (**Figure 2E**), and this also occurred for total MAT volume in the 0-, 4-, and 8-week TZD groups (**Figure 2F**).

Cortical Bone Ruptures Significantly Decrease Detectable rMAT Volume

The above observations suggest that *Ocn*-Wnt10b males and females partially resist TZD-induced MAT expansion, predominantly as a result of a lower cMAT volume than WT mice. Indeed, rMAT volume did not differ between genotypes in any of the TZD treatment groups. However, when analyzing the μCT scans, we noticed that the decalcified cortical bone had ruptured in tibiae from all male mice and in a subset of females. The ruptures always occurred in proximal tibial diaphysis, as indicated by representative scans of non-ruptured (intact) and ruptured tibiae (**Figure 3A**). Cross sections show that ruptures allowed escape of the bone marrow, resulting in decreased osmium staining compared to intact tibiae (**Figure 3A**). This loss of signal suggests that the ruptures might have confounded measurement of MAT volume. To address this, we quantified the volumes of cMAT, rMAT, and total MAT in female tibiae, comparing bones from non-TZD-treated mice (all of which were intact) with intact or ruptured bones from TZD-treated mice. The volume of cMAT did not differ between intact and ruptured bones (**Figure 3B**), indicating that these ruptures did not affect detection of cMAT in the distal tibia. However, in TZD-treated WT mice, the detectable volume of rMAT and total MAT was significantly lower in ruptured compared to intact bones (**Figure 3B**). Indeed, in both WT and *Ocn*-Wnt10b mice, TZD-induced expansion of rMAT and total MAT was strongly significant for intact bones, but not when ruptures were present (**Figure 3B**). This impaired rMAT detection likely explains why TZD-induced rMAT expansion was less marked in male than in female mice (**Figure 2B** vs. **Figure 2E**), because all male bones were ruptured. Importantly, for intact tibiae, TZD-induced expansion of rMAT and total MAT was significantly blunted in *Ocn*-Wnt10b compared to WT mice (**Figure 3B**). This suggests that, in addition to decreased cMAT (**Figures 2B,E**), *Ocn*-Wnt10b mice are at least mildly resistant to rMAT expansion during TZD treatment.

Adipocyte Transcript Expression in Tibiae Confirms TZD-Induced MAT Expansion

Given the confounding influence of these bone ruptures, we next pursued other approaches to further assess tibial MAT content. MAT expansion during CR or rosiglitazone treatment has previously been monitored by qPCR analysis of adipocyte marker expression in intact bones, including transcripts for adiponectin (*Adipoq*) and fatty acid-binding protein 4 (*Fabp4*) (3, 26). Thus, we next used qPCR to assess *Adipoq* and *Fabp4* expression in whole tibiae. As shown in **Figures 4A–D**, across all groups of female or males, expression of *Adipoq* and *Fabp4* was significantly affected by TZD treatment ($P < 0.0001$ for each). Multiple comparisons confirmed that 4- or 8-week TZD significantly increased *Adipoq* in WT males and females (**Figures 4A,C**) and *Fabp4* in males and females of each genotype (**Figures 4B,D**). TZD treatment for 2 weeks was also associated with increased *Adipoq* in *Ocn*-Wnt10b males (**Figure 4C**); increased *Fabp4* in WT females (**Figure 4B**); and increased *Fabp4* in males of each genotype (**Figure 4D**). Transcript expression within each TZD treatment group generally did not differ between WT and *Ocn*-Wnt10b mice, with the exception of decreased *Adipoq* in 4-week TZD females (**Figure 4A**) and decreased *Fabp4* in 8-week TZD males (**Figure 4D**). However, two-way ANOVA revealed that genotype significantly influenced *Fabp4* in females ($P = 0.0184$) and males ($P = 0.0339$), while there was a significant genotype–TZD interaction that influenced *Adipoq* expression in females ($P = 0.0193$) and males ($P = 0.0297$).

Collectively, these results suggest that TZD increases tibial adipocyte content and that there is some level of resistance to this effect in *Ocn*-Wnt10b mice. Thus, together with the osmium

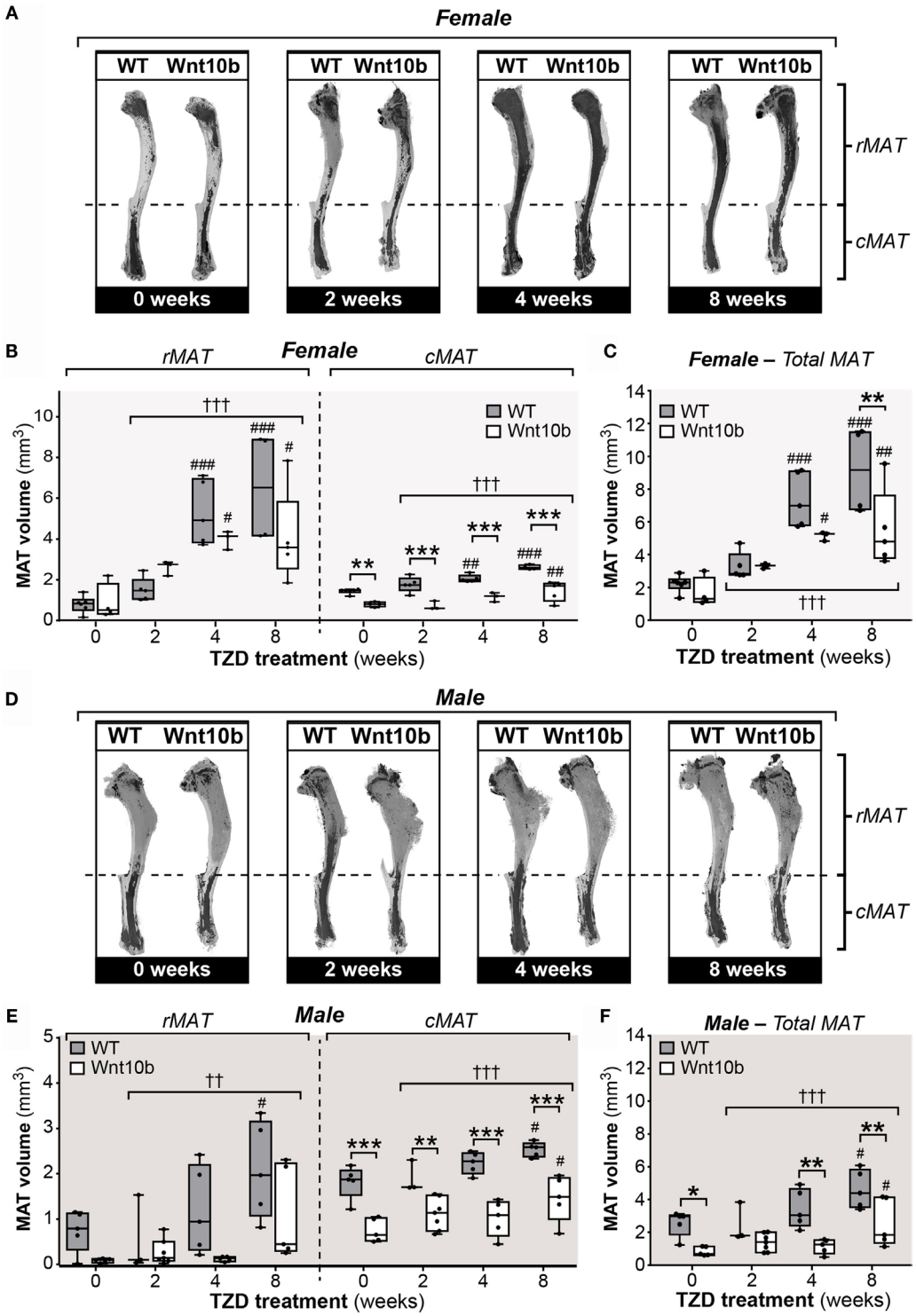

FIGURE 2 | **Rosiglitazone increases rMAT and cMAT volume in WT mice and cMAT expansion is blunted in *Ocn*-Wnt10b mice**. Male and female tibiae were dissected at necropsy. For each mouse, one tibia was decalcified in EDTA, stained with 1% osmium tetroxide, and analyzed by μCT scanning, as described in Section "Materials and Methods." **(A,D)** Representative μCT scans of stained tibiae from female **(A)** and male mice **(D)**. The dashed line indicates the tibia–fibula junction as the boundary between rMAT and cMAT. **(B,C,E,F)** For female **(B,C)** and male mice **(E,F)**, μCT scans were used to determine the volumes of rMAT (proximal to tibia–fibula junction), cMAT (distal to tibia–fibula junction), and total MAT (whole tibia), as indicated. In **(B,E)**, volumes of rMAT and cMAT are presented on the same *y*-axis scale. A significant influence of TZD treatment, across all treatment groups, is indicated by † ($P < 0.05$), †† ($P < 0.01$) or ††† ($P < 0.001$). Within each genotype, significant differences between TZD-treated mice and untreated controls are indicated by # ($P < 0.05$), ## ($P < 0.01$) or ### ($P < 0.001$). Within each TZD treatment group, statistically significant differences between WT and *Ocn*-Wnt10b mice are indicated by * ($P < 0.05$), ** ($P < 0.01$), or *** ($P < 0.001$).

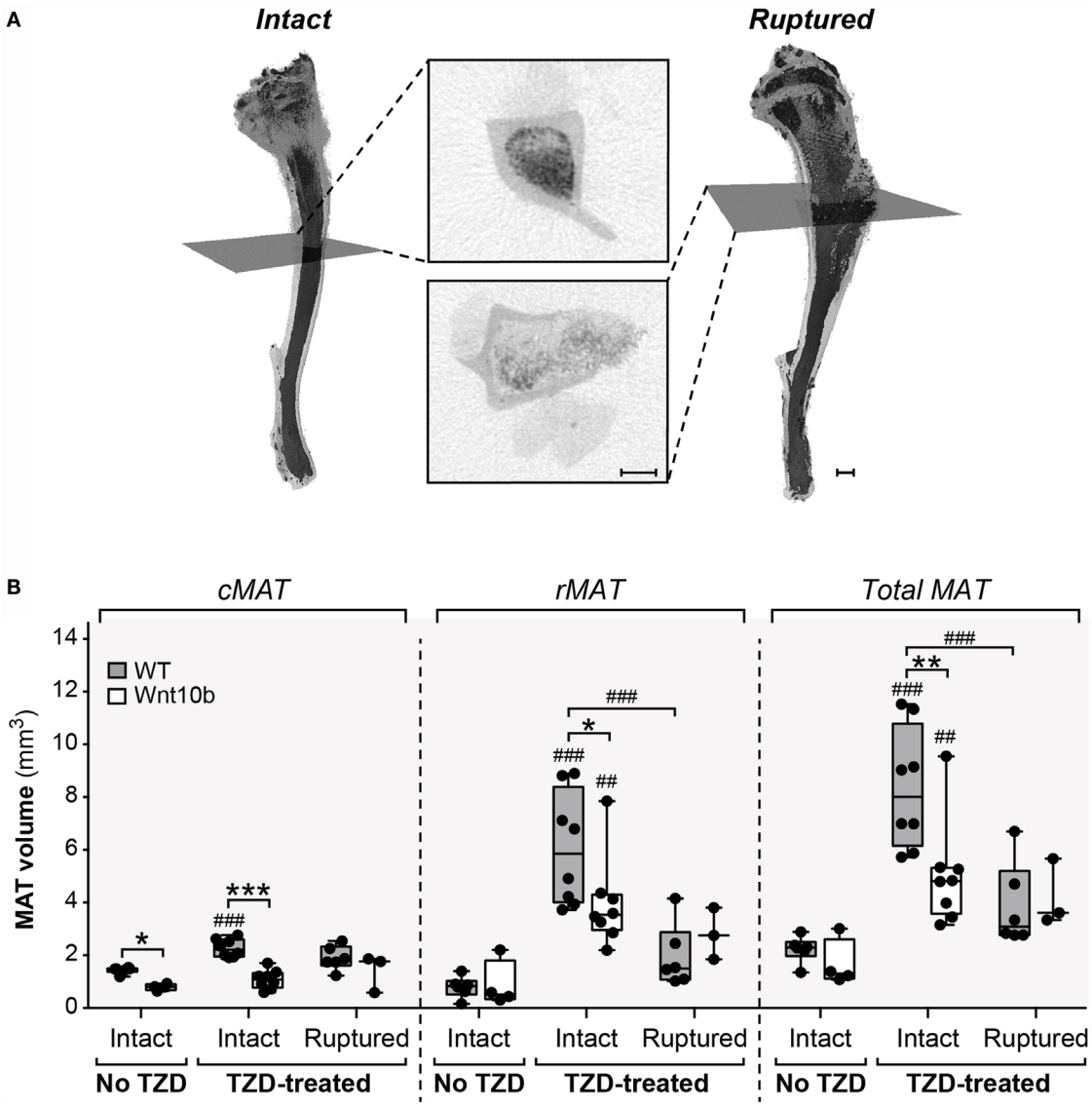

FIGURE 3 | **Cortical bone ruptures significantly decrease detectable rMAT volume**. All male and some female tibiae had ruptured cortical bone near the proximal end, causing a large reduction in signal. **(A)** Representative 3D models of intact (non-ruptured) and ruptured tibiae from 8-week-TZD-treated females, with cross-sectional images showing loss of MAT signal (dark regions within bone marrow cavity). Gray squares across the 3D models indicate the slices from which cross-sectional images are taken. Scale bars = 500 μm. **(B)** Tibiae from female WT or *Ocn*-Wnt10b mice were categorized into bones from mice untreated with TZD, all of which were intact; intact bones from TZD-treated mice; and ruptured bones from TZD-treated mice. The volume of cMAT, rMAT, and total MAT in these bones was determined from μCT scans. Statistically significant differences between untreated (intact), TZD-treated (intact), and TZD-treated (ruptured) samples are indicated by ## ($P < 0.01$) or ### ($P < 0.001$). Within each group, statistically significant differences between WT and *Ocn*-Wnt10b mice are indicated by * ($P < 0.05$), ** ($P < 0.01$), or *** ($P < 0.001$).

tetroxide analyses of MAT volume (**Figures 2** and **3**), it seems likely that *Ocn*-Wnt10b mice partially resist TZD-induced MAT expansion, but this is not prevented entirely.

TZD Induces Hyperadiponectinemia to a Similar Extent in WT and *Ocn*-Wnt10b Mice

Given this mild resistance of *Ocn*-Wnt10b mice to MAT expansion, we next investigated if TZD-induced hyperadiponectinemia was altered in these mice. To do so, we used an ELISA to measure serum adiponectin concentrations. Across both genotypes and all TZD groups, treatment with TZD was associated with significantly increased circulating adiponectin ($P < 0.0001$ for males or females) (**Figure 5**). Genotypic differences were not detected in males; however, in females, there was a significant influence of genotype ($P = 0.0466$) and a significant interaction between genotype and TZD treatment ($P = 0.0248$), indicating that effects of TZD differ between WT and *Ocn*-Wnt10b females. Consistent with this, multiple comparisons showed significantly

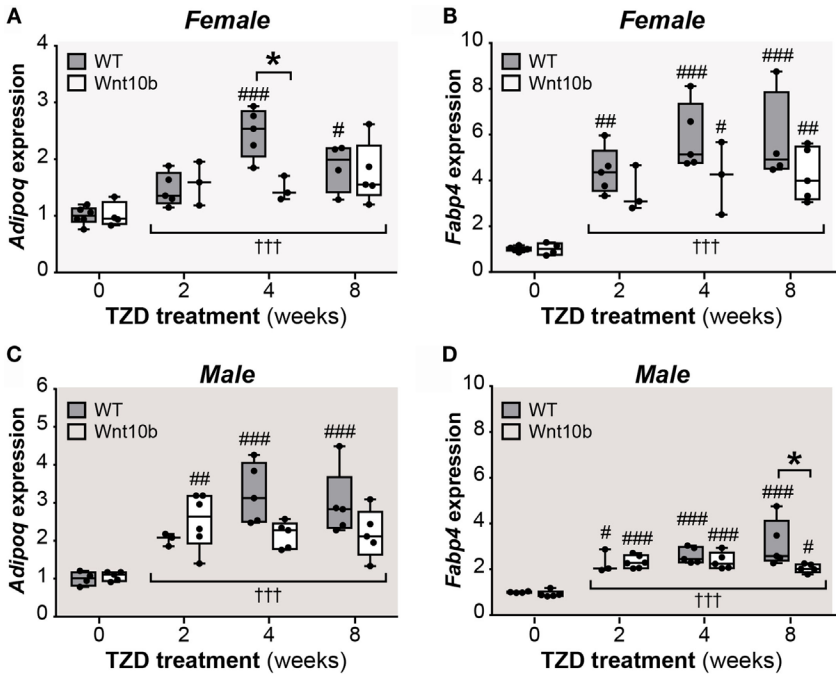

FIGURE 4 | TZD increases adipocyte marker expression in tibiae, suggesting MAT expansion. Male and female tibiae were dissected at necropsy, and total RNA was isolated from one tibia of each mouse. Expression of *Adipoq* **(A,C)** and *Fabp4* transcripts **(B,D)** in female and male mice was determined by qPCR and is presented normalized *Ppia* mRNA expression. Statistical significance is presented, as described in **Figure 2**, for the influence of TZD across all groups, and for differences between TZD-treated and untreated mice (within each genotype) or WT and *Ocn*-Wnt10b mice (within each TZD group).

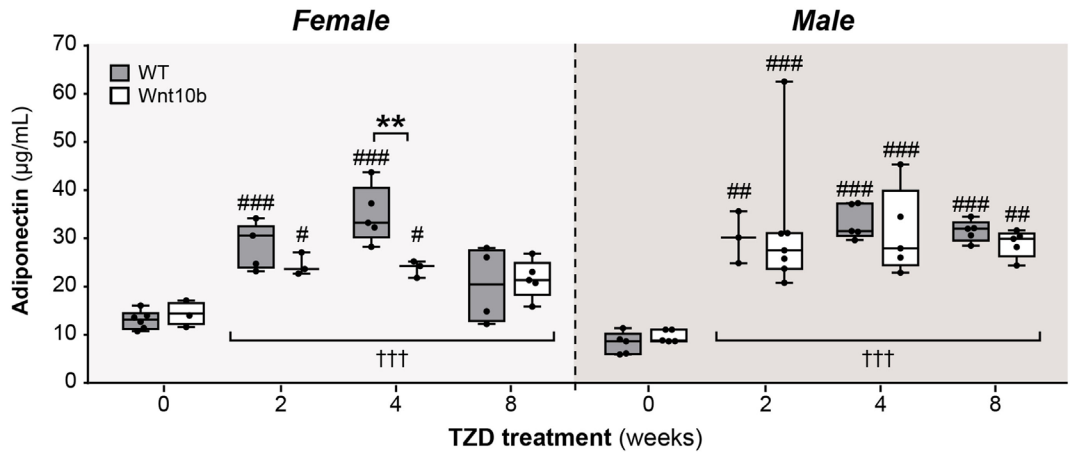

FIGURE 5 | TZD induces hyperadiponectinemia to a similar extent in WT and *Ocn*-Wnt10b mice. Serum was isolated from mice at 30 weeks of age and ELISA used to determine concentrations of total adiponectin in female and male mice, as indicated. For each sex, statistical significance for the influence of TZD across all groups, and for differences between TZD-treated and untreated mice (within each genotype) or WT and *Ocn*-Wnt10b mice (within each TZD group), are presented as described for **Figure 2**.

decreased circulating adiponectin in *Ocn*-Wnt10b compared to WT females following 4 weeks' TZD (**Figure 5**). Thus, while TZD-induced hyperadiponectinemia was similar between WT and *Ocn*-Wnt10b males, this effect of TZD was mildly blunted in female *Ocn*-Wnt10b mice.

TZD Increases Adiponectin Protein Expression in WAT

The above observations demonstrate that, despite having significantly decreased cMAT and being partially resistant to TZD-induced rMAT expansion, *Ocn*-Wnt10b mice undergo

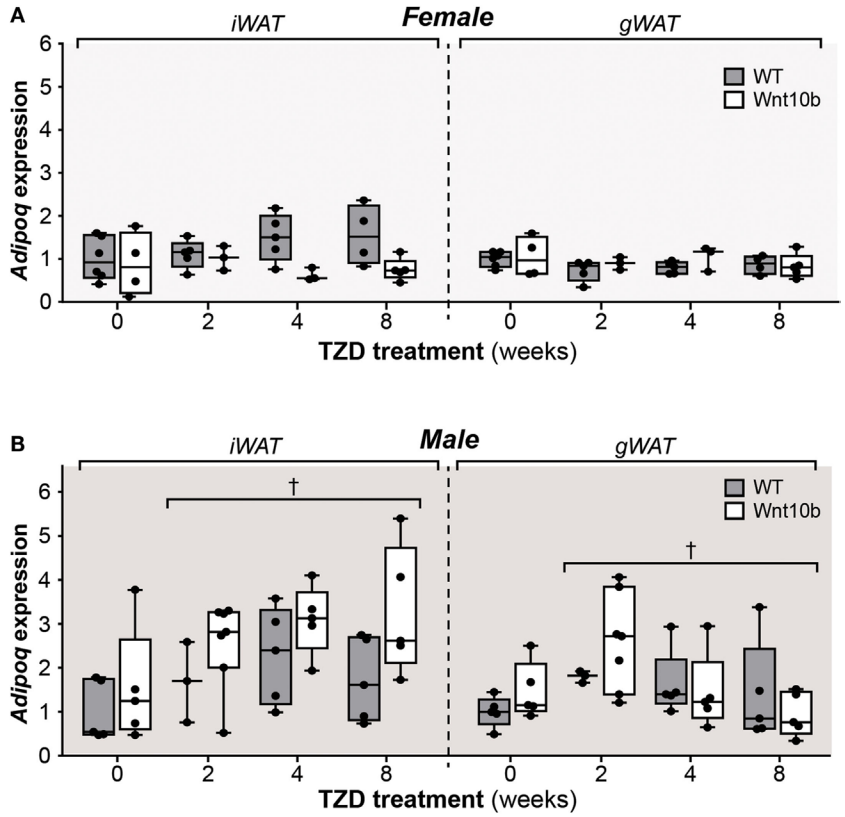

FIGURE 6 | **Rosiglitazone treatment or Wnt10b transgene expression does not alter adiponectin transcript expression in WAT**. At necropsy, iWAT and gWAT were dissected, and total RNA was isolated from portions of each tissue. Expression of *Adipoq* in female **(A)** and male mice **(B)** was determined by qPCR and is presented normalized *Ppia* mRNA expression. Across all groups, statistically significant effects of TZD are presented as described for **Figure 2**, while significant effects of genotype are described in the text. There were no statistically significant differences between TZD-treated and untreated mice (within each genotype) or between WT and *Ocn*-Wnt10b mice (within each TZD group), as determined by two-way ANOVA.

hyperadiponectinemia to a similar extent to their WT counterparts. Thus, factors beyond MAT might have a greater influence over TZD-induced hyperadiponectinemia. To address this possibility, we next investigated the effects of TZD and genotype on adiponectin expression in WAT. In WT and *Ocn*-Wnt10b females, TZD did not influence *Adipoq* expression in iWAT or gWAT, either when comparing individual treatment durations or when effects were assessed across all groups (**Figure 6A**). However, in female iWAT, *Adipoq* transcripts varied significantly by genotype ($P = 0.0095$), with expression diverging as TZD duration increased (**Figure 6A**). Given that Wnt10b transgene expression is restricted to osteoblasts, this genotypic difference in WAT was unexpected. Across all groups of males, TZD treatment had a minor influence on *Adipoq* transcript levels in both iWAT and gWAT ($P = 0.0269$ and $P = 0.0461$, respectively), although multiple comparisons found no significant effects of TZD between individual treatment groups (**Figure 6B**). As for females, male iWAT also exhibited genotypic variation ($P = 0.0096$), although in this case *Adipoq* expression tended to be greater in *Ocn*-Wnt10b than in WT mice (**Figure 6B**).

These findings show that WAT *Adipoq* expression is influenced only modestly by TZD, in contrast to the marked TZD-mediated increases in circulating adiponectin (**Figure 5**). Indeed, our above observations in female mice are consistent with previous reports demonstrating that TZDs can increase circulating adiponectin without increasing *Adipoq* expression in WAT (23, 24). However, other studies have reported a disparity between adiponectin expression at the transcript and protein level (32, 33). Therefore, we next used fluorescence-based immunoblotting to detect and quantify adiponectin protein expression. As shown in **Figure 7A**, across all groups of female mice, there was a significant influence of TZD on adiponectin protein expression in iWAT and gWAT ($P < 0.0001$ for both), with adiponectin typically increased in WAT of TZD-treated mice compared to untreated controls. Multiple comparisons further confirmed that, for females of each genotype, TZD treatment for 2 or 8 weeks significantly increased adiponectin protein in gWAT or iWAT, respectively (**Figure 7A**). As for females, across all groups of male mice, TZD had a significant influence on adiponectin protein in iWAT ($P = 0.004$) and gWAT ($P = 0.0004$) (**Figure 7B**). Based on multiple comparisons, adiponectin was significantly elevated in iWAT and gWAT of WT males after 2 weeks of TZD, and in gWAT of *Ocn*-Wnt10b males after 2 or 4 weeks of TZD (**Figure 7B**). These results demonstrate that rosiglitazone significantly increases expression

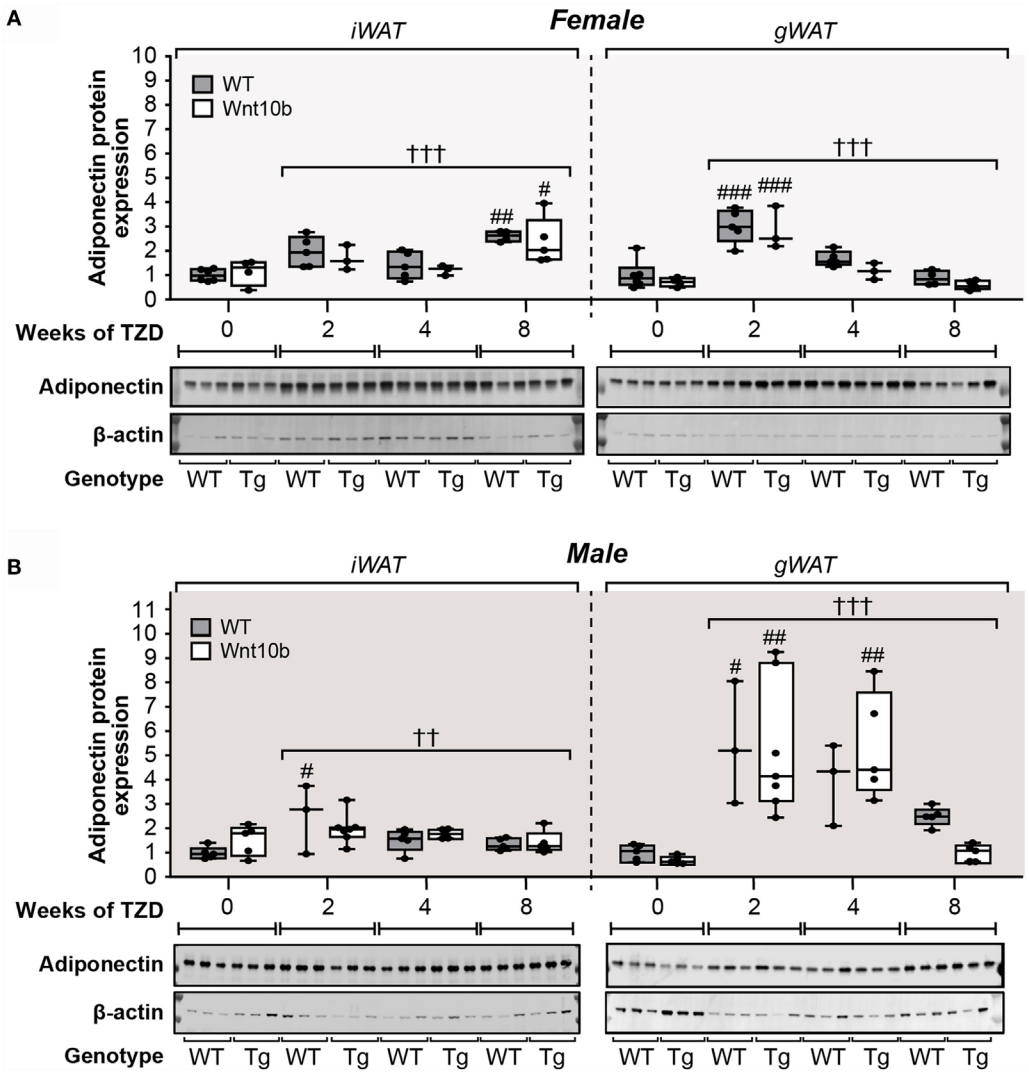

FIGURE 7 | **Rosiglitazone increases adiponectin protein expression in WAT in a depot- and sex-specific manner**. At necropsy, iWAT and gWAT were dissected, and total protein was isolated from portions of each tissue. Lysates were separated by SDS-PAGE and expression of adiponectin protein determined by immunoblotting; β-actin expression was analyzed as a loading control. Immunoblots shown in **(A,B)** are representative of three mice per group. Samples from *Ocn*-Wnt10b mice are labeled "Tg." Band intensities from these blots and further blots of the remaining samples were quantified using Image Studio Lite software. Adiponectin expression was then normalized to expression of β-actin for **(A)** Males and **(B)** Females, with representative blots shown beneath. For each sex, statistically significant differences between TZD-treated and untreated mice (within each genotype) or between WT and *Ocn*-Wnt10b mice (within each TZD group) are presented as described for **Figure 2**.

of adiponectin protein in WAT of female and male mice. Thus, it seems likely that, with this regimen of rosiglitazone treatment, WAT makes at least a partial contribution to TZD-induced hyperadiponectinemia.

TZD Induces UCP1 Protein Expression in BAT but Not in WAT or Tibiae

While these studies focused on the relationship between MAT and adiponectin, they also provided the opportunity to assess other properties of MAT; indeed, it remains unclear to what extent MAT's characteristics overlap with those of WAT and BAT. The key function of BAT is to mediate adaptive thermogenesis *via* uncoupled respiration, which is dependent on expression of uncoupling protein 1 (UCP1). TZDs dose-dependently increase UCP1 protein and *Ucp1* transcripts in BAT and can upregulate *Ucp1* in WAT and whole tibiae (26, 34). Based on the latter, it has been suggested that MAT may have BAT-like characteristics (26). However, others have argued that elevated *Ucp1* expression alone, without assessment of UCP1 protein, is insufficient evidence for a tissue's thermogenic capacity (35). Indeed, the relative protein expression of UCP1 between MAT and BAT remains to be firmly established. Thus, to further study the BAT-like properties of MAT, we next analyzed UCP1 expression in BAT, WAT, and tibiae, both at the transcript and protein level.

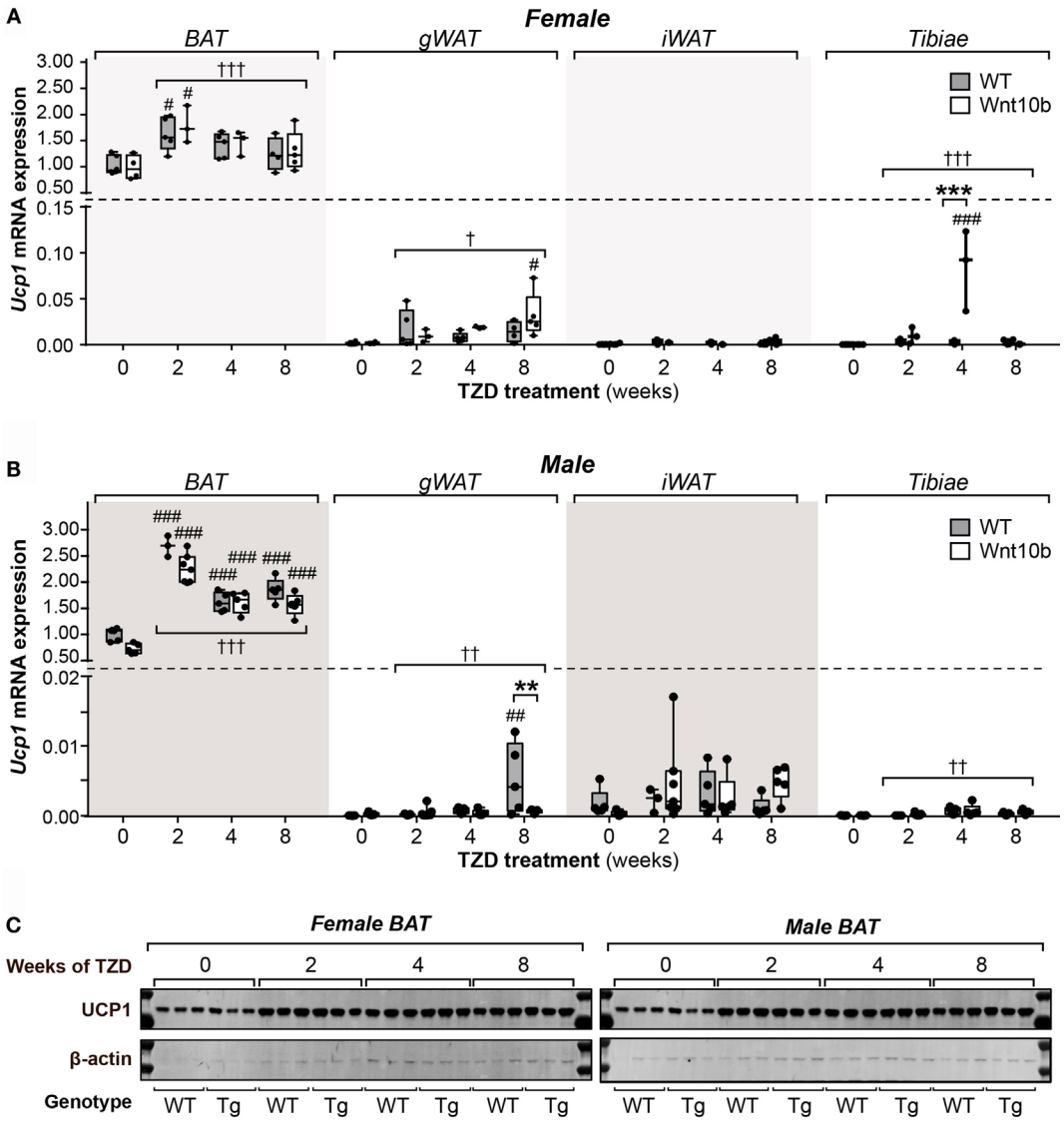

FIGURE 8 | Rosiglitazone increases UCP1 mRNA and protein in BAT not in WAT or tibiae. Total RNA and protein were isolated from interscapular BAT, gWAT, iWAT, and whole tibiae. **(A,B)** *Ucp1* transcript expression in each tissue of female **(A)** and male mice **(B)** was quantified by qPCR and normalized to expression of *Ppia* mRNA. In each tissue, statistically significant differences between TZD-treated and untreated mice (within each genotype) or between WT and *Ocn*-Wnt10b mice (within each TZD group) were determined by two-way ANOVA and are presented as described for **Figure 2**. **(C)** Protein lysates from BAT were separated by SDS-PAGE and expression of UCP1 protein determined by immunoblotting; β-actin expression was analyzed as a loading control. Immunoblots are representative of three mice per group. Samples from *Ocn*-Wnt10b mice are labeled "Tg." UCP1 protein could not be detected in gWAT, iWAT, or tibiae (data not shown).

As shown in **Figures 8A,B**, across all groups of female or male mice, TZD strongly influenced *Ucp1* expression in BAT (females, $P = 0.0002$; males, $P < 0.0001$). Multiple comparisons further confirmed that, relative to untreated controls, each duration of TZD significantly increased BAT *Ucp1* in males of each genotype (**Figure 8B**), while this also occurred for females with 2 weeks' TZD treatment (**Figure 8A**). Across-group effects of TZD were also detected in female gWAT ($P = 0.014$), female tibiae ($P < 0.0001$), male gWAT ($P = 0.0051$), and male tibiae ($P = 0.0017$), wherein TZD-treated groups typically had greater *Ucp1* expression than untreated controls (**Figures 8A,B**). Analysis of genotypic differences *via* multiple comparisons confirmed that, relative to untreated mice, *Ucp1* was significantly elevated in *Ocn*-Wnt10b female tibiae or gWAT after 4 or 8 weeks' TZD, respectively, and in WT male gWAT, after 8 weeks' TZD (**Figures 8A,B**). Each of these groups also had significantly greater *Ucp1* expression than their untreated WT or *Ocn*-Wnt10b counterparts, respectively; however, such genotypic differences were uncommon, and genotype generally did not influence *Ucp1* expression in any of the tissues analyzed.

These data demonstrate that rosiglitazone increases *Ucp1* expression in BAT, gWAT, and tibiae, consistent with results in previous studies (26, 34). However, relative to expression in BAT, *Ucp1* expression in untreated mice was over 500-fold lower in gWAT, 1,500-fold lower in iWAT, and 10,000-fold lower in tibiae (**Figures 8A,B**). Thus, even with TZD treatment, *Ucp1* expression in these tissues is negligible, raising questions over its functional relevance. To further address this, we next analyzed UCP1 expression at the protein level. As shown in **Figure 8C**, in females and males of either genotype, TZD robustly increased UCP1 expression in BAT; however, in gWAT, iWAT, or whole tibiae, we could not detect UCP1 protein expression (data not shown). Together, these observations suggest that MAT is unlikely to possess the thermogenic properties of BAT.

DISCUSSION

Herein, we pursued studies in *Ocn*-Wnt10b mice to investigate the hypothesis that MAT expansion contributes to TZD-induced hyperadiponectinemia. We found that, regardless of TZD treatment, *Ocn*-Wnt10b mice have significantly less cMAT than WT mice and likely resist TZD-induced rMAT accumulation. Despite this loss of cMAT and mild resistance to rMAT expansion, circulating adiponectin is generally similar between WT and *Ocn*-Wnt10b mice. Moreover, we found that TZD significantly increases adiponectin protein expression in WAT. Together, these findings suggest that WAT, rather than MAT, is the key mediator of TZD-induced hyperadiponectinemia, at least under these conditions of TZD treatment. However, as discussed in Section "Contribution of MAT and WAT to TZD-Induced Hyperadiponectinemia," further consideration of these findings suggests that MAT makes at least some contribution to TZD-induced hyperadiponectinemia. As a secondary aim, we also addressed the hypothesis that MAT has BAT-like properties. We found that, in contrast to BAT, UCP1 protein is undetectable in tibiae, suggesting that MAT is unlikely to have the thermogenic capacity of BAT.

As further discussed below, these findings shed new light on the function of MAT and have implications worth considering for future MAT research.

Contribution of MAT and WAT to TZD-Induced Hyperadiponectinemia

We previously identified MAT as a source of increased circulating adiponectin during CR, a conclusion based, in part, on the finding that *Ocn*-Wnt10b mice resist both CR-associated MAT expansion and hyperadiponectinemia (2, 3).

Herein, we find that, regardless of TZD treatment, cMAT volume is significantly lower in *Ocn*-Wnt10b than in WT mice. Unfortunately, tibial ruptures confounded measurement of rMAT volume; however, analysis of intact tibiae, without ruptured samples, suggests strongly that *Ocn*-Wnt10b mice also partially resist rMAT accumulation in response to TZD treatment. Despite this loss of cMAT and mild resistance to rMAT expansion, circulating adiponectin is generally similar between WT and *Ocn*-Wnt10b mice. Superficially, this suggests that MAT expansion *per se* does not contribute to hyperadiponectinemia under these TZD treatment conditions. However, this conclusion is less certain when several other key factors are taken into account.

One such factor is the likely contribution of WAT. Unlike during CR, adiponectin protein expression in WAT is increased under these conditions of TZD treatment, which may override any effects of suppressed MAT expansion. These increases are more pronounced for adiponectin protein than for *Adipoq* transcripts, with TZD affecting the *Adipoq* transcripts only in male WAT (**Figure 6**). These findings echo previous reports of sex-specific differences in WAT adiponectin expression, and of a disconnect between adiponectin expression at the transcript and protein level (32, 33). Notably, these effects on WAT are inconsistent with the finding that TZDs can increase circulating adiponectin without increasing adiponectin expression in WAT (23, 24). This disparity is likely a result of the higher dose of rosiglitazone used in our study. Indeed, WAT adiponectin expression is unaltered by lower TZD doses (24, 36) but significantly increased at higher rosiglitazone concentrations (18). Thus, as discussed further below ("Implications of TZD Dose on the Capacity of *Ocn*-Wnt10b Mice to Resist MAT Expansion and Hyperadiponectinemia"), a lower dose of rosiglitazone would likely be required if we were to further investigate the contribution of MAT to TZD-associated hyperadiponectinemia.

Considering these findings, it seems likely that WAT makes at least some contribution to hyperadiponectinemia under these conditions of rosiglitazone treatment. However, the effect of TZD on WAT adiponectin expression (**Figures 6** and **7**) is far less consistent and pronounced than that which occurs for circulating adiponectin concentrations (**Figure 5**). In contrast, these changes in circulating adiponectin are closely reflected by the increases in tibial adiponectin expression (**Figure 4**). For example, when comparing *Ocn*-Wnt10b and WT mice, circulating adiponectin is lower only in the 4-week TZD females (**Figure 5**); hence, it is striking that this is also the only group in which tibial adiponectin expression is lower in *Ocn*-Wnt10b mice (**Figure 4A**). Together, these observations show that circulating adiponectin is closely associated with tibial adiponectin expression and less tightly associated with gross changes in rMAT and cMAT volume. This underscores the importance of analyzing MAT through multiple approaches, including transcriptional markers, rather than focusing solely on MAT volume *via* osmium tetroxide staining. Perhaps, more importantly, this close association suggests that adiponectin production from MAT contributes, at least in part, to TZD-induced hyperadiponectinemia.

Implications of TZD Dose on the Capacity of *Ocn*-Wnt10b Mice to Resist MAT Expansion and Hyperadiponectinemia

Previous studies have used a wide range of doses of rosiglitazone to investigate its impact on adiponectin or bone marrow adiposity. For example, Nawrocki et al. treated mice with 10 mg/kg/day to examine the effects on circulating adiponectin and glucose homeostasis (20), while 20 mg/kg/day was used in two more recent studies investigating effects of rosiglitazone on bone marrow adiposity (26, 27). A much lower dose of 3 mg/kg/day was also found to cause MAT expansion in mice, but whether

this promotes hyperadiponectinemia was not reported (28, 37). Thus, in the present study, we used 15 mg/kg/day to ensure robust effects on MAT and circulating adiponectin. As in the above studies (26–28), we did so by administering rosiglitazone in the diet, based on measurements of body mass and estimated daily food intake. However, because of variation in body masses and daily food consumption, some mice may have exceeded the target dose of 15 mg/kg/day. As discussed above, this relatively high dose may explain the increased adiponectin expression in WAT, thereby complicating interpretation of any contribution from MAT. Such high doses may also have overwhelmed the ability of *Ocn*-Wnt10b mice to more robustly resist MAT expansion. Thus, a lower rosiglitazone dose may limit these confounding effects and thereby be more suitable for addressing our hypothesis in *Ocn*-Wnt10b mice.

Limitations of *Ocn*-Wnt10b Mice as a Model Resistant to MAT Expansion

One reason that we have not pursued such follow-up studies is that *Ocn*-Wnt10b mice may be too limited a model in which to robustly address MAT's endocrine functions. For example, while CR- or TZD-induced MAT expansion is blunted in these mice, such expansion is still marked in comparison to untreated *Ocn*-Wnt10b controls (**Figures 2** and **3**) (3). Moreover, distal tibiae of *Ocn*-Wnt10b mice remain laden with MAT (**Figures 2A,D**) and, while cMAT volume is lower in *Ocn*-Wnt10b mice, this likely reflects restrictions imposed by decreased bone marrow volume (3), rather than resulting from a direct inhibition of adipogenesis. Thus, as we have recently argued elsewhere (7), future research of MAT would benefit enormously from development of new mouse models that more robustly resist MAT formation, developmentally and/or in response to CR, TZDs, or other stimuli that promote MAT expansion.

Confounding Effects of Bone Ruptures on Osmium Tetroxide-Based rMAT Analysis

The present study reveals that cortical bone ruptures can confound osmium-based MAT detection. This issue, which has not been reported previously, provides further support for taking a multifaceted approach to MAT analysis. While TZDs can cause bone loss and fractures (38), it is unlikely that the ruptures occurred *in vivo* over the course of rosiglitazone treatment: such an injury would have dramatically impacted mobility and behavior of the mice, which was not apparent during daily inspections; and the ruptures also occurred in tibiae of males untreated with rosiglitazone, demonstrating that they are not a consequence of TZD treatment. Instead, it is likely that ruptures occurred *ex vivo* as a result of methodological issues. In particular, after fixing tibiae in formalin post-necropsy there was a very long time span, ~30 months, before most of these bones were decalcified and analyzed by osmium tetroxide staining. This holdup largely resulted from delays associated with one of our lead authors moving to a new institution, during which time the fixed tibiae were stored in PBS at 4°C and shipped by air from the USA to the UK. Although these storage conditions would not be expected to promote cortical ruptures, it is notable that no ruptures occurred in a subset of female tibiae that were stored in PBS for a shorter duration (~12 months), without air transport, before decalcification and osmium analysis. Moreover, at both the University of Michigan and the University of Edinburgh, we have analyzed hundreds of osmium-stained mouse bones from other studies, none of which has undergone such long-term storage or air transport, and among which no ruptures have ever been detected. Thus, one possibility is that exposure to low air pressure during air transport can cause a pressure differential that promotes bone ruptures. It remains possible that other factors also contributed to this phenomenon; however, our findings strongly suggest that fixed bones should not undergo long-term storage or exposure to low atmospheric pressure if MAT volume is to be determined accurately using osmium tetroxide staining.

BAT-Like Thermogenic Function Is Unlikely in MAT

There is extensive interest in "beige" or "brite" (brown-in-white) adipocytes, which develop in WAT in response to diverse external stimuli, including cold exposure or TZD treatment, and which share some properties of brown adipocytes (39–41). This so-called "browning" of WAT can increase energy consumption and may thereby contribute to TZD-associated improvement in metabolic health. Therefore, whether MAT can also undergo browning or has BAT-like characteristics has been a subject of some interest. Krings et al. found that, in mice treated for 4 weeks with rosiglitazone (20 mg/kg/day), transcript expression of brown adipocyte markers is increased in tibiae, supporting the possibility that MAT has BAT-like characteristics (26). This is consistent with our finding that rosiglitazone influences tibial *Ucp1* mRNA expression (**Figure 8**). However, Krings et al. further highlighted that, compared to BAT, *Ucp1* expression is 16,000-fold lower in tibiae, which agrees closely with our data showing a 10,000- to 25,000-fold decrease in tibiae compared to BAT. In addition, even with rosiglitazone treatment, we find that *Ucp1* transcripts remain 400- to 7,000-fold lower in tibiae than in BAT (**Figures 8A,B**). Crucially, at this level of *Ucp1* expression, we could not detect UCP1 protein, whereas rosiglitazone-induced increases in UCP1 protein in BAT are readily detectable (**Figure 8C**).

UCP1 is the hallmark of brown adipocytes and the key mediator of adaptive thermogenesis, and therefore the above findings strongly suggest that bone marrow adipocytes are unlikely to possess BAT-like thermogenic properties. One limitation of our study, and that of Krings et al., is that we analyzed whole bones rather than isolated marrow adipocytes. However, both brown and beige adipocytes are further defined by their high mitochondrial content and the multilocular morphology of their lipid droplets (41), neither of which is observed in bone marrow adipocytes (3, 4, 12, 42). This raises further doubts about the notion that MAT has BAT-like characteristics, an issue that we recently discussed in greater depth elsewhere (5). Nevertheless, it remains possible that, under a different TZD treatment regimen or in response to other stimuli, MAT is capable of undergoing browning. Indeed, while we were unable to detect UCP1 protein in WAT or whole tibiae, previous studies have detected UCP1 in

WAT following TZD treatment (41). Moreover, effects of TZDs on *Ucp1* expression in BAT are dose-dependent (34). This supports the possibility that TZD-mediated browning of WAT and MAT requires an optimal regimen of TZD treatment, in which case the conditions in our study may simply have been unsuitable for inducing a browning response. Thus, there is ample scope for future studies to further investigate whether MAT has BAT-like properties, both at the molecular and functional levels.

Other Strengths and Limitations of This Study

This study is the first to address the novel hypothesis that MAT contributes to hyperadiponectinemia in conditions beyond CR. The experimental design is strengthened by including both male and female mice, as well as by analysis of several durations of TZD treatment. The discovery of the confounding effects of cortical ruptures is partly a strength, in that it highlights an important technical consideration for future MAT research; however, presently this was a limitation because it prevented thorough measurement of rMAT volume. As discussed above, another limitation is that the dose of rosiglitazone may have been too high, and may have varied slightly between mice because of differences in body mass and daily food intake. Administration of lower doses by daily injection or oral gavage could be one approach to overcome this issue. Finally, a key limitation of this study is that our findings are based on only a single cohort of mice. Ideally, these experiments would be repeated in a second cohort, with particular care taken to avoid cortical ruptures; this would allow more robust determination of rMAT volume in *Ocn*-Wnt10b mice. However, as noted above ("Limitations of *Ocn*-Wnt10b Mice as a Model Resistant to MAT Expansion"), *Ocn*-Wnt10b mice may not be sufficiently robust as a model of impaired MAT formation. For example, adipocyte marker expression in tibiae is generally similar between WT and *Ocn*-Wnt10b mice (**Figure 4**). This limitation of the *Ocn*-Wnt10b model undermines the rationale for repeating the present studies in a second cohort. Instead, we feel strongly that it would be more productive and scientifically beneficial to focus efforts on developing new mouse models that more robustly resist MAT expansion. Such models could then be used to better address the present hypothesis, as well as other aspects of MAT function.

Beyond these particular issues, one broader limitation is that our experiments were based only in mice; it remains unclear if the relationship between TZD-induced MAT expansion and hyperadiponectinemia also exists in humans. It is well established that TZDs increase circulating adiponectin in humans (16), but their effects on MAT are less clear. Indeed, one study finds that rosiglitazone *decreases* bone marrow adiposity in the lumbar vertebrae (43), whereas a more recent report finds that pioglitazone, another TZD, increases femoral and lumbar vertebral bone marrow adiposity (44). Unfortunately, neither of these studies assessed circulating adiponectin, and there remain very few clinical studies assessing the effect of TZDs on MAT. Thus, there is a strong rationale for future research to establish how TZDs affect MAT accumulation in humans and whether this is associated with changes in circulating adiponectin.

CONCLUSION

There are four main conclusions from our study. First, under these TZD treatment conditions, it is likely that both WAT and MAT make some contribution to TZD-induced hyperadiponectinemia. Second, UCP1 expression in MAT is negligible, and therefore MAT is unlikely to have the thermogenic capacity of BAT. Third, cortical bone ruptures confound measurement of MAT volume by osmium tetroxide staining, and therefore care must be taken when processing bones for such analysis. Moreover, osmium-based assessment of MAT volume can differ from measurement of MAT content based on expression of bone marrow adipocyte transcripts; hence, multiple approaches should be used to assess MAT content, including analysis of molecular markers, rather than relying solely on osmium tetroxide staining. Finally, while *Ocn*-Wnt10b mice have been useful as a model resistant to MAT formation, development of more robust loss-of-MAT models would be of great benefit to future MAT research.

AUTHOR CONTRIBUTIONS

RS and WC designed all figures and wrote the manuscript, with ES, HM, and OM providing additional critical revisions. WC, BL, ES, VK, and OM contributed to the conception and design of the experiments. BL oversaw mouse breeding and colony management. RS, BL, BZ, ES, SP, BS, HM, AB, RW, OM, and WC contributed to data acquisition, analysis, and/or interpretation. All authors gave final approval for publication of the manuscript and agree to be accountable for all aspects of the work presented herein.

FUNDING

This work was supported by grants from the National Institutes of Health (R24 DK092759 to OM; K99-DE024178 to ES; R25 DK088752 to BZ; S10-RR026475-01 to the University of Michigan School of Dentistry microCT Core; and P30 DK089503 to the Michigan Nutrition Obesity Research Center, which oversaw NMR analysis of mouse body composition and provided a Pilot/Feasibility grant to HM). RS is supported by a British Heart Foundation 4-year PhD Studentship. WC is supported by a Career Development Award (MR/M021394/1) from the Medical Research Council (UK) and by a Chancellor's Fellowship from the University of Edinburgh, and previously by a Lilly Innovation Fellowship Award and a Postdoctoral Research Fellowship from the Royal Commission for the Exhibition of 1851 (UK). SP and BS were supported by a Training Grant from the University of Michigan Training Program in Organogenesis (T32-HD007505). Analysis of microCT imaging data was supported by a Bioinformatics Award provided through a British Heart Foundation Centre of Research Excellence grant.

REFERENCES

1. Rosen ED, Spiegelman BM. What we talk about when we talk about fat. *Cell* (2014) 156(1–2):20–44. doi:10.1016/j.cell.2013.12.012
2. Scheller EL, Burr AA, MacDougald OA, Cawthorn WP. Inside out: bone marrow adipose tissue as a source of circulating adiponectin. *Adipocyte* (2016) 5(3):251–69. doi:10.1080/21623945.2016.1149269
3. Cawthorn WP, Scheller EL, Learman BS, Parlee SD, Simon BR, Mori H, et al. Bone marrow adipose tissue is an endocrine organ that contributes to increased circulating adiponectin during caloric restriction. *Cell Metab* (2014) 20(2):368–75. doi:10.1016/j.cmet.2014.06.003
4. Scheller EL, Doucette CR, Learman BS, Cawthorn WP, Khandaker S, Schell B, et al. Region-specific variation in the properties of skeletal adipocytes reveals regulated and constitutive marrow adipose tissues. *Nat Commun* (2015) 6:7808. doi:10.1038/ncomms8808
5. Scheller EL, Cawthorn WP, Burr AA, Horowitz MC, MacDougald OA. Marrow adipose tissue: trimming the fat. *Trends Endocrinol Metab* (2016) 27(6):392–403. doi:10.1016/j.tem.2016.03.016
6. Suchacki KJ, Cawthorn WP, Rosen CJ. Bone marrow adipose tissue: formation, function and regulation. *Curr Opin Pharmacol* (2016) 28:50–6. doi:10.1016/j.coph.2016.03.001
7. Sulston RJ, Cawthorn WP. Bone marrow adipose tissue as an endocrine organ: close to the bone? *Horm Mol Biol Clin Investig* (2016). doi:10.1515/hmbci-2016-0012
8. Zhang Y, Proenca R, Maffei M, Barone M, Leopold L, Friedman JM. Positional cloning of the mouse obese gene and its human homologue. *Nature* (1994) 372(6505):425–32. doi:10.1038/372425a0
9. Scherer PE, Williams S, Fogliano M, Baldini G, Lodish HF. A novel serum protein similar to C1q, produced exclusively in adipocytes. *J Biol Chem* (1995) 270(45):26746–9. doi:10.1074/jbc.270.45.26746
10. Hu E, Liang P, Spiegelman BM. AdipoQ is a novel adipose-specific gene dysregulated in obesity. *J Biol Chem* (1996) 271(18):10697–703. doi:10.1074/jbc.271.18.10697
11. Devlin MJ. Why does starvation make bones fat? *Am J Hum Biol* (2011) 23(5):577–85. doi:10.1002/ajhb.21202
12. Cawthorn WP, Scheller EL, Parlee SD, Pham HA, Learman BS, Redshaw CM, et al. Expansion of bone marrow adipose tissue during caloric restriction is associated with increased circulating glucocorticoids and not with hypoleptinemia. *Endocrinology* (2016) 157(2):508–21. doi:10.1210/en.2015-1477
13. Bennett CN, Ouyang H, Ma YL, Zeng Q, Gerin I, Sousa KM, et al. Wnt10b increases postnatal bone formation by enhancing osteoblast differentiation. *J Bone Miner Res* (2007) 22(12):1924–32. doi:10.1359/jbmr.070810
14. Zgheib S, Mequinion M, Lucas S, Leterme D, Ghali O, Tolle V, et al. Long-term physiological alterations and recovery in a mouse model of separation associated with time-restricted feeding: a tool to study anorexia nervosa related consequences. *PLoS One* (2014) 9(8):e103775. doi:10.1371/journal.pone.0103775
15. Lehmann JM, Moore LB, Smith-Oliver TA, Wilkison WO, Willson TM, Kliewer SA. An antidiabetic thiazolidinedione is a high affinity ligand for peroxisome proliferator-activated receptor γ (PPARγ). *J Biol Chem* (1995) 270(22):12953–6. doi:10.1074/jbc.270.22.12953
16. Yki-Jarvinen H. Thiazolidinediones. *N Engl J Med* (2004) 351(11):1106–18. doi:10.1056/NEJMra041001
17. Cabre A, Lazaro I, Girona J, Manzanares JM, Marimon F, Plana N, et al. Fatty acid binding protein 4 is increased in metabolic syndrome and with thiazolidinedione treatment in diabetic patients. *Atherosclerosis* (2007) 195(1):e150–8. doi:10.1016/j.atherosclerosis.2007.04.045
18. Maeda N, Takahashi M, Funahashi T, Kihara S, Nishizawa H, Kishida K, et al. PPARgamma ligands increase expression and plasma concentrations of adiponectin, an adipose-derived protein. *Diabetes* (2001) 50(9):2094–9. doi:10.2337/diabetes.50.9.2094
19. Yu JG, Javorschi S, Hevener AL, Kruszynska YT, Norman RA, Sinha M, et al. The effect of thiazolidinediones on plasma adiponectin levels in normal, obese, and type 2 diabetic subjects. *Diabetes* (2002) 51(10):2968–74. doi:10.2337/diabetes.51.10.2968
20. Nawrocki AR, Rajala MW, Tomas E, Pajvani UB, Saha AK, Trumbauer ME, et al. Mice lacking adiponectin show decreased hepatic insulin sensitivity and reduced responsiveness to peroxisome proliferator-activated receptor gamma agonists. *J Biol Chem* (2006) 281(5):2654–60. doi:10.1074/jbc.M505311200
21. Nissen SE, Wolski K. Effect of rosiglitazone on the risk of myocardial infarction and death from cardiovascular causes. *N Engl J Med* (2007) 356(24):2457–71. doi:10.1056/NEJMoa072761
22. Loke YK, Singh S, Furberg CD. Long-term use of thiazolidinediones and fractures in type 2 diabetes: a meta-analysis. *Can Med Assoc J* (2009) 180(1):32–9. doi:10.1503/cmaj.080486
23. Rasouli N, Yao-Borengasser A, Miles LM, Elbein SC, Kern PA. Increased plasma adiponectin in response to pioglitazone does not result from increased gene expression. *Am J Physiol Endocrinol Metab* (2006) 290(1):E42–6. doi:10.1152/ajpendo.00240.2005
24. Pita J, Panadero A, Soriano-Guillén L, Rodríguez E, Rovira A. The insulin sensitizing effects of PPAR-γ agonist are associated to changes in adiponectin index and adiponectin receptors in Zucker fatty rats. *Regul Pept* (2012) 174(1–3):18–25. doi:10.1016/j.regpep.2011.11.004
25. Burant CF, Sreenan S, Hirano K, Tai TA, Lohmiller J, Lukens J, et al. Troglitazone action is independent of adipose tissue. *J Clin Invest* (1997) 100(11):2900–8. doi:10.1172/JCI119839
26. Krings A, Rahman S, Huang S, Lu Y, Czernik PJ, Lecka-Czernik B. Bone marrow fat has brown adipose tissue characteristics, which are attenuated with aging and diabetes. *Bone* (2012) 50(2):546–52. doi:10.1016/j.bone.2011.06.016
27. Lazarenko OP, Rzonca SO, Hogue WR, Swain FL, Suva LJ, Lecka-Czernik B. Rosiglitazone induces decreases in bone mass and strength that are reminiscent of aged bone. *Endocrinology* (2007) 148(6):2669–80. doi:10.1210/en.2006-1587
28. Ackert-Bicknell CL, Shockley KR, Horton LG, Lecka-Czernik B, Churchill GA, Rosen CJ. Strain-specific effects of rosiglitazone on bone mass, body composition, and serum insulin-like growth factor-I. *Endocrinology* (2009) 150(3):1330–40. doi:10.1210/en.2008-0936
29. Turer AT, Scherer PE. Adiponectin: mechanistic insights and clinical implications. *Diabetologia* (2012) 55(9):2319–26. doi:10.1007/s00125-012-2598-x
30. Carey DG, Cowin GJ, Galloway GJ, Jones NP, Richards JC, Biswas N, et al. Effect of rosiglitazone on insulin sensitivity and body composition in type 2 diabetic patients [corrected]. *Obes Res* (2002) 10(10):1008–15. doi:10.1038/oby.2002.137
31. Scheller EL, Troiano N, Vanhoutan JN, Bouxsein MA, Fretz JA, Xi Y, et al. Use of osmium tetroxide staining with microcomputerized tomography to visualize and quantify bone marrow adipose tissue in vivo. *Methods Enzymol* (2014) 537:123–39. doi:10.1016/B978-0-12-411619-1.00007-0
32. Combs TP, Berg AH, Rajala MW, Klebanov S, Iyengar P, Jimenez-Chillaron JC, et al. Sexual differentiation, pregnancy, calorie restriction, and aging affect the adipocyte-specific secretory protein adiponectin. *Diabetes* (2003) 52(2):268–76. doi:10.2337/diabetes.52.2.268
33. Wiesenborn DS, Menon V, Zhi X, Do A, Gesing A, Wang Z, et al. The effect of calorie restriction on insulin signaling in skeletal muscle and adipose tissue of Ames dwarf mice. *Aging (Albany NY)* (2014) 6(10):900–12. doi:10.18632/aging.100700
34. Kelly LJ, Vicario PP, Thompson GM, Candelore MR, Doebber TW, Ventre J, et al. Peroxisome proliferator-activated receptors gamma and alpha mediate in vivo regulation of uncoupling protein (UCP-1, UCP-2, UCP-3) gene expression. *Endocrinology* (1998) 139(12):4920–7. doi:10.1210/endo.139.12.6384
35. Nedergaard J, Cannon B. UCP1 mRNA does not produce heat. *Biochim Biophys Acta* (2013) 1831(5):943–9. doi:10.1016/j.bbalip.2013.01.009
36. Moore GB, Pickavance LC, Briscoe CP, Clapham JC, Buckingham RE, Wilding JP. Energy restriction enhances therapeutic efficacy of the PPARgamma agonist, rosiglitazone, through regulation of visceral fat gene expression. *Diabetes Obes Metab* (2008) 10(3):251–63. doi:10.1111/j.1463-1326.2007.00697.x
37. Styner M, Pagnotti GM, Galior K, Wu X, Thompson WR, Uzer G, et al. Exercise regulation of marrow fat in the setting of PPAR gamma agonist treatment in female C57BL/6 mice. *Endocrinology* (2015) 156(8):2753–61. doi:10.1210/en.2015-1213
38. Riche DM, King ST. Bone loss and fracture risk associated with thiazolidinedione therapy. *Pharmacotherapy* (2010) 30(7):716–27. doi:10.1592/phco.30.7.716
39. Petrovic N, Walden TB, Shabalina IG, Timmons JA, Cannon B, Nedergaard J. Chronic peroxisome proliferator-activated receptor gamma (PPARgamma) activation of epididymally derived white adipocyte cultures

reveals a population of thermogenically competent, UCP1-containing adipocytes molecularly distinct from classic brown adipocytes. *J Biol Chem* (2010) 285(10):7153–64. doi:10.1074/jbc.M109.053942
40. Ohno H, Shinoda K, Spiegelman BM, Kajimura S. PPAR agonists induce a white-to-brown fat conversion through stabilization of PRDM16 protein. *Cell Metab* (2012) 15(3):395–404. doi:10.1016/j.cmet.2012.01.019
41. Harms M, Seale P. Brown and beige fat: development, function and therapeutic potential. *Nat Med* (2013) 19(10):1252–63. doi:10.1038/nm.3361
42. Tavassoli M. Ultrastructural development of bone marrow adipose cell. *Acta Anat (Basel)* (1976) 94(1):65–77. doi:10.1159/000144545
43. Harslof T, Wamberg L, Moller L, Stodkilde-Jorgensen H, Ringgaard S, Pedersen SB, et al. Rosiglitazone decreases bone mass and bone marrow fat. *J Clin Endocrinol Metab* (2011) 96(5):1541–8. doi:10.1210/jc.2010-2077
44. Grey A, Beckley V, Doyle A, Fenwick S, Horne A, Gamble G, et al. Pioglitazone increases bone marrow fat in type 2 diabetes: results from a randomized controlled trial. *Eur J Endocrinol* (2012) 166(6):1087–91. doi:10.1530/EJE-11-1075

Conflict of Interest Statement: RS, BL, BZ, ES, SP, BS, HM, AB, and RW have nothing to disclose. WC held a postdoctoral fellowship funded by Eli Lilly and Company. VK is employed by Eli Lilly and Company. OM has received research funding from Eli Lilly and Company.

3.2. Discussion

The overall aim of this chapter was to test if, as for CR, TZD-induced hyperadiponectinaemia is significantly blunted when BMAT expansion is impaired. As discussed in the paper, some elements of the experiment limited the interpretation of the results. It appeared that the TZD dose, which was relatively high, was powerful enough to overcome the resistant effect of the Ocn-Wnt10b transgene on BMAT expansion. Multiple comparisons showed that, following TZD treatment, the Ocn-Wnt10b mice have significantly lower cBMAT volume than wild-type mice. However, this may reflect a decrease in medullary cavity volume rather than a specific decrease in BMAT volume given that, anecdotally, the medullary cavity appeared full of BMAT in the distal portion of the tibia. I was unable to measure the medullary cavity volume in these mice because this requires μCT analysis of calcified bones, but in this study the bones underwent μCT scanning only after decalcification. In the proximal tibia fewer significant differences were seen, indicating that the Ocn-Wnt10b mice may not effectively resist TZD-induced BMAT expansion. Additionally, the issue of bone ruptures also added uncertainty to the interpretation of the results by limiting the confidence in rBMAT volumes of some bones. Fortunately, the adipocyte transcript data helped fill some knowledge gaps left by the ruptures and allow some firmer conclusions to be gained from the results.

The results have been discussed in depth in the published paper; however, several other relevant, papers have since been published. Thus, MRI analyses of human premenopausal women found that vertebral BMAT volume is a significant predictor of circulating adiponectin, although so were other white adipose tissue depots[181]. This provides further evidence for the role of BMAT contributing to hyperadiponectinaemia in alternative contexts to calorie restriction. Despite this, it has also been shown that there is no association between BMAT and circulating adiponectin in control, obese and type II diabetic groups[182]. This is a diverse group of subjects so it is not clear if the relationship between BMAT and adiponectin only exists in more controlled subsets of people i.e. premenopausal women or non-obese diabetics.

Studies in anorexic patients show that adiponectin is negatively correlated with BMD[183] and given that BMAT is often inversely associated with BMD, there is support for the possibility that in anorexia nervosa, BMAT and adiponectin may be positively associated.

Little further work has been performed using the Ocn-Wnt10b mice given their presumed limited ability to resist BMAT expansion in the face of robust stimuli. Future work from others in the Cawthorn Lab is attempting to develop a mouse model that

completely lacks BMAT whilst maintaining normal development of other adipose depots. If successful, these models will enable researchers to examine how stimuli that normally cause BMAT expansion and hyperadiponectinaemia affect adiponectin plasma concentrations when BMAT is absent.

4. Skeletal changes caused by variation in calorie restriction duration.

4.1. Introduction

4.1.1. How CR affects the skeleton

CR causes a wide variety of skeletal changes. As described previously, calorie restriction increases BMAT but the causes and consequences of BMAT expansion during CR remain to be firmly established. The increase in BMAT has been hypothesised to occur for a variety of reasons. One proposed mediator is low concentrations of circulating leptin, an adipocyte-derived satiety hormone that acts by inducing feeding behaviours when its concentration falls[184]. CR is known to decrease leptin levels [185]. Indications for leptin driving the accumulation of BMAT can be seen in experiments showing that mice lacking leptin (*ob/ob* mice) or leptin receptors (*db/db* mice) have very high volumes of BMAT, and leptin administration to *ob/ob* mice causes a reduction in BMAT[140,186,187]. The relationship between leptin and haematopoiesis may also influence BMAT expansion: leptin is required for effective haematopoiesis[188] and BMAT has been shown to be a negative regulator of overall haematopoesis[189]. Low leptin may therefore cause a reduction in red, haematopoietic marrow, which would then allow space for the BMAT to expand into.

Some evidence exists that leptin is neither sufficient nor required for BMAT expansion and that glucocorticoids, such as corticosterone, are a more important regulator[129]. Indeed, leptin administration to mice not deficient in leptin actually causes a decrease in BMAT[187,190]. A caveat to the observation that BMAT expansion is more closely associated with glucocorticoids than leptin during CR is that the results were obtained in rabbits and therefore more research is required into the relationship between glucocorticoids, leptin and BMAT. An alternative to both glucocorticoids and leptin as regulators of BMAT expansion is the role of IGF-1 and GH. Rats with low IGF-1, either through hypophysectomy or genetic alteration, showed significantly more BMAT in female tibiae[141].

Along with increases in BMAT, reductions in bone mineralisation and strength are also observed in response to CR. Bone loss is associated with age and weight loss[191] and a chronic 20% reduction in calories has also been shown to reduce bone mass[192]. It could be suggested that bone integrity decreases in these contexts due to reduced mechanical stress on the bone caused by reduced weight; however, research has shown that,

compared to girls with typical body weight, both ballet dancers and girls with anorexia nervosa show reduced bone mineral density despite ballet dancers having increased physical activity [193]. These differences were only present when adjusted to be relative to fat mass, indicating that fat mass is important for determining bone mineral density[193]. Site-specific differences within bone have also been observed in response to calorie restriction. Cortical bone decreases during CR but trabecular bone does not[194].

Insulin has been proposed as a potential molecular influencer of bone, particularly in CR. High fat mass and obesity are associated with hyperinsulinaemia[195] and, conversely, insulin is lower in lean and calorie-restricted states[196]. It has been shown that, *in vitro*, insulin is able to stimulate osteoblast-like cell growth[197]. *In vivo*, localised injection of insulin has been shown to increase bone formation in mice[198]. This suggests that CR-induced bone loss may be caused by hypoinsulinaemia.

As mentioned above, leptin is significantly decreased during calorie restriction. Leptin treatment in *ob/ob* mice has been shown to greatly increase bone growth[199] and leptin is also able to inhibit osteoclast formation in vitro[200]. Therefore, leptin may also be a positive regulator of bone mass.

Glucocorticoids are an anti-inflammatory group of steroid hormones. Glucocorticoids are elevated during caloric restriction[129] and are well established to cause a reduction in bone density and strength[201,202]. Given the overlapping roles of glucocorticoids and leptin on both bone mineral density and BMAT expansion I aimed to evaluate the relationship between changes in these hormones and effects on both bone integrity and BMAT expansion during CR. If these endocrine factors are mediators of bone loss and BMAT expansion, then we would expect the changes in their circulating levels to precede or coincide with these skeletal effects of CR.

Finally, adiponectin has also been proposed as regulator of bone density. Research in humans has shown that increased circulating adiponectin is associated with reduced bone mineral density [203] and although the association with bone density was maintained, another study did not show an association between adiponectin and fracture risk[204]. Transgenic mice overexpressing adiponectin show reduced bone mineral content in the femurs of the females but not the males[205] and a further study using the same model showed significant decreases in tibial bone parameters[206].

4.2. Results

4.2.1. Body mass changes during caloric restriction

In order to confirm if the CR protocol had functioned as expected I first measured the body mass of the mice over the course of the experiment. I expected to observe a

decrease in body mass in the CR mice compared to the *ad libitum* (AL)-fed mice. Figure 4.1 shows the body mass of both male (A) and female (B) mice measured every week for 6 weeks. In both sexes, mice were randomly assigned to AL or CR diet and so at the start of the experiment (week 0) both groups had the same body mass, indicating no pre-existing difference between the two dietary groups. After one week of the experiment both male and female CR mice showed a sharp and significant decrease in body mass whilst the AL mice continued at the same rate of body mass increases observed prior to intervention (data not shown). In both sexes, CR mice continued to decrease their body mass until 3 weeks post-intervention, at which point they both reached minimal body mass. From 4-6 weeks post-intervention, the CR mice showed increases in body mass compared to their nadir but remained significantly reduced compared to the AL mice, which continued to increase in body mass. Two-way ANOVA showed that both diet and duration of the experiment were significant contributors to the variance in the data. A significant interaction was also detected in both sexes, confirming a divergence between the AL and CR diets. Whilst these results are not surprising, they confirm that the CR intervention was acting as predicted and thereby lay a foundation for the further characterisation these mice, as discussed below.

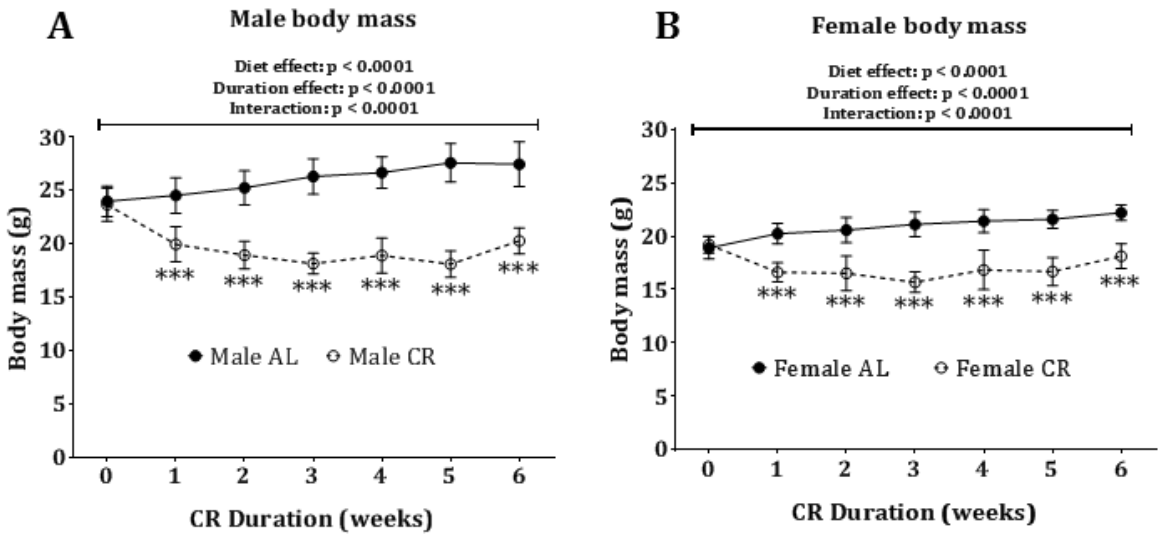

Figure 4.1 – Body mass in male and female mice across 6 weeks CR diet. Male **(A)** and female **(B)** mice were weighed weekly. Mean body mass is shown with error bars indicating ± SD. Statistical significance was determined by 2-way ANOVA, source of variance significance is shown above the data and multiple comparisons for AL vs CR at each time point determined using Sidak's correction are indicated on the data, ***: $p < 0.001$. Number used Male AL 0w – 21; 1w – 21; 2w – 16; 3w – 13; 4w – 11; 5w – 8; 6w – 6. Male CR 0w – 22; 1w – 22; 2w – 17; 3w – 11; 4w – 11; 5w – 6; 6w – 6. Female AL 0w-

23; 1w – 23; 2w – 23; 3w – 12; 4w – 12; 5w – 7; 6w – 6. Female CR 0w – 23; 1w – 23; 2w – 23; 3w – 16; 4w – 13; 5w – 9; 6w – 6.

4.2.2. Tibial and femoral changes in bone marrow adipose tissue

We have previously observed large increases in tibial BMAT after 6 weeks of CR compared to mice on an AL diet[121,129] yet the mechanisms underlying this effect and over what time frame it occurs are less well understood. Additionally, the BMAT changes in bones other than tibiae are also less well characterised. To address these gaps in knowledge, we analysed BMAT at several skeletal sites after mice had undergone CR for 1-6 weeks. Both sexes underwent CR for 2, 4 or 6 weeks and a 1-week CR group was also included for males; a 1-week CR in females could not be completed owing to time constraints. Figure 4.2 shows tibial BMAT separated into proximal and distal regions, which correspond to rBMAT and cBMAT, respectively. The interface between the proximal and distal section is located at the junction between the tibia and fibula. In male mice (Fig. 4.2.A) proximal tibial BMAT showed significant regulation by both diet and duration, and an interaction between these factors. Additionally, multiple comparison analysis showed a significant difference between the 6-week AL and CR groups. This pattern of significance was repeated in proximal tibial BMAT of females (B). In the distal tibia both males (C) and females (D) the % BMAT was greater than in the proximal tibia, consistent with previous observations[121]. In male distal tibiae ANOVA identified duration, but not diet itself, as a significant source of variance. This may reflect the 'constitutive' nature of distal tibial BMAT, which is less influenced by diet and other exogenous stimuli[207]. In the female distal tibia both diet and duration were significant but no interaction was seen. Multiple comparisons did not reveal any significant differences in male or female distal BMAT. Male and female humeri were also analysed but no BMAT was detectable in these bones and therefore the data is not shown.

Here we see that, as expected, there are large increases in tibial BMAT, particularly in the proximal regions. It is likely that we observe larger differences in BMAT volume in the proximal tibia compared to the distal tibia because the distal region is constitutively full of BMAT as indicated by the BMAT percentage occupancy in the region of 100% in all groups of the distal tibia. In some cases the measured BMAT volume exceeded 100% of the measured marrow cavity volume; this likely results from dilation of the marrow cavity after decalcification and because osmium-stained samples are scanned at a slightly lower resolution than the calcified samples (from which the marrow cavity volume is measured). For durations under 6 weeks we see very few significant

differences, indicating that the CR-induced increases in BMAT occur predominantly between 4-6 weeks of CR. Yet, diet was a significant source of variance in proximal tibiae for both sexes, indicating that there is likely a mild effect on BMAT over all durations of CR.

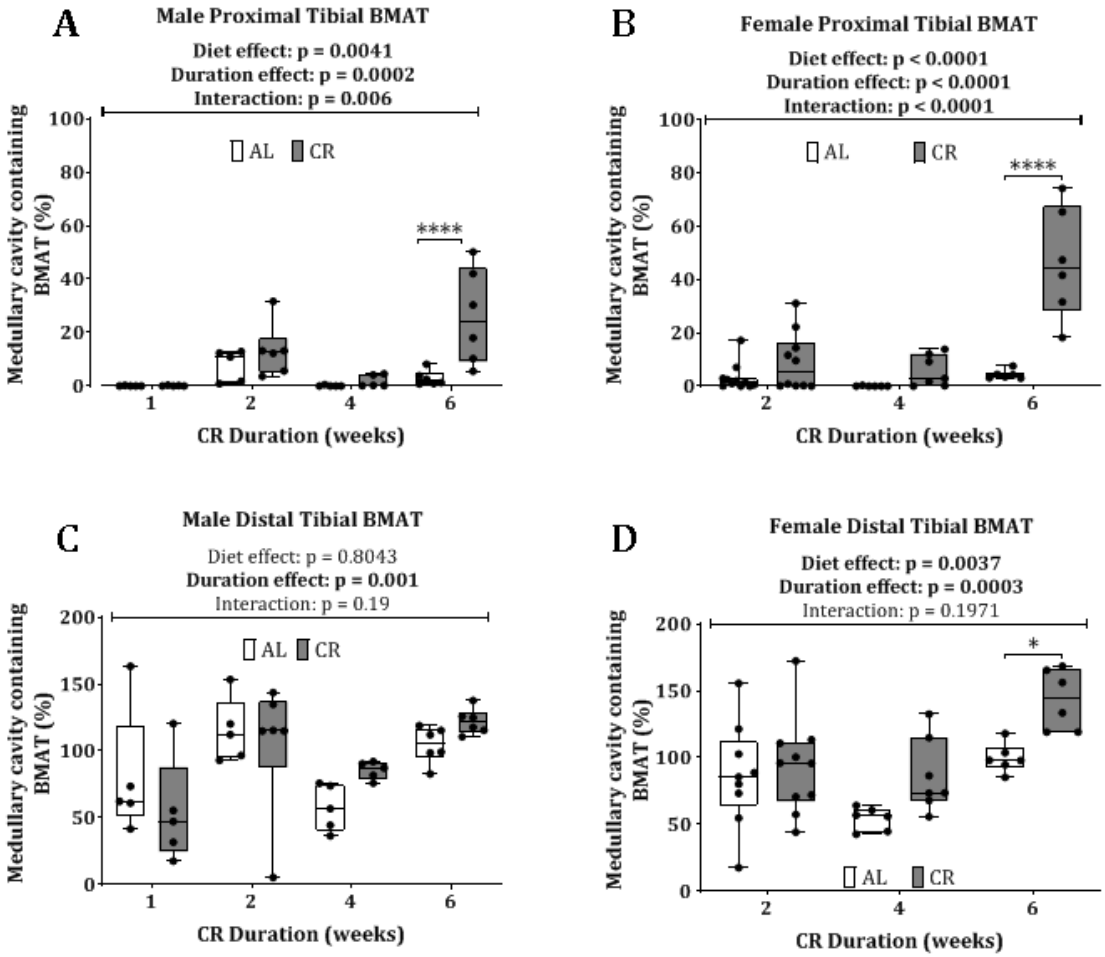

Figure 4.2 – Tibial BMAT percentage occupancy of medullary cavity. Tibiae were dissected from mice post-cull, decalcified and stained with osmium tetroxide. µCT was used to quantify BMAT volume and medullary cavity volume. BMAT (% medullary cavity) was then calculated for **(A)** male proximal tibia, **(B)** female proximal tibia, **(C)** male distal tibia and **(D)** female distal tibia. All data are presented as box-and-whisker plots showing median, interquartile range and range. Statistical significance was determined by 2-way ANOVA, source of variance significance is shown above the data and multiple comparisons determined using Sidak's correction are indicated on the data,*: $p < 0.05$; ****: $p < 0.0001$. Numbers per group: Male AL 1w – 5; Male CR 1w – 5; Male AL 2w – 5; Male CR 2w – 6; Male AL 4w – 5; Male CR 4w – 5; Male AL 6w – 6; Male CR 6w – 6; Female AL 2w – 9; Female CR 2w – 10; Female AL 4w – 6; Female CR 4w – 7; Female AL 6w – 6; Female CR 6w – 6.

Given that there were strong data to support CR induced BMAT increases all (1, 2, 4 and 6 week) durations were analysed. Femoral BMAT accumulation has been shown after 6 and 12 weeks of CR[133] but whether this occurs with shorter durations remains unknown. Given the expense of μCT analysis, I focussed my femoral BMAT analysis on my 2- and 6-week groups, reasoning that there may be no differences before 6 weeks and so to analyse all time points preceding this could be fruitless. Figure 4.3 shows the percentage of BMAT in whole femurs of both male and female mice. In male femurs (A) ANVOA detected a borderline-significant interaction between duration and diet, with multiple comparisons revealing a significant difference between CR and AL mice after 6 weeks. Female femoral BMAT showed greater differences with both diet and duration identified as significant sources of variance with a significant interaction between these factors (Figure 4.3B). Multiple comparisons showed significant differences between AL and CR females at both 2- and 6-week time points.

From these data it appears that the female mice are more responsive than males to CR-induced increases in femoral BMAT. Females also appear to exhibit more rapid increases in BMAT than males.

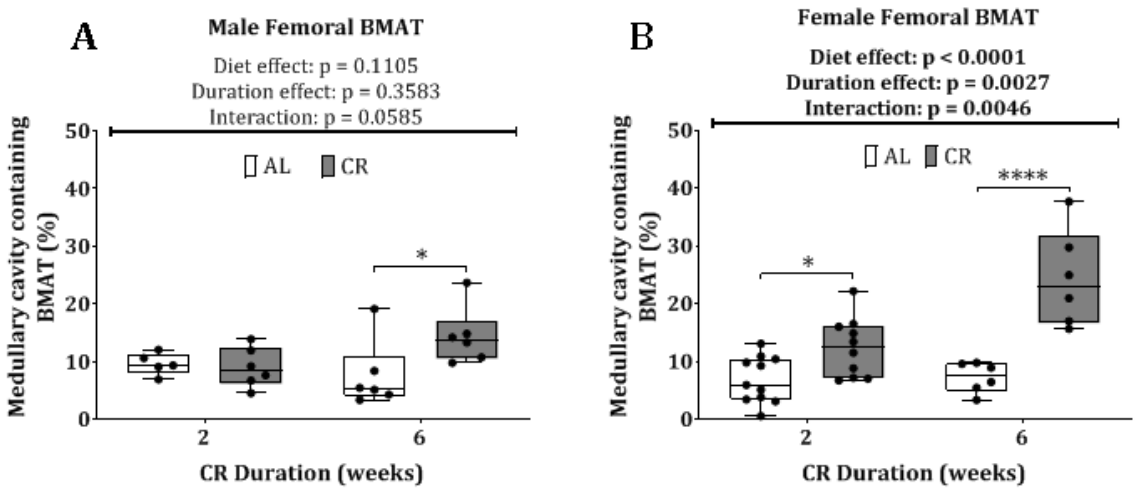

Figure 4.3 – Femoral BMAT percentage occupancy of medullary cavity. Femurs were dissected from mice post-cull, were decalcified and stained with osmium tetroxide. μCT was used to quantify BMAT volume and medullary cavity volume. **(A)** BMAT percentage occupancy of the medullary cavity in male femur. **(B)** BMAT percentage occupancy of the medullary cavity in female femur. Data are presented and statistical significance was determined as described for Figure 4.2. Numbers per group: Male AL 2w – 5; Male CR 2w – 6; Male AL 6w – 6; Male CR 6w – 6; Female AL 2w – 9; Female CR 2w – 10; Female AL 6w – 6; Female CR 6w – 6.

Figure 4.4 shows 3D reconstructions of tibiae and femurs scanned by μCT. One representative bone with the median BMAT volume was selected per group. A and B show the male and female tibiae whilst panels C and D show the male and female femurs. Qualitative increases in BMAT volume can be observed as duration on the diet increases, particularly in 6-week mice, which agrees with the quantitative data above. The boundary between proximal and distal tibia at the tiba/fibula (T/F) junction is shown for reference.

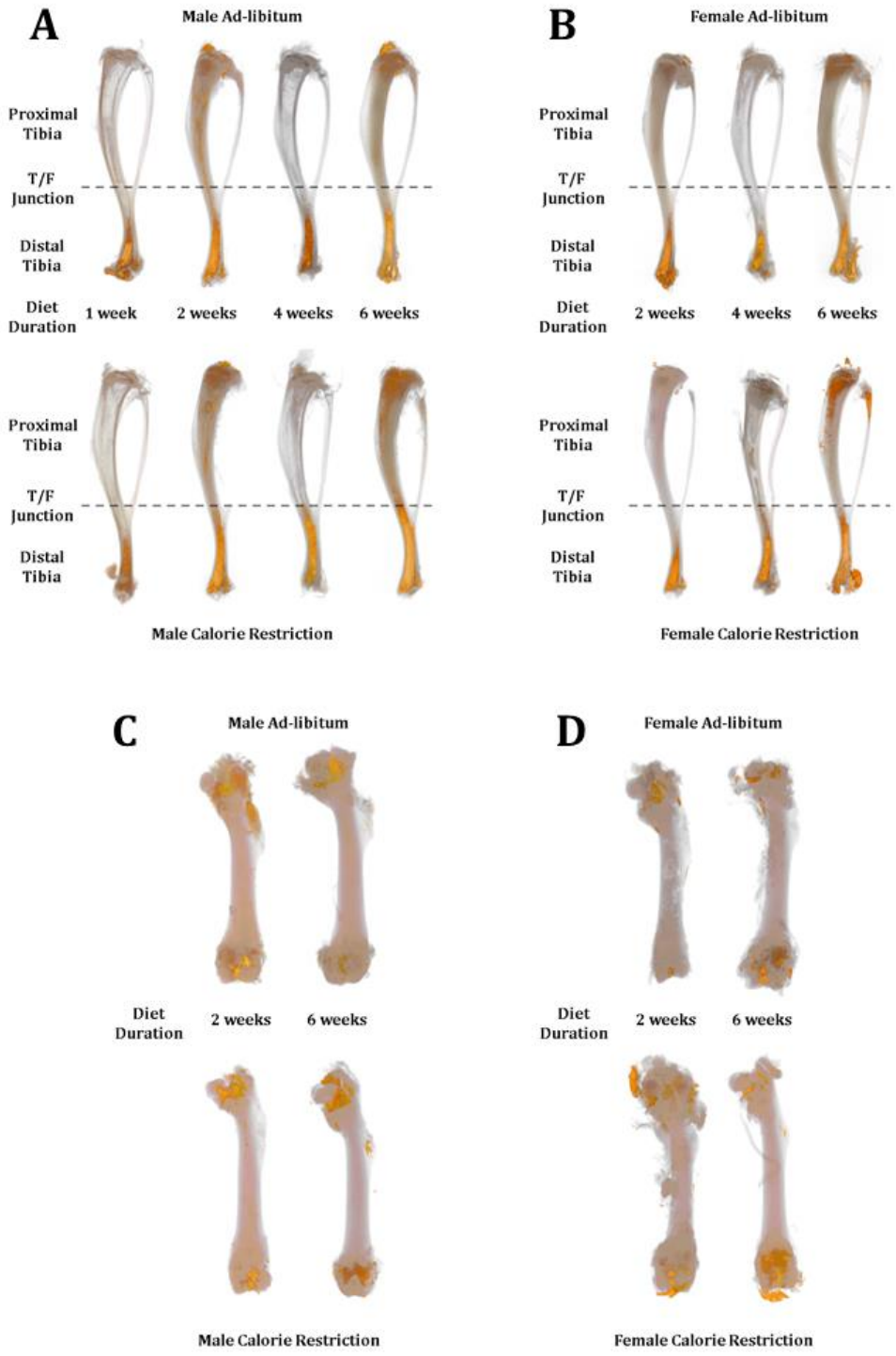

Figure 4.4 – 3D renders of tibias and femurs staining with osmium tetroxide. Tibia and femurs were dissected from mice post-cull, were decalcified and stained with osmium tetroxide. µCT was used to scan the bones and the resulting scans were visualised using CTvox (Bruker) software. T/F junction represents tibia/fibula junction. **(A)** Male tibia. **(B)** Female tibia. **(C)** Male femur. **(D)** Female femur.

4.2.3. Transcript level changes in adiposity

A secondary method for the measurement of adiposity in bones is to quantify mRNA transcripts associated with adipocytes. Here we examine transcript levels of *Adipoq* (Adiponectin), *Lep* (Leptin) and *Fabp4* (Fatty Acid Binding Protein 4), all of which are primarily expressed by adipocytes. We can infer that bone tissue with higher concentrations of these adipocyte transcripts is likely to have higher volumes of BMAT.

In Figure 4.5 tibial expression of these adipocyte markers is shown. ANOVA revealed that, in male tibiae, diet contributed significantly to variance in *Adipoq* and *Fabp4*, while experiment duration was significant for all three adipocyte markers. Additionally, multiple comparisons revealed significant differences in *Adipoq* expression tibiae of 4-week males. No interaction effects were seen. In females fewer significant differences were observed; diet was a significant source of variance for *Lep* expression whilst duration was significant for *Adipoq* expression. These data indicate some tibial BMAT expansion caused by CR, at least in some markers.

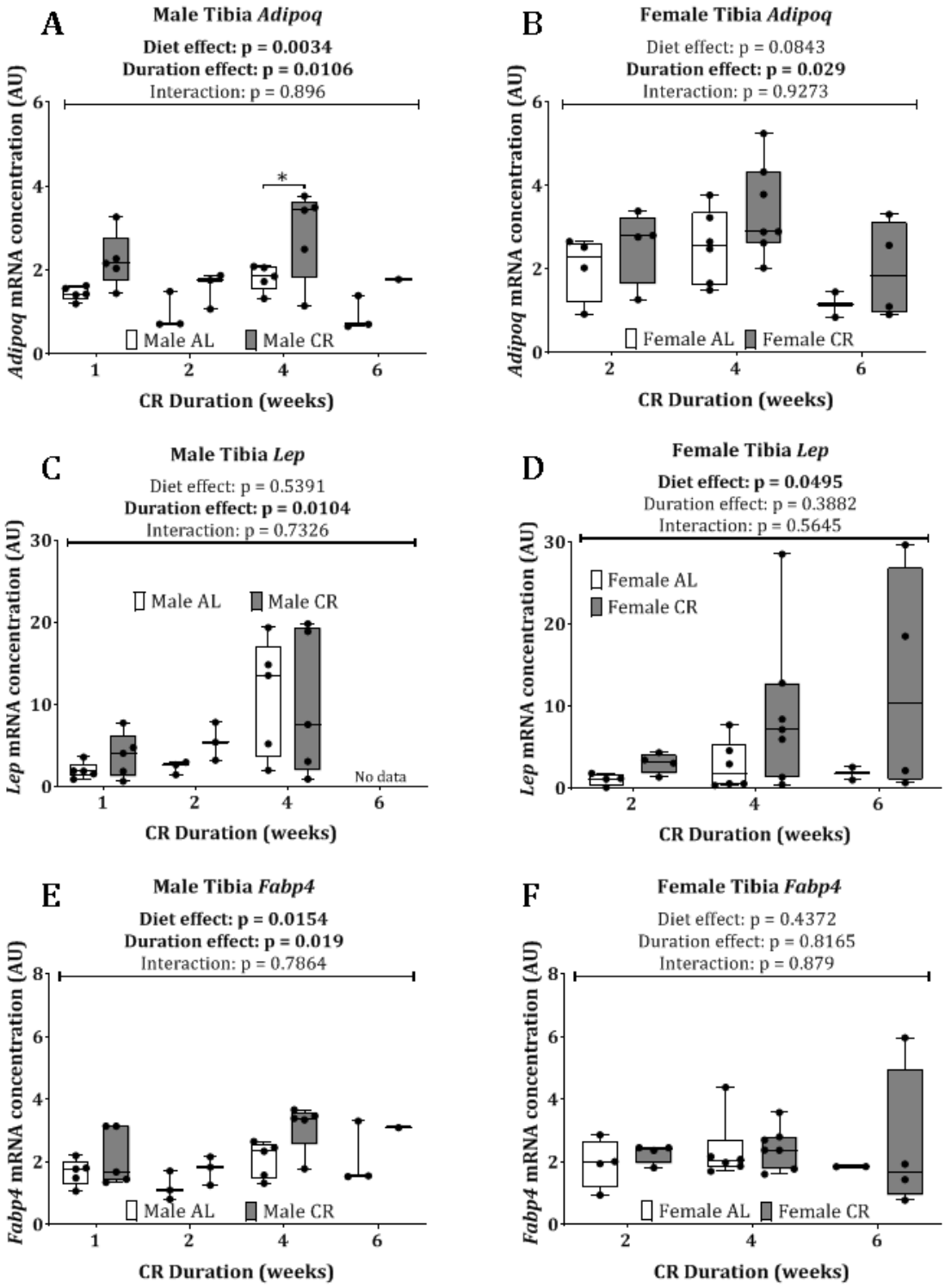

Figure 4.5 – Adipocyte transcript markers of male and female tibia. Tibiae were dissected from mice post-cull and frozen. They were homogenised in liquid nitrogen and RNA extracted. The RNA was reverse transcribed to cDNA and qPCR used to quantify expression of *Adipoq*, *Lep* and *Fabp4*. Data are presented in arbitrary units relative to the geometric mean concentration of housekeeping gene *Ppia* and ribosomal RNA 18S (*Rn18s*). **(A)** *Adipoq* in the male tibia. **(B)** *Adipoq* in the female tibia **(C)** *Lep* in the male

tibia. **(D)** *Lep* in the female tibia. **(E)** *Fabp4* in male tibia. **(F)** *Fabp4* in female tibia. Data are presented and statistical significance was determined as described for Figure 4.2. Numbers per group: see Figure 4.2.

Figure 4.6 shows expression of these adipocyte markers in femurs of the mice. No significant variance is attributable to diet in either sex for any of the transcript markers. Experimental duration was a significant source of variance in male and female Adipoq and male and female Fabp4. These data do not show the same pattern observed in femurs stained by osmium tetroxide, which showed significant effects of CR, particularly in female femurs. Therefore, the transcript markers may not be an accurate marker of bone adiposity, at least in femurs.

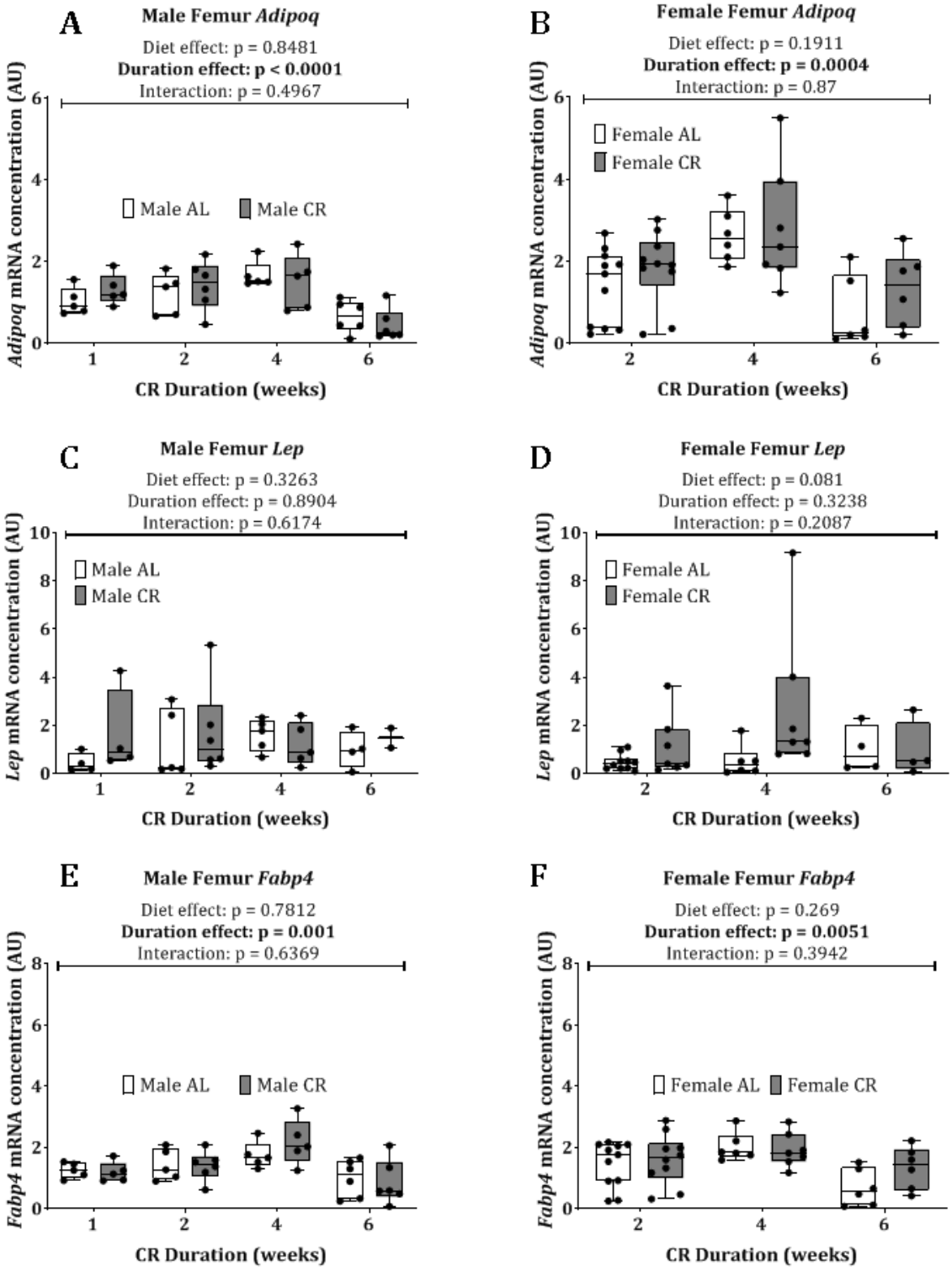

Figure 4.6 – Adipocyte transcript markers of male and female femur. Transcript expression in femurs was done as described for tibiae in Figure 4.5. **(A)** Adipoq in the male femur. **(B)** Adipoq in the female femur **(C)** Lep in the male femur. **(D)** Lep in the female femur. **(E)** Fabp4 in male femur. **(F)** Fabp4 in female femur. Data are presented, numbers used and statistical significance was determined as described for Figure 4.2

Finally, humeri were also analysed for the same adipocyte transcript markers. My rationale was that, despite not seeing any BMAT by osmium staining, transcript markers may be more sensitive in detecting changes on a molecular level, which might precede the lipid accumulation that osmium staining detects on a more gross anatomical level. No significant effects of diet were detected on overall variance in any markers, yet a significant difference by multiple comparison was seen in *Lep* expression in male humeri. Notably, humeral *Lep* expression was far lower than that seen in tibiae and femurs, which is consistent with the lack of detectable BMAT in osmium-stained humeri. Some significant durational effects were observed in male and female *Adipoq*, male *Lep* and male *Fabp4*. The durational effects seen in all bones likely reflect a change in expression of these factors as mice age and may be related to the increased BMAT detected as mice get older[207].

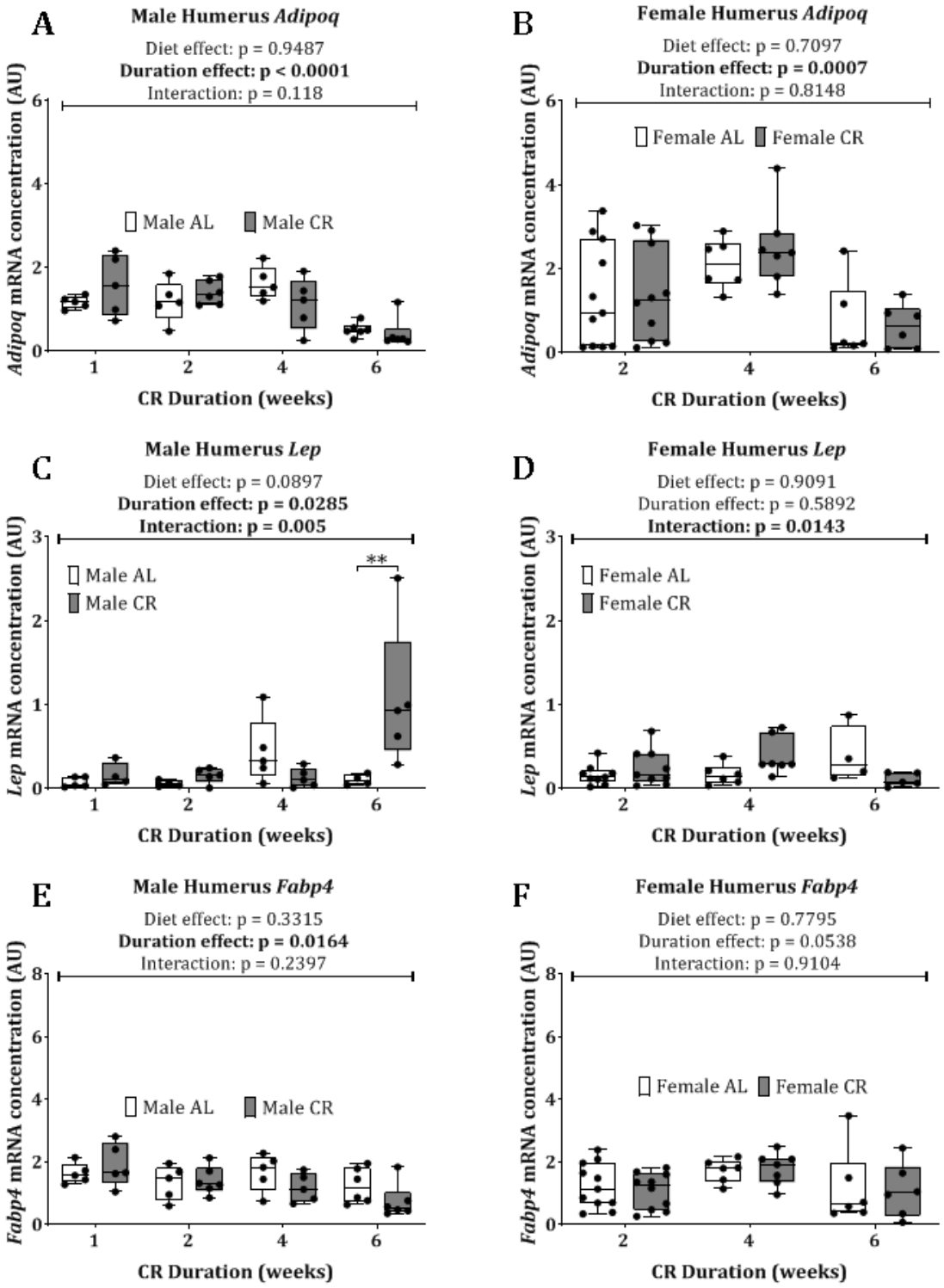

Figure 4.7 – Adipocyte transcript markers of male and female humerus. Transcript expression in femurs was done as described for tibiae in Figure 4.5. **(A)** Adipoq in the male humerus. **(B)** Adipoq in the female humerus **(C)** Lep in the male humerus. **(D)** Lep in the female humerus. **(E)** Fabp4 in male humerus. **(F)** Fabp4 in female humerus. Data are presented, numbers used and statistical significance was determined as described for Figure 4.2.

4.2.4. Calcified tissue measurement of tibia, femur and humerus

The above findings show that the effects of CR on BMAT volume are both duration dependent and skeletal site specific. Differences were also seen between males and females. It is well known that there is a strong link between increased BMAT volume and decreased bone tissue integrity, but it is unclear if BMAT expansion plays a causal role in bone loss. Thus, to explore the temporal relationship between these phenomena during CR, I next measured the architecture of the tibia, femur and humerus by μCT and also examined the transcript expression of osteocalcin (*Bglap*), an osteoblast-derived hormone that can be used as a biomarker of bone formation and osteoblast activity[208].

To determine how tibiae, femurs and humeri respond to CR these bones were scanned by μCT prior to osmium staining, allowing the quantification of markers of trabecular and cortical integrity. These data are presented in tables over the following pages, which show the mean +/- standard deviation (SD) as well as the ANOVA results for the contribution of diet and duration on total variance of the dataset. Additionally, p values for multiple comparisons between the AL and CR mice are shown.

The methodology for scanning and analysis of the bones was performed in accordance with the recommendations set out in Bouxsein et al.[209] which also shows representative images and 3D renders for the trabecular and cortical bone[209].

In trabecular bone the primary readouts include the bone volume fraction (BV/TV, %), which is a measure of the ratio of the volume of calcified tissue in the trabecular region to the total volume within the trabecular region of interest; trabecular number (Tb.N, 1/mm), which is a count of the number of trabeculae per unit of length; trabecular thickness (Tb.Th, mm), which is a measure of the mean thickness of the trabeculae.; and trabecular separation (Tb.Sp, mm), which is a measure of the mean distance between trabeculae. These four factors have been described as the key variables to be shown when describing trabecular bone morphology[209].

In the cortical bone I analysed the following: the total cross-sectional area inside the periosteal envelope (the tissue on the outside of the bone) (Tt.Ar, mm^2), which is a measure of the tissue found within the periosteum, calcified or otherwise; cortical bone area (Ct.Ar), which is the total bone area found within the periosteum; and the cortical area fraction (Ct.Ar/Tt.Ar, %), which is a measure of the percentage of the total endosteal area that is bone tissue. As with the trabecular bone, these are the key readouts for describing cortical bone morphology[209]; however, the readout for average

cortical thickness is not shown here for reasons described in the discussion of this chapter.

Table 4.1 shows the morphological parameters described above for the trabecular bone of the tibia in male and female mice. In males we see that there were significant effects in all parameters caused by duration of diet yet none in relation to diet itself. The same pattern emerges in the females. This indicates that the tibial trabeculae do not respond to CR yet changes are observed with age of the mice. The trabeculae region analysed (as described in the methods) is near the proximal region of the long bones, therefore these results appears to be counterintuitive based on previous data showing large increases in BMAT volume in the proximal tibia of both males and females and considering that such BMAT expansion is often associated with loss of calcified tissue. However, they are consistent with previous studies showing that CR does not cause trabecular bone loss in mice[194].

In table 4.2 shows parameters for the cortex of the tibia. Some significant effects were caused by diet, with the tibial cortex of male CR mice being smaller than AL controls. This was particularly evident for Ct.Ar, indicating that the endosteum has shrunk whilst the periosteum has remained constant. The same effect occurred in females with CR mice exhibiting lower Ct.Ar and Ct.Ar/Tt.Ar than the AL controls. This again indicates that the endosteum is shrinking and likely to a greater extent than the male mice given the greater degrees of significance seen in the Ct.Ar/Tt.Ar parameter. This bone loss in males and females may reflect the previously observed CR-induced increase in BMAT volume, especially considering that it is the inner membrane of the cortical bone that is being reduced.

Table 4.3 shows the trabecular parameters for the femurs. In male mice no significance was observed for any of the parameters whereas in females both diet and duration were significant effectors of total variance of the data with multiple comparisons showing that BV/TV was significantly down and Tb.Sp up in CR mice compared to AL. This indicates a modest and longer-term reduction in the trabecualae of female femurs. These results reflect the BMAT volume data which showed small increases in BMAT volume of male femurs compared to far larger increases in female femur BMAT. This may show that the femoral trabeculae respond more rapidly to changes in BMAT volume when compared to the tibial trabeculae.

Quantification of the femoral cortex morphology is shown in table 4.4. Diet was a significant source of variation in the male mice in the Ct.Ar and Ct.Ar/Tt.Ar with significant differences detected by multiple comparison after 6 weeks of CR compared to 6 weeks of AL diet in these parameters. Female mice showed far greater losses in femoral cortex caused by CR. Diet was a significant source of variance in all parameters measured and multiple comparisons showed significant differences after 2 weeks of CR

diet in Ct.Ar and Ct.Ar/Tt.Ar. This indicates a more rapid loss of bone tissue in the femurs of females mice compared to males which is reflective of the greater CR-induced increases in femoral BMAT volume of female mice giving further evidence of a link between bone loss and BMAT volume.

The final bone to be analysed was the humerus, given the previous results showing no detectable BMAT in the humeri of male or female mice we hypothesised that there would be no significant changes in bone parameters if there is a link between BMAT and bone loss in CR. As shown in table 4.5, neither male nor female mice displayed diet related significant differences in trabecular parameters. In the cortex of the humeri some significant effects of the diet were observed. In males the Ct.Ar and Ct.Ar/Tt.Ar showed diet as a significant source of variance, additionally, multiple comparisons showed 6 week differences in Ct.Ar and 4 and 6 week differences in Ct.Ar/Tt.Ar. In the females a similar pattern was observed but to a slightly greater extent, with all parameters showing diet as a significant source of variance, Ct.Ar with 4 and 6 week differences in CR compared to AL and a 6 week difference in Ct.Ar/Tt.Ar. This again shows that the cortex of bones appears to be more reactive to CR-induced bone loss than the trabeculae.

A summary of the effect of calorie restriction on bone morphology parameters are as follows:

CR-induced changes	Tibia		Femur		Humerus	
	Trabeculae	Cortex	Trabeculae	Cortex	Trabeculae	Cortex
Male	No change	↓	No change	↓	No change	↓
Female	No change	↓↓	↓	↓↓↓	No change	↓↓

Tibial Trabecular Analysis

Male	Mean ± SD								Source of variance						Multiple comparisons AL vs CR P value			
	Experiment duration								Diet		Duration		Interaction		Experiment duration			
	1 week		2 weeks		4 weeks		6 weeks		% total variance	P value	% total variance	P value	% total variance	P value	1 week	2 weeks	4 weeks	6 weeks
Diet	AL	CR	AL	CR	AL	CR	AL	CR										
BV/TV	88.6 ± 3.40	89.1 ± 4.94	67.1 ± 2.09	64.6 ± 4.40	85.3 ± 1.44	84.1 ± 1.75	76.0 ± 6.77	74.0 ± 7.47	0.4382	0.3717	79.43	**<0.0001**	0.3045	0.9028	0.9998	0.864	0.9892	0.926
Tb.Th	0.0636 ± 0.00565	0.0656 ± 0.0134	0.078 ± 0.00375	0.0770 ± 0.00505	0.0555 ± 0.00570	0.0503 ± 0.00375	0.0811 ± 0.00588	0.0753 ± 0.00568	1.062	0.2269	72.59	**<0.0001**	1.705	0.4969	0.9834	0.999	0.6408	0.448
Tb.Sp	0.0161 ± 0.00114	0.0157 ± 0.00179	0.0416 ± 0.00143	0.0447 ± 0.00308	0.0165 ± 0.000427	0.0168 ± 0.000552	0.0356 ± 0.00341	0.0362 ± 0.00393	0.128	0.2549	95.22	**<0.0001**	0.2885	0.4013	0.998	0.18	0.9998	0.987
Tb.N	14.0 ± 0.777	13.9 ± 1.94	8.62 ± 0.387	8.40 ± 0.324	15.51 ± 1.47	16.78 ± 0.966	9.36 ± 0.204	9.817 ± 0.372	0.3007	0.2314	91.43	**<0.0001**	0.7914	0.2894	0.9998	0.993	0.1567	0.878

Table 4.1a – Tibial trabeculae morphological parameters. Tibiae of male mice were dissected post-cull and scanned by μCT. A representative section containing 100 slices was isolated and analysed with CTAn automation software. Statistical significance was determined by 2-way ANOVA and multiple comparisons determined using Sidak's correction are indicated on the data. *P* values in bold represent statistical significance. Numbers used as described in Figure 4.2.

Female	Mean ± SD						Source of variance						Multiple comparisons AL vs CR P value		
	Experiment duration						Diet		Duration		Interaction		Experiment duration		
	2 weeks		4 weeks		6 weeks		% total variance	P value	% total variance	P value	% total variance	P value	2 weeks	4 weeks	6 weeks
Diet	AL	CR	AL	CR	AL	CR									
BV/TV	78.5 ± 6.68	77.1 ± 12.8	84.2 ± 1.88	81.8 ± 1.64	73.7 ± 7.19	62.8 ± 7.40	5.962	0.0503	32.7	**1E-04**	4.403	0.2346	0.9721	0.9362	0.0642
Tb.Th	0.0666 ± 0.0128	0.0663 ± 0.0150	0.0509 ± 0.00332	0.0458 ± 0.00239	0.0761 ± 0.00650	0.0679 ± 0.00428	2.614	0.1482	47.42	**<0.0001**	1.558	0.5284	>0.9999	0.7473	0.4166
Tb.Sp	0.0286 ± 0.00979	0.0290 ± 0.0125	0.0167 ± 0.00049	0.0170 ± 0.000454	0.0364 ± 0.00316	0.0417 ± 0.00405	0.7619	0.4111	54.26	**<0.0001**	0.9137	0.664	0.9992	0.9997	0.5936
Tb.N	12.3 ± 3.33	12.2 ± 3.83	16.6 ± 0.776	17.9 ± 0.693	9.67 ± 0.250	9.24 ± 0.789	0.1172	0.7286	59.6	**<0.0001**	0.8635	0.6408	0.9998	0.726	0.9874

Table 4.1b – Tibial trabeculae morphological parameters. Tibiae of female mice were analysed as disclosed in table 4.1a.

Tibial Cortical analysis

Male	Mean ± SD								Source of variance						Multiple comparisons AL vs CR P value			
	Experiment duration								Diet		Duration		Interaction		Experiment duration			
	1 week		2 weeks		4 weeks		6 weeks		% total variance	P value	% total variance	P value	% total variance	P value	1 week	2 weeks	4 weeks	6 weeks
Diet	AL	CR	AL	CR	AL	CR	AL	CR										
Tt.Ar	2.60 ± 0.107	2.314 ± 0.226	2.40 ± 0.172	2.36 ± 0.142	2.74 ± 0.255	2.50 ± 0.217	2.50 ± 0.141	2.41 ± 0.327	13.05	**0.0145**	13.74	0.0918	4.881	0.4887	0.1369	0.9942	0.2838	0.9239
Ct.Ar	1.15 ± 0.0508	1.01 ± 0.122	1.11 ± 0.0730	1.042 ± 0.0481	1.15 ± 0.0674	1.00 ± 0.108	1.20 ± 0.0497	1.04 ± 0.0891	41.19	**<0.0001**	3.617	0.4891	3.364	0.5202	**0.0358**	0.5123	**0.0249**	**0.0044**
Ct.Ar/Tt.Ar	44.1 ± 2.21	43.6 ± 3.30	46.2 ± 0.770	44.3 ± 2.49	42.1 ± 2.23	40.2 ± 2.54	48.1 ± 2.19	43.3 ± 3.06	12.85	**0.005**	30.44	**0.0007**	6.26	0.2388	0.9967	0.6001	0.6347	**0.0081**

Table 4.2a – Tibial cortical morphological parameters. Tibiae of male mice were analysed as disclosed in table 4.1a.

Female	Mean ± SD						Source of variance						Multiple comparisons AL vs CR P value		
	Experiment duration						Diet		Duration		Interaction		Experiment duration		
	2 weeks		4 weeks		6 weeks		% total variance	P value	% total variance	P value	% total variance	P value	2 weeks	4 weeks	6 weeks
Diet	AL	CR	AL	CR	AL	CR									
Tt.Ar	2.12 ± 0.138	2.10 ± 0.127	2.04 ± 0.180	2.01 ± 0.142	2.13 ± 0.137	2.11 ± 0.243	0.5221	0.6373	6.601	0.252	0.06976	0.985	0.9916	0.971	0.9975
Ct.Ar	1.16 ± 0.0737	1.10 ± 0.0674	1.16 ± 0.124	0.987 ± 0.0977	1.23 ± 0.0882	1.07 ± 0.119	32.85	**<0.0001**	6.91	0.1043	4.916	0.1952	0.2797	**0.0048**	**0.0131**
Ct.Ar/Tt.Ar	55.0 ± 2.18	52.3 ± 1.76	56.9 ± 4.26	49.2 ± 3.06	57.9 ± 2.66	50.8 ± 3.38	51.73	**<0.0001**	1.513	0.5091	8.767	**0.0265**	0.0895	**<0.0001**	**0.0002**

Table 4.2b – Tibial cortical morphological parameters. Tibiae of female mice were analysed as disclosed in table 4.1a.

Femoral Trabecular analysis

Male	Mean ± SD				Source of variance						Multiple comparisons AL vs CR P value	
	Experiment Duration				Diet		Duration		Interaction		Experiment duration	
	2 weeks		6 weeks		% total variance	P value	% total variance	P value	% total variance	P value	2 weeks	6 weeks
Diet	AL	CR	AL	CR								
BV/TV	85.66 ± 1.384	85.83 ± 2.107	85.62 ± 1.202	85.221 ± 1.977	0.1248	0.878	1.074	0.6532	0.7951	0.6988	0.9835	0.9073
Tb.Th	0.056 ± 0.00219	0.0565 ± 0.00234	0.0566 ± 0.00302	0.0536 ± 0.00265	5.897	0.2459	4.294	0.3197	10.69	0.1235	0.9506	0.1088
Tb.Sp	0.0164 ± 0.000428	0.0166 ± 0.000634	0.0166 ± 0.000260	0.0165 ± 0.000545	0.07605	0.9043	0.488	0.7609	2.273	0.5133	0.8339	0.9086
Tb.N	15.31 ± 0.589	15.22 ± 0.492	15.14 ± 0.649	15.92 ± 0.562	7.81	0.1719	4.741	0.2825	12.66	0.0866	0.9566	0.06

Table 4.3a – Femoral trabeculae morphological parameters. Tibiae of male mice were analysed as disclosed in table 4.1a.

Female	Mean ± SD				Source of variance						Multiple comparisons AL vs CR P value	
	Experiment Duration				Diet		Duration		Interaction		Experiment duration	
	2 weeks		6 weeks		% total variance	P value	% total variance	P value	% total variance	P value	2 weeks	6 weeks
Diet	AL	CR	AL	CR								
BV/TV	85.9 ± 1.89	85.3 ± 1.42	84.22 ± 2.00	80.6 ± 2.31	14.56	**0.0052**	35.3	**<0.0001**	8.258	**0.0304**	0.7892	**0.0048**
Tb.Th	0.0567 ± 0.00378	0.0544 ± 0.00298	0.0511 ± 0.00395	0.0467 ± 0.00378	10.52	**0.0157**	42.38	**<0.0001**	1.175	0.3983	0.3069	0.079
Tb.Sp	0.0165 ± 0.000372	0.0165 ± 0.000360	0.0166 ± 0.000450	0.0174 ± 0.000580	14.09	**0.0134**	20.76	**0.0034**	11.53	**0.024**	0.9733	**0.0076**
Tb.N	15.2 ± 0.829	15.7 ± 0.700	16.5 ± 0.950	17.4 ± 1.05	7.94	**0.0419**	40.56	**<0.0001**	0.4198	0.6281	0.3354	0.2103

Table 4.3b – Femoral trabeculae morphological parameters. Tibiae of female mice were analysed as disclosed in table 4.1a.

Femoral Cortical Anlaysis

Male	Mean ± SD				Source of variance						Multiple comparisons AL vs CR P value	
	Experiment Duration				Diet		Duration		Interaction		Experiment duration	
	2 weeks		6 weeks		% total variance	P value	% total variance	P value	% total variance	P value	2 weeks	6 weeks
Diet	AL	CR	AL	CR								
Tt.Ar	2.37 ± 0.145	2.35 ± 0.137	2.39 ± 0.150	2.42 ± 0.321	0.04509	0.9264	1.766	0.5647	0.4589	0.7683	0.9876	0.9512
Ct.Ar	0.977 ± 0.0373	0.922 ± 0.0710	1.01 ± 0.0425	0.907 ± 0.0966	28.73	**0.01**	0.4623	0.7208	2.873	0.3771	0.348	**0.0266**
Ct.Ar/Tt.Ar	41.3 ± 1.56	39.2 ± 1.02	42.4 ± 1.74	37.5 ± 2.57	47.72	**0.0002**	0.3576	0.6949	7.35	0.0869	0.1325	**0.0004**

Table 4.4a – Femoral cortical morphological parameters. Femur of male mice were analysed as disclosed in table 4.1a.

Female	Mean ± SD				Source of variance						Multiple comparisons AL vs CR P value	
	Experiment Duration				Diet		Duration		Interaction		Experiment duration	
	2 weeks		6 weeks		% total variance	P value	% total variance	P value	% total variance	P value	2 weeks	6 weeks
Diet	**AL**	**CR**	**AL**	**CR**								
Tt.Ar	2.25 ± 0.0708	2.17 ± 0.102	2.26 ± 0.102	2.03 ± 0.172	34.33	**0.0003**	5.519	0.1091	7.07	0.0714	0.1391	**0.0015**
Ct.Ar	1.01 ± 0.0466	0.916 ± 0.0620	1.12 ± 0.0502	0.865 ± 0.0682	68.37	**<0.0001**	1.177	0.2854	12.68	**0.0013**	**0.001**	**<0.0001**
Ct.Ar/Tt.Ar	44.9 ± 2.11	42.3 ± 2.46	49.0 ± 0.902	42.8 ± 1.88	48.24	**<0.0001**	12.31	**0.0053**	7.99	**0.0214**	**0.0128**	**<0.0001**

Table 4.4b – Femoral cortical morphological parameters. Femur of female mice were analysed as disclosed in table 4.1a.

Humeral Trabecular Analysis

Male	Mean ± SD						Source of variance						Multiple comparisons AL vs CR P value		
	Experiment duration						Diet		Duration		Interaction		Experiment duration		
	2 weeks		4 weeks		6 weeks		% total variance	P value	% total variance	P value	% total variance	P value	2 weeks	4 weeks	6 weeks
Diet	AL	CR	AL	CR	AL	CR									
BV/TV	90.52 ± 0.907	90.75 ± 1.008	89.59 ± 2.17	88.45 ± 2.40	89.75 ± 0.270	90.01 ± 1.131	0.5058	0.676	18.34	0.055	4.487	0.4634	0.9915	0.537	0.9854
Tb.Th	0.0628 ± 0.00405	0.0639 ± 0.00311	0.0613 ± 0.003851	0.0620 ± 0.00417	0.0604 ± 0.00280	0.0624 ± 0.00435	3.223	0.3331	6.058	0.4133	0.5611	0.9192	0.9485	0.9852	0.7383
Tb.Sp	0.0164 ± 0.000298	0.0164 ± 0.000405	0.0167 ± 0.000807	0.0173 ± 0.000775	0.0167 ± 0.000285	0.0166 ± 0.000353	2.747	0.322	18.62	**0.0463**	6.285	0.3272	>0.9999	0.2424	0.9979
Tb.N	14.45 ± 0.818	14.22 ± 0.572	14.65 ± 0.633	14.296412 ± 0.701	14.88 ± 0.660	14.47 ± 0.776	6.198	0.1804	4.58	0.506	0.3326	0.9506	0.9287	0.8116	0.6712

Table 4.5a – Humeral trabeculae morphological parameters. Humeri of male mice were analysed as disclosed in table 4.1a.

Female	Mean ± SD						Source of variance						Multiple comparisons AL vs CR P value		
	Experiment duration						Diet		Duration		Interaction		Experiment duration		
	2 weeks		4 weeks		6 weeks		% total variance	P value	% total variance	P value	% total variance	P value	2 weeks	4 weeks	6 weeks
Diet	AL	CR	AL	CR	AL	CR									
BV/TV	91.0 ± 0.899	89.9 ± 0.857	88.6 ± 1.95	88.1 ± 2.23	90.2 ± 0.987	89.6 ± 1.57	4.326	0.1717	27.36	**0.0056**	0.6201	0.8695	0.5675	0.9307	0.8838
Tb.Th	0.0633 ± 0.00257	0.0614 ± 0.00417	0.0596 ± 0.00316	0.0588 ± 0.00484	0.0599 ± 0.00326	0.0592 ± 0.00544	1.855	0.4252	11.64	0.1464	0.5056	0.9151	0.824	0.9823	0.9914
Tb.Sp	0.0163 ± 0.000312	0.0166 ± 0.000241	0.0171 ± 0.000642	0.0172 ± 0.000907	0.0163 ± 0.000244	0.0165 ± 0.000408	2.762	0.266	31.14	**0.0027**	0.6847	0.8535	0.6691	0.9877	0.9106
Tb.N	14.4 ± 0.460	14.7 ± 0.863	14.9 ± 0.584	15.0 ± 0.998	15.1 ± 0.656	15.2 ± 1.24	1.342	0.5054	9.372	0.2212	0.2121	0.9648	0.917	0.9832	0.9931

Table 4.5b – Humeral trabeculae morphological parameters. Humeri of female mice were analysed as disclosed in table 4.1a.

Humeral Cortex Analysis

Male	Mean ± SD						Source of variance						Multiple comparisons AL vs CR P value		
	Experiment duration						Diet		Duration		Interaction		Experiment duration		
	2 weeks		4 weeks		6 weeks		% total variance	P value	% total variance	P value	% total variance	P value	2 weeks	4 weeks	6 weeks
Diet	AL	CR	AL	CR	AL	CR									
Tt.Ar	1.55 ± 0.0952	1.55 ± 0.0456	1.65 ± 0.106	1.67 ± 0.0315	1.66 ± 0.0805	1.62 ± 0.140	0.1673	0.8099	22.25	**0.0319**	0.9998	0.8392	0.9997	0.9995	0.8928
Ct.Ar	0.745 ± 0.0579	0.711 ± 0.0354	0.767 ± 0.0443	0.693 ± 0.0340	0.796 ± 0.0203	0.714 ± 0.0992	26.22	**0.0029**	4.022	0.4511	2.834	0.568	0.6766	0.1259	**0.0499**
Ct.Ar/Tt.Ar	48.1 ± 1.562	45.7 ± 1.129	46.5 ± 1.88	41.8 ± 1.79	48.1 ± 2.53	43.8 ± 2.87	42.08	**<0.0001**	13.95	**0.021**	2.976	0.3959	0.1961	**0.0039**	**0.0042**

Table 4.6a – Humeral cortical morphological parameters. Humeri of male mice were analysed as disclosed in table 4.1a.

Female	Mean ± SD						Source of variance						Multiple comparisons AL vs CR P value		
	Experiment duration						Diet		Duration		Interaction		Experiment duration		
	2 weeks		4 weeks		6 weeks		% total variance	P value	% total variance	P value	% total variance	P value	2 weeks	4 weeks	6 weeks
Diet	AL	CR	AL	CR	AL	CR									
Tt.Ar	1.57 ± 0.117	1.51 ± 0.0258	1.55 ± 0.140	1.43 ± 0.0649	1.61 ± 0.0850	1.486 ± 0.0290	24.68	**0.0019**	6.696	0.2256	1.966	0.6358	0.6186	0.0585	0.0706
Ct.Ar	0.801 ± 0.0552	0.723 ± 0.0231	0.802 ± 0.105	0.683 ± 0.0430	0.881 ± 0.0892	0.698 ± 0.0466	45.65	**<0.0001**	4.48	0.2232	5.172	0.1794	0.1801	**0.0093**	**0.0001**
Ct.Ar/Tt.Ar	51.2 ± 2.57	48.0 ± 1.99	51.7 ± 3.35	47.8 ± 1.65	54.8 ± 3.44	47.0 ± 2.30	46.03	**<0.0001**	2.362	0.4499	7.648	0.0867	0.1527	0.0356	**<0.0001**

Table 4.6b – Humeral cortical morphological parameters. Humeri of female mice were analysed as disclosed in table 4.1a.

In addition to the μCT measurements of bone integrity we can also measure transcript markers of bone turnover to assess bone loss or gain in response to CR. *Bglap* is the gene encoding osteocalcin, a protein secreted exclusively by osteoblasts that is a marker of bone formation and increased mineralisation[210]. We measured transcript concentrations in the tibia, femur and humerus of male and female mice.

In male tibiae, duration was a significant source of variation but no other effects were seen. In female tibiae, diet was a significant effect indicating that female tibiae are more responsive to CR than male tibia, at least with regards to *Bglap*.

In the femurs both diet and duration were significant sources of variation in the data set in male mice. Multiple comparisons showed significant effects in 1, 2 and 4 weeks but not in 6 weeks. No significant effects were seen in the female mice. This early effect in the male femurs may show that Bglap transcript levels responds early to calorie deficit but adaption has occurred by 6 weeks of being on the diet.

In male humeri diet and duration are both significant with a significant interaction between them. There were significant differences between AL and CR mice in the 1-, 2- and 4-week groups, again indicating a rapid response followed by possible adaptation to CR by 6 weeks. This is further confirmed in female humeri, where diet was a significant source of variance and significant differences occurred between AL and CR mice in the 2-week group.

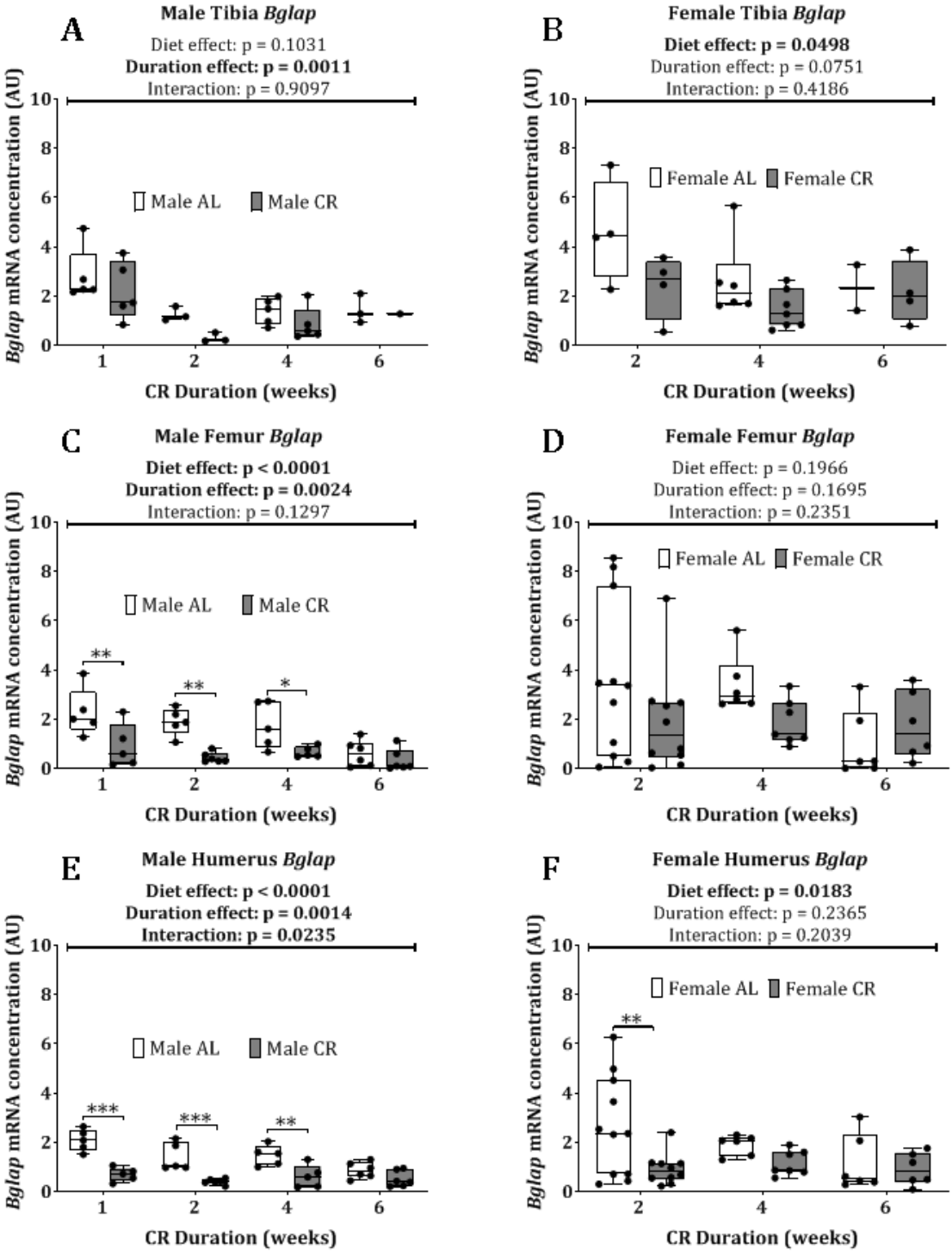

Figure 4.8 – *Bglap* expression of male and female tibia, femur and humerus. Tibiae, femurs and humeri were dissected from mice post-cull and frozen. They were homogenised in liquid nitrogen and RNA extracted. The RNA was reverse transcribed to cDNA and qPCR used to quantify concentrations of Bglap. Data is presented in arbitrary units relative to the geometric mean concentration of housekeeping gene Ppia and ribosomal RNA 18S **(A)** Bglap in the male tibia. **(B)** Bglap in the female tibia **(C)** Bglap in the male femur. **(D)** Bglap in the female femur. **(E)** Bglap in male humerus. **(F)** Bglap in

female humerus. All data points shown with median, interquartile range and range shown by box and whisker plot. Statistical significance was determined by 2-way ANOVA, source of variance significance is shown above the data and multiple comparisons determined using Sidak's correction are indicated on the data, *: $p < 0.05$; **: $p < 0.01$; ***: $p < 0.001$. Numbers used as described in Figure 4.2.

Overall, we see that, as expected, CR does exert large effects on bone morphology. Whilst transcript analysis cannot provide information on the site of bone loss it can help in confirming results seen by μCT.

4.2.5. Circulating factors that can affect bone structure

As mentioned in the introduction to this chapter, corticosterone, leptin and IGF-1 have each be proposed to play a role in both BMAT expansion and bone loss during CR. Thus, I measured the circulating concentrations of these 3 factors at weekly time points throughout the experiment to further establish their relationship with BMAT expansion and bone loss during CR.

AS shown in Figure 4.9A, in males, circulating corticosterone was significantly different between AL and CR mice, shown by diet being a significant source of variance. Additionally, duration was a significant source of variance and there was a significant interaction between diet and duration. At 1 and 2 weeks into the experiment, multiple comparisons showed significant differences between AL and CR mice. In the female mice, diet and duration were both significant sources of variance and a significant interaction was also detected. No multiple comparison differences were found to be significant. In males there appears to be a rapid increase in circulating corticosterone followed by a gradual reduction, perhaps indicating an initial stress response followed by acclimatisation to the diet. This effect can also be seen in the females. Data for the 6 week time point was collected but showed a very large spike in concentration across all groups. This increase is almost certainly caused by different blood sampling conditions at the 6-week time point compared to the preceding time points. This was caused by the blood being taken in an unfamiliar setting at with differing housing conditions immediately prior to blood sampling. The reason for this variation in conditions was due to the mice being culled immediately after the blood sampling. For this reason, the 6 week data was excluded from the analysis to prevent this erroneous data from confounding the other results. This technical issue was rectified for subsequent experiment including the data shown in chapter 6.

Diet was a significant source of variance in male leptin circulating concentrations and an interaction effect was also detected (Figure 4.9C). Multiple comparisons showed that there were significant differences between AL and CR mice at 4 and 5 weeks into the experiment. It appears that leptin gradually decreased in CR mice until 2 weeks, after

which they maintain a constant but low level of circulating leptin. The AL mice gradually increased their circulating leptin levels, with no plateau detected after 5 weeks. In females, diet was a significant source of variance and an interaction between diet and duration was also detected. There were significant differences between AL and CR groups at the 3- and 4-week time points. The female mice appear to follow a similar pattern to the male mice but within a smaller dynamic range, the leptin on the CR mice did not go as low as the male mice and likewise, the leptin of the female AL mice did not go as high as the male mice. This may relate to sex differences in total fat mass, as reported in Chapters 5 and 6. The 6-week time point was excluded as previously mentioned.

For circulating IGF-1 in both males and females, diet was a significant source of variance with an interaction also detected in the females. Duration was also a significant source of variance in male mice. Multiple comparisons did not reveal any significant differences between AL and CR males at any time points but did show a significant difference at 3 weeks in female mice. In both male and female mice IGF-1 concentrations declined in response to CR but the data showed more variation across the duration of the experiment and within each time point, making it harder to draw firmer conclusions from the data.

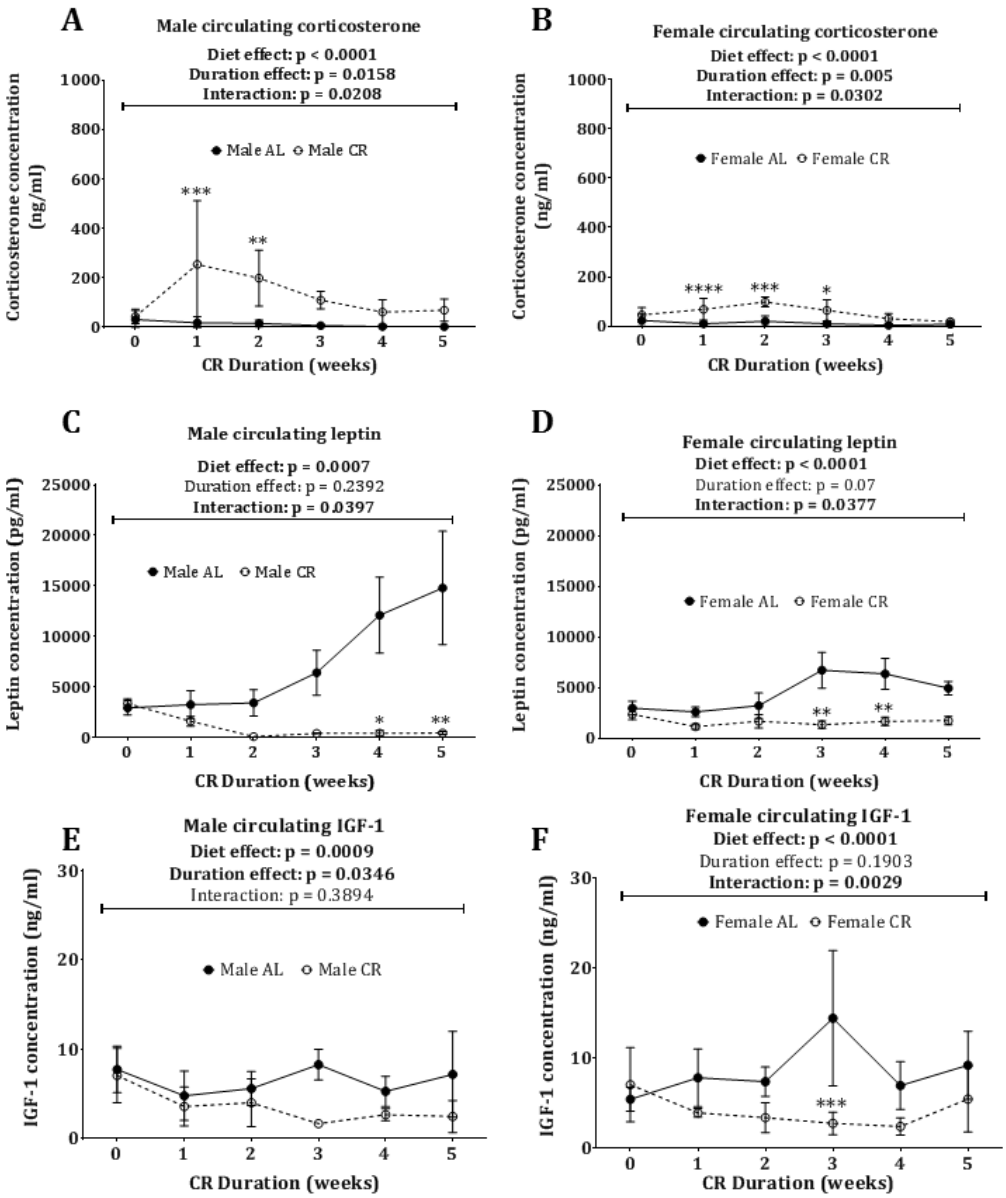

Figure 4.9 – Circulating corticosterone, leptin and IGF-1 in male and female plasma over 5 weeks of CR diet. (A) Male circulating corticosterone increased during CR. **(B)** Female circulating corticosterone showed moderate increases in response to CR. **(C)** Male leptin was significantly decreased during CR. **(D)** Female leptin was moderately decreased during CR. **(E)** Male circulating IGF-1 was mildly decreased by CR. **(F)** Female circulating IGF-1 was mildly decreased by CR. Mean concentration is shown with error bars indicating ± SD. Statistical significance was determined by 2-way ANOVA, source of variance significance is shown above the data and multiple comparisons determined using Sidak's correction are indicated on the data, *: $p < 0.05$; **: $p < 0.01$; ***: $p < 0.001$. Numbers used: all male groups 5 per group. Female AL 0w – 8; 1w – 8; 2w to 5w – 5. Female CR 0w – 9; 1w – 10; 2w to 5w – 5.

4.3. Discussion

Preceding this work, little was known about the interaction between duration of CR and BMAT increases. Six weeks of CR has been well established to increase BMAT[121,133] yet little is known about whether shorter CR durations can also promote BMAT expansion. When combining all the previous results we can build up a picture of what is happening in each bone during CR, both in terms of BMAT expansion and loss of calcified tissue. My findings show that in male tibiae there are no changes in distal BMAT volume. This is consistent with previous results showing near maximal occupation of the marrow cavity, leaving very little room for BMAT expansion[118,207]. In the proximal tibia there are large increases in BMAT volume after 6 weeks but very few changes preceding this, although at 4 weeks some of the CR mice do show an increase over their AL counterparts. The adipocyte transcript markers are inconsistent in reflecting these changes, with only milder overall diet effects seen, and so these may not be a good reflection of overall BMAT volume despite their use previously[129,211].

4.3.1. Relationship between BMAT expansion and bone loss during CR

BMAT has been suggested to contribute to bone loss[212]. Thus, given that we see large increases in BMAT volume only at 6 weeks in male tibiae, I also expected to see large decreases in calcified bone parameters at this timepoint. In both the cortex and the trabeculae of male tibiae I saw large durational effects, indicating that male tibiae are changing over the course of the experiment, irrespective of diet. Despite seeing no dietary changes in trabeculae, the cortex does show a reduction in %BV, specifically after 6 weeks of CR. This is consistent with previous research highlighting the preferential loss of cortical bone over trabecular bone during CR[194]. Moreover, it supports the possibility that BMAT expansion contributes to cortical bone loss during CR. However, *Bglap* expression in male tibiae does not show any dietary effects and so this may not be an accurate measure of overall bone integrity.

In female tibiae there is also a large increase in the proximal BMAT volume after 6 weeks of CR. As for males, this change generally is not mirrored by increases in adipocyte transcript gene concentrations. In contrast to males, females did show increases in distal tibial BMAT during CR. From the calcified measures of female tibiae I did not see any effects on trabecular bone but instead saw large effects in the cortex of these bones. Like male mice, *Bglap* transcripts in the female tibiae did not reflect the decreases in bone parameters seen by μCT, again highlighting μCT as a more robust approach to assess skeletal effects. Notably, the loss of cortical bone in female tibiae occurred by 4 weeks of CR, yet no significant increases in BMAT volume were detected at this timepoint. Thus, it may be that calcified bone loss precedes the expansion of BMAT.

In male femurs I saw modest increases in BMAT volume after 6 weeks but no changes after 2 weeks. As for tibiae, this change was not reflected in the adipocyte transcript markers in the femur. Relating these BMAT changes to μCT parameters of bone loss, we do not see any overlap in trabecular bone, but cortical %BV decreases significantly after 6 weeks. This provides further evidence for concurrent BMAT expansion and bone loss, particularly in the cortex. *Bglap* expression in male femurs shows a starkly opposite pattern to the μCT parameters, with significant differences seen at 1, 2 and 4 weeks of CR, but not 6 weeks. Thus, it may be that *Bglap* expression is a rapid responder to calorie deficit and its longer-term effects are not seen until osteocalcin concentrations have been altered for a greater period of time. Female femurs show more rapid increases in BMAT volume, with significant differences at both 2 and 6 weeks of CR. If the hypothesis that BMAT expansion causes bone loss is true, then we would expect to see more rapid decreases in bone occurring around 2 weeks of CR. The cortex of female femurs showed significant differences between AL and CR at both 2 and 6 weeks, whilst trabecular losses were limited to just 6 weeks. As before, *Bglap* expression is not reflective of bone loss parameters, with no changes in *Bglap* seen as a result of CR. Given that we see few trabecular losses it may be the case that trabecular degradation occurs more slowly or with a lower priority than cortical bone, given that here we see far earlier changes in cortical bone. These data show that, in the femur, BMAT expansion coincides with bone loss, supporting the concept of BMAT-expansion-induced bone loss.

As no BMAT was detectable in male or female humeri the adipocyte transcript data may not reflect adipocyte content, but instead may give hints to the early adipogenesis direction of skeletal stem cells within the bone marrow. We saw a large increase in *Lep* in male humeri after 6 weeks of CR, which may represent early programming prior to increased adipogenesis. However, humeral *Lep* expression is far lower than in the tibia or femur and so may not present much biological relevance. Despite seeing no BMAT in humeri, we saw large CR-associated decreases in cortical bone of both male and female humeri and large decreases in *Bglap* transcripts, particularly in males. This suggests that BMAT may be entirely unrelated to bone loss, at least in the humerus.

4.3.2. Endocrine mediators of BMAT expansion during CR

I found that, as previously proposed[129,187], leptin is decreased and corticosterone is increased in response to CR. This makes it hard to determine if one over the other is more important in the expansion of BMAT. Speculatively, the magnitude of change in leptin is great than that of corticosterone and so this could indicate that leptin plays a more significant role, however further work is required to confirm this.

4.3.3. Limitations and future directions

Whilst the adipocyte genes did not reveal any major changes and ended up being non-reflective of osmium-tetroxide-measured changes in BMAT, it may be the case that the transcript concentrations of these genes are disconnected from the protein

concentrations. It could be that these genes are further regulated at the protein level rather than transcript and if this is the case protein analysis by western blot or ELISA would give more accurate answers on bone adiposity. The same could be said for *Bglap*, analysis of the osteocalcin protein could give more answers regarding bone turnover. Additionally, considering that osteocalcin is a secreted protein, osteocalcin concentrations could also be determined from plasma samples taken throughout the experiment.

For tibial analysis of *Adipoq, Lep, Fabp4* and *Bglap*, at some time points not all mice could be included. This was caused by early attempts to split the frozen tibia at the tibia/fibula junction prior to RNA extraction to allow analysis of the proximal and distal tibia separately. Unfortunately, these attempts failed as the RNA yield from the smaller portions of bone, particularly the distal tibia, was too low to allow for effective reverse transcription. This resulted in lower than normal number for these groups and so the results may be less reliable given that they were underpowered.

Additionally, the BMAT quantification via osmium tetroxide staining may also be limited by the number of animals analysed. There appear to be trends for increased BMAT at earlier time points in the male and female tibiae that do not breach the significance threshold. More mice per group would raise the power to statistically detect these more nuanced changes.

Based on visual inspection of the data it appears that the µCT intensities in the 4 week tibia are lower than the other times points in male and female tibiae. This is likely a technical effect given that the 4 week bones were analysed later than the others. The differing intensities are likely due to unintentional variation introduced either during staining or scanning. This could be in the form of different batches of osmium tetroxide or differing amounts of time between staining and scanning introduced by variation in availability of the µCT scanner.

Interestingly, it has been demonstrated that adiponectin can have a positive effect on bone mineral density. Mice with adenoviral overexpression of adiponectin have increased bone mass compared to lacZ-overexpressing controls[213]. It was shown that this effect is caused by a dual action of adiponectin to suppress osteoclasts and induce osteoblasts[213]. This is paradoxical to our results here where we see large increases in adiponectin coinciding with losses in bone density.

We observed very large increases in the concentration of corticosterone in both female CR and AL mice at the 6-week time point (data excluded). This may have been caused by a change in location at this time point prior to blood sampling. Specifically, at the point of cull the mice were transferred to our *ex vivo* facility to allow for rapid processing of tissues. In the cohort analysed for corticosterone the blood was taken from the mice in this ex-vivo facility and transfer of the animals may have caused a large stress response,

confounding the results. In future cohorts we performed the blood sampling in the normal animal facility in which the mice were well habituated to having blood sampled in. Future work could quantify circulating corticosterone in my later cohorts to obtain more representative concentrations for corticosterone at the 6-week time point. This procedure was also performed on the mice used for leptin and IGF-1 quantification and so this data was also excluded despite showing a smaller stress effect.

5. Determination of the temporal relationships between BMAT expansion, adiponectin and metabolic adaptations induced by caloric restriction

.

5.1. Introduction

Our previous work found that BMAT is an important source of adiponectin during CR[121], based on the observation that mice resistant to BMAT expansion also showed blunted hyperadiponectinaemia. In parallel to this, the mice also showed attenuation of CR-induced mitochondrial biogenesis in skeletal muscle but not in liver; however, they also had unaltered glucose homeostasis, as determined by glucose tolerance testing. These findings suggest that BMAT, through adiponectin or perhaps other factors, may be contributing to a subset of systemic metabolic effects of CR. However, this remains to be firmly established. Thus, the goal of the studies in this chapter was to determine the temporal relationships between BMAT expansion and metabolic adaptations to CR.

5.1.1. Metabolic consequences and mechanism of CR

The reported metabolic benefits of CR are numerous, including reducing cholesterol, fasting glucose and insulin, C-reactive protein and systolic and diastolic blood pressure[214]. In addition to reduced fasting insulin, insulin sensitivity is also improved[196] as well as improved mitochondrial function[215]. Despite the effects of CR being well defined, the mechanism behind these effects is less so, with many hypotheses focussing on the effect of CR on mitochondrial function. In particular, adiponectin is known to be elevated in CR and correlates inversely with fat mass[101] but positively correlates with increased fatty acid oxidation and a reduction in peripheral lipid accumulation[216]. Overexpression of adiponectin has been shown to prevent some of the damaging effects of diet-induced obesity such as hyperinsulinemia and hyperglycaemia[217] and can even prevent metabolic dysregulation in morbidly obese *ob/ob* mice[218]. Furthermore, chronic treatment of *db/db* mice with adiponectin has been shown to alleviate some of the diabetic symptoms of these mice, including hyperglycaemia and hepatic steatosis[219]. Despite these effects being well known, the time frame in which adiponectin increases and induces metabolic effects is less well understood. Despite this, there is some evidence that adiponectin acts as a rapid mediator of insulin sensitivity. For example, administration of the hormone fibroblast growth factor 21 (FGF21) causes very rapid increases in insulin sensitivity yet this effect is abrogated in *Adipoq* KO mice, indicating that adiponectin contributes to these rapid metabolic improvements. However, whether this is the case in CR is unknown[220].

Mitochondria are classically described as the power houses of the cell and are the site of oxidative phosphorylation, where large quantities of ATP are synthesised via the electron transport chain and ATP synthase. CR has been shown to have an important effect of increasing mitochondrial number and this has been proposed to be a mechanism of action for CR's beneficial metabolic effects[221]. Data from rats exposed to a 40% CR diet from weaning to 12 months of age show that CR induces an increase in proliferation of mitochondria with a decrease in ROS generation and no reduction in ATP output[222]. Additionally, they showed that this effect was dependent on peroxisome proliferation-activated receptor coactivator 1α (PGC-1α)[222]. This phenomenon is also observed in humans: healthy participants fed a 25% CR diet for 6 months showed increased expression of mitochondrial function genes including PGC-1α and transcription factor A mitochondria (TFAM) in Vastus lateralis muscle from the quadriceps[215]. However, the ability of CR to increase mitochondrial number is controversial, with some data suggesting no role for CR in these increases[223-225]. A final gene of interest is medium-chain acyl-CoA dehydrogenase (*Acadm* or *Mcad*), a mitochondrial gene involved in fatty acid metabolism. Along with PGC1α and TFAM, *Acadm* has been shown to increase with CR and may provide another readout of mitochondrial function and number[226].

5.1.2. Long-term vs short-term CR

Fasting can be considered the shortest duration of CR. Despite the short time involved, large metabolic effects are seen as the body acts to maintain energy homeostasis[77]. Few studies have investigated the durational effects of CR and the time frames needed to elicit particular effects. One study feeding rats a 40% restricted diet for either 2 weeks, 2 months or 6 months showed that some effects occur rapidly and are maintained, such as a reduction in reactive oxygen species (ROS) production, whilst some effects occur rapidly but are lost over time, including decreased serum non-esterified fatty acid (NEFA) levels[227]. Furthermore, some effects take a long time to develop, such as decreased mass-adjusted oxygen consumption[227]. Crucially, no studies have examined the relationship between CR duration, BMAT expansion, hyperadiponectinaemia and metabolic adaption.

5.1.3. Sexual dimorphisms in response to CR

Differential effects of CR have been reported with males and females. The most widely studied is the effect on fertility: CR has been shown to have a negative effect on female fertility yet no effect on males[228-230]. This may link back to cardio-metabolic health given that premenopausal women are more resistant to obesity-induced heart disease compared to males[231]. In addition, some metabolic adaptations that are present in males are absent in females in response to CR including reduced plasma lipoprotein concentrations[232]. One striking difference between males and females is the difference in

loss of fat mass in response to CR. Men loose more fat mass than females but the exact mechanism causing this is not well known[233] and interestingly, not all studies show this effect[234]. One recent study also revealed sex differences in CR-induced weight loss and improvements in glucose homeostasis: compared to females, males displayed greater weight loss, decreases in fasting insulin and the HOMA-IR index (a proxy for insulin resistance), and improvements in an oral glucose tolerance test[235]. However, the mecahnisms underlying these sex differences, and whether they relate to effects on BMAT and/or circulating adiponectin, remain unknown.

5.1.4. Aims of the chapter

This present chapter aims to address two interconnected questions. Firstly, given the results presented in the previous chapter, here I examined the corresponding metabolic effects present across the same time points of CR. This is to provide answers about the contribution of expanding BMAT to metabolic adaptions during calorie restriction. The second question is the role adiponectin is playing during CR, by looking at the temporal increases in adiponectin and how these correspond with the temporal metabolic adaptions. Whilst both the BMAT expansion, hyperadiponectinaemia and metabolic adaptions will be purely associative, establishing these temporal relationships will begin to inform the potential causal role of BMAT expansion and/or hyperadiponectinaemia in the metabolic benefits of CR.

5.2. Results

5.2.1. Basic measures of CR on whole body composition

As shown in Chapter 4, CR decreased body mass in both male and female mice,. However, to assess the metabolic effects it is necessary to measure the impact of CR on body composition. Indeed, lipectomy recapitulates many of the metabolic benefits of CR[236], suggesting that loss of fat mass contributes to such CR-induced metabolic effects. Moreover, lean tissues such as skeletal muscle are a key site of glucose disposal and thereby influence metabolic homeostasis[237]. Therefore, to begin addressing the time-dependent metabolic effects of CR, I first analysed body composition to assess fat and lean mass.

Given that both sexes of mice are displaying a decrease in body mass, we can further characterise the tissue loses to specific tissue groups by time domain nuclear magnetic resonance (TD-NMR) which can quantify body composition based on the local environment of the protons in the mice as either in a lean, fat or liquid environment. Mice were analysed every 2 weeks. Figure 5.1 shows the fat and lean masses of both male and female mice expressed in absolute amount (g) and as a percentage of total body mass for each mouse. For both sexes there were no differences between AL and CR groups at the baseline (0 week) time-point, indicating no pre-existing differences in body

composition between the groups. For male fat mass, both in absolute terms (5.1A) and as a percentage (5.1C), significant decreases occurred after the first measurement at 2-weeks post-CR. This was followed by a maintenance of fat mass from weeks 2 to 4 and an increase between weeks 4 to 6. Multiple comparisons revealed that, at all time points, fat masses in CR males were significantly lower than the corresponding time point in AL mice, except for percentage fat mass at the 6-week time point. This indicates that the body mass decreases observed in figure 5.1 are, at least in part, driven by catabolism of fatty tissues. These is likely to be mostly accounted for by white adipose tissues, however this cannot be determined by TD-NMR alone. The other major tissue type detectable by TD-NMR is lean mass. In males, absolute lean mass (E) significantly decreased across 2,4 and 6 weeks of CR. However, unlike fat mass, percentage lean mass (G) was greater in CR vs AL males at the 2- and 4-week time points, with no significant differences detected after 6 weeks of CR. This indicates that CR differentially affects lean mass and fat mass in male mice. Whilst lean mass decreases in absolute terms, CR males become leaner in terms of percentage body mass. This indicates that whilst males catabolise some lean tissue during CR, this is being relatively protected whilst fat loss accounts disproportionately for their overall loss of body mass.

In female mice a different result is seen to the males. ANOVA revealed that, for female absolute fat mass (B), diet was not a significant source of variance. A similar result was seen for females' percentage fat mass (D), where there was no significant effect from diet over the entire data set and only duration is a source of variance; however, the effect of diet ($p = 0.062$) was near the threshold for significance, albeit with CR females tending to have *higher* percent fat mass than their AL counterparts. This result shows that, rather than catabolising fat, females may preferentially be protecting their fat mass during CR. As seen previously, the female mice have decreased body mass during CR (Figure 4.1) and so given that they are not losing fat mass it seems likely that they may show a reduction in lean mass. This was observed in absolute terms (F), with a significant source of variation caused by diet and multiple comparisons revealing significant differences at all post-intervention time points. When quantified as percentage of body mass the dietary effect is no longer observed, showing that the female mice are losing lean mass proportionally to the loses in body mass during CR.

Together, these data show that male mice catabolise both fat and lean tissue in response to CR, with a preference for fatty tissues. In contrast, females do not catabolise fat mass in response to CR and instead utilise lean mass in a manner proportional to body mass decreases.

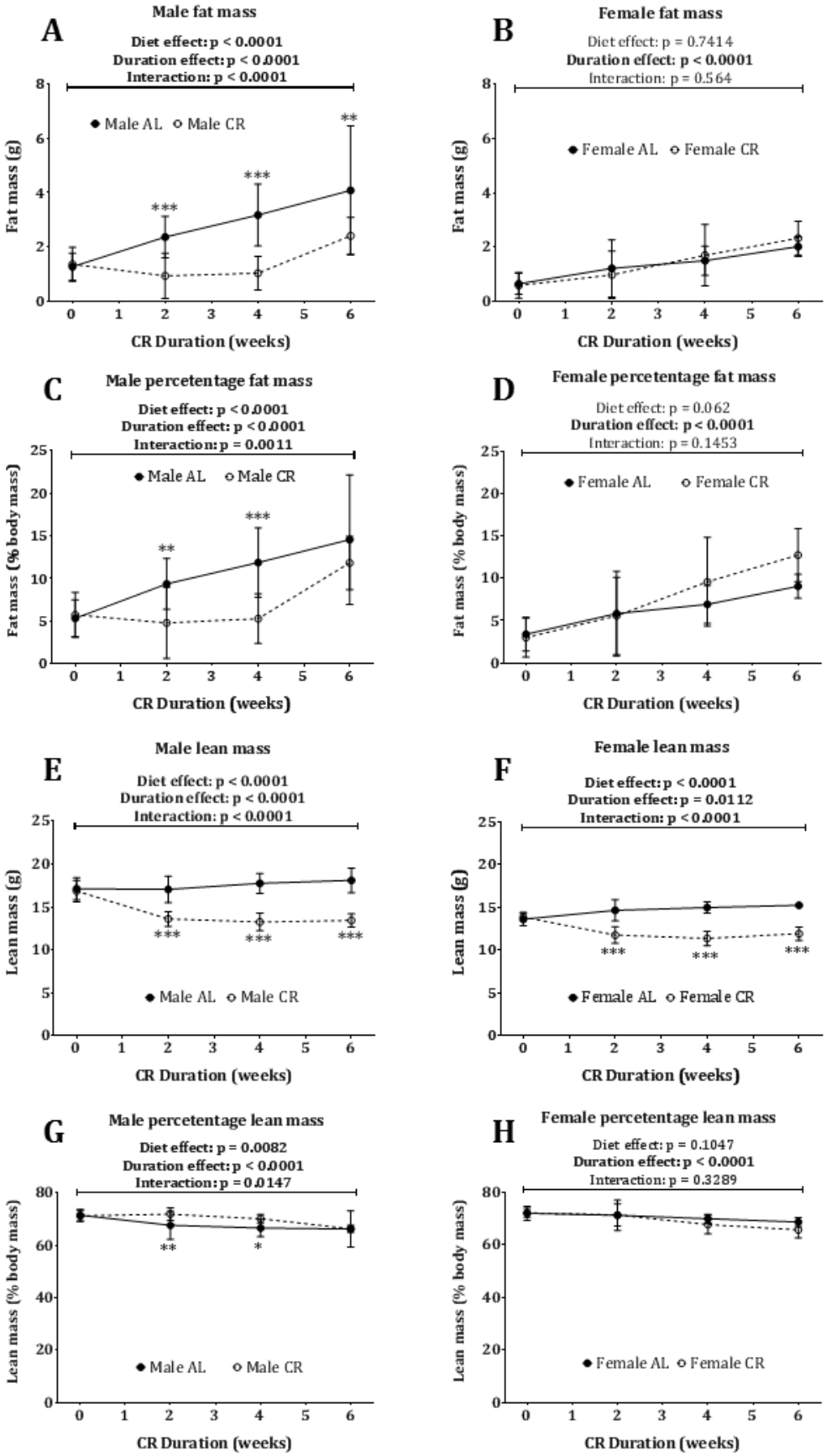

Figure 5.1 – Body composition determined by TD-NMR in male and female mice

over 6 weeks CR diet. Male and female mice underwent TD-NMR every two weeks. **(A)** Male fat mass expressed in grams. **(B)** Female fat mass expressed in grams. **(C)** Male fat mass expressed as percentage of body mass. **(D)** Female fat mass expressed as percentage of body mass. **(E)** Male lean mass expressed in grams. **(F)** Female lean mass expressed in grams. **(G)** Male lean mass expressed as percentage of body mass. **(H)** Female lean mass expressed as percentage of body mass. |Data are presented as mean ± SD of the following numbers of mice per group: male AL (n=x), male CR (n=x), female AL (n=x), female CR (n=x). Statistical significance was determined by 2-way ANOVA, source of variance significance is shown above the data and multiple comparisons determined using Sidak's correction are indicated on the data, *: $p < 0.05$; **: $p < 0.01$; ***: $p < 0.001$. Number used Male AL 0w – 21; 1w – 21; 2w – 16; 3w – 13; 4w – 11; 5w – 8; 6w – 6. Male CR 0w – 22; 1w – 22; 2w – 17; 3w – 11; 4w – 11; 5w – 6; 6w – 6. Female AL 0w- 23; 1w – 23; 2w – 23; 3w – 12; 4w – 12; 5w – 7; 6w – 6. Female CR 0w – 23; 1w – 23; 2w – 23; 3w – 16; 4w – 13; 5w – 9; 6w – 6.

5.2.2. Absolute adipose depot mass changes caused by different durations of CR

Whilst TD-NMR can detect changes in lipid-associated protons, it cannot specifically attribute these changes to adipose tissue given that lipids exist in many other tissue types. To investigate if WAT mirrors the gross changes in fat mass, specific adipose depots from each group of mice were dissected and weighed post-mortem. Figure 5.2 shows the absolute mass of three typical WAT depots as well as the thermogenic BAT. Inguinal WAT (iWAT) is found subcutaneously around the groin and can extend into the dorso-lumbar region. Gonadal WAT (gWAT) is found around the gonads and is a visceral adipose depot. Also found viscerally is the mesenteric WAT (mWAT) which is found outside the intestines of the mice. For male iWAT and gWAT (5.2A), diet was a significant source of variation indicating that the reduced fat mass detected by TD-NMR is at least partly related to decreased iWAT and gWAT mass. Duration also significantly affected gWAT mass, which increased over time in the AL mice but not in the CR males. Indeed, multiple comparisons revealed that CR males had significantly less gWAT than AL males at 4 and 6 weeks (5.2A). In the mWAT (A) of the male mice, no significant differences were observed.

Findings for females were also consistent with the TD-NMR, with female WAT depots (B) not showing any significant differences caused by diet. Duration of the experiment significantly influenced both iWAT and gWAT masses in females, but not the mass of mWAT. These data further support the conclusion that, during CR, male mice catabolise fat mass whilst female mice do not. Moreover, it shows that the fat mass in question is adipose tissue, specifically gWAT and to a lesser extent iWAT.

A further fatty tissue that is distinct to WAT is BAT, which acts to burn fatty acids to generate heat, rather than to synthesise ATP. Some studies have found that CR in rodents

or humans decreases BAT activity[238-240], although variable effects on BAT mass have been reported[238,241]. Nevertheless, given that BAT contains a high proportion of lipid, I postulated that altered BAT mass may contribute to some of the fat mass changes seen by TD-NMR. Thus, BAT was dissected from the interscapular region and weighed. In males (C) no significant differences were observed in absolute BAT mass, indicating that the fat mass differences seen by TD-NMR are not influenced by changes in BAT mass. In contrast, in females (D) diet was a significant source of variation, with a significant difference detected by multiple comparison between AL and CR after 2 weeks of CR and a trend after 4 weeks. There was also a significant interaction in females, with BAT mass tending to increase over time in AL females but decrease over time in CR females.

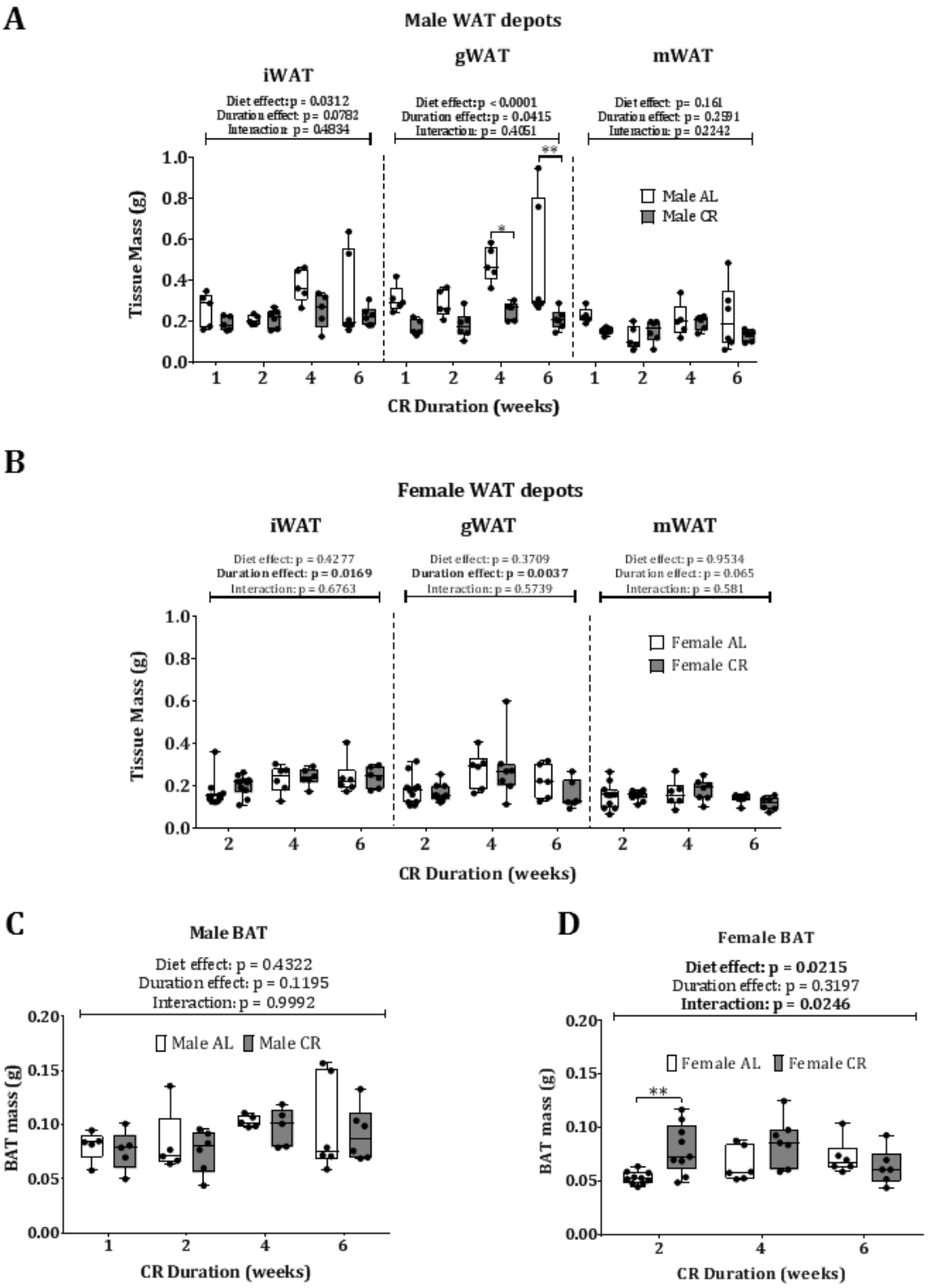

Figure 5.2 – WAT and BAT depot masses in male and female mice across 6 weeks CR diet. Male and female mice were culled by cervical dislocation and tissues were dissected and weighed. **(A)** iWAT, gWAT and mWAT depot masses in male mice. **(B)** iWAT, gWAT and mWAT depot masses in female mice. **(C)** Male BAT mass. **(D)** Female BAT mass. All data points shown as box and whisker plots with median, interquartile range and range. Statistical significance was determined by 2-way ANOVA, source of

variance significance is shown above the data and multiple comparisons determined using Sidak's correction are indicated on the data,*: $p < 0.05$; **: $p < 0.01$. Numbers used as described in figure 4.2.

5.2.3. Relative adipose depot mass changes caused by different durations of CR

As for TD-NMR, these tissue masses can also be quantified as a percentage of the total body mass for each mouse. This can provide more insight into the relative bias for tissue gains or losses compared to the absolute changes. In the male WAT depots, no significant effect was seen for iWAT or mWAT; however a significant effect caused by both diet and duration was observed in the gWAT (5.3A). No significant effects were seen for BAT (C), in concordance with results for absolute BAT mass. These findings indicate that, of the depots analysed, gWAT is the most preferentially metabolised adipose depot in males. In females (D) ANOVA showed that diet was a significant source of variation for iWAT and BAT, with interactions detected for BAT. Thus, percent iWAT tended to be greater in CR vs AL females across all time points, while multiple comparisons revealed significantly increased BAT in CR vs AL females at 2 and 4 weeks of CR. Again, this is in concordance with results for absolute mass of BAT and further indicates that BAT increases during CR in females, but not in males.

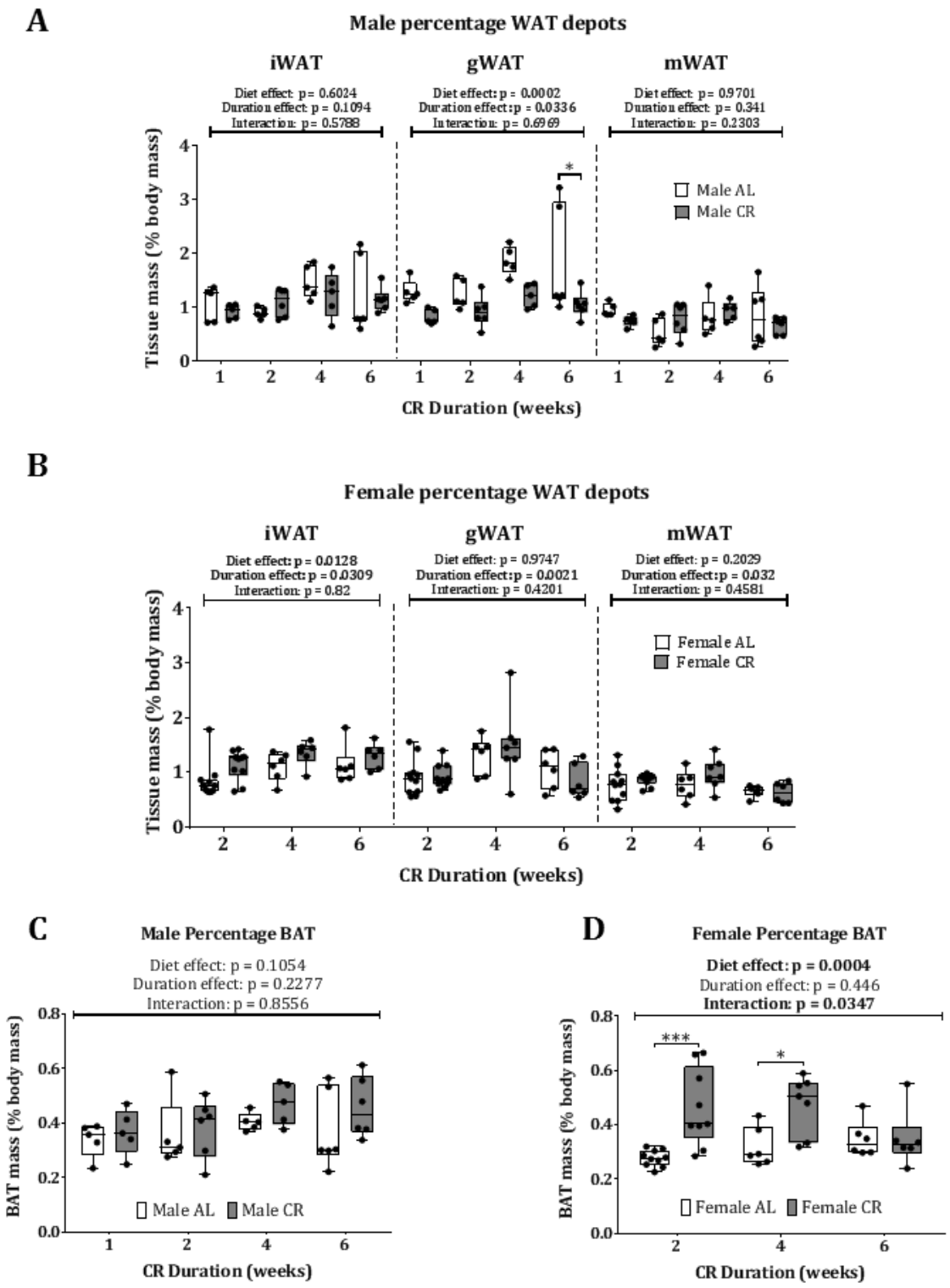

Figure 5.3 – WAT and BAT depot mass percentages in male and female mice across 6 weeks CR diet. Male and female mice were culled by cervical dislocation and tissues were dissected, weighed and presented as a percentage of total body mass for individual mice. **(A)** iWAT, gWAT and mWAT depot masses in male mice. **(B)** iWAT, gWAT and mWAT depot masses in female mice. **(C)** Male BAT mass. **(D)** Female BAT mass. All data points shown with median, interquartile range and range shown by box and whisker

plot. Statistical significance was determined by 2-way ANOVA, source of variance significance is shown above the data and multiple comparisons determined using Sidak's correction are indicated on the data,*: $p < 0.05$; ***: $p < 0.001$. Numbers used as described in figure 4.2.

5.2.4. Total and percentage masses of liver and spleen in response to different durations of CR.

In addition to adipose depots other tissues typically lose mass during CR, but the speed at which these changes occur is not well characterised. Both liver and spleen have been shown to decrease in mass in response to CR over a duration of 3 months[160]. However, only male mice were analysed and so little is known how the liver and spleen of females reacts to CR. Both sexes showed diet as a significant source of variation in total liver mass, with males also showing significant differences by multiple comparisons after 4 and 6 weeks of CR (Figure 5.4 A and B). In terms of liver as a percentage of total body mass, both sexes showed no significant diet effects (E and F). Thus, whilst the livers of the CR mice are smaller than the AL controls, the loses are proportional to decreases in body mass and there is not preferential catabolism or protection of the liver in response to CR.

Even greater effects of CR were noted for spleen masses, which significantly decreased after 2, 4 and 6 weeks of CR in both sexes (C, D). In males there was also a significant duration effect, with spleen masses tending to decrease from weeks 1-2 and then remaining near week 2 levels at weeks 4 and 6 (C). When spleen mass was expressed as a percentage of total body mass, males continued to show a significant effect of duration but decreases associated with CR were only borderline significant (G). In contrast, females (H) maintained the significant CR influence seen for total spleen mass (D), with a strong effect both overall and at the 2-, 4- and 6-week time points. This indicates that whilst both sexes are decreasing spleen mass in response to CR, the decreases in males are less disproportionate to their body mass losses whereas females exhibit a greater preferential decrease in spleen mass relative to their body mass changes.

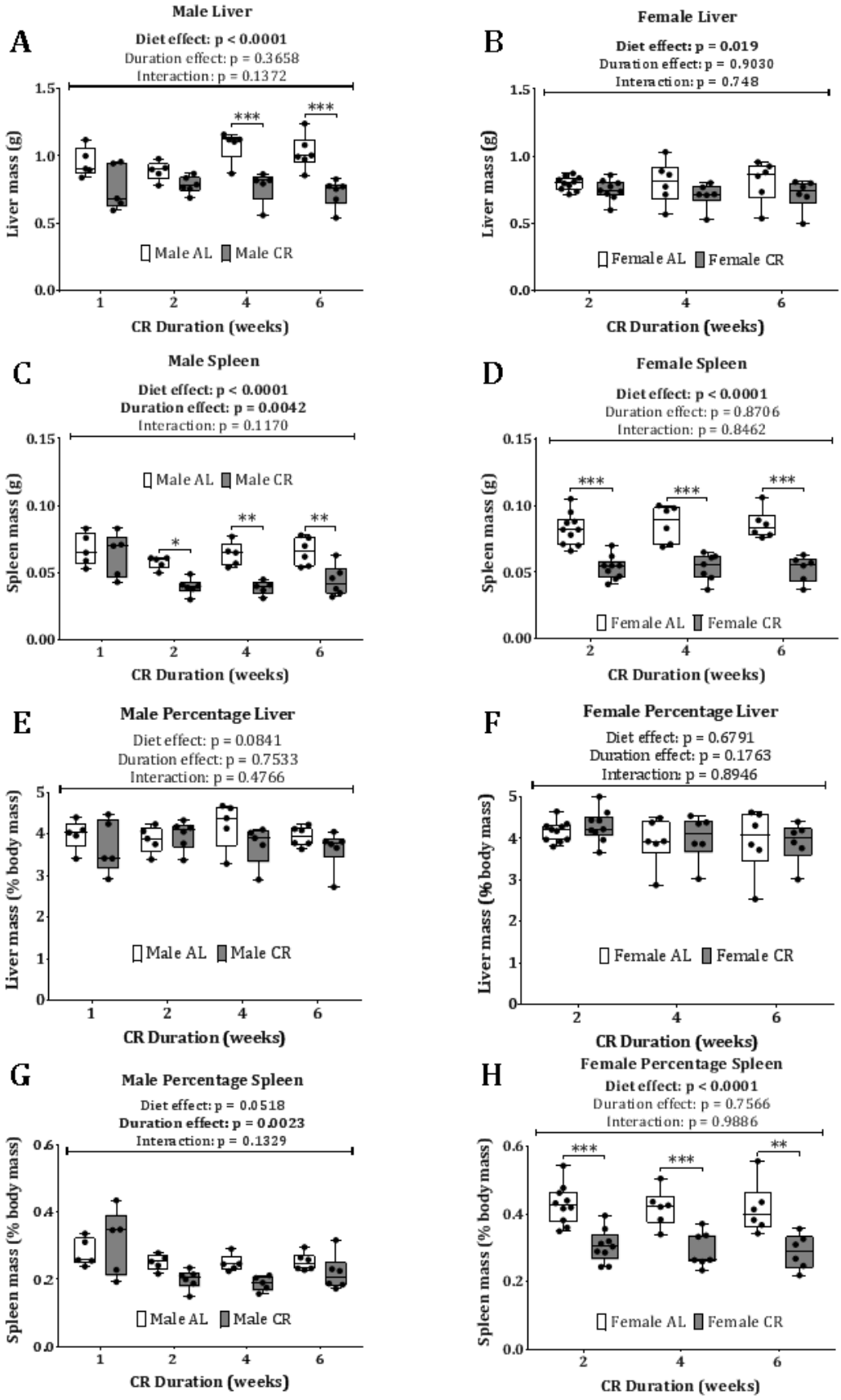

Figure 5.4 – Liver and spleen masses and percentage masses in male and female mice over 6 week CR diet. The liver and spleen were dissected and weight once the

mice had been culled **(A)** Male liver mass expressed in grams. **(B)** Female liver mass expressed in grams. **(C)** Male spleen mass expressed in grams. **(D)** Female spleen mass expressed in grams. **(E)** Male liver mass expressed as percentage of body mass. **(F)** Female liver mass expressed as percentage of body mass. **(G)** Male spleen mass expressed as percentage of body mass. **(H)** Female spleen mass expressed as percentage of body mass. All data points shown with median, interquartile range and range shown by box and whisker plot. Statistical significance was determined by 2-way ANOVA, source of variance significance is shown above the data and multiple comparisons determined using Sidak's correction are indicated on the data,*: $p < 0.05$; **: $p < 0.01$; ***: $p < 0.001$. Numbers used as described in figure 4.2.

5.2.5. Circulating total and HMW adiponectin

A primary aim of these CR studies was to determine the relationship between CR-induced hyperadiponectinaemia and CR-induced metabolic adaptions, as well as changes in BMAT and bone microarchitecture (as assessed in Chapter 4). Once the basic physiology of the mice had been established, and the model validated by confirming the basic and well-known effects of CR, work to quantify the concentrations of circulating adiponectin could begin. I measured total and HMW adiponectin by ELISA and also calculated the ratio between the two. Male total circulating adiponectin (Figure 5.5A) was significantly influenced by both diet and duration of CR, with an interaction between these factors. The same pattern occurred in females (Figure 5.5B), with multiple comparisons also revealing a similar pattern between males and females at each week of CR. Both sexes showed increases in circulating adiponectin until 4 weeks after commencement of CR, followed by a relative plateau in concentrations. HMW adiponectin in males (C) and females (D) showed significant variance caused by both diet and duration of the experiment. By multiple comparison, male mice showed differences between AL and CR groups at 1 and 4 weeks after starting the diet whilst females showed differences after 2, 3 and 4 weeks. Males also showed a drop in HMW adiponectin at week 3 of CR, though the reasons for this are unclear. When combining these two measurements into the ratio of total adiponectin as high molecular weight multimers we see no significant differences in females (F) and an effect only from duration of the experiment in males (E). This indicates that the changes in HMW adiponectin result from changes in total adiponectin rather than specific effects on adiponectin multimerisation.

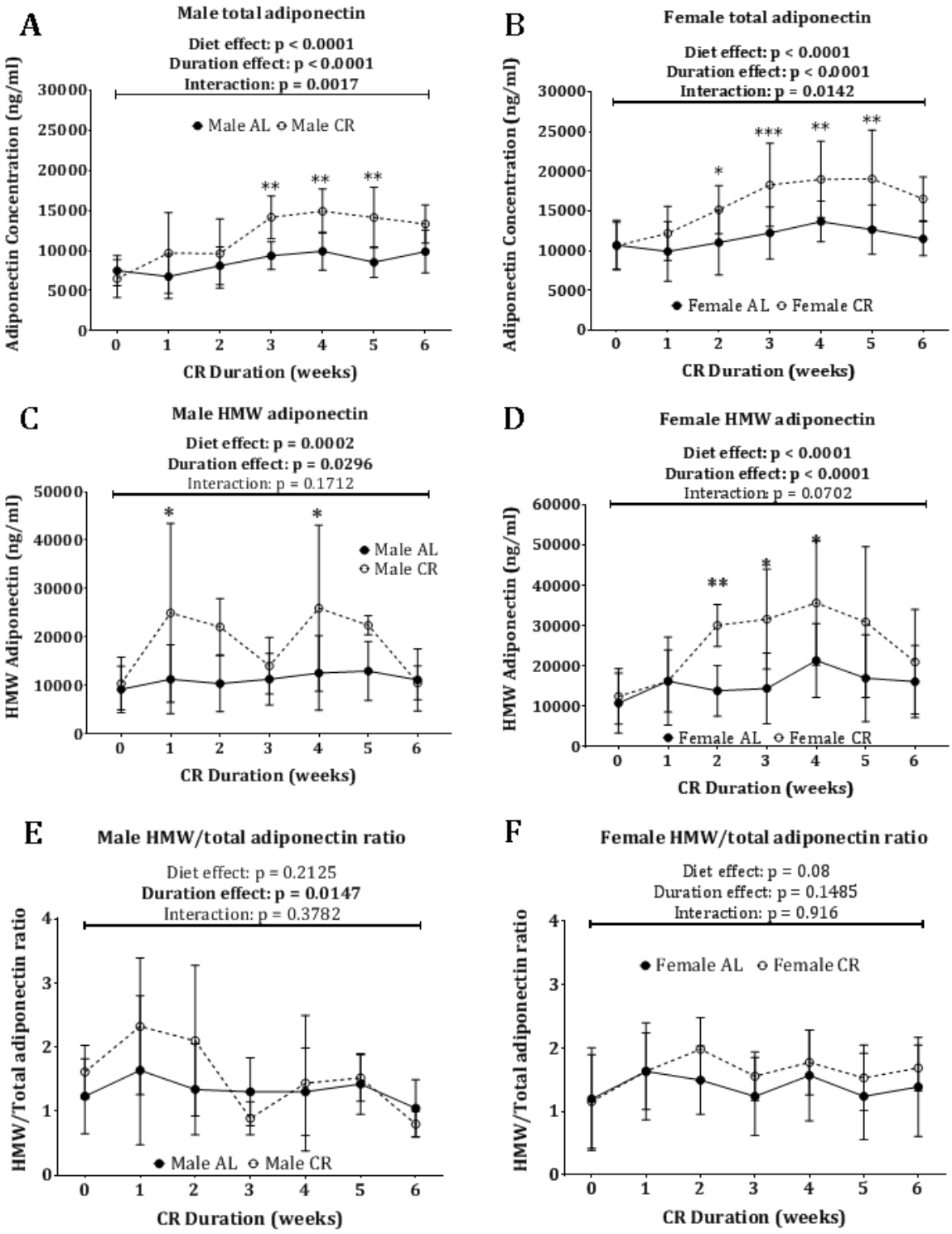

Figure 5.5 – Total, HMW and ratio of adiponectin in male and female mice over 6 weeks CR diet. Plasma obtained from tail vein bleeds and decapitation was quantified for circulating concentrations of total adiponectin and high molecular weight multimers by ELISA. **(A)** Male total adiponectin. **(B)** Female total adiponectin. **(C)** Male high molecular weight adiponectin. **(D)** Female high molecular weight adiponectin. **(E)** Male high molecular weight to total adiponectin ratio. **(F)** Female high molecular weight to total adiponectin ratio. Mean measurement is shown with error bars indicating ± SD.

Statistical significance was determined by 2-way ANOVA, source of variance significance is shown above the data and multiple comparisons determined using Sidak's correction are indicated on the data,*: $p < 0.05$; **: $p < 0.01$; ***: $p < 0.001$. Number used as described in figure 4.9.

5.2.6. CR-induced improvements in glucose tolerance

The above observations showed that hyperadiponectinaemia occurs after two weeks of CR in females but only after three weeks of CR in males and is not maximal until week 4 of CR in either sex. This raises the question of how such hyperadiponectinaemia relates to metabolic benefits of CR. Glucose tolerance tests (GTT) are used to assess the speed and extent to which organisms react to a glucose load; this reflects both glucose-stimulated insulin secretion and also insulin sensitivity. Therefore, I next used GTTs in to assess effects of CR on systemic glucose homeostasis. Mice were given an oral dose of glucose by gavage and their ability to clear the glucose was measured (figure 5.6). In all GTTs 2-way ANOVAs were performed but, unlike previous analysis, the effect of duration of the test was not considered, solely the contribution to variance by diet. In all sexes and durations, diet was a significant source of variance within the data indicating that, by 1 week in male mice and by 2 weeks in female mice, improvements in glucose tolerance were already being caused by CR. Multiple comparisons revealed some sex differences in these effects of CR. Thus, compared to their AL counterparts, CR males showed significant differences between all time points across the GTTs except for 15-minutes post-gavage in the 4-week CR group. In contrast, in females fewer time points differed significantly between AL and CR groups. This indicates that the females are showing improvements in glucose tolerance to a lesser extent than the males in response to the CR diet, consistent with observations in humans[235].

To further quantify the glucose tolerance response, area under the curve (AUC) analysis was performed in two different ways. The first was to take the bottom of the area as the 0 mM glucose measurement, whereas the second method used the fasting glucose concentration for each individual mouse as the baseline for AUC analysis; each method has its benefits. For example, when looking at the 0 mM AUC calculation we can measure the total glucose load experienced by the mouse over the course of the procedure, but the downside of this is that fasting glucose differences can significantly affect the result irrespective of any relative differences across other time points. For this reason, AUCs calculated against the fasting glucose baseline for each individual mouse are also used. This removes differences in fasting glucose as a confounding factor in the analysis and purely looks at the increases from the baseline and the speed at which the mice are able to reduce their glucose to pre-gavage concentrations. In summary, using a value of zero as the base of the area under the curve we can acquire a measure of the total glucose present in the circulation over the course of the test. Using the fasting glucose

concentration as the bottom of the area allows us to quantify the response to the glucose bolus specifically without being influenced by the initial fasting glucose concentration.

In the male AUC relative to 0 mM glucose (A) all time points show a significant difference between AL and CR groups indicating improved glucose tolerance, likely due to improvements in initial fasting glucose. However, when comparing to the AUC baselined to the fasting glucose some of these differences were no longer present. The CR mice after 2 and 6 weeks of CR maintain their reduced AUC, indicating improved glucose clearance irrespective of fasting glucose; this was not observed after 4 weeks of CR, the reasons for which are unclear. In females a similar pattern to the males is seen for AUCs relative to 0 mM glucose, with improvements in glucose tolerance seen at all time points. Unlike the males, the female mice showed no differences in AUC relative to fasting glucose concentrations. This indicates that the improvements seen in the female GTT are solely due to improvements in fasting glucose and that the response to the glucose dose is the same between AL and CR mice. This represents an important sex difference between the male and female mice in their response to CR.

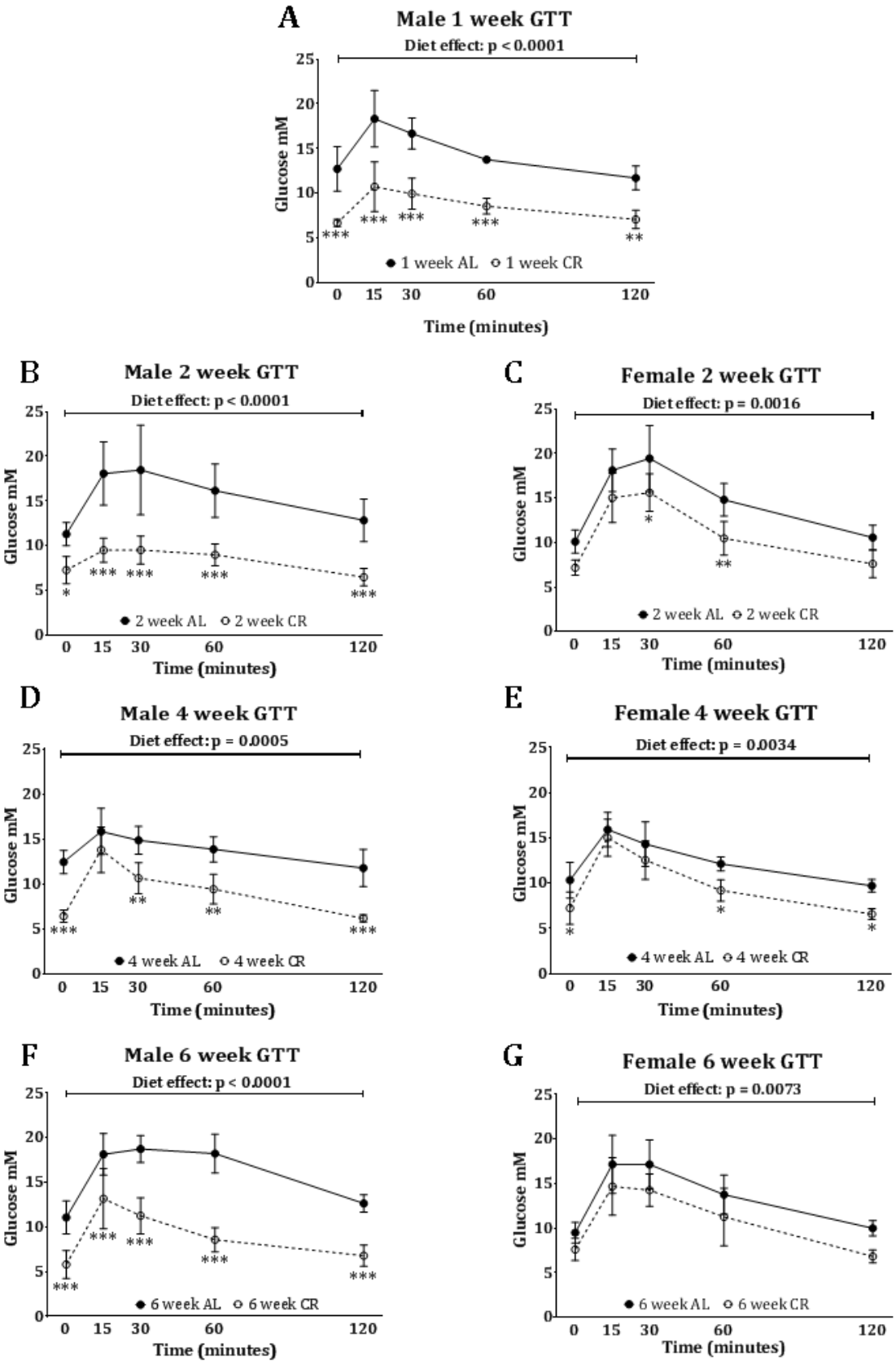

Figure 5.6 – Glucose tolerance tests blood glucose over time in male and female mice over 6 weeks CR diet/ Blood concentrations of glucose were measured using

Verio blood glucose monitor from tail vein incisions. Measurements were taken before oral glucose dose then 15, 30 60 and 120 minutes after administration. **(A)** GTT in male 1 week diet mice. **(B)** GTT in male 2 week diet mice. **(C)** GTT in female 2 week diet mice. **(D)** GTT in male 4 week diet mice. **(E)** GTT in female 4 week diet mice. **(F)** GTT in male 6 week diet mice. **(G)** GTT in female 6 week diet mice Mean measurement is shown with error bars indicating ± SD. Statistical significance was determined by 2-way ANOVA, source of variance significance is shown above the data and multiple comparisons determined using Sidak's correction are indicated on the data,*: $p < 0.05$; **: $p < 0.01$; ***: $p < 0.001$. Number used male AL and CR 1w – 5; AL and CR 2w – 6; AL 4w – 5; CR 4w – 4; AL and CR 6w – 6. Female AL 2w – 7; CR 2w – 6; AL 4w – 5; CR 4w – 6; AL and CR 6w – 6.

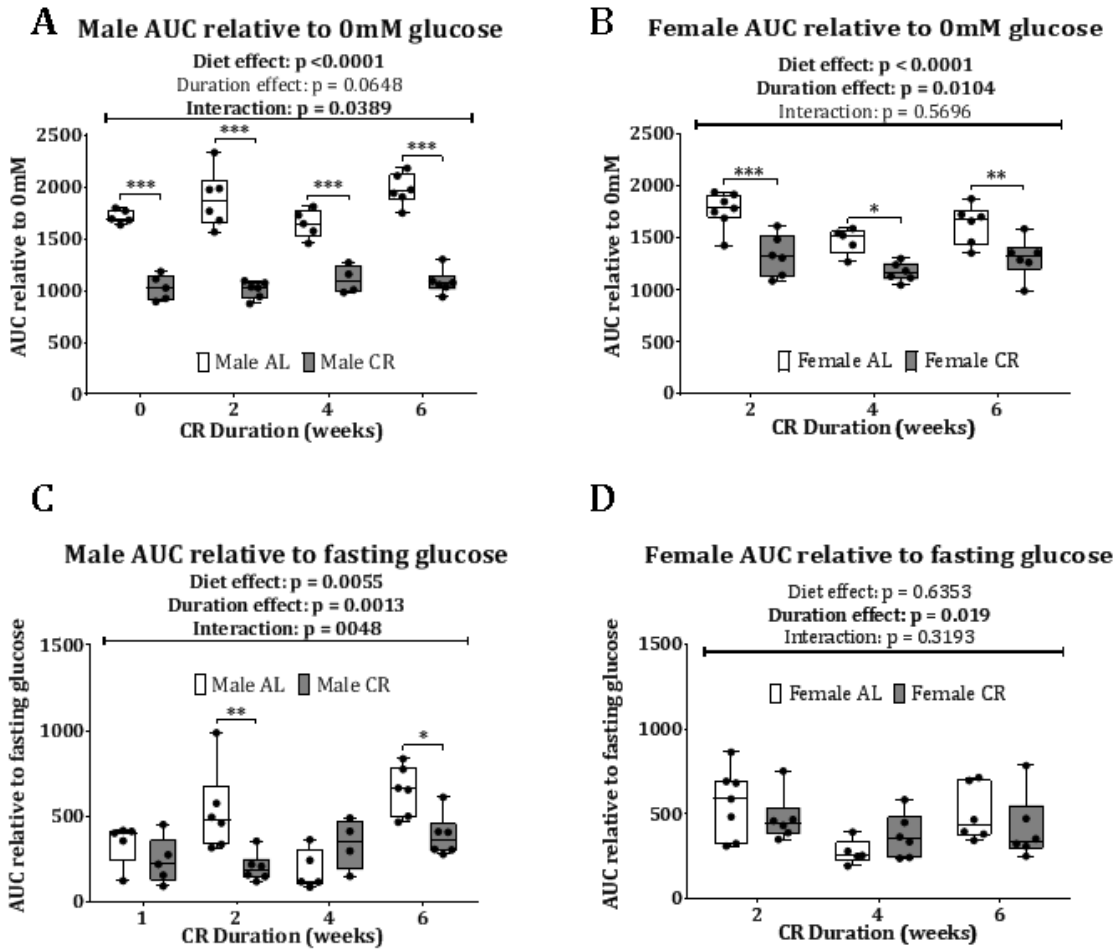

Figure 5.7 – AUC for glucose tolerance test for glucose analysed relative to 0mM and individual fasting glucose in male and female mice across 6 weeks CR diet. AUC analysis was performed on GTT plots for individual mice and the baseline for calculation was either the 0 mM glucose concentration or the glucose concentration of the fasting glucose at 0 minutes into the test. **(A)** Male GTT AUC relative to 0 mM glucose. **(B)**Female GTT AUC relative to 0 mM glucose. **(C)** Male GTT AUC relative to fasting

glucose concentration. **(D)** Female GTT AUC relative to fasting glucose concentration. All data points shown with median, interquartile range and range shown by box and whisker plot. Statistical significance was determined by 2-way ANOVA, source of variance significance is shown above the data and multiple comparisons determined using Sidak's correction are indicated on the data,*: $p < 0.05$; **: $p < 0.01$; ***: $p < 0.001$. Numbers used as described in figure 5.6.

5.2.7. Reverse feeding and lean mass GTT

One possibility is that technical issues were influencing the diet and sex effects observed in the GTT. On the evening before the GTT, AL mice were re-fed with a full daily ration of AL diet and CR mice were re-fed a full daily ration of CR diet, i.e. 70% of the mass of the AL ration. The logic for this approach is that both groups of mice will have consumed all of their diet by 07.00 the following morning, such that doing the GTT at 12.00 would represent a fast of at least 5 hours. However, it is likely that the CR mice will have consumed all of their diet sooner, leading to a longer fasting period than for the AL groups. Therefore, to test if this feeding regimen was adversely influencing the outcome, a subsequent GTT was performed which involved feeding the CR mice the normal AL pre-GTT ration, and the AL mice the normal CR pre-GTT ration. This was to test if the effects observed above resulted from long-term CR and not from short-term fasting effects. Mice underwent the GTT procedure as usual and the plots of the GTT are shown in figure 5.8A. The mean points for both the standard pre-GTT feeding and reversed diet are shown. I saw that the AL mice fed the CR diet pre-GTT performed in a similar manner to the AL mice fed the normal pre-GTT AL diet. In contrast the CR mice, when fed the AL diet before the GTT, had higher glucose levels than CR mice that had been fed the CR diet pre-GTT (Figure 5.8A). However, whether mice were fed an AL ration or a CR ration pre-GTT, CR significantly improved glucose tolerance. This validated my previous GTT results by showing that reversing the feeding between the AL and CR mice before the GTT does not alter the conclusion that long-term CR improves glucose tolerance.

Another technical issue to address relates to whether the administered glucose dose is calculated relative to lean body mass or to total body mass. Lean mass is a major site of glucose uptake and this plays a large role during a GTT [242]. In our GTTs (Fig. 5.6) we administered glucose based on total body mass; however, unlike males, female mice lose lean mass rather than fat mass during CR. Therefore, we hypothesised that females may be resisting CR-induced improvements in glucose tolerance because, compared to males, they have a lower proportional lean mass and are therefore receiving a higher relative dose of glucose relative to lean mass. To test this, a group of female mice were fed either AL or CR diet for 2 weeks then underwent a GTT with glucose administered relative to lean mass ('lean mass GTT') rather than body mass ('body mass GTT'). The plot for this lean mass GTT is shown in figure 5.8. All points, excluding 0 minutes, were significantly

different by multiple comparison between AL and CR mice, this is more than for the body mass GTTs in figure 5.6 and may indicate that glucose administration relative to lean mass-produces greater differences between the dietary groups. To directly assess this, I next compared AUCs from the lean mass GTT with those from the body mass GTT (C and D). Glucose dosing alone did significantly influence the outcome, with lower AUCs for the lean mass than for the body mass GTTs, regardless of how the AUCs were calculated (Figure. 5.8C-D). This was expected, because the lean mass dosing provided a lower total amount of glucose to the mice than the body mass dosing. However, if females' altered body composition were a major explanation for their resistance to CR-induced GTT improvements, then we would expect the CR effect to be greater for the lean mass GTT than for the body mass GTT. This was not the case: for both the 0 MM AUCs and the fasting glucose AUCs, glucose dosing did not affect the influence of CR on the GTT outcome (no interaction detected by two-way ANOVA). Indeed, for either glucose dosing regimen, CR significantly decreased the 0 mM AUCs (Fig. 5.8C) but not the fasting glucose AUCs (Fig. 5.8D). As discussed above, the improvements in the 0 mM AUCs are likely driven by decreased fasting glucose in the CR mice. Together, these data show that the lean mass GTT did not significantly influence the CR effect. Thus, we can conclude that the lean mass deficiency in the female mice is not responsible for the differing glucose tolerance phenotype seen between males and females.

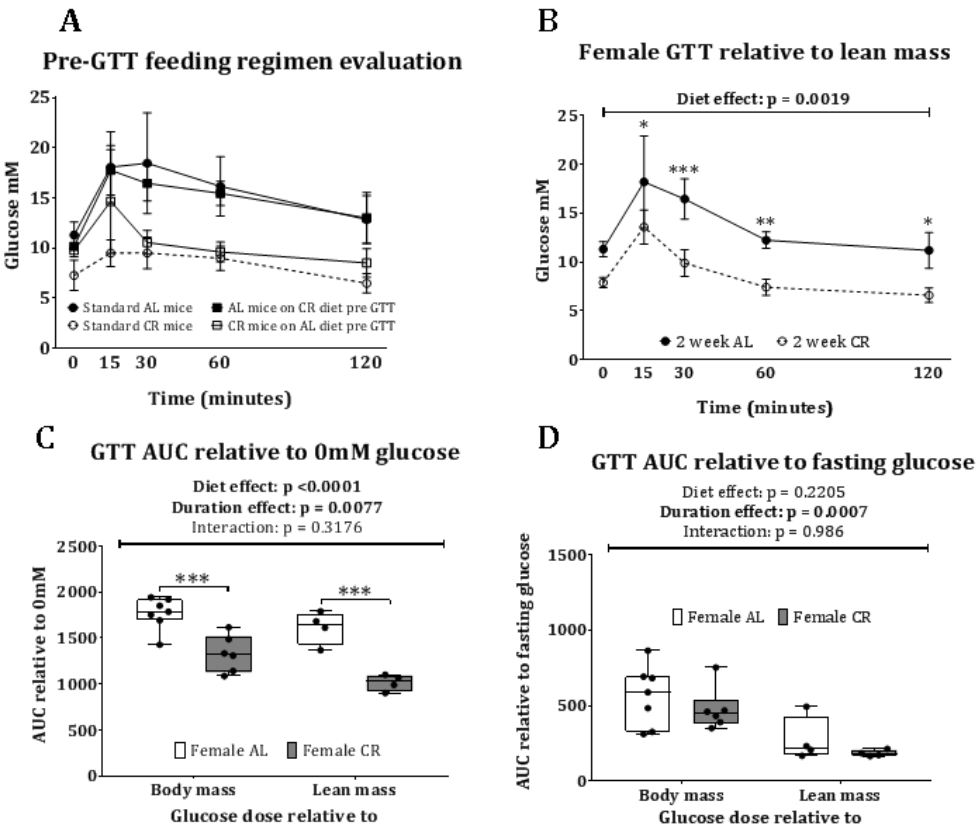

Figure 5.8 – Reversed pre-GTT feeding regime and lean mass relative glucose dose alterations on glucose tolerance tests. Male CR mice were given AL diet before the GTT fast whilst AL mice were given the CR diet pre-fast, a GTT was performed as normal. In female mice glucose was administered relative to lean mass and compared to previously acquired body mass data. AUC was calculated relative to 0 mM glucose and fasting glucose concentration. **(A)** Male mice fed either normal or alternate diet pre-fast. **(B)**Female mice given glucose relative to either body mass or lean mass. Mean measurement is shown with error bars indicating ± SD. **(C)** AUC from body or lean mass glucose dose relative to 0 mM glucose concentration. **(D)** AUC from body or lean mass glucose dose relative to fasting glucose concentration. All data points shown with median, interquartile range and range shown by box and whisker plot. Statistical significance was determined by 2-way ANOVA, source of variance significance is shown above the data and multiple comparisons determined using Sidak's correction are indicated on the data,*: $p < 0.05$; **: $p < 0.01$; ***: $p < 0.001$. Numbers used standard diet AL and CR 2w – 6; reverse fed groups AL and CR – 2. AL relative to body mass – 7; CR relative to body mass 6; AL relative to lean mass – 4; CR relative to lean mass – 4.

5.2.8.Insulin changes during GTT

One reason for variation in response to glucose tolerance tests is altered secretion of insulin into the blood. We measured plasma concentrations of insulin during GTTs in the

2- and 6-week cohorts to examine if glucose-induced insulin secretion was altered between CR and AL mice and could account for the diet and/or sex differences in glucose tolerance. Two and six weeks were chosen for analysis as these were the minimum and maximum durations present for both sexes. A significant diet effect was seen by ANOVA for both durations of diet and both sexes, however a significant effect caused by the duration of the GTT was only present in the male 2-week diet group. This was a surprise given that previous studies suggest that insulin should increase post—glucose administration[243]. One possibility is that the peak in insulin preceded the first measurement at 15 minutes, which may also explain why AUC analysis did not show any differences (data not shown) Of importance, CR did not enhance insulin secretion in any of the groups assessed; hence, it is clear that the ability of CR to improve glucose tolerance in males, but not in females, is not related to diet- or sex-associated effects on on insulin secretion.

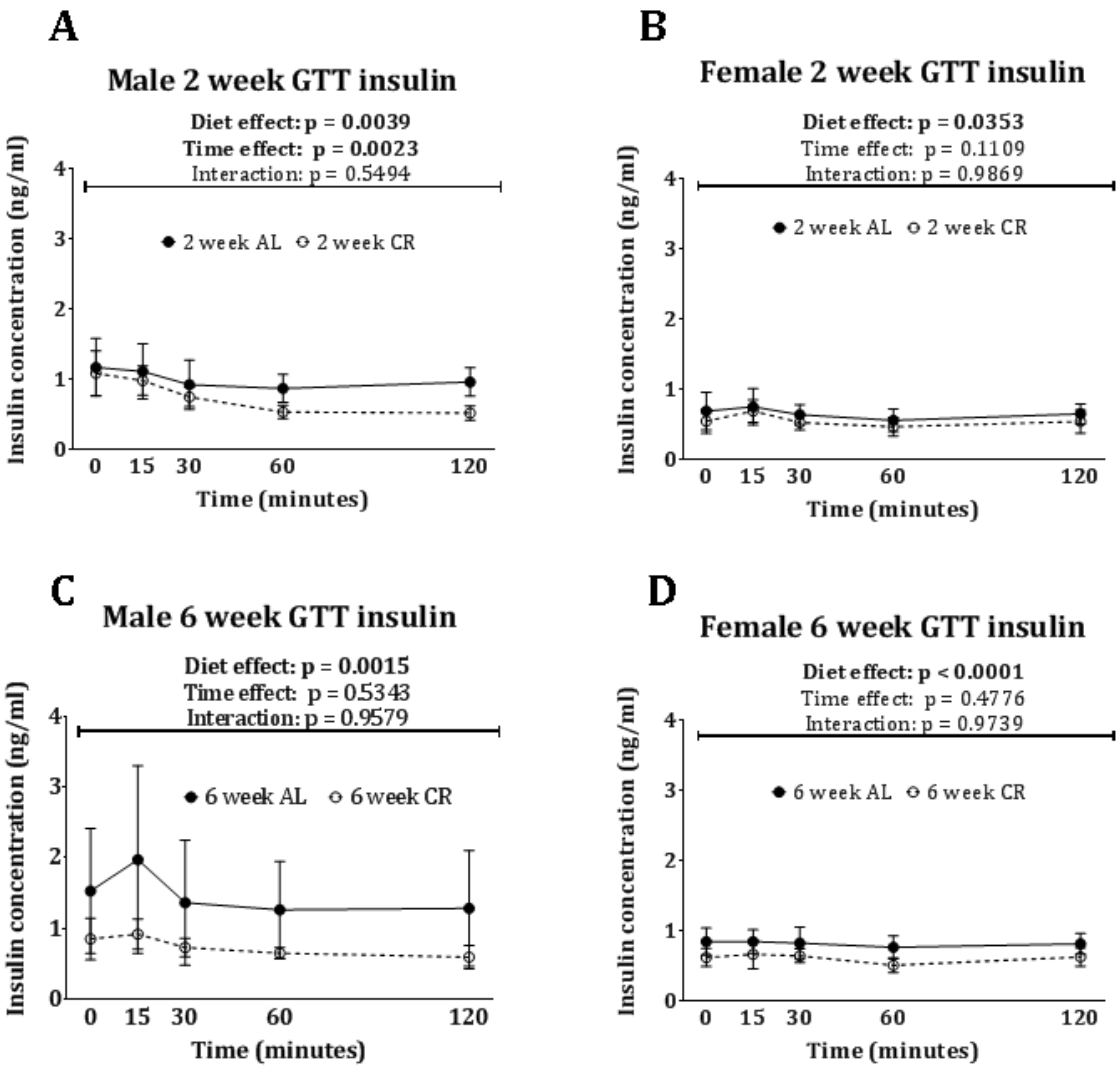

Figure 5.9 – Plasma insulin concentrations during GTT in male and female mice scorss 6 week CR diet. Plasma insulin concentrations were measured by ELISA. Measurements were taken before oral glucose dose then 15, 30 60 and 120 minutes after

administration. **(A)** Insulin concentration across GTT in male 2 week diet mice. **(B)** Insulin concentration across GTT in female 2-week diet mice. **(C)** Insulin concentration across GTT in male 6-week diet mice. **(D)** Insulin concentration across GTT in female 6 week diet mice Mean measurement is shown with error bars indicating ± SD. Statistical significance was determined by 2-way ANOVA, source of variance significance is shown above the data. No multiple comparisons determined using Sidak's correction were found to be significant. Number used as described in figure 5.6.

5.2.9. Effects on mitochondrial biogenesis in gastrocnemius muscle

Previous research has suggested that certain mRNA transcripts are altered in muscle tissue during CR, many of which are also reported targets of adiponectin. Peroxisome proliferator-activated receptor gamma coactivator 1-alpha (PGC1α, encoded by *Pcg1a*) is a transcriptional co-activator able to regulate mitochondrial function, and is often induced by CR. Mitochondrial transcription factor A (*Tfam*) is a downstream target of PGC1α that can regulates mitochondrial function and replication. Acyl-coenzyme A dehydrogenase, C-4 to C-12 straight chain (*Acadm*) is another downstream target of PGC1α that also has important mitochondrial functions. Despite previous studies showing an induction of *Pgc1a*[121] in this study we saw no significant differences between AL and CR in the gastrocnemius muscle. Both male and female mice also showed no significant differences between AL and CR mice in *Tfam* expression and females did not exhibit any significant differences in *Acadm* expression. Diet did significantly affect *Acadm* expression in males;, however, the effect was for a decrease in CR mice compared to AL, which was not the expected result. Thus, despite robust increases in circulating adiponectin during CR in both males and females, expression of these reported adiponectin targets was not increased during CR in either sex.

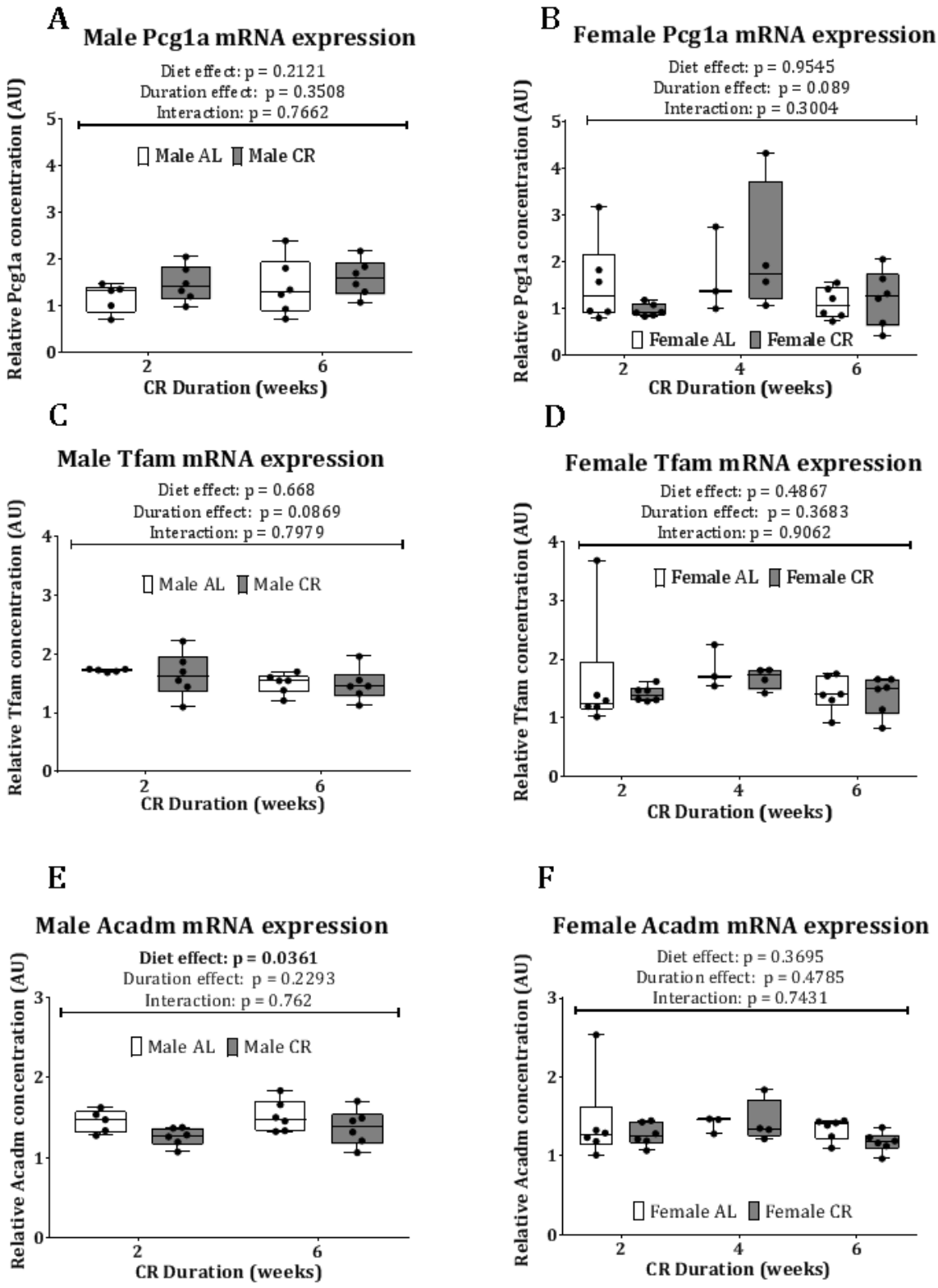

Figure 5.10 – Mitochondrial biogenesis gene transcript analysis of skeletal muscle in male and female mice across 6 week CR diet. RNA was extracted from gastrocnemius muscle and reverse transcribed to cDNA. Transcript concentration of mitochondrial biogenesis genes was quantified by qPCR relative to a standard curve. **(A)** Male *Pgc1a* gastrocnemius transcript concentrations. **(B)** Female *Pgc1a* gastrocnemius

transcript concentrations. **(C)** Male *Tfam* gastrocnemius transcript concentrations. **(D)** Female *Tfam* gastrocnemius transcript concentrations. **(E)** Male *Acadm* gastrocnemius transcript concentrations. **(F)** Female *Acadm* gastrocnemius transcript concentrations. All data points shown with median, interquartile range and range shown by box and whisker plot. Statistical significance was determined by 2-way ANOVA, source of variance significance is shown above the data. No multiple comparisons determined using Sidak's correction were found to be significant. Numbers used male AL 2w – 5, all other male groups – 6. Female AL 2w – 6; CR 2w – 6; AL 4w – 3; CR 4w – 4; AL and CR 6w – 6.

5.3. Discussion

5.3.1. Adiponectin as a mediator of metabolic benefits of CR

The contribution of this chapter to the overall hypothesis and aims of the thesis was to investigate the timing of adiponectin increases in relation to the beneficial metabolic effects of CR, namely improved glucose homeostasis and mitochondrial biogenesis. The rationale being that if metabolic changes are preceding increases in adiponectin, then adiponectin may not be a crucial hormone in conveying these benefits of CR. On the other hand, if the metabolic changes were occurring at or after the point at which adiponectin increased, or in a manner proportional to adiponectin increases, we could conclude that adiponectin may be a causal factor. In both male and female mice, we observed a maximal increase in adiponectin after 4 weeks of CR with a maintenance in concentration from 4 weeks to 6 weeks. In the female mice, between the start of the diet and 4-weeks post-diet, the increases in adiponectin were gradual and continuous whereas the male mice showed a more dramatic and sudden increase between 2 and 3 weeks post-commencement of CR. The improvements in male glucose tolerance were first apparent after 1 week of CR and were statistically significant after 2 week of CR, which is before the increases in circulating adiponectin. This suggests that hyperadiponectinaemia is not a pre-requisite for improvements in glucose tolerance. Furthermore, whilst the female mice showed robust increases in adiponectin, few metabolic adaptions were seen, giving more indication that adiponectin increases are not required. This is a surprising conclusion, because during CR energy is scarce and to invest resources into robust induction of hyperadiponectinaemia suggests that this response must yield an evolutionary benefit that confers a survival advantage in a low-calorie environment.

Decreases in mitochondrial number, function, and enzyme activity in skeletal muscle have been shown to contribute to insulin resistance and worsening of glucose homeostasis[244]. Additionally, genes involved in mitochondrial biogenesis have been shown to be increased during CR[121]. We hypothesised that the CR-induced improvements in glucose tolerance could be caused by improvements in mitochondrial

biogenesis and function. The gastrocnemius was chosen for analysis as a large and readily isolated skeletal muscle. As shown above, we saw very few significant differences in the transcripts evaluated. This was in opposition to previously published data and could have occurred for two reasons. Firstly, the muscle used in previous research was the quadriceps[121] as opposed to the gastrocnemius here, however it seems unlikely that this would cause such a big difference in results. Another contributing factor could be the pre-cull fasting procedure because, in the previously mentioned study, the AL mice were not fasted before the cull[121] and so differences in muscle transcript expression may be caused by differences in fasting duration, rather than longer-term CR effects. To further evaluate mitochondrial number and function, confocal microscopy could be used to examine cross-sections of muscle tissue stained with fluorescent probes, such as mitotracker[245]. Given the lack of changes it is difficult to examine the hypothesis that adiponectin is driving the metabolic benefits of CR given that in this experiment it appeared not to be any benefits imparted.

5.3.2. Sex differences in the metabolic effects of CR

One of the most striking findings of this chapter was the vast differences between male and female mice in their response to CR. Male mice preferentially metabolised adipose tissue and displayed large improvements in glucose tolerance whilst female mice showed a preference to maintain fat mass and metabolise lean mass instead and did not exhibit any improvements in glucose tolerance aside from improvements in fasting glucose. Some CR studies have shown that female mice do show reduced fat mass in response to CR[246,247], whilst some, in concordance with the results presented here, show that female's fat mass is unaltered or can even increase in response to CR[248,249]. One potential reason for some studies showing reduced fat mass in females is diet duration, in the above cited studies mice underwent CR for 20 weeks[246] or 3 months[247] indicating that females may lose fat mass after longer durations of CR. Mouse strain may also be an important determinant with some strains showing large decreases in female fat mass whilst others showed no change or even increases in fat mass[247]. The picture in humans is also complicated, with females showing reduced fat mass in response to CR in some studies but not in others[233,234]. No consensus has been reached regarding the nature of fat loss discrepancies between male and females in mice, humans or indeed other species. Future work could focus on ovariectomised mice to evaluate the contribution of female sex hormones on these differences with the hypothesis being that female mice without ovaries would react to CR with a more male-like phenotype.

The dissected adipose tissue masses mirror the lipid mass changes observed by TD-NMR, with male mice showing a decrease in both lipid mass and adipose tissue mass, whilst females did not show reductions in either lipid mass by TD-NMR nor less massive adipose depots by dissection. This indicates that the changes seen in fat mass by TD-

NMR are indicative of gross changes in adipose depots rather than more generic changes in total body lipids and can be trusted to recapitulate the effects of CR on adipose depots. Here we chose to measure the inguinal WAT as a representative depot of subcutaneous adipose and gonadal and mesenteric WAT was representative of visceral depots. Whilst we saw effects in these depots there are also other WAT depots present in mice which could also have been used to quantify WAT mass and may have shown different results. These include perirenal WAT[250] and perivascular WAT[251].

The lean mass GTT in females was performed given the hypothesis that the lack of response in glucose homeostasis induced by CR may be caused by a reduction in lean mass rather than fat mass as observed from the TD-NMR and WAT dissection data. Given that skeletal muscle, a type of lean tissue, is a very large source of peripheral glucose uptake[252,253], it seemed likely that if females had less lean mass relative to their total body mass then the glucose dose they were receiving relative to their body mass may be too high. By administering glucose relative to the lean mass of the mice we sought to give the female mice an appropriate glucose dose relative to the major site of uptake. We expected that if this hypothesis was correct the GTT plots and AUC analysis in the female mice would appear more male-like. We did not see this, the female mice continued to exhibit the same response to the glucose tolerance test irrespective to the glucose dose being calculated relative to total body mass or lean mass. This indicates that the sex differences observed between males and females are not a result of inappropriate glucose doses and instead reflect an underlying biological difference between males and females.

5.3.3. Are the metabolic effects of CR concordant with previous studies

Body mass reduction is well established as a result of CR, it has been observed in humans[254], rats[255], rhesus monkey[256], rabbits[129] and, importantly, mice[257]. Reductions in body mass seen in these mice indicates that the CR intervention is working as anticipated and further analysis can be performed. Both male and female mice were showing reductions in body mass and the contribution of various tissue types was elucidated by TD-NMR body composition and post-cull tissue dissection.

5.3.4. Technical considerations and limitations

The TD-NMR measurements were performed fortnightly, this duration was chosen in order to reduce the stress caused to the mice that might be caused by more regular measurement, given that the procedure involves placing the mouse in a confined space for approximately 40 seconds. Despite these concerns the mice appeared to habituate to the procedure rapidly and therefore for future experiments, weekly measures by TD-NMR were performed. A major advantage of using TD-NMR for body composition is the non-invasive nature of the procedure, this allows longitudinal measures to be made and changes in composition of individual mice to be tracked. This provides more insight into the overall effect of CR as well as enhancing the statistical analysis performed by

allowing for paired analysis. One small disadvantage of using TD-NMR is the inability to attribute changes to specific tissues. The local environment of protons is measured but these protons cannot be located to a specific tissue type. For example, we see a reduction in fat mass in male mice induced by CR, but this change cannot be attributed to a reduction in adipose tissue by TD-NMR alone, merely that fewer protons are in a lipid microenvironment, which may be a reduction in lipid in other tissues such as the liver. For this reason, tissue dissection was also performed to gain an understanding of changes in specific tissues. This, however, is a terminal procedure and therefore cannot be performed longitudinally.

A potential confounding factor during the dissection of adipose depots and other tissues post-mortem is variability in the dissection technique. For well-defined organs, such as the liver, dissection is easy as the tissues are separated and adjoined to the surrounding tissue at few locations. However, in more diffuse tissues, such as BAT, the edges of the tissue are not clearly defined and the boundary is more subjective. In order to control for variation in dissection technique, the number of people performing the dissection across the multiple cohorts was kept to a minimum. In this case two different people dissected tissues and organs but no differences were seen in tissue masses between these people (data not shown). Additionally, the dietary group of the mouse was blinded in the people involved in the dissection as best as possible to prevent unconscious bias when the tissues were removed. This was difficult given the AL diet and CR diet were different colours, to prevent confusion when feeding, and could be seen in the digestive tract of the mice upon opening of the peritoneum. Another issue to overcome in the dissection procedure of the mice is the feeding regimen prior to cull. The nature of administration of the CR diet meant that the CR mice were receiving their food once per day and were effectively short-term fasting between daily feeds. In contrast, the AL mice had 24-hour free access to their food and so experienced very little fasting. If these mice were culled in a free-fed state it is likely that the CR mice would be in a fasted state whilst the AL mice would be in a fed state. This would confound the results of the experiment as the aims were to investigate the longer-term effects of CR and not the effects of short term fasting. Therefore, it was required that both groups of mice were in fasted states, such that any differences observed would not be influenced by an alteration in fed state. The pre-cull feeding regimen is described in the methods and allowed both groups of mice be fasted to a similar degree. Unfortunately, it was not possible to match the fasting duration perfectly and so many have added to some of the variation in the data between CR and AL groups.

When quantifying the concentrations of adiponectin in the circulation an ELISA was used, this is a well-established and reliable method for quantifying adiponectin and has been widely used in the past[12,258-260]. A potentially confounding element of the adiponectin quantification is the collection of plasma samples that were used in the

ELISA. Blood sampling was performed in the morning, prior to administration of diet to the CR mice. This means that the CR mice were in their maximally fasted state whilst the AL mice had had free access to food during the night and therefore were likely more fed than the CR mice. Additionally, the plasma taken from the endpoint of the experiment was taken from mice fasted in both CR and AL groups as described previously. Despite this, it was not expected that this affected the results in a significant manner. Fasting or leptin administration (a molecular mimic of fasting) have been shown to not cause significant variation in circulating adiponectin concentrations[261]. The plasma isolated from the mice was frozen which can have a negative effect on proteins, particularly storage time in the freezer[262]. Despite this, adiponectin has been shown to be stable across multiple freeze-thaw cycles[10] whilst the plasma used in this experiment only experienced one freeze-thaw cycle. Additionally, adiponectin in fresh frozen plasma samples, used clinically, has been shown to exert a specific beneficial effect in trauma patients[263] further indicating the stability of adiponectin during freeze-thawing.

A surprising observation from the adiponectin quantification was the higher concentration of high molecular weight adiponectin multimers than total adiponectin concentrations. This indicates a technical issue in the quantification given that the total adiponectin ELISA should measure the high molecular weight multimers in addition to the medium and low weight multimers. One explanation for these findings could be that ELISAs from different manufacturers were used for total and high molecular weight, as therefore, different antibodies were used in the detection of the protein. This means a different affinity which could result in different relative concentration. Despite this, the relative differences between total and HMW adiponectin are still valid given that all samples for either total or HMW were analysed with the same kit and thus whilst the absolute concentrations may not be comparable, the relationship between the multimers is still valid.

Whilst the GTT plots and AUC in the male mice were all fairly similar across the differing durations of CR, the 4-week time-point appeared to show a slightly different pattern to the 1-, 2- and 6-week points. The reduction in fasting glucose was still present in the CR mice at 4 weeks but the initial increase in blood glucose was greater in the CR mice compared to the AL group and increased to nearly the same point 15 minutes after glucose administration. When this was analysed in the AUC the typical pattern was seen relative to 0 mM glucose, indicative of an improvement in fasting glucose, which was also seen in the glucose-over-time plots. However, when looking at the AUC relative to fasting glucose concentrations the 4-week dietary groups do not mirror the other time points. The 2- and 6-week time points show a reduction in AUC in the CR mice with a similar

(yet non-significant) trend after 1 week. In the 4-week group, no significant differences are observed yet the mean of the CR group is higher than the mean in the AL group, the opposite of what is seen in the other time points. There are two potential explanations for this observation: firstly, there may be metabolic changes that occur after 2 weeks of CR and then revert between 4 and 6 weeks, but this seems fairly unlikely given the short time frame and the lack of rationale for a transient abolition of glucose tolerance improvements induced by CR. The alternative explanation is that this is a technical issue. The glucose gavage can be a difficult technique and the potential for slightly incorrect administration is not insignificant, and whilst there were no signs of technical variation during the GTT this does not discount the possibility of it occurring and influencing the result.

As mentioned previously the fasting of CR and AL mice is problematic and required some compromise, therefore it was deemed necessary to confirm that the effect from the fasting regime was not causing the differences seen between AL and CR mice. In order to test this, the CR mice were fed the AL ration before the fast and the AL mice were fed a CR ration. If the pre-GTT diet was causing the differences seen, we would have expected to see either a reversal in difference between AL and CR or the abrogation in difference. When the GTT was performed the reverse-fed mice performed in an equivalent manner to the normally fed mice, we therefore concluded that the short-term diet before the GTT was not a causative factor in the differences between AL and CR and that the long-term diet was the influencing factor.

When differences in glucose tolerance are seen, insulin is the most likely cause of these effects and has been previously reported to show significant differences across a glucose tolerance test[264]. Yet when we evaluated plasma insulin concentrations across the glucose tolerance test we saw very little difference between AL and CR groups, which was not necessarily expected, but also no differences across the duration of the glucose tolerance test which was not in concordance with previous literature. One reason for this may be that the 15-minute time point was not rapid enough to be able to catch the rapid increase in insulin caused by the bolus of glucose, especially given that these mice were lean and therefore likely to have a far more rapid insulin response compared to obese mice or humans undergoing glucose tolerance tests. In order to confirm or rectify this in future tests, a 5-minute and/or 10-minute plasma sample could be taken to confirm if insulin was increasing or staying constant as indicated here. This would also allow more accurate blood glucose concentrations to be measured and may allow further conclusions to be drawn regarding the glucose homeostasis during CR.

5.3.5. Future directions

Future directions for this chapter, not included in subsequent chapters, will primarily focus on the sex differences between males and females in their response to CR. The primary goal would be to ascertain if the results seen in mice are recapitulated in humans. Whilst human CR experiments are more complex and expensive to perform, a large amount of historical data exists and it would be possible to evaluate previously taken whole-body scans of humans undergoing CR to examine any sex differences in regards to fat and lean mass changes. Glucose tolerance data may be harder to come by in calorie restricted humans; however, fasting glucose and insulin concentrations can provide a rough measure of glucose and insulin tolerance. For more murine experimentation, female mice could be ovariectomised and calorie restricted to evaluate the hypothesis that female sex hormones are contributing to the phenotype seen. If this hypothesis is correct, we would expect female mice that have undergone ovariectomy to respond to CR in a more male-like manner. To further evaluate the hypothesis that adiponectin is driving some of the metabolic adaptions to CR we used an adiponectin knockout mouse model to examine how lack of this hormone affects response to CR, this data is shown and discussed in chapter 6.

6. Mice lacking adiponectin show altered responses to caloric restriction

6.1. Introduction

Adiponectin -inversely correlates with BMI[12] as well as subcutaneous and intra-abdominal fat[265], waist circumference[13] and blood pressure[13]. This inverse relationship with adiposity has been dubbed the 'adiponectin paradox', given that adiponectin is secreted exclusively by adipose tissue[12] yet when adipose tissue is at the highest levels hypoadiponectinaemia is observed. Conversely, leanness is associated with hyperadiponectinaemia. Understanding the mechanisms behind hypoadiponectinaemia is important, because this has implications for metabolic disease. For example, circulating concentrations of adiponectin are also reduced in patients with type 2 diabetes compared to BMI-matched non-diabetics[17]. In addition, people with higher circulating adiponectin concentrations are at a significantly reduced risk of developing type 2 diabetes in later life[266].

6.1.1. Past adiponectin studies

Much of the previous work on adiponectin knockout mice has focussed on conditions of high-fat diet. While this makes sense in terms of addressing the role of adiponectin in obesity and diabetes, it is also perplexing considering that obesity is the condition in which adiponectin is at its lowest. Despite this, mice lacking adiponectin on a high-fat diet develop more rapid glucose intolerance compared to wild-type mice[267]. Additionally, the effects of insulin-sensitising PPARγ agonists such as thiazolidines (TZD) are ameliorated in adiponectin knockout mice, supporting a role for adiponectin in glucose sensitivity[268]. One study of particular note aimed to examine the role of adiponectin during CR but focussed on outcomes relating to ischemia-reperfusion injury. CR is known to restore the hearts ability to resist ischemia reperfusion injury[107] indicating that CR has the ability to enhance the hearts defence mechanism against ischemic stress. Given this, the role of adiponectin during ischemic stress was examined using Ad-As mice which over express an anti-sense oligonucleotide against adiponectin[108]. They found that the Ad-As mice resisted the CR-induced hyperadiponectinaemia, especially the HMW multimers[108] and they also showed a corresponding resistance to positive recovery from ischemia-reperfusion injury and reduced myocardial glycogen content in the Ad-As mice[108]. Interestingly, they also showed that administration of recombinant adiponectin to the Ad-As mice via an osmotic minipump restored the CR-induced improved recovery response to ischemia reperfusion injury including a reduced infarct size[108]. In addition, they also showed that treatment with an AMPK inhibitor abrogates the cardioprotective effect of CR[108]. Overall this indicates that adiponectin contributes to the cardioprotective effects of CR and it may be mediated through stimulating AMPK activity in the myocardium. This effect has also been reproduced in a model of hind limb ischemia, with CR enhancing the revascularisation of ischemia hind limbs in WT mice but

not in adiponectin KO mice[109]. This is important for this thesis because it shows that adiponectin plays an important role during calorie restriction and therefore it seems likely that adiponectin will also exert other CR-induced effects, especially given the previously described metabolic effects of adiponectin.

Treatment with adiponectin causes a decrease in plasma glucose in wild-type mice, but not in mice with a double knockout of both adiponectin receptors[30]. Additionally, these double knockout mice showed markedly higher plasma insulin concentrations, indicating insulin resistance[30]. Glucose tolerance tests in these mice, when fed a high-fat diet, showed impaired glucose tolerance and increased plasma insulin compared to wild type mice[30]. Additionally, euglycaemia-hyperinsulinaemic clamp studies have demonstrated that mice lacking adiponectin have significantly impaired suppression of insulin-stimulated hepatic glucose production[268]. Treatment of mice with globular adiponectin decreased plasma free fatty acid concentrations[8] indicating a role for adiponectin in lipid metabolism as well as insulin sensitivity.

Body fat may not be the ultimate determinant of adiponectin concentrations during CR. Studies examining the effect of genetically low insulin during calorie restriction on mice showed that CR caused paradoxical increases in fat mass, yet adiponectin was still elevated as normal[241]. This could be reflective of previously discussed studies showing a role for BMAT in CR-induced hyperadiponectinaemeia.

Indirect calorimetry was used gain a better understanding of the adaptions in energy expenditure, basal metabolism and substrate utilisation during CR. Rats on CR diet had decreased O_2 usage and reduced resting metabolic rate[269]. The ratio between O_2 usage and CO_2 production is termed the respiratory exchange ratio (RER) was increased[269]. With regards to energy expenditure and resting metabolic rate alterations during calorie restriction, the literature shows a variety of conclusions with some showing that resting metabolic rate is not altered during calorie restriction when taking into account the body size of the animals[81,270]. Whereas others have shown that the tissue calorie restricted animals reduce their energy expenditure even when taking into account reduced size[227,271]. An additional parameter is the energy expended by activity. Mice exhibited decreased physical activity in response to CR as a strategy to conserve energy[272]. Mice also displayed increased activity in the hours immediately preceding feeding in a phenomenon known as food anticipatory activity.

6.1.2. Aims of the chapter

This present chapter aims to address the impact of adiponectin on imparting the metabolic benefits of CR. The first aim is to generate and maintain a stock of adiponectin knockout mice. We will then place these mice on AL or CR and characterise the basic physical parameters of the mice including body mass, composition and specific tissue masses. We will then aim to evaluate both the glucose and lipid metabolic phenotype of these mice. The glucose homeostasis phenotyping will comprise oral glucose tolerance

tests whilst the lipid homeostasis phenotyping will comprise liver and plasma lipid analysis. Finally, both glucose and lipid homeostasis will be evaluated on a whole organism scale via indirect calorimetry. If adiponectin is mediating at least some of the effects of calorie restriction, we will expect to see differences in response CR between the AL and CR diet mice in any of the above parameters. This will answer important questions about the physiological benefit of investing resources to increasing concentrations of adiponectin during times of calorie scarcity.

6.2. Results

6.2.1. Confirmation of genotype

It was essential to show that the adiponectin knockout was successful. Immunoblotting was performed on mouse plasma in order to detect the presence of the hormone in the blood. The resulting Western blot confirms that the wild-type mice had detectable plasma adiponectin whereas the KO mice did not (Figure 6.1). A total protein stain was used to confirm that the poly-acrylamide gel was loaded correctly and that all lanes contained protein. This showed that the absence of adiponectin in the knockout mice was not a result of lack of protein loaded. This procedure was performed on all experimental mice, however only a representative gel is shown here.

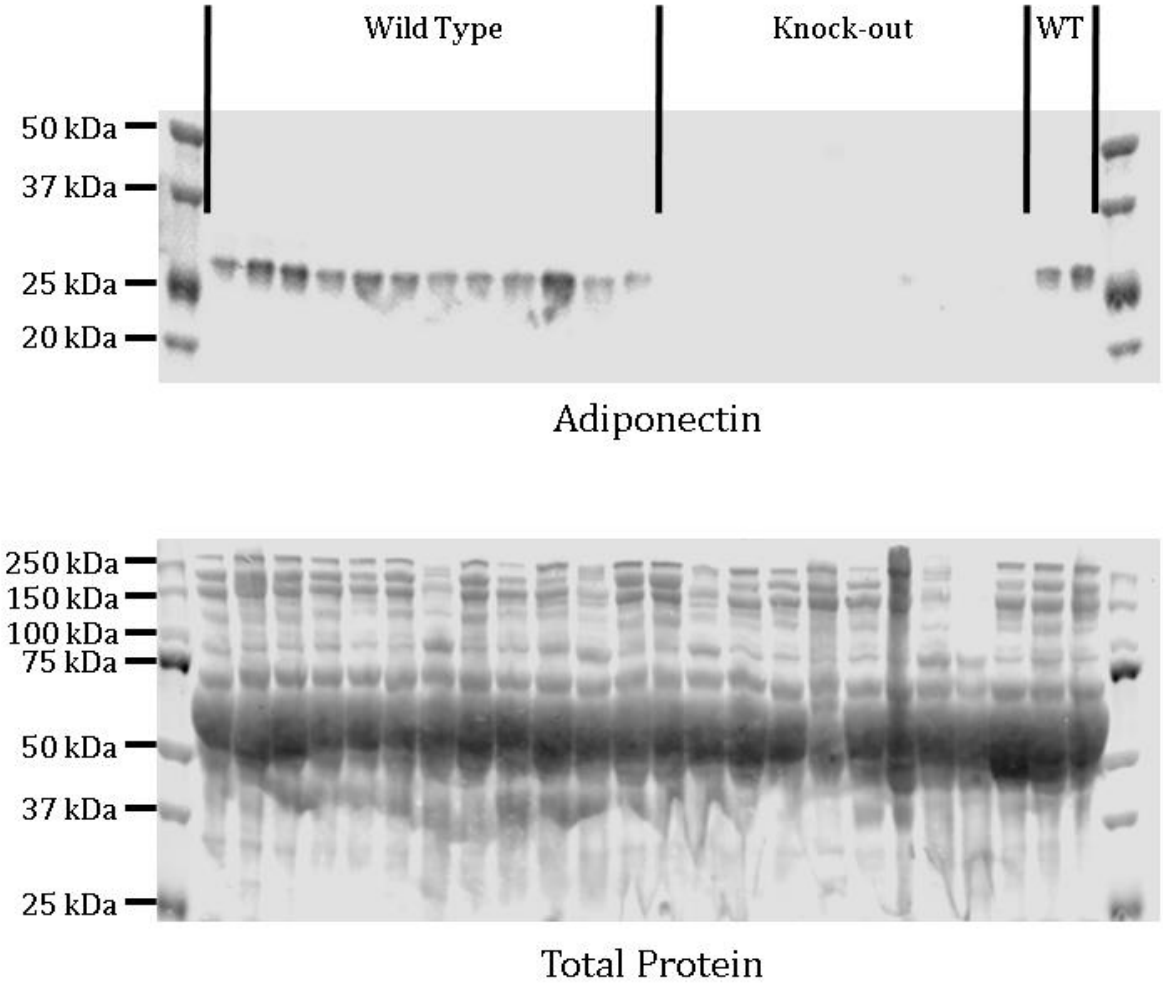

Figure 6.1 – Immunoblot for adiponectin and total protein stain from mouse plasma. Mouse plasma was denatured in loading buffer containing SDS. Electrophoresis was performed through a polyacrylamide gel then the protein transferred to a nitrocellulose membrane. The total protein was stained and visualised using LiCor total protein stain. After washing this stain, anti-adiponectin antibody was used to detect the absence or presence of adiponectin in the samples.

6.2.2. Basic measures of whole-body composition

As with the CR time course, one method to confirm that the dietary intervention was successful was to measure the body composition of the animals. CR induced weight loss in males and females (Figure 6.2). Given that this data in wild type mice has already been presented, the only statistical test performed was to detect differences between wild type and knockout mice within each dietary group. No differences were detected in body mass between WT and KO mice. However, visual inspection on the data reveals that female KO mice in the AL group were heavier than their WT counterparts.

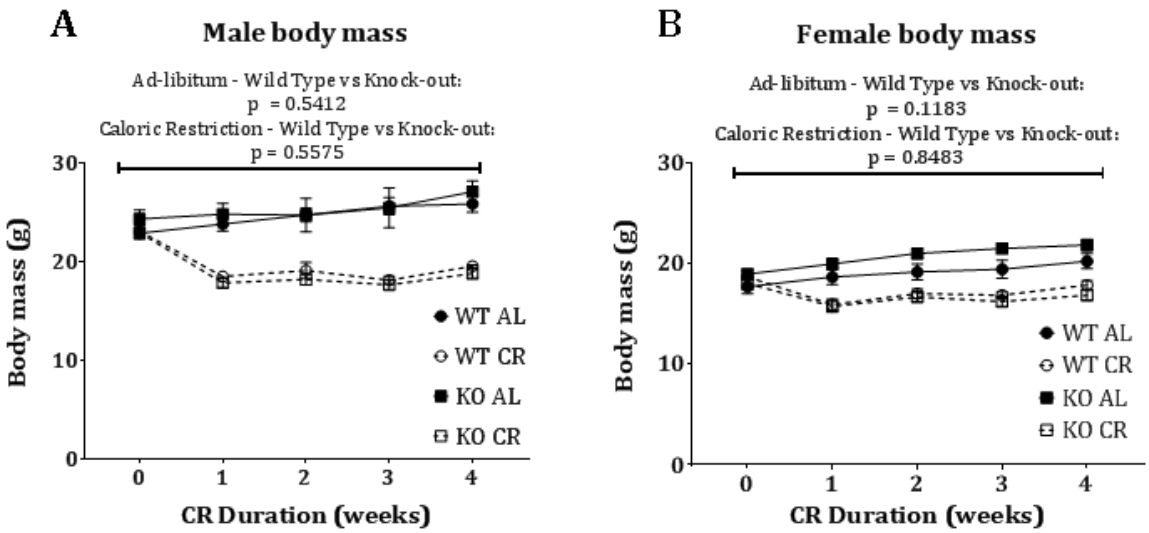

Figure 6.2 –Adiponectin deficiency does not affect body mass

Male **(A)** and female **(B)** mice were weighed weekly. Mean body mass is shown with error bars indicating ± SD. Statistical significance was determined by 2-way ANOVA, multiple comparisons between wild type and knockout mice were determined using Sidak's correction and p values are shown above the data. Numbers used Male WT AL – 10; male WT CR – 9; male KO AL – 6; male KO CR – 9. Female WT AL – 7; female WT CR – 8; female KO AL – 9; female KO CR – 8.

TD-NMR was performed to quantify their lean and fat masses. Male mice showed decreased fat and lean mass, whilst the females exclusively lost lean mass in response to CR (Figure 6.3). KO mice showed significantly different lean mass compared to WTs on the AL diet. This effect was present before commencing the diet, and so may not be related to the diet. Furthermore, the effect is not seen in the CR mice prior to beginning the diet indicating this may not be a legitimate effect.

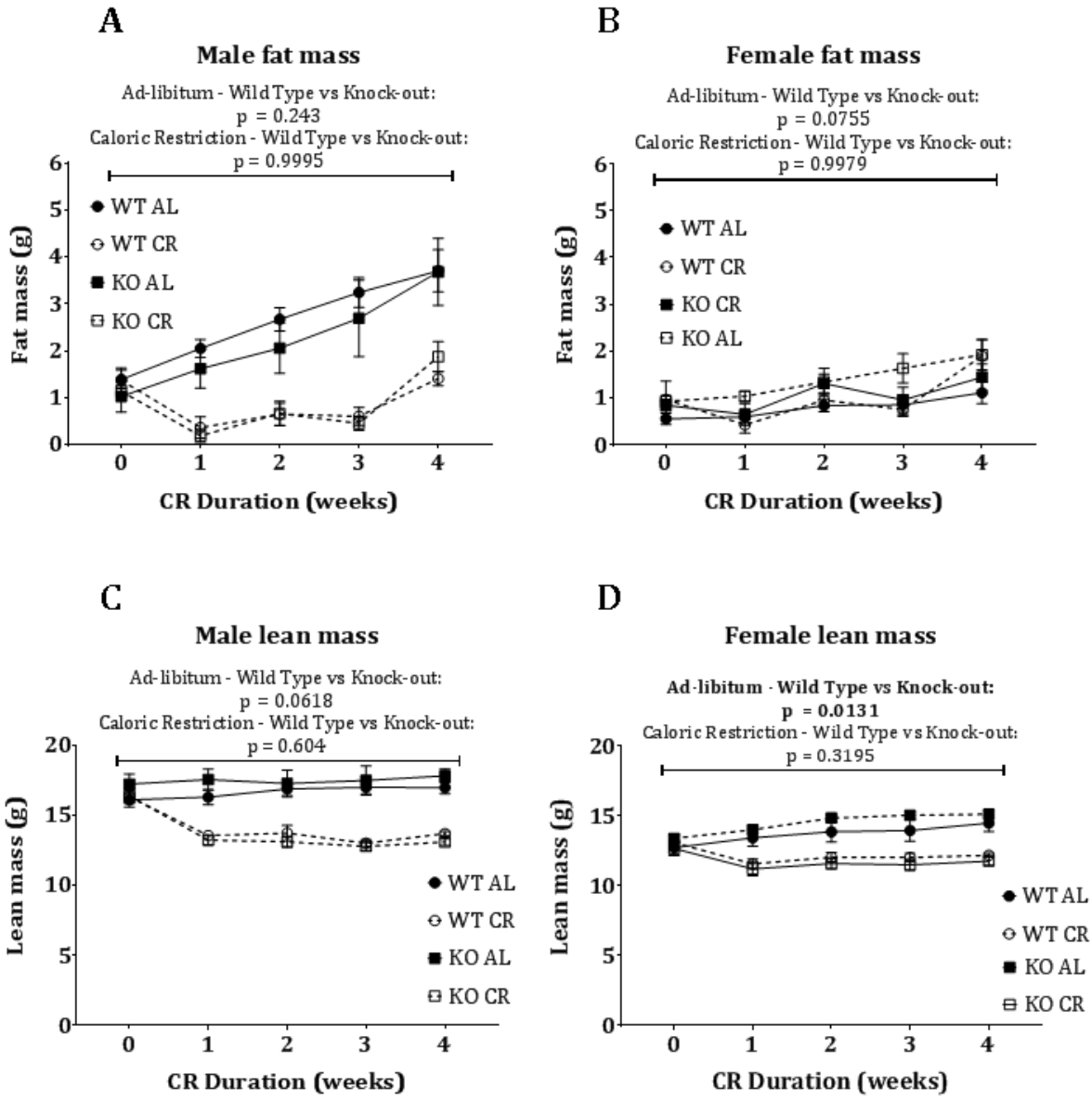

Figure 6.3 – The effects of adiponectin deficiency on body composition determined by TD-NMR Male and female mice underwent TD-NMR every week. **(A)** Male fat mass expressed in grams. **(B)** Female fat mass expressed in grams. **(C)** Male lean mass expressed in grams. **(D)** Female lean mass in grams. Mean measurement is shown with error bars indicating ± SD. Statistical significance was determined by 2-way ANOVA, multiple comparisons between wild type and knockout mice were determined using Sidak's correction and p values are shown above the data. Numbers used as described in figure 6.2.

6.2.3.Necropsy masses

Given our hypothesis that adiponectin mediates metabolic benefits of CR, we investigated the possibility that adiponectin was involved in adipose tissue distribution and metabolism during CR. To further assess fat distribution, WAT depots were dissected from subcutaneous and visceral locations during necropsy of the mice (figure

6.4). As previously observed by TD-NMR and preceding experiments, the male mice showed significantly lower WAT masses caused by CR diet, whilst female mice did not. In terms of genotypic differences, nothing was detected in the male mice. In the female mice, those lacking adiponectin had significantly higher iWAT when looking across both AL and CR groups however this effect was not seen in the gWAT or mWAT. In the gWAT a significant interaction was observed in the female mice, with the gWAT mass higher in KO mice in the AL group but lower in KO mice in the CR group; a similar trend was also observed for mWAT.

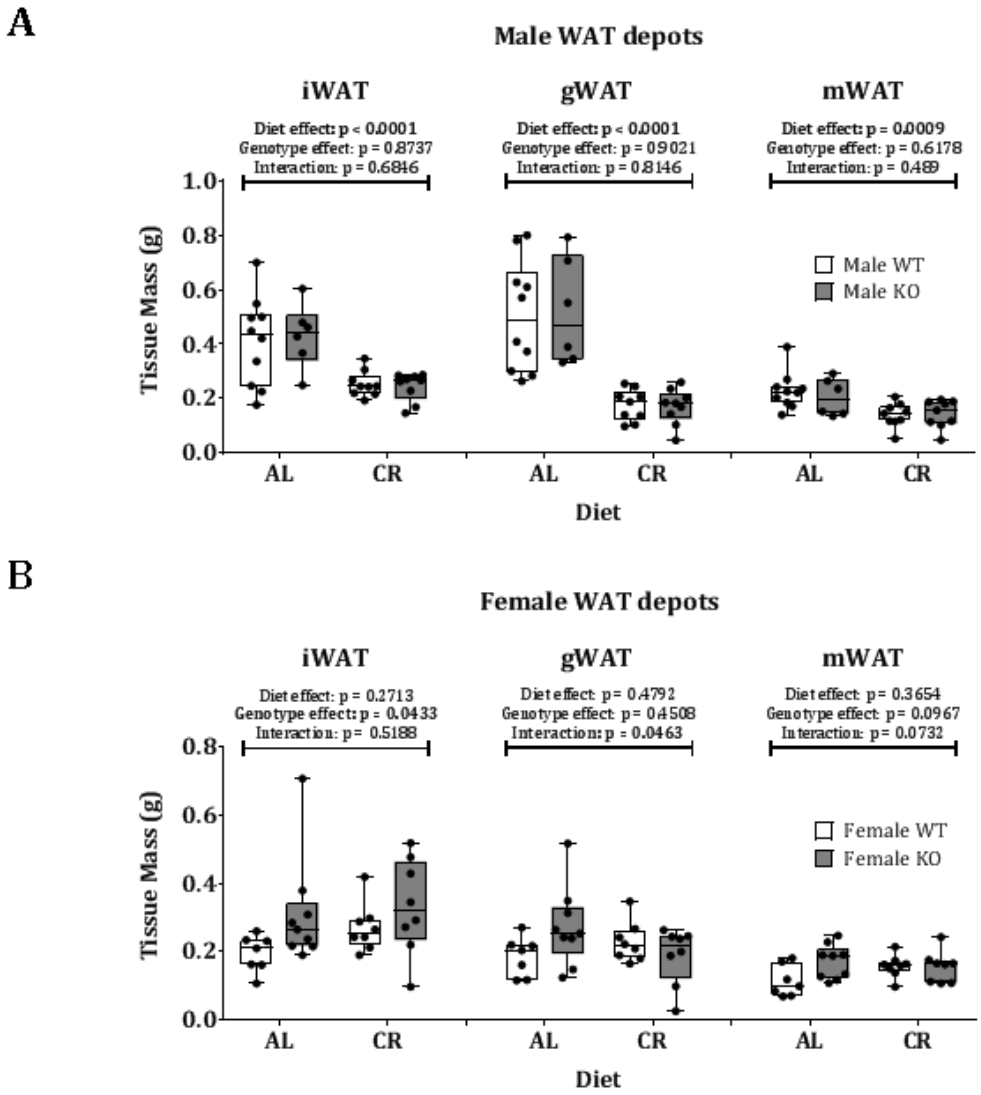

Figure 6.4 – Dissected adipose in males do not show any differences in mice lacking adiponectin, female mice may have altered iWAT mass when lacking adiponectin. Male and female mice were culled by cervical dislocation and tissues were dissected and weighed. **(A)** iWAT, gWAT and mWAT depot masses in male mice. **(B)** iWAT, gWAT and mWAT depot masses in female mice. All data points shown with median, interquartile range and range shown by box and whisker plot. Statistical significance was determined by 2-way ANOVA, source of variance significance is shown

above the data and multiple comparisons between wild type and knockout determined using Sidak's correction are indicated on the data. Number used as in figure 6.2.

As previously seen during the time course experiment, there were significant effects on BAT, liver and spleen masses during CR. To test if the absence of adiponectin alters these CR effects, these tissues were weighed during necropsy (figure 6.5). Additionally, no genotypic effects were detected for BAT mass in either sex. This indicates that BAT is unaffected by CR or the absence of adiponectin. The masses of liver and spleen were, once again, significantly reduced by CR but there was no effect caused by lack of adiponectin, further indicating that adiponectin does not influence the reduced mass of these organs during CR.

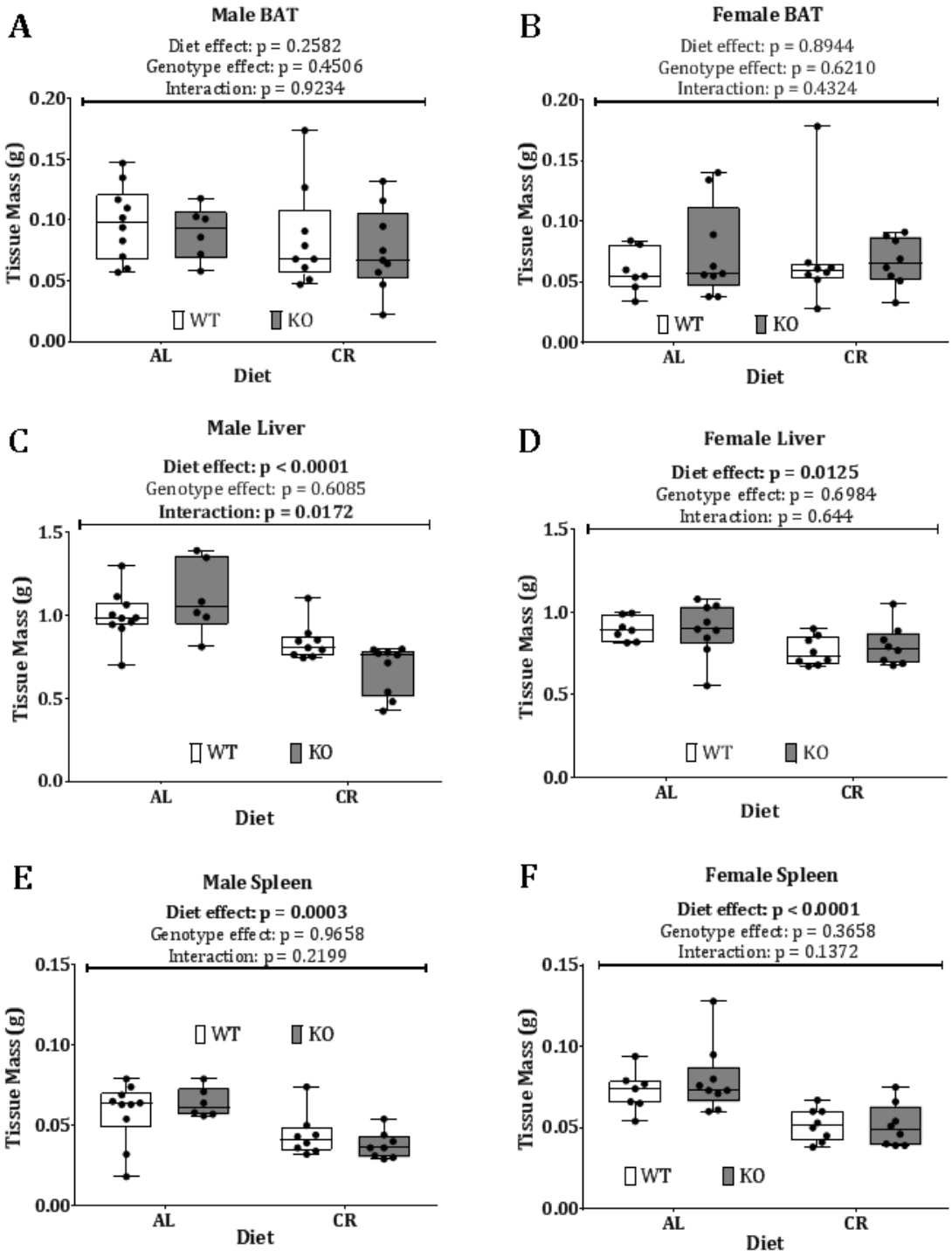

Figure 6.5 – The effects of adiponectin deficiency on BAT, liver and spleen masses. Male and female mice were culled by cervical dislocation and tissues were dissected and weighed. **(A)** Male BAT. **(B)** Female BAT. **(C)** Male liver. **(D)** Female liver. **(E)** Male spleen. **(F)** Female spleen. All data points shown with median, interquartile range and range shown by box and whisker plot. Statistical significance was determined by 2-way ANOVA, source of variance significance is shown above the data and multiple comparisons between wild type and knockout determined using Sidak's correction are indicated on the data. Numbers used as in figure 6.2.

6.2.4. Glucose tolerance greater in Adipoq KO male mice than WT on a CR diet

Previous studies have reported that adiponectin KO results in impaired glucose tolerance and insulin sensitivity. Therefore, we hypothesised that adiponectin contributes to CR-induced improvements in glucose tolerance. On this basis, we predicted that adiponectin KO mice would resist the improved glucose tolerance associated with CR. The same GTT procedure was used as described previously; briefly, mice were fasted for ~6-8 hours and given an oral dose of glucose relative to their whole body mass. Blood glucose was quantified before the glucose bolus and at multiple time points across the experiment.

Blood glucose was significantly higher in ad libitum-fed male KO mice at the 15-minute time point of the GTT (Figure 6.6). In contrast, blood glucose was significantly lower in CR male AdKO mice at the 15-minute time point of the GTT. This result indicated that adiponectin may be a negative factor in CR-induced improvements in glucose homeostasis.

When analysing glucose tolerance by AUC analysis, males and females showed a significant reduction caused by CR for AUC calculated relative to 0 mM, (6.6 E & F) but not when relative to the fasting glucose of each animal (6.6 C & D). Thus, as in Chapter 5, this indicates that fasting glucose improvements are a major driving force for CR-associated improvements in glucose tolerance. There were no genotypic effects present when looking at the overall performance in the test, indicating that the time-point-specific effects in male mice were not large enough to influence these results.

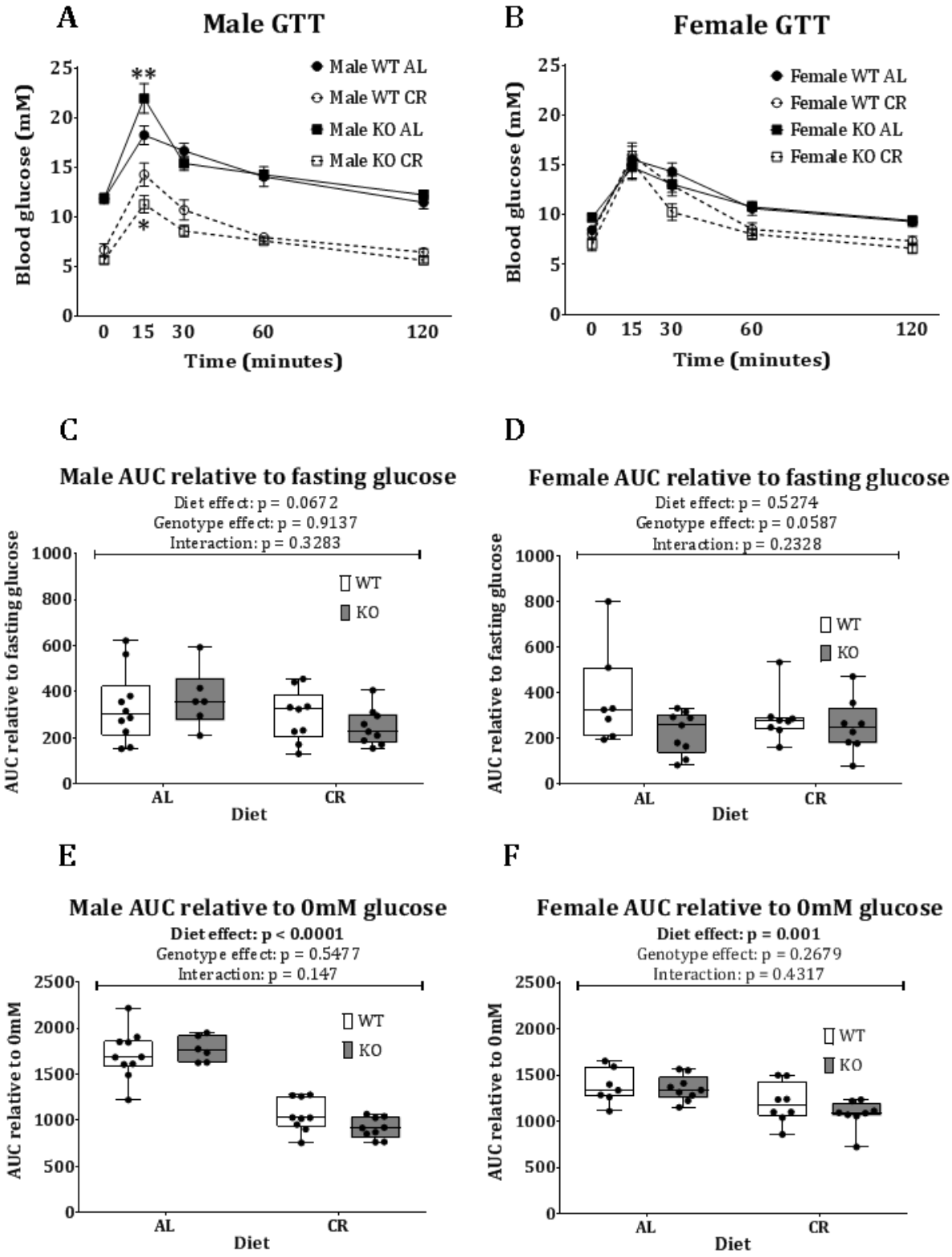

Figure 6.6 – The effects of adiponectin deficiency on glucose tolerance of male and female mice. Male and female mice were fasted then given an oral dose of glucose relative to their body mass. Blood glucose concentrations were measured before glucose administration and 15, 30, 60 and 120 minutes after. AUC analysis was performed on the resulting glucose concentration plots relative to the fasting glucose of individual mice

and to 0 mM glucose. **(A)** Male blood glucose concentrations. **(B)** Female blood glucose concentrations. Mean measurement is shown, with error bars indicating ± SD. Statistical significance was determined by 2-way ANOVA, multiple comparisons between wild type and knockout mice were determined using Sidak's correction, *: $p < 0.05$, **: $p < 0.01$. **(C)** Male AUC relative to fasting glucose. **(D)** Female AUC relative to fasting glucose. **(E)** Male AUC relative to 0 mM glucose. **(F)** Female AUC relative to 0 mM glucose. All data points shown with median, interquartile range and range shown by box and whisker plot. Statistical significance was determined by 2-way ANOVA, source of variance significance is shown above the data and multiple comparisons between wild type and knockout determined using Sidak's correction are indicated on the data. Numbers used as described in figure 6.2.

6.2.5. Liver and plasma lipid concentration

Given the greater improvements in glucose tolerance observed in adiponectin KO mice there is a possibility that the mice lacking adiponectin have a reduced ability to metabolise fats and therefore are more reliant on glucose as an energy source; if so, this may account for the improved glucose tolerance of KO mice during CR. To test this, I first quantified the concentrations non-esterified fatty acids (NEFA) in the plasma of the mice, after the full 4 weeks of dietary intervention. Male CR mice showed elevated plasma NEFA concentrations. Within the CR group the adiponectin KO mice showed an elevation in NEFA concentrations. In contrast, the females did not show any significant differences in plasma NEFA concentrations.

Given the lipid accumulation in the plasma we then examined the triacylglycerol concentration in the liver, a major site of lipid metabolism[273]. In contrast to plasma NEFA, hepatic TG concentrations were not influenced by diet or genotype in males or females. This indicates that, in our cohorts, adiponectin KO or CR does not influence lipid accumulation in the liver, despite the anecdotal evidence of observing some livers to be much fattier than others upon necropsy.

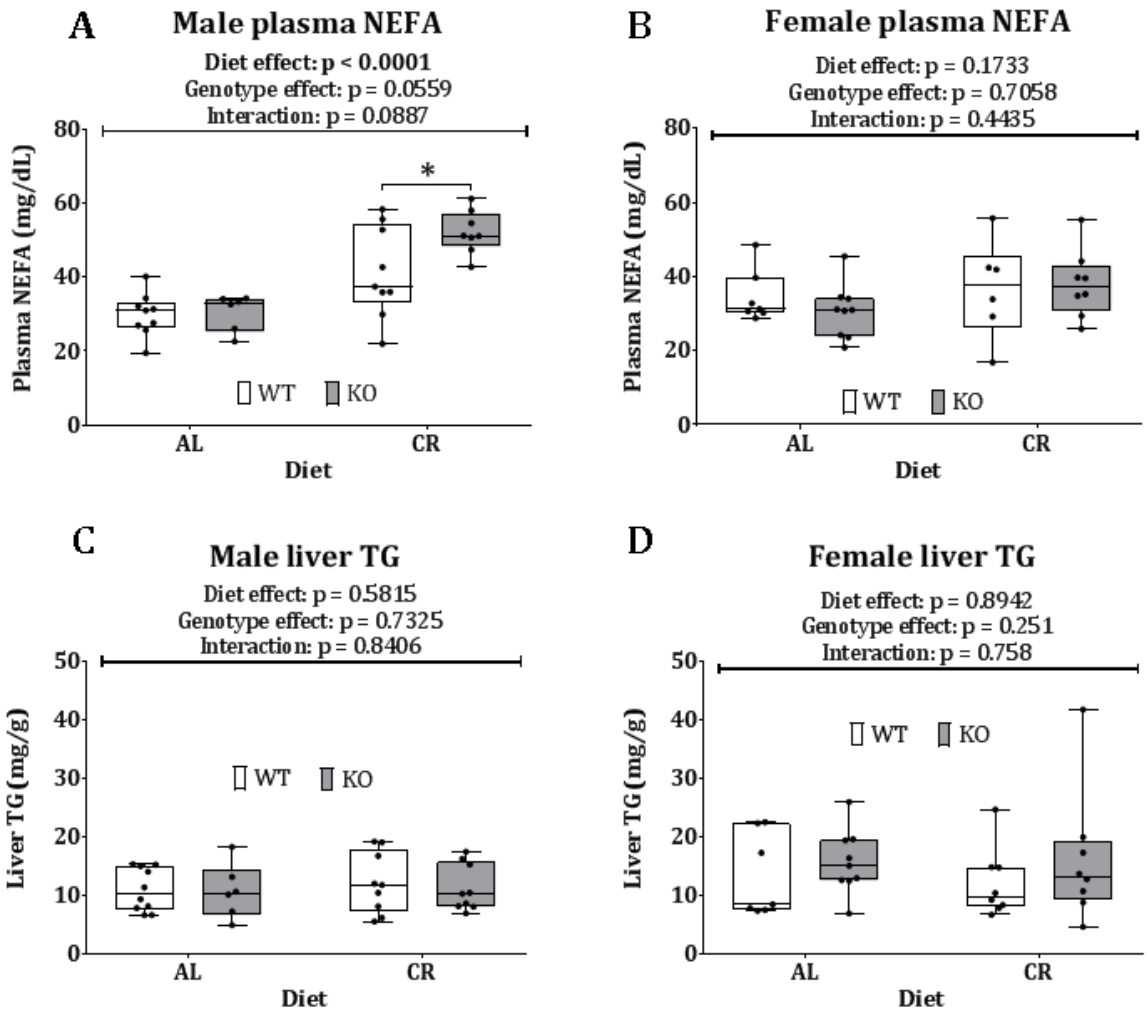

Figure 6.7 – The effects of adiponectin deficiency on plasma NEFA and liver triglycerides. Plasma from male and female mice was analysed for NEFA and liver for triacylglycerides, both by colorimetric assay. **(A)** Male plasma NEFA. **(B)** Female plasma NEFA. **(C)** Male liver TG. **(D)** Female liver TG. All data points shown with median, interquartile range and range shown by box and whisker plot. Statistical significance was determined by 2-way ANOVA, source of variance significance is shown above the data and multiple comparisons between wild type and KO determined using Sidak's correction are indicated on the data. *: $p < 0.05$. Numbers used as described in figure 6.2.

Another class of lipids present in the liver and with a link to adiponectin signalling are the sphingolipids, including ceramide species. Adiponectin decreased hepatic ceramides perhaps explaining why adiponectin improves insulin sensitivity[274]. Therefore, it was hypothesised that mice lacking adiponectin have altered ceramide profiles and that this may be a causal factor in their altered glucose tolerance. To address this, ceramides and their precursors, dihydroceramides, were quantified from frozen liver tissue by mass spectrometry I analysed male livers only, reasoning that males showed greater diet and

genotype effects on glucose homeostasis and therefore would be more likely to reveal effects on hepatic ceramides. The total ceramide concentrations were not altered by diet or genotype. However, many specific ceramide species were changed. Shorter-chain ceramides, 14:0, 16:0, 18:0, 18:1 and 20:1, and the long chain ceramide 23:0 were all increased in CR mice (Figure 6.8); ceramide 20:0 was unaffected. In contrast, medium-length ceramide 22:0 and 22:1 were lower in CR mice. There was no effect of adiponectin deficiency on short or medium or the 23:0 ceramides. Adiponectin deficiency had a specific effect on ceramide 23:1, whereby, CR increased 23:1 in WT mice but tended to decrease this species in KO mice (Figure 6.8). Both 24:0 and 24:1 ceramides were unaffected by diet and genotype whilst long-chain ceramides 26:0 and 26:1 were increased by CR.

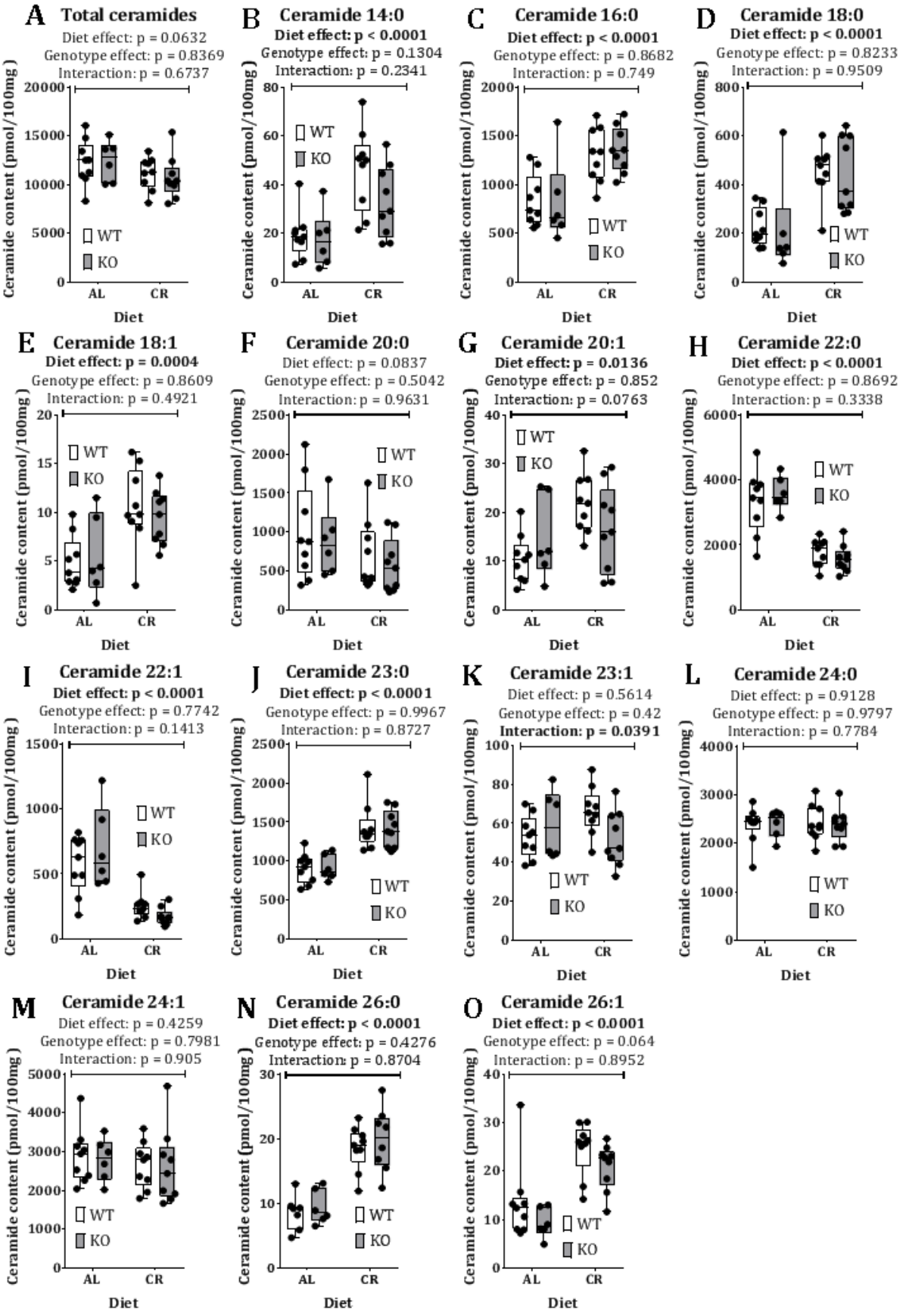

Figure 6.8 –. The effects of adiponectin deficiency on ceramide species in liver of AL and CR fed males. Liver from male mice was quantified for ceramide concentration

by mass spectrometry. **(A)** Total ceramides. **(B)** Ceramide 14:0. **(C)** Ceramide 16:0. **(D)** Ceramide 18:0 **(E)** Ceramide 18:1 **(F)** Ceramide 20:0 **(G)** Ceramide 20:1 **(H)** Ceramide 22:0 **(I)** Ceramide 22:1 **(J)** Ceramide 23:0 **(K)** Ceramide 23:1 **(L)** Ceramide 24:0 **(M)** Ceramide 24:1 **(N)** Ceramide 26:0 **(O)** Ceramide 26:1. All data points shown with median, interquartile range and range shown by box and whisker plot. Statistical significance was determined by 2-way ANOVA, source of variance significance is shown above the data and multiple comparisons between wild type and KO determined using Sidak's correction are indicated on the data. Numbers used male WT AL – 9; WT CR – 9; KO AL – 6; KO CR – 9.

To further assess the impact of CR and adiponectin on ceramide biosynthesis and function, I next quantified hepatic dihydroceramide content. The dishydroceramids are the immediate precursors to the corresponding chain length ceramides[275]; hence, measuring their concentrations may further reveal if altered biosynthesis was contributing to the effects of CR on ceramide concentration. In a very similar fashion to the ceramides, the short-chain dihydroceramides were mostly upregulated by CR, with 14:0, 16:0, 18:0 and 18:1 each elevated (Figure 6.9). This indicates a strong association between ceramides and their dihydro-precursors, at least at these chain lengths. Unlike its 20:1 its ceramide counterpart, dihydroceramide 20:1 was not affected by diet or genotype. Dihydroceramides 20:0 and 24:1 were also unaltered, although this was also observed for the 20:0 and 24:1 ceramide counterparts. The 22-carbon dihydroceramides also mirrored their ceramide analogues, with CR downregulating 22:0 and 22:1, but upregulating 23:0 species (Figure 6.9). The 23:1, 26:0 and 26:1 species were all undetectable as dihydroceramides (Figure 6.9). In contrast, 24:0 dihydroceramide was upregulated by CR despite being unchanged at the ceramide level. Generally, the dihydroceramides and ceramides showed parallel regulation, Notably, Adiponectin KO generally had no effect on hepatic dihydroceramide content.

The ratio of DHC:Cermide concentration is also a useful measure of ceramide metabolism. When analysed, these ratios showed no differences between WT and KO mice. Therefore the data is not shown here.

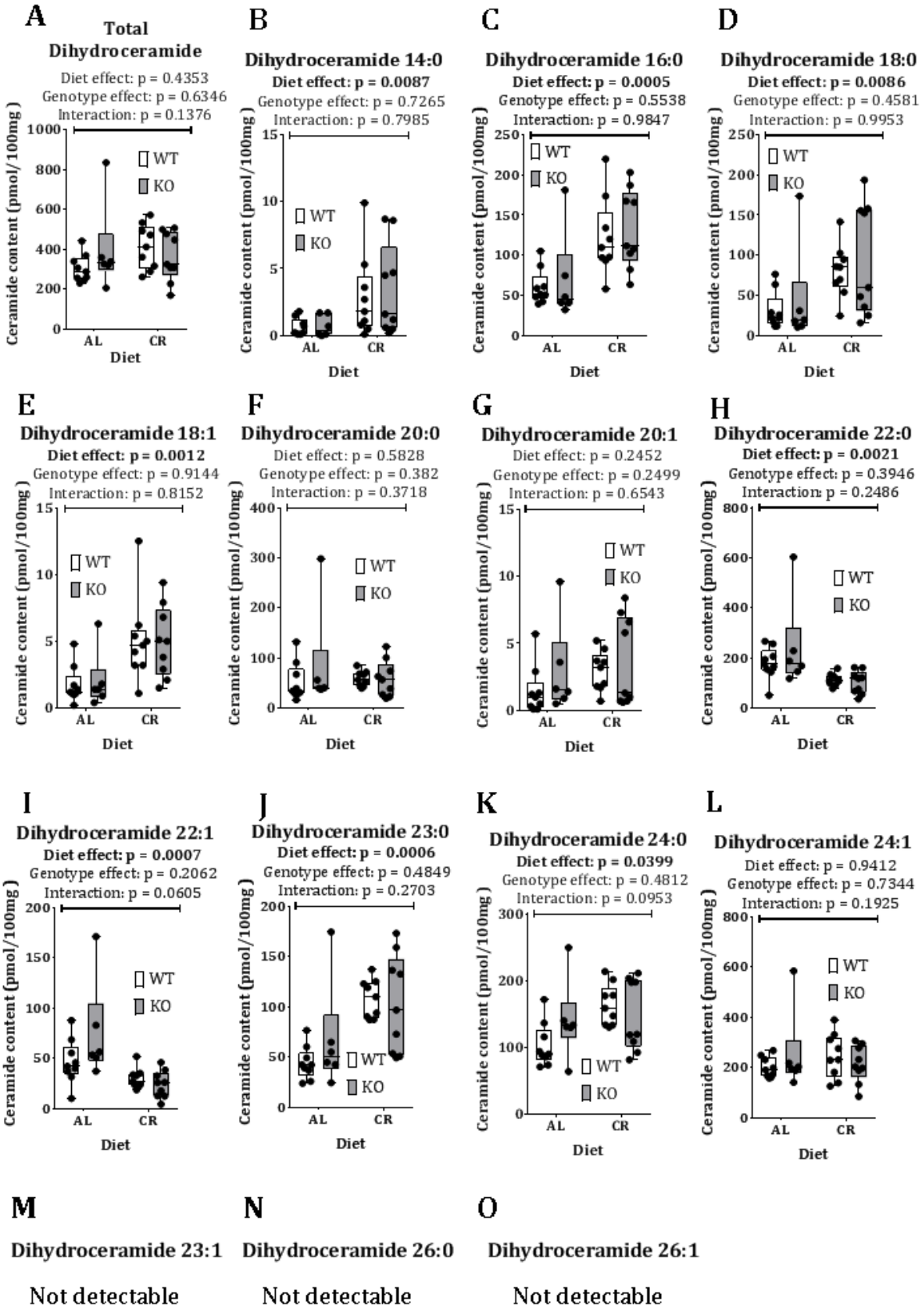

Figure 6.9 – The effects of adiponectin deficiency on dihydroceramide species in liver of AL and CR fed males. Liver from male mice was quantified for dihydroceramide

concentration by mass spectrometry. **(A)** Total dihydroceramides. **(B)** Dihydroceramide 14:0. **(C)** Dihydroceramide 16:0. **(D)** Dihydroceramide 18:0 **(E)** Dihydroceramide 18:1 **(F)** Dihydroceramide 20:0 **(G)** Dihydroceramide 20:1 **(H)** Dihydroceramide 22:0 **(I)** Dihydroceramide 22:1 **(J)** Dihydroceramide 23:0 **(K)** Dihydroceramide 24:0 **(L)** Dihydroceramide 24:1 **(M)** Dihydroceramide 23:1 **(N)** Dihydroceramide 26:0 **(O)** Dihydroceramide 26:1. All data points shown with median, interquartile range and range shown by box and whisker plot. Statistical significance was determined by 2-way ANOVA, source of variance significance is shown above the data and multiple comparisons between wild type and KO determined using Sidak's correction are indicated on the data. Number used as described inn figure 6.8.

6.2.6. Metabolic cages and indirect calorimetry

A technique for assessing whole body lipid metabolism is indirect calorimetry. Measurement of oxygen consumption and carbon dioxide production in a defined space allows determination of total energy expenditure and preferential fuel utilisation, specifically the ratio of carbohydrate to fat catabolism. If an altered lipid metabolism phenotype is responsible for the altered glucose tolerance response, then we would expect to see a differential response to CR in the adiponectin KO mice in respiratory quotient.

Figure 6.10A shows male oxygen consumption, to adjust for individual variation, mean oxygen consumption was calculated across the entire 24-hour period and split into the light and dark phases which delimit the feeding and torpor cycles of mice. Note that the dark phase of mice, which are nocturnal, is normally accompanied by a robust increase in feeding behaviour, increased activity and energy expenditure and a switch to carbohydrate utilisation with ingestion of a normal chow diet. Across the entire 24-hour period, CR caused a significant decrease in oxygen consumption. Notably, decreased oxygen consumption is observed selectively over the dark phase. Adiponectin deficiency did not affect male oxygen consumption.

In females, shown in figure 6.11, we observed the same phenomenon. They had lower oxygen consumption caused by CR and this was driven by a reduction during the night, but not during the day.

As for oxygen, carbon dioxide in male mice is decreased across 24 hours with this effect being solely down to a difference during the night. There was also a significant interaction between diet and genotype during the night, with CR-induced decreases in carbon dioxide being more pronounced in WT mice (Figure 6.12). However, given the low numbers of mice studied, additional experiments should be done before firm conclusions can be drawn.

Female carbon dioxide exhalation was also decreased with CR and this was caused by effects during the night and not during the day (Figure 6.13). However, unlike the males, females did not show a significant interaction over night between diet and genotype.

We then combined the oxygen consumption and carbon dioxide production to give the respiratory quotient (RER), a ratio between the two gasses which give information on the energy substrate utilisation of the animals. A ratio of 1 is indicative of glucose metabolism, a ratio of 0.8 represents protein or a mixed diet metabolism and 0.7 indicates that lipids are being metabolised. This change in ratio is caused by additional oxygen being required for metabolising fats and proteins prior to them entering glycolysis or the TCA cycle.

The male RER 24-hour plot shows an easily recognisable pattern, with the RER elevated during the day phase in the CR mice (Figure 6.14). When this was averaged out across the entire 24-hour period we saw a significant elevation caused by CR. When broken into day and night we saw that the 24-hour increase in RER was caused solely by an increase during the day; at night CR tended to decrease RER and this effect appeared to be greater in the WT than in the KO mice. This tentatively would support the possibility that CR-mediated enhancement of fat catabolism is impaired in the KO males; however, this is highly speculative, underscoring the need for additional mice to be studied.

In females the same is observed, with RER elevated in CR mice across a 24-hour period as a result of significant increases during the day; however, unlike in males, there was no trend in females for CR to decrease RER nocturnally.

These results for male and female mice were surprising considering that all the differences we had observed in oxygen and carbon dioxide had been observed during the night, yet the differences in RER were observed purely during the day. No genotypic differences in RER were observed in males or females, indicating that, generally, lack of adiponectin does not influence these metabolic effects of CR.

The final metabolic measurement available from the metabolic cage measurement is energy expenditure. Male energy expenditure was significantly reduced by CR, no differences were detected during the day and all differences were accounted for by a reduction during the night. This pattern was mirrored in females with a reduction in energy expenditure during the night but no differences detected during the night.

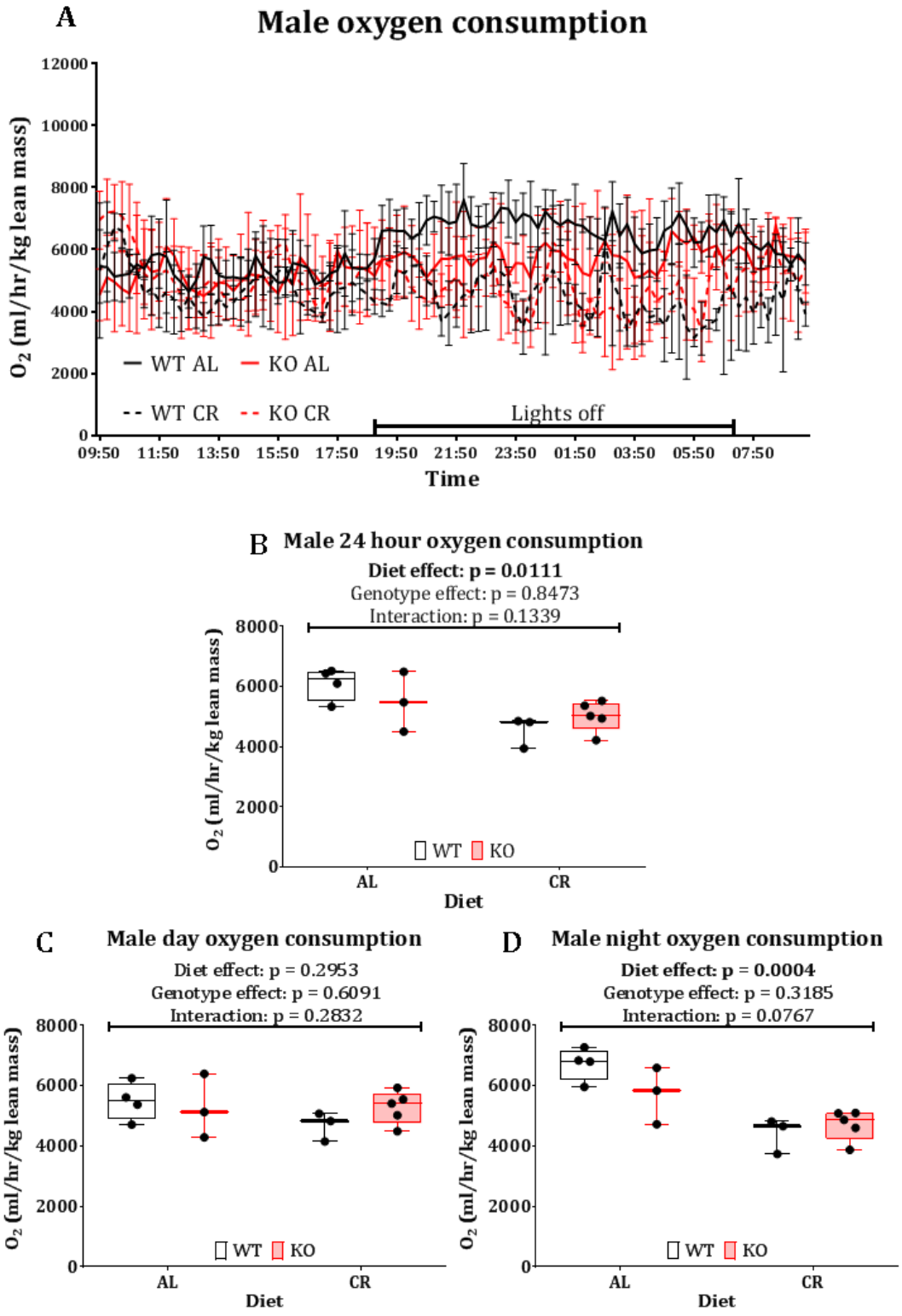

Figure 6.10 – The effects of adiponectin deficiency on male oxygen consumption. Oxygen consumption was measured by quantifying differences between reference air and exhaled air from metabolic cages over 24 hours. All data was normalised to lean body mass measurement by TD-NMR. **(A)** Male oxygen consumption measured every 15 minutes over 24 hours. Mean rate for each group plotted every 15 minutes with error bars indicating ± SD **(B)** Average oxygen consumption rate over 24 hours. **(C)** Average oxygen consumption rate during the day. **(D)** Average oxygen consumption rate during

the night. All data points shown with median, interquartile range and range shown by box and whisker plot. Statistical significance was determined by 2-way ANOVA, source of variance significance is shown above the data and multiple comparisons between wild type and KO determined using Sidak's correction are indicated on the data. Numbers used male WT AL – 4; WT CR – 3; KO AL – 3; KO CR – 5.

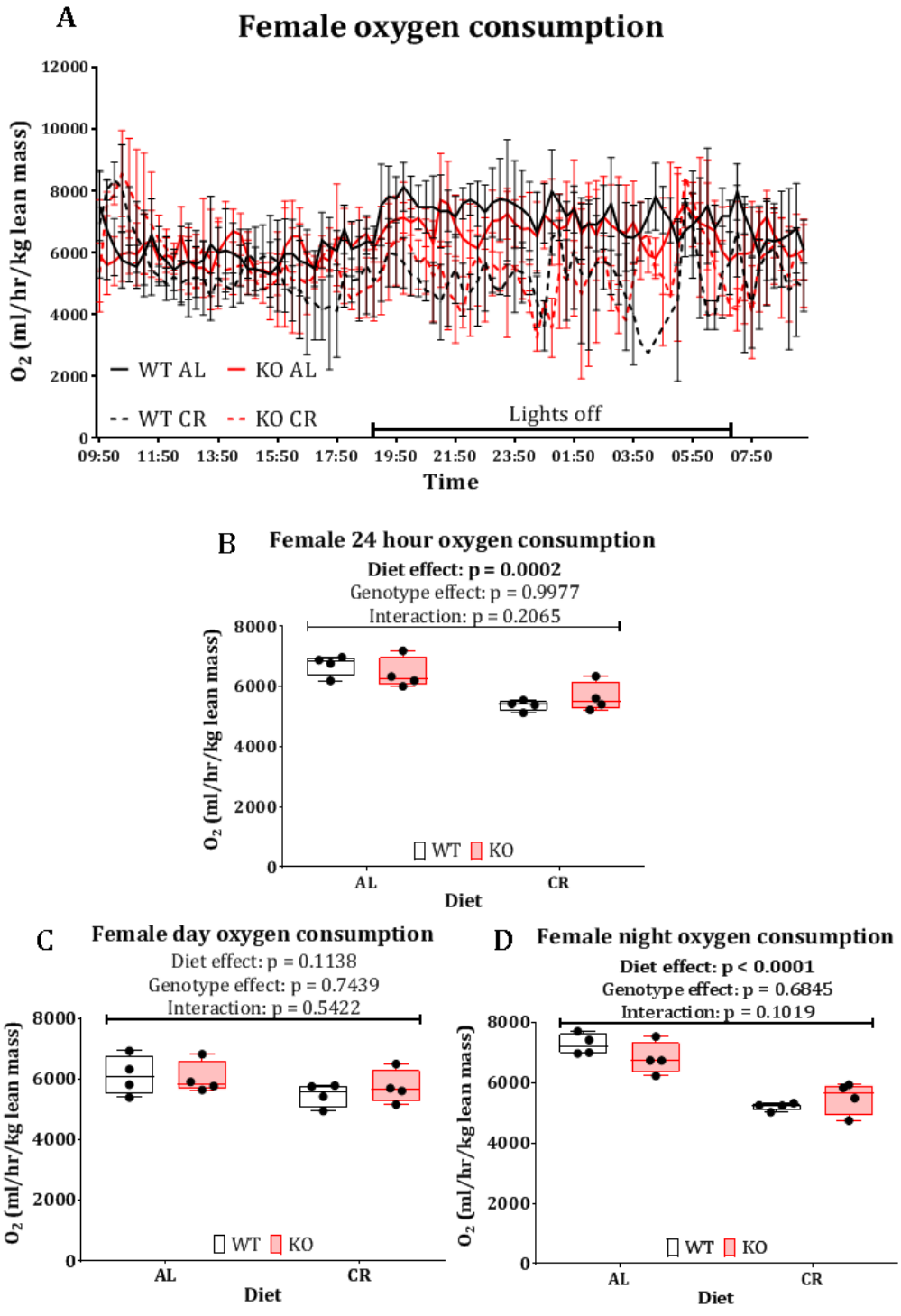

Figure 6.11 – The effects of adiponectin deficiency on female oxygen consumption. Oxygen consumption was measured by quantifying differences between reference air

and exhaled air from metabolic cages over 24 hours. All data was normalised to lean body mass measurement by TD-NMR. **(A)** Female oxygen consumption measured every 15 minutes over 24 hours. Mean rate for each group plotted every 15 minutes with error bars indicating ± SD **(B)** Average oxygen consumption rate over 24 hours. **(C)** Average oxygen consumption rate during the day. **(D)** Average oxygen consumption rate during the night. All data points shown with median, interquartile range and range shown by box and whisker plot. Statistical significance was determined by 2-way ANOVA, source of variance significance is shown above the data and multiple comparisons between wild type and KO determined using Sidak's correction are indicated on the data. Numbers used in all groups – 4.

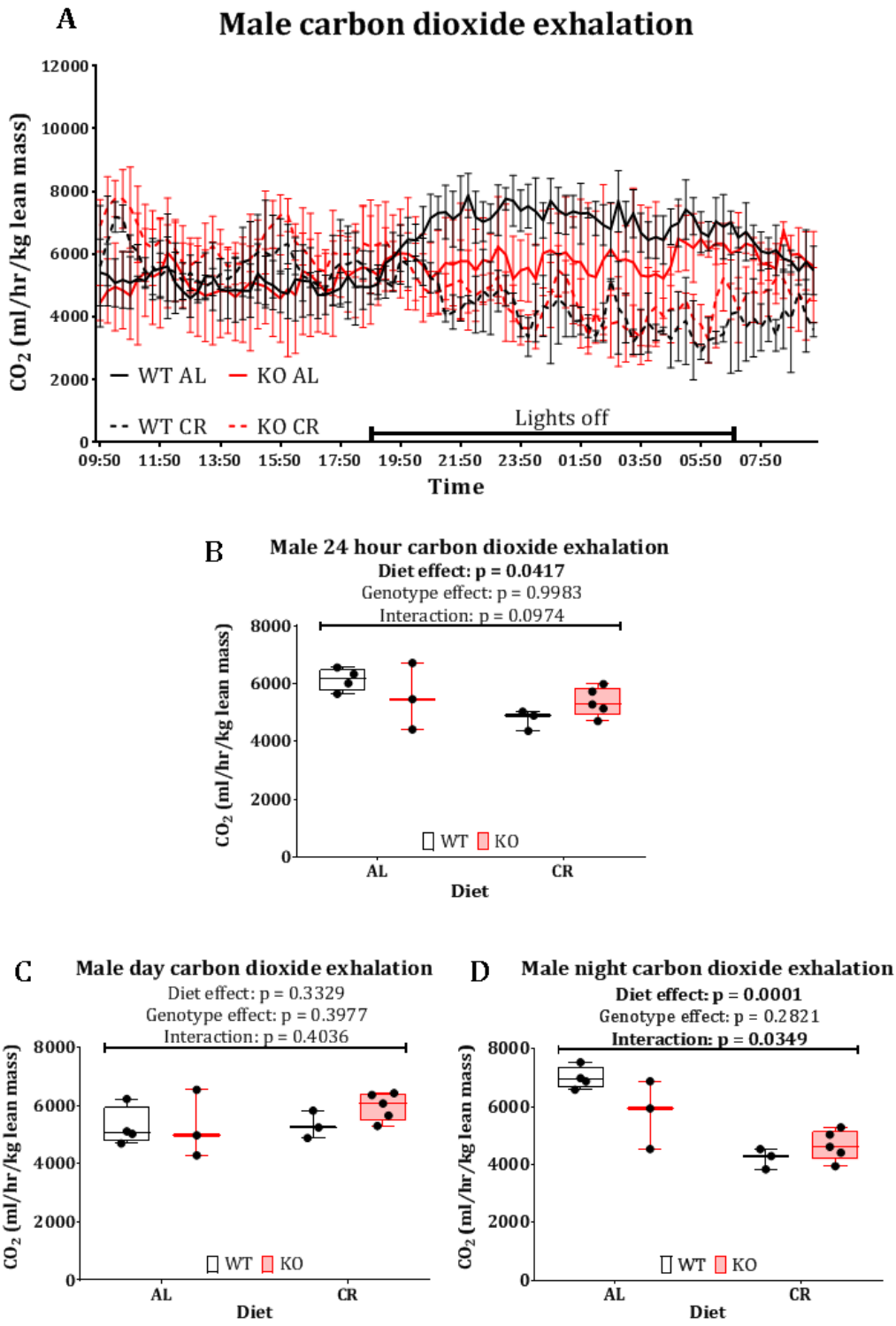

Figure 6.12 – – The effects of adiponectin deficiency on male carbon dioxide exhalation. Carbon dioxide exhalation was measured by quantifying differences between reference air and exhaled air from metabolic cages over 24 hours. All data was normalised to lean body mass measurement by TD-NMR. **(A)** Male carbon dioxide production measured every 15 minutes over 24 hours. Mean rate for each group plotted every 15 minutes with error bars indicating ± SD **(B)** Average carbon dioxide production rate over 24 hours. **(C)** Average carbon dioxide production rate during the day. **(D)** Average carbon dioxide production rate during the night. All data points shown with

median, interquartile range and range shown by box and whisker plot. Statistical significance was determined by 2-way ANOVA, source of variance significance is shown above the data and multiple comparisons between wild type and KO determined using Sidak's correction are indicated on the data. Numbers used as described in figure 6.10.

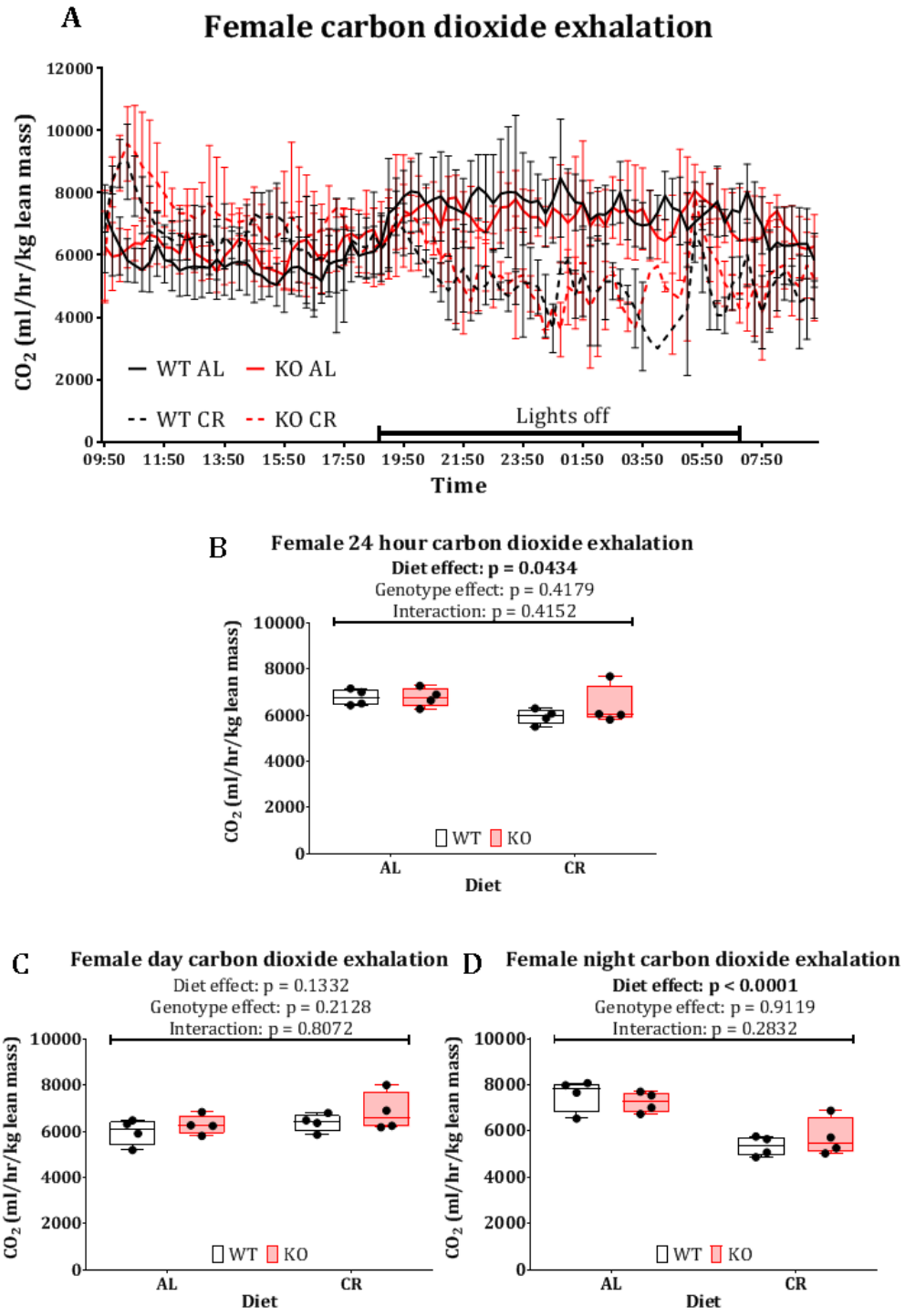

Figure 6.13 – – The effects of adiponectin deficiency on female carbon dioxide exhalation. Carbon dioxide exhalation was measured by quantifying differences between reference air and exhaled air from metabolic cages over 24 hours. All data was

normalised to lean body mass measurement by TD-NMR. **(A)** Female carbon dioxide production measured every 15 minutes over 24 hours. Mean rate for each group plotted every 15 minutes with error bars indicating ± SD **(B)** Average carbon dioxide production rate over 24 hours. **(C)** Average carbon dioxide production rate during the day. **(D)** Average carbon dioxide production rate during the night. All data points shown with median, interquartile range and range shown by box and whisker plot. Statistical significance was determined by 2-way ANOVA, source of variance significance is shown above the data and multiple comparisons between wild type and KO determined using Sidak's correction are indicated on the data. Numbers used as described in figure 6.11.

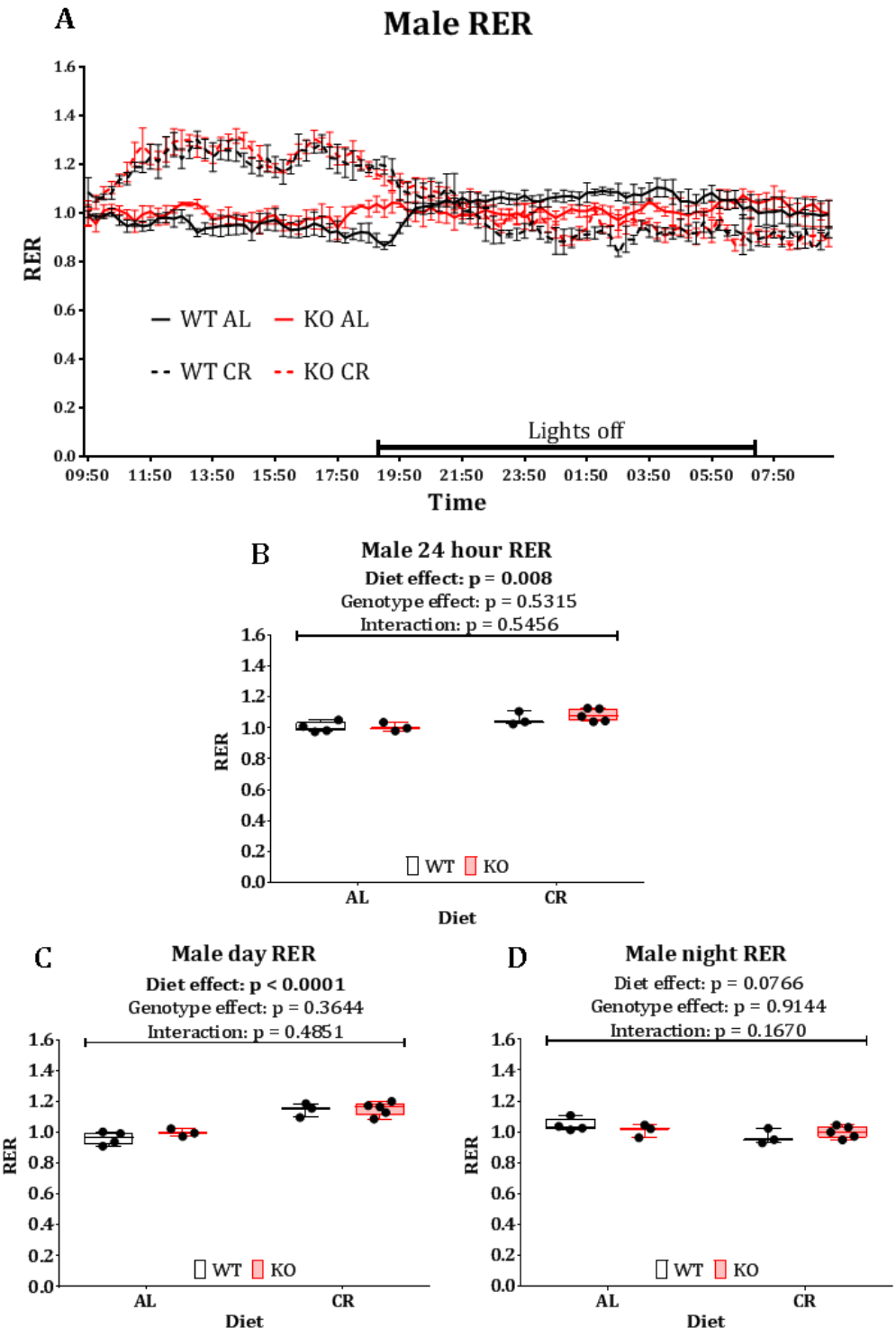

Figure 6.14 – – The effects of adiponectin deficiency on male respiratory exchange ratio. The ratio of oxygen consumed and carbon dioxide produced was calculated over 24 hours. All data was normalised to lean body mass measurement by TD-NMR. **(A)** Male respiratory exchange ratio measured every 15 minutes over 24 hours. Mean ratio for each group plotted every 15 minutes with error bars indicating ± SD **(B)** Average respiratory exchange ratio over 24 hours. **(C)** Average respiratory exchange ratio during the day. **(D)** Average respiratory exchange ratio during the night. All data points shown with median, interquartile range and range shown by box and whisker plot. Statistical

significance was determined by 2-way ANOVA, source of variance significance is shown above the data and multiple comparisons between wild type and KO determined using Sidak's correction are indicated on the data. Numbers used as described in figure 6.10.

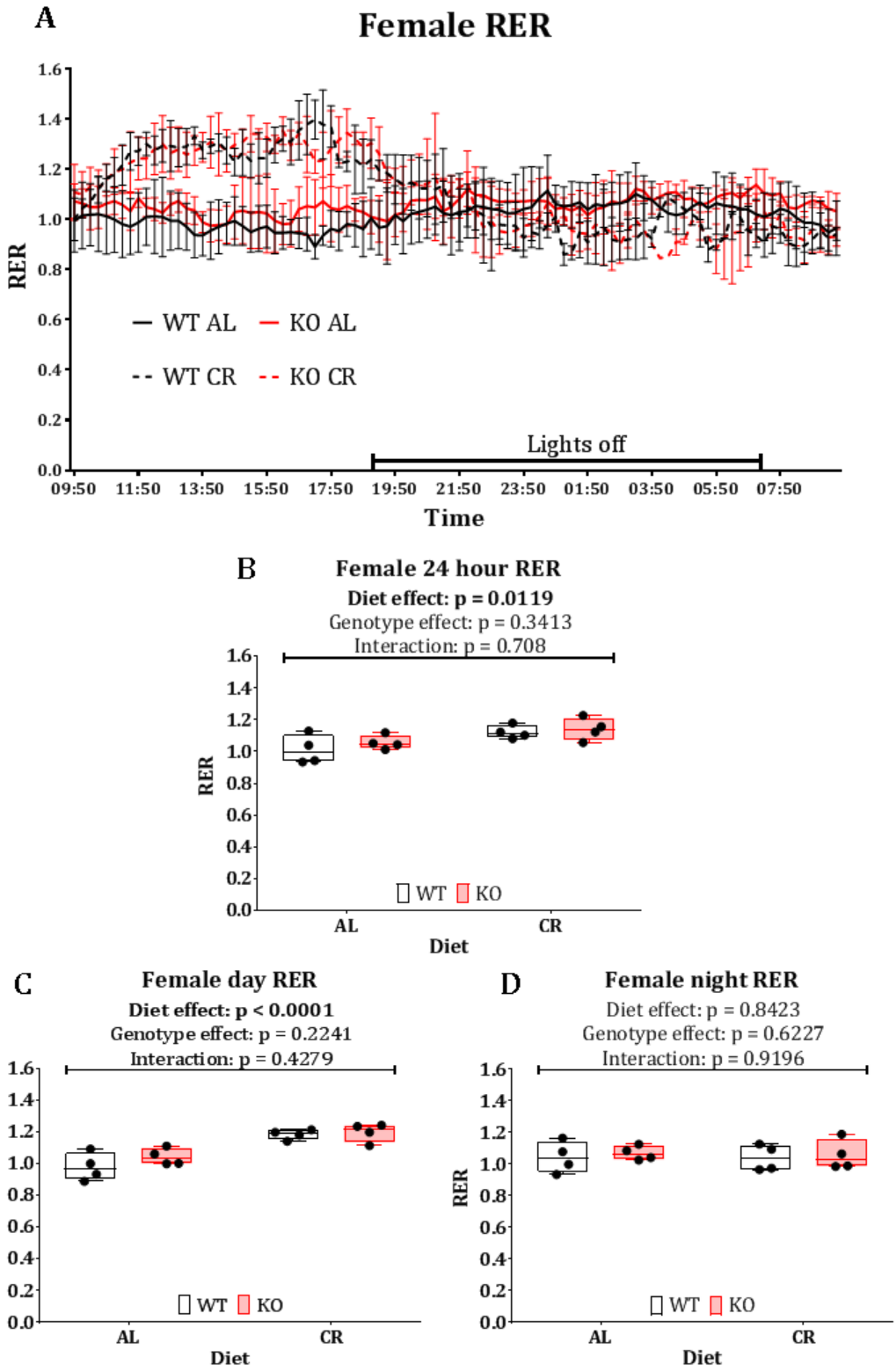

Figure 6.15 – The effects of adiponectin deficiency on female respiratory exchange ratio. The ratio of oxygen consumed and carbon dioxide produced was calculated over 24 hours. All data was normalised to lean body mass measurement by TD-NMR. **(A)**

Female respiratory exchange ratio measured every 15 minutes over 24 hours. Mean ratio for each group plotted every 15 minutes with error bars indicating ± SD **(B)** Average respiratory exchange ratio over 24 hours. **(C)** Average respiratory exchange ratio during the day. **(D)** Average respiratory exchange ratio during the night. All data points shown with median, interquartile range and range shown by box and whisker plot. Statistical significance was determined by 2-way ANOVA, source of variance significance is shown above the data and multiple comparisons between wild type and KO determined using Sidak's correction are indicated on the data. Numbers used as described in figure 6.11.

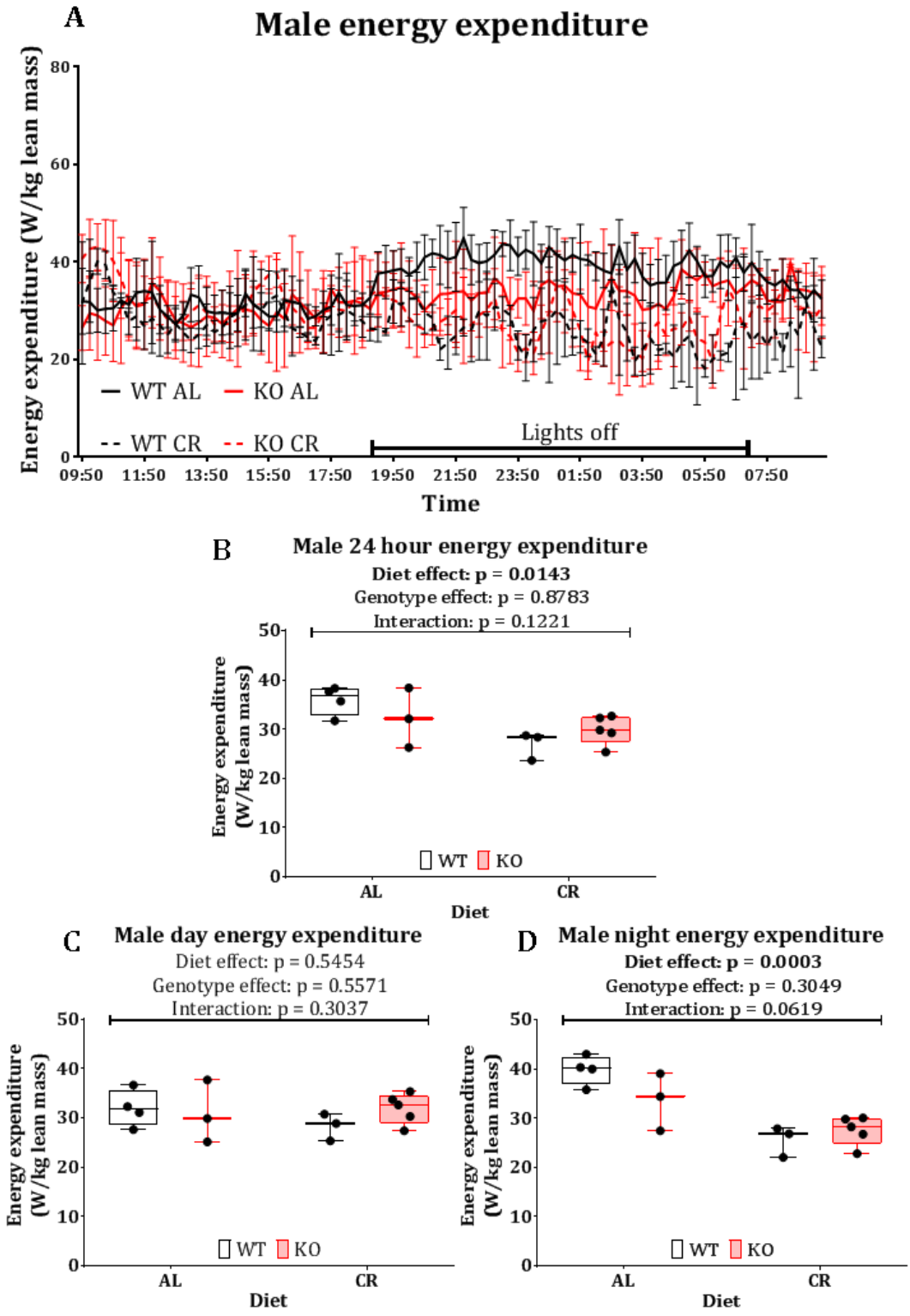

Figure 6.16 – The effects of adiponectin deficiency on male energy expenditure. The energy expenditure was calculated over 24 hours. All data was normalised to lean body mass measurement by TD-NMR. **(A)** Male energy expenditure measured every 15 minutes over 24 hours. Mean ratio for each group plotted every 15 minutes with error bars indicating ± SD **(B)** Average energy expenditure over 24 hours. **(C)** Average energy expenditure during the day. **(D)** Average energy expenditure during the night. All data points shown with median, interquartile range and range shown by box and whisker

plot. Statistical significance was determined by 2-way ANOVA, source of variance significance is shown above the data and multiple comparisons between wild type and KO determined using Sidak's correction are indicated on the data. Numbers used as described in figure 6.10.

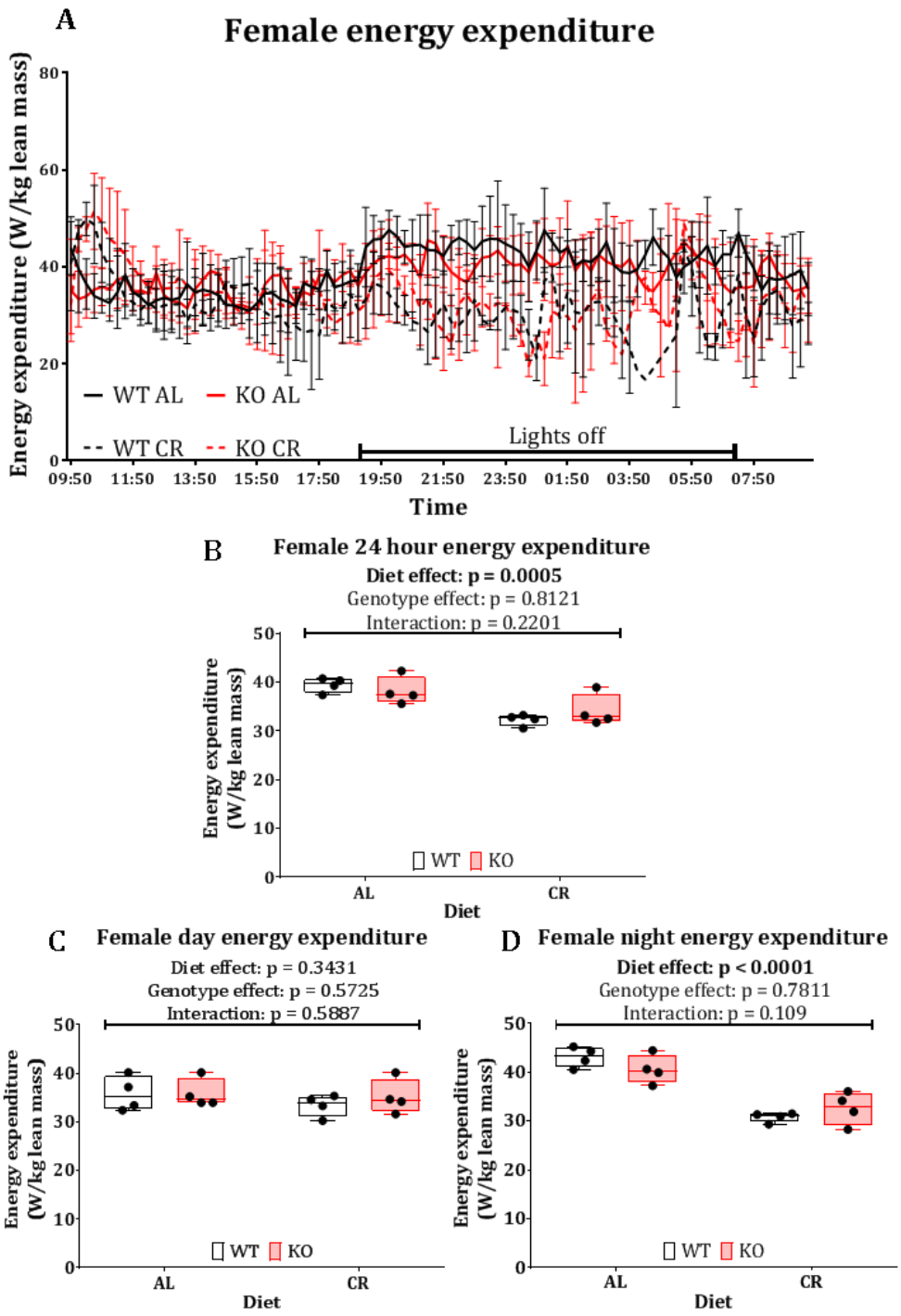

Figure 6.17 – The effects of adiponectin deficiency on female energy expenditure. The energy expenditure was calculated over 24 hours. All data was normalised to lean body mass measurement by TD-NMR. **(A)** Female energy expenditure measured every 15 minutes over 24 hours. Mean ratio for each group plotted every 15 minutes with error bars indicating ± SD **(B)** Average energy expenditure over 24 hours. **(C)** Average

energy expenditure during the day. **(D)** Average energy expenditure during the night. All data points shown with median, interquartile range and range shown by box and whisker plot. Statistical significance was determined by 2-way ANOVA, source of variance significance is shown above the data and multiple comparisons between wild type and KO determined using Sidak's correction are indicated on the data. Numbers used as described in figure 6.11.

The cages used during the indirect calorimetry are equipped with light beam sensors that can detect movement of the mice within the cages. They exist on both the x and y axis of the cage and the number of times the beams are broken is used as a measure of physical activity of the mice. Here, I present the number of beam breaks across a 24-hour period as well as this same period broken into the day (lights on) phase and night (lights off) phase. A strong diet effect was present in both males and females across the 24-hour measurement period, but this was strongly sexually dimorphic: the male CR mice were more active than their AL counterparts whilst the female CR mice were significantly less active than AL females (Figure 6.18). When we break this down into the day and night phase, we observed that the male CR mice were more active during the day than the AL mice but showed the same activity levels as the AL mice during the night. Conversely, in females, the CR group showed the same amount of activity as AL controls during the day phase and less activity during the night phase (Figure 6.18). Overall, CR increased physical activity in males and this was due to an increase during the day, whereas CR decreased activity in females and this was due to a decrease during the night. These activity differences could provide some rationale for the sexual dimorphisms in glucose tolerance observed in this chapter and chapter 5. No genotypic differences were observed in males or females, indicating no contribution of adiponectin to activity programming during CR.

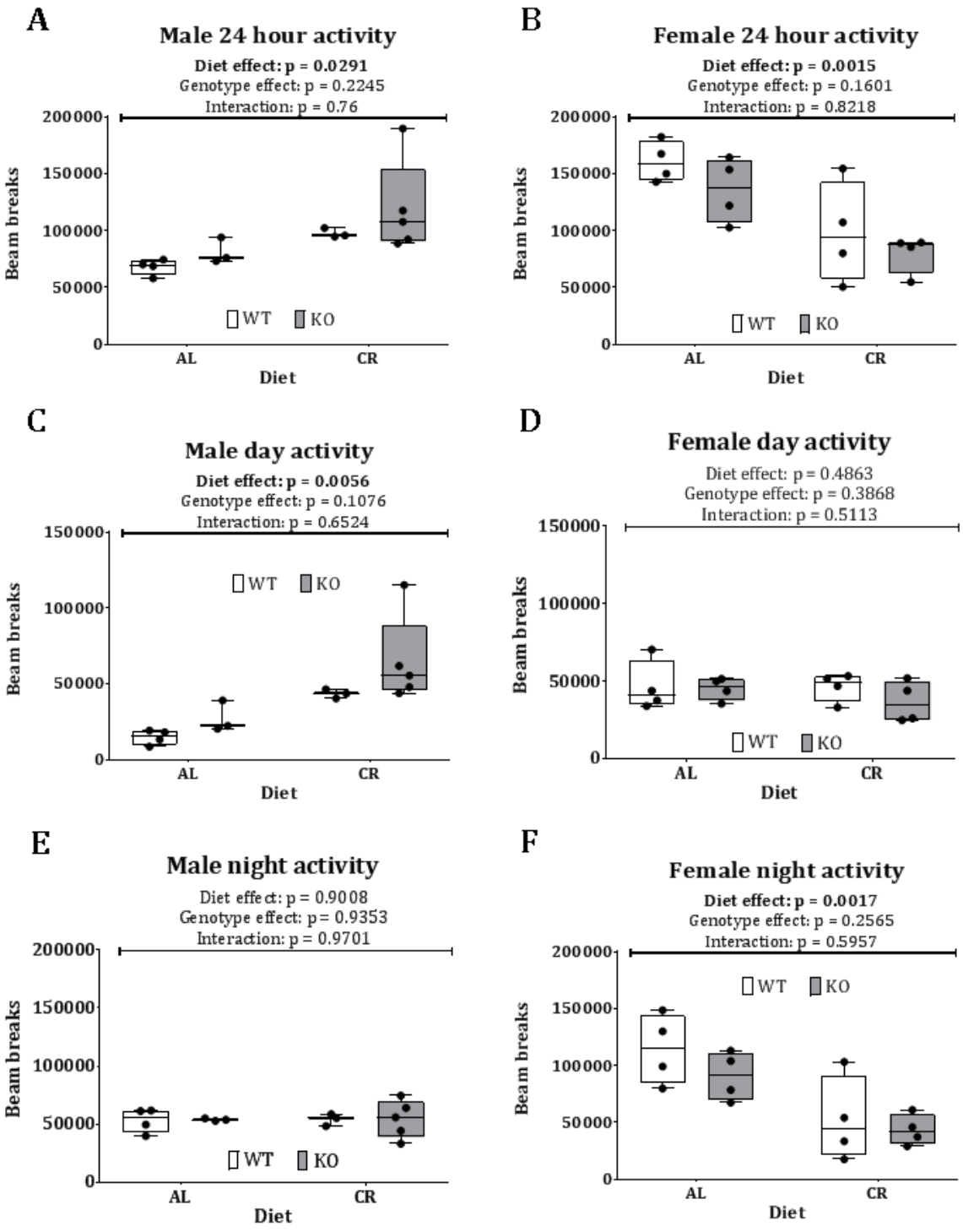

Figure 6.18 – Male CR mice are more active during the day and female CR mice are less active during the night than their AL counterparts. Light beam breaks in the x and y axis were counted over a 24 hour period and summed over this entire period as well as for the day and night phase. **(A)** Male 24 hour activity. **(B)** Female 24 hour activity. **(C)** Male day activity. **(D)** Female day activity **(E)** Male night activity **(F)** Female night activity. All data points shown with median, interquartile range and range shown by box and whisker plot. Statistical significance was determined by 2-way ANOVA, source of variance significance is shown above the data and multiple comparisons

between wild type and KO determined using Sidak's correction are indicated on the data. Numbers used as described in figure 6.10 and 6.11.

6.3. Discussion

Four weeks of CR was chosen for the adiponectin KO study given previously acquired results from the time-course study (Chapters 4-5). We observed that 4 weeks of CR induced the maximal increases in adiponectin and that after this point adiponectin plasma concentrations remained fairly constant in CR mice. Therefore, to minimise the amount of time animals were required to be in the experiment, we chose to restrict the animals to the point of maximal hyperadiponectinaemia, but no further. One disadvantage of this is that we saw smaller changes in glucose tolerance in the time course after 4 weeks when compared to both 2-week and 6-week restrictions. Despite this, we still saw improvements in glucose tolerance between AL and CR WT males and, unexpectedly, this CR effect was even greater in KO mice of each sex, indicating that the 4-week time point was sufficient to observe differences between the diets and genotypes.

Given that adiponectin has been shown to act in the liver to reduce gluconeogenesis[57], it was expected that mice lacking adiponectin would not be able to reduce their hepatic glucose production as well as the WT mice in response to the glucose bolus received during the glucose tolerance test. As we see here, the glucose tolerance response of the adiponectin KO mice was better, indicating that the mice are better at reducing their gluconeogenesis and/or at increasing their peripheral glucose uptake. This is counter intuitive to the previously cited literature showing that adiponectin inhibits gluconeogenesis and that adiponectin can increase peripheral glucose uptake[44]. Unlike on the CR diet, KO males fed an AL diet displayed impaired glucose tolerance compared to WT AL males, which is consistent with previous studies reporting impaired glucose tolerance with adiponectin KO. Thus, it may be that CR alters the mechanism for action of adiponectin which causes the opposite effects of adiponectin KO on glucose tolerance.

Unlike previous chapters the data for lean and fat mass by TD-NMR and tissue necropsy masses were not plotted as percentages of total body mass and were only expressed in absolute terms. This decision was taken given that no great differences were observed between absolute and percentage previously and given that there were no changes caused by genotype in absolute tissue masses no differences were seen for percentages and so the data was not shown.

We saw large increases in plasma NEFA in response to CR, which is a phenomenon that has been previously reported[276]. However, it should be noted that this effect was reversed after longer term CR[276]. It has been previously observed that adiponectin KO causes an increase in plasma triglyceride concentrations but not in plasma free fatty

acids[267], and the impact of adiponectin on CR-induced changes in plasma lipids has never previously been determined. My findings show that, in males, adiponectin KO increases plasma NEFA during CR, suggesting that adiponectin promotes NEFA clearance and/or impairs lipolytic NEFA production during CR. Future studies should explore these possibilities, for example through fatty acid tolerance tests and analysis of rates of lipolysis *in vivo.*

The triacylglyceride assay used to quantify TG concentrations in the liver works by lysing the fatty acids from the glycerol backbone and then using the glycerol to produce a quantifiable colour change. A disadvantage of this procedure is that it does not take into account any constitutive glycerol in the liver prior to TG cleavage. A more robust method for TG quantification would be to quantify constitutive glycerol present in the liver, not bound to fatty acids, then to quantify the total cleaved and constitutive glycerol and calculate the contribution of TG incorporated glycerol as a measure of TG concentration.

The results of the ceramide analysis indicate that despite the cytotoxic effects of some ceramides, many species are increased in CR, suggesting potential beneficial effects on cellular and physiological function. The lack of genotypic differences was also surprising given the reported role of adiponectin signalling on ceramide synthesis, and suggest that adiponectin is not a major mediator of the effects of CR on ceramide metabolism

The observed increase daytime activity induced by CR has been previously observed, a previous study involved looking at feeding time on CR experiments saw that CR mice fed during the day or overnight on a restricted diet were more active during the day[277]. However, this was only performed in male mice so does not corroborate the behaviour we observed in females. Male CR mice have also been observed to be more active during the day in another study, which found that this effect occurred after one month of CR [278]. This further validates our finding, yet this previous study also showed that the effect does not persist after 6 months of CR[278]. An explanation for the increase in male CR mice activity may be food anticipatory activity (FAA), whereby organisms react to circadian rhythms associated with feeding[279]. Far less research has been performed on female mice to verify our findings of reduced activity during the night. However, these sex differences might contribute to the other sexually dimorphic effects of CR, such as on fat mass and glucose tolerance (Chapter 5). Thus, future studies should further explore if the effects of CR on energy homoestasis differ between males and females, as this may have widespread implications for the use of CR as a therapeutic strategy against chronic diseases.

The feeding regimen was likely to have confounded the above results, given that the AL mice had 24 hour free access to food, which they ate gradually over the dark phase, and that the CR mice were fed a once daily diet ration at around 9:00am which they ate over approximately 2 hours. A potential improvement to this feeding regimen that would

more faithfully recapitulate normal feeding behaviour in CR mice would be to administer small doses of food overnight, allowing them to eat gradually during the dark phase in a similar fashion to the AL group. Whist manual administration of food in this manner would not be possible, a mechanical feeding device could solve the problem. Such a device is disclosed by a research group from The University of Texas Southwestern Medical Centre, this device allows single pellets of diet at a defined weight to be administered with removal time recorded and a programmed delay before a new pellet is dispensed[277]. This allows for very precise feeding regimens to be implemented and additional feeding data to be collected.

The lack of differences between KO and WT mice was surprising. This is because during times of calorie scarcity it is beneficial to the organism to conserve as much energy as possible to increase the chances of survival. Therefore, during mammalian evolution (and potentially even earlier) the increased adiponectin concentrations during CR must have imparted a survival benefit considering the energy investment in synthesising the additional protein. Given the mild phenotype of adiponectin knockout *in vivo* it seems likely that adiponectin is not playing a major role during times of calorie sufficiency, excess or mild deficiency. However, the effects of adiponectin on glucose and lipid homeostasis *in vitro* are well known showing that adiponectin does exert a strong signalling effect. Therefore, it may be that adiponectin acts most strongly during times of extreme calorie deficiency, at times of near starvation. This would explain why we do not see a large phenotype caused by adiponectin knockout during moderate CR. Unfortunately, this hypothesis is not easily testable given the ethical issues with severe CR. One potential way to test this would be to use drosophila which are not protected by law and have some conserved adiponectin signalling[280].

Future directions for further elucidating the role of adiponectin in mediating some of the benefits of CR will primarily focus on the glucose tolerance result and how and if this relates to the increased plasma NEFA concentrations. In order to determine the contribution of insulin to the improved glucose tolerance in adiponectin KO mice when exposed to CR, clamp studies could be used. A hyperglycaemic clamp in which glucose is perfused into the blood to reach a steady state concentration can be used to measure the insulin secretion and glucose uptake capacity of the mice. Based on our findings, we would expect the adiponectin KO mice to have elevated insulin secretion and/or increased glucose uptake during CR, given my finding that the KO mice have improved glucose tolerance during CR. A hyperinsulinemic-euglycemic clamp could also be used, in which insulin is perfused at a concentration above basal levels whilst glucose is infused to maintain blood glucose concentration at basal level. The rate of glucose infusion can give a measure of the insulin-induced glucose uptake in the body, and therefore the sensitivity to insulin; under these clamp conditions, the glucose infusion rate is generally considered a mark of how insulin resistant the mice are. The literature

reports adiponectin to play an insulin-sensitising role so we may expect the KOs to be less insulin sensitive, at least on an AL diet; however, no previous studies have applied such in-depth metabolic phenotyping to adiponectin KO mice during CR. Based on the present findings, I would expect glucose infusion rate to increase in the CR-fed KO mice, relative to WT counterparts, as a result of improved insulin sensitivity in the KO mice.

To further examine the impact and source of the increased NEFAs in the blood of the CR mice, and the augmentation of this effect in the adiponectin KO mice, mass spectrometry could be used to determine which lipid species are specifically increased or if the effect is generic across all species. Long-term aims could evaluate the effect of tissue specific adiponectin KO receptors during CR to further elucidate the role adiponectin plays during this dietary intervention. A liver specific KO for both adiponectin receptors could tell us if this increase in plasma lipid is derived from the liver, additionally an adipose tissue KO could answer the same question for this organ.

A fundamental issue with the indirect calorimetry data is the low number of mice per group: due to time constraints, fewer mice than would be ideal had been processed through the system and so it was hard to draw strong conclusions from the data. In the future, more cohorts will be analysed to further elucidate any genotypic differences here. Our results show an RER greater than one, which is fairly uncommon but can be explained by a variety of reasons. One reason could be metabolism of a highly oxygen-rich energy source, such as malic or tartaric acid[281]; however, given that the diet consumed by the mice is highly controlled and the formulation known, this does not seem likely. Additionally, these acids are generally only present in trace amounts in food and are toxic in large quantities[282] so could not contribute to the overall RER of the animals; hence, we can rule this out as a contributing factor. An alternative reason is that the CR mice are converting the ingested carbohydrates into fats, i.e. de novo fatty acid biosynthesis. This process requires oxygen and so more oxygen must be used from the air, resulting in a RER greater than one[283].

The values for energy expenditure and O_2 and CO_2 flow rates are expressed relative to lean mass. This is to mitigate the effects caused by varying body size of the mice, particularly due to the effects of CR. Whilst the calculation could have been performed using body mass, adipose tissue has a far lower metabolic rate than lean tissues, therefore lean mass is a more accurate scaling factor for the above mentioned parameters. One problem with this is that whilst adipose tissue has been shown to be fairly metabolically inert in vitro this may not be representative of adipose tissue in vivo[284]. Additionally, using lean mass also make the assumption that the adipose tissue is completely metabolically inert which is obviously not the case. Despite this, expressing

the values relative to lean mass remains a well-used measurement and can still provide useful conclusions.

Given that the main differences in oxygen and carbon dioxide utilisation rates were during the night in the CR mice, it was surprising that the differences in RER were observed during the day, with no changes during the night compared to the AL mice. This means the change in RER is likely caused by a more subtle change in ratio between oxygen and carbon dioxide and that the nocturnal decreases in both are proportional, bringing the CR mice onto the same level as the AL mice. A topic touched on in previous discussion chapters is the feeding regimen for the CR mice, with the mice receiving all their food in one dose in the morning. This causes variation compared to the AL mice, which eat their food gradually across the night. This is the likely cause of the large increase in RER in the day, immediately after the CR mice have been fed and are digesting and metabolising their diet.

The lack of genotypic differences observed in the metabolic cages experiment indicates that there are no organism-wide differences in lipid metabolism in opposition to our hypothesis. However, speculatively, it seems that there is a trend in males for the CR to decrease nocturnal RER in the WT mice, but not in the KO mice (Figure 6.14D). If so, this would support the possibility that adiponectin is required for CR-induced increases in lipid oxidation. As mentioned above, the low numbers per group mean that firm conclusions cannot yet be drawn. What is clear, from the results herein, is that lack of adiponectin does influence at least some of the metabolic effects of CR, but in a manner that goes directly against our original hypothesis. Therefore, these studies highlight unexpected roles of adiponectin in conditions of CR, which might relate to the evolutionary role of adiponectin as a hormone that is important for surviving periods of energy deficit.

7. Discussion

One of the fundamental aims of this thesis was to further test the contribution of BMAT to hyperadiponectinaemia, both in CR and in other contexts. The other fundamental aim was to discover to what extent adiponectin contributes to the metabolic adaptions induced by CR, given the large overlap in the effects of CR and hyperadiponectinaemia.

7.1. BMAT as a source of adiponectin

With regard to examining BMAT as a secretory source of adiponectin, I was only able to draw limited conclusions from the TZD study given the lack of resistance to TZD-induced BMAT expansion in the Ocn-Wnt10b mice. I still observed TZD-induced increases in WAT adiponectin production, which indicates that adiponectin is secreted from both WAT and BMAT in response to TZD, as previously shown in CR[121]. Further tests of this hypothesis can be drawn from the CR time-course experiment. I see that adiponectin increases occur moderately rapidly, with maximal increases observed around 4 weeks of CR. This does not correspond to a mutual rise in tibial BMAT volume, which may indicate that the BMAT is not a major contributor to circulating adiponectin. This, however, is based on the assumption that BMAT volume increase is required for it to be able to increase adiponectin. It may be that increased transcription and/or translation of adiponectin is able to occur from a constant volume of BMAT. Importantly, I saw some increases in tibial *Adipoq* transcript expression, particularly around 4 weeks of CR, indicating a potential contribution from BMAT.

There is some evidence that BMAT is acting as a contributory source of adiponectin during CR. We observed that in female mice, adiponectin is increased by CR after 2 weeks whereas in males it is increased after 3 weeks. Similarly, femoral BMAT in female mice was increased after 2 weeks but not in males. Additionally, female mice tended to have increased tibial BMAT after 2 weeks whereas males did not. Based on this there appears to be an association between the timing of increased BMAT and increased circulating adiponectin.

To further test this hypothesis, femoral BMAT volume could be quantified in the 4-week group of mice to examine if this bone is a more important contributor to overall CR-induced hyperadiponectinaemia. Additionally, the transcript and/or protein expression of *Adipoq*/adiponectin in WAT could be assessed. If a large increase in expression is observed around 4 weeks into CR, it could be concluded that the WAT may be providing a greater contribution to hyperadiponectinaemia. However, previous studies have shown that CR generally does not increase adiponectin expression or secretion in WAT[110], supporting the conclusion that BMAT makes a greater contribution to hyperadiponectinaemia in this context. Another limitation is that transcript expression of adipoq and other adipose markers was done for whole bones, but not for isolated

bone marrow or BMAds. In part this is because, when I began these studies, methods for isolation of mouse BMAds had not yet been optimised, and such methods only started to be published after my whole-bone transcript analyses had been completed[285]. Thus, future studies could better resolve the effects of CR on BM adiposity, and on adiponectin production from BMAT, by specifically measuring transcript expression in isolated BM and BMAds. Ideally, both the CR and TZD experiments could be performed in genetically altered mice that completely lack BMAT, to further test if they would have blunted hyperadiponectinaemia in response to these stimuli. Unfortunately, despite efforts from our lab and others, a transgenic mouse model that specifically lacks BMAT has yet to be established.

7.2. Adiponectin as a mediator of the effects of CR

The second hypothesis that adiponectin contributes to CR-induced metabolic adaptions was tested both via the CR timecourse studies and through CR studies in the adiponectin KO mice. I aimed to evaluate the coincidence of hyperadiponectinaemia and the metabolic adaptions to CR. If we saw the adaptions occur at the same time or after the rise in adiponectin, this would give evidence that adiponectin may be driving some of these benefits. However, if the benefits preceded hyperadiponectinaemia it would suggest that adiponectin is not playing a significant role. We saw very rapid improvements in glucose tolerance following CR, prior to any significant increases in adiponectin in males or females. This indicates that hyperadiponectinaemia is not required for the improvements in glucose tolerance induced by CR. This is consistent with data from the adiponectin KO mice. Looking at AL mice only, we see an effect consistent with previous studies, whereby adiponectin KO males show a higher blood glucose concentration following glucose administration. This could be caused by an impairment in peripheral glucose uptake and/or a reduced ability for insulin to supress hepatic glucose production, with the latter being more likely given previous literature[268]. Yet, when these mice are calorie restricted, we see a lower glucose peak following glucose administration in the adiponectin KO mice and greater effect of CR in decreasing the AUC. This is indicative of more rapid uptake of glucose peripherally and/or a more rapid or effective suppression of hepatic gluconeogenesis. From these data we can see that glucose homeostasis improvements in response to CR are not dependent on adiponectin. To the contrary, the results of these studies suggest that hyperadiponectinaemia impairs CR-induced improvements in glucose tolerance, such that this CR effect is enhanced in the absence of adiponectin. Insulin tolerance tests would be one way to determine if these GTT differences reflect corresponding differences in insulin responsiveness. As previously mentioned, a hyperinsulinaemic-euglycaemic clamp study would give a further, more precise determination of the nature of these changes.

An interesting future direction for this work would be to characterise the BMAT volumes and skeletal microarchitecture of adiponectin KO mice. It may be that BMAT expansion is halted once adiponectin concentrations reach a certain maximal amount. If true, this would manifest as larger increases in BMAT volume in calorie-restricted adiponectin KO mice compared to wild-type controls. On the other hand, increases in adiponectin could help to drive the expansion of BMAT and so, without adiponectin, BMAT may not increase in response to CR. Some research does exist on the effects of adiponectin on BMAT. It has been demonstrated *in vivo* that adiponectin is able to block adipocyte formation[286] and this may represent a paracrine mechanism of limiting excessive BMAT expansion. Additional bone research in adiponectin knockout mice could also focus on the cortical bone loss caused by CR. Given that adiponectin is implicated in improving bone mineral density[213] it could be the case that CR-induced bone loss is even more severe in adiponectin KO mice.

7.3. Sexual differences in the response to CR

None of the experiments in this thesis were designed to specifically test the differences between males and females. In many cases, males and females in the same cohort were analysed on different days given the scale of mice involved. Therefore, drawing conclusions on the differences between males and females should be done cautiously. The reason for this was that our focal hypothesis related to the response to CR and what differences existed between either the duration of CR or the difference between WT and adiponectin KO mice. Therefore, when designing the methodology for the experiments, the cohorts were designed such that there were equal numbers of AL and CR, and WT and KO mice to allow accurate comparisons to be made. If sex of the mice was also included in this matching, it would have reduced the number of mice used in each cohort. This would result in an increase in the total number of mice used and greater numbers of mice unused given they were in excess of the strict matching criteria. Work succeeding this thesis will focus on designing and implementing CR experiments to directly compare the differences between male and female mice in greater detail.

Regardless the above considerations, there appears to be many differences in the response to CR between males and females. Fundamentally, female mice appear to lose less weight in response to CR than males. This is a well-known phenomenon in humans[65]. We also see large sexual dimorphisms in body composition with males showing large reductions in fat mass with no differences in females. A further difference between males and females appeared to be the response to glucose tolerance tests with greater improvements in males compared to females. These differences need further research and could have implications in the far future regarding the use of adiponectin agonists or antagonists. Whilst much research has been performed on adiponectin agonists[287] little has been performed on adiponectin antagonists. Based on the glucose tolerance results in the adiponectin knockout mice it could be possible that adiponectin

antagonism could improve glucose tolerance although more research is required to establish the mechanism behind this effect.

7.4. Concluding Remarks

In conclusion, we cannot say that any of our initial hypotheses can be confidently confirmed. However, these studies have provided valuable insights into the temporal dynamics of CR that were previously unknown. In addition to the data here, large amounts of tissue are still frozen and fixed for future analysis allowing further hypotheses to be tested from these experiments. We also gained valuable information regarding the response to CR in both the presence and absence of circulating adiponectin. We revealed no situations in which adiponectin is required for a beneficial response to CR, yet, given the large resource commitment to increase this hormone in a time of energy scarcity, we still believe there is a reason for adiponectin to be so elevated in CR.

8. References

1. Scherer, P.E., Williams, S., Fogliano, M., Baldini, G. & Lodish, H.F. A novel serum protein similar to C1q, produced exclusively in adipocytes. *The Journal of biological chemistry* **270**, 26746-26749 (1995).
2. Hu, E., Liang, P. & Spiegelman, B.M. AdipoQ is a novel adipose-specific gene dysregulated in obesity. *The Journal of biological chemistry* **271**, 10697-10703 (1996).
3. Maeda, K.*, et al.* cDNA cloning and expression of a novel adipose specific collagen-like factor, apM1 (AdiPose Most abundant Gene transcript 1). *Biochem Biophys Res Commun* **221**, 286-289 (1996).
4. Nakano, Y., Tobe, T., Choi-Miura, N.H., Mazda, T. & Tomita, M. Isolation and characterization of GBP28, a novel gelatin-binding protein purified from human plasma. *Journal of biochemistry* **120**, 803-812 (1996).
5. Wang, Y., Xu, A., Knight, C., Xu, L.Y. & Cooper, G.J.S. Hydroxylation and Glycosylation of the Four Conserved Lysine Residues in the Collagenous Domain of Adiponectin: POTENTIAL ROLE IN THE MODULATION OF ITS INSULIN-SENSITIZING ACTIVITY. *Journal of Biological Chemistry* **277**, 19521-19529 (2002).
6. Tsao, T.-S., Murrey, H.E., Hug, C., Lee, D.H. & Lodish, H.F. Oligomerization State-dependent Activation of NF-κB Signaling Pathway by Adipocyte Complement-related Protein of 30 kDa (Acrp30). *Journal of Biological Chemistry* **277**, 29359-29362 (2002).
7. Waki, H.*, et al.* Impaired multimerization of human adiponectin mutants associated with diabetes. Molecular structure and multimer formation of adiponectin. *The Journal of biological chemistry* **278**, 40352-40363 (2003).
8. Fruebis, J.*, et al.* Proteolytic cleavage product of 30-kDa adipocyte complement-related protein increases fatty acid oxidation in muscle and causes weight loss in mice. *Proceedings of the National Academy of Sciences of the United States of America* **98**, 2005-2010 (2001).
9. Waki, H.*, et al.* Generation of Globular Fragment of Adiponectin by Leukocyte Elastase Secreted by Monocytic Cell Line THP-1. *Endocrinology* **146**, 790-796 (2005).
10. Schraw, T., Wang, Z.V., Halberg, N., Hawkins, M. & Scherer, P.E. Plasma adiponectin complexes have distinct biochemical characteristics. *Endocrinology* **149**, 2270-2282 (2008).
11. Kishida, K., Funahashi, T. & Shimomura, I. Adiponectin as a routine clinical biomarker. *Best practice & research. Clinical endocrinology & metabolism* **28**, 119-130 (2014).
12. Arita, Y.*, et al.* Paradoxical decrease of an adipose-specific protein, adiponectin, in obesity. *Biochem Biophys Res Commun* **257**, 79-83 (1999).
13. Ryo, M.*, et al.* Adiponectin as a biomarker of the metabolic syndrome. *Circulation journal : official journal of the Japanese Circulation Society* **68**, 975-981 (2004).
14. Okauchi, Y.*, et al.* Changes in Serum Adiponectin Concentrations Correlate With Changes in BMI, Waist Circumference, and Estimated Visceral Fat Area in Middle-Aged General Population. *Diabetes Care* **32**, e122-e122 (2009).
15. Kishida, K.*, et al.* Relationships between Circulating Adiponectin Levels and Fat Distribution in Obese Subjects. *Journal of Atherosclerosis and Thrombosis* **18**, 592-595 (2011).
16. Ng, T.W.K., Watts, G.F., Barrett, P.H.R., Rye, K.-A. & Chan, D.C. Effect of Weight Loss on LDL and HDL Kinetics in the Metabolic Syndrome. *Associations with changes in plasma retinol-binding protein-4 and adiponectin levels* **30**, 2945-2950 (2007).
17. Hotta, K.*, et al.* Plasma concentrations of a novel, adipose-specific protein, adiponectin, in type 2 diabetic patients. *Arterioscler Thromb Vasc Biol* **20**, 1595-1599 (2000).

18. Lindsay, R.S*., et al.* Adiponectin and development of type 2 diabetes in the Pima Indian population. *The Lancet* **360**, 57-58 (2002).
19. Pischon, T*., et al.* Plasma adiponectin levels and risk of myocardial infarction in men. *JAMA* **291**, 1730-1737 (2004).
20. von Eynatten, M*., et al.* Serum Adiponectin Levels Are an Independent Predictor of the Extent of Coronary Artery Disease in Men. *Journal of the American College of Cardiology* **47**, 2124-2126 (2006).
21. Nakamura, T*., et al.* Association of Hyperadiponectinemia With Severity of Ventricular Dysfunction in Congestive Heart Failure. *Circulation Journal* **70**, 1557-1562 (2006).
22. Tamura, T*., et al.* Serum Adiponectin Level as an Independent Predictor of Mortality in Patients With Congestive Heart Failure. *Circulation Journal* **71**, 623-630 (2007).
23. Van Berendoncks, A.M*., et al.* Functional Adiponectin Resistance at the Level of the Skeletal Muscle in Mild to Moderate Chronic Heart Failure. *Circulation: Heart Failure* **3**, 185-194 (2010).
24. Kollerits, B*., et al.* Gender-specific association of adiponectin as a predictor of progression of chronic kidney disease: The Mild to Moderate Kidney Disease Study. *Kidney International* **71**, 1279-1286 (2007).
25. Jorsal, A*., et al.* Serum adiponectin predicts all-cause mortality and end stage renal disease in patients with type I diabetes and diabetic nephropathy. *Kidney International* **74**, 649-654 (2008).
26. Adamczak, M*., et al.* Decreased plasma adiponectin concentration in patients with essential hypertension. *American Journal of Hypertension* **16**, 72-75 (2003).
27. Iwashima, Y*., et al.* Hypoadiponectinemia Is an Independent Risk Factor for Hypertension. *Hypertension* **43**, 1318-1323 (2004).
28. Biver, E*., et al.* Influence of Adipokines and Ghrelin on Bone Mineral Density and Fracture Risk: A Systematic Review and Meta-Analysis. *The Journal of Clinical Endocrinology & Metabolism* **96**, 2703-2713 (2011).
29. Xie, L*., et al.* Intracellular trafficking and secretion of adiponectin is dependent on GGA-coated vesicles. *Journal of Biological Chemistry* **281**, 7253-7259 (2006).
30. Yamauchi, T*., et al.* Targeted disruption of AdipoR1 and AdipoR2 causes abrogation of adiponectin binding and metabolic actions. *Nature Medicine* **13**, 332 (2007).
31. Denzel, M.S*., et al.* T-cadherin is critical for adiponectin-mediated cardioprotection in mice. *The Journal of Clinical Investigation* **120**, 4342-4352 (2010).
32. Kadowaki, T*., et al.* Adiponectin and adiponectin receptors in insulin resistance, diabetes, and the metabolic syndrome. *The Journal of Clinical Investigation* **116**, 1784-1792 (2006).
33. Pajvani, U.B*., et al.* Complex distribution, not absolute amount of adiponectin, correlates with thiazolidinedione-mediated improvement in insulin sensitivity. *Journal of Biological Chemistry* **279**, 12152-12162 (2004).
34. Lara-Castro, C., Luo, N., Wallace, P., Klein, R.L. & Garvey, W.T. Adiponectin multimeric complexes and the metabolic syndrome trait cluster. *Diabetes* **55**, 249-259 (2006).
35. Liu, M*., et al.* Fat-Specific DsbA-L Overexpression Promotes Adiponectin Multimerization and Protects Mice From Diet-Induced Obesity and Insulin Resistance. *Diabetes* (2012).
36. Tomas, E*., et al.* Enhanced muscle fat oxidation and glucose transport by ACRP30 globular domain: acetyl-CoA carboxylase inhibition and AMP-activated protein kinase activation. *Proceedings of the National Academy of Sciences of the United States of America* **99**, 16309-16313 (2002).
37. Kubota, N*., et al.* Adiponectin stimulates AMP-activated protein kinase in the hypothalamus and increases food intake. *Cell Metabolism* **6**, 55-68 (2007).
38. Kos, K*., et al.* Adiponectin and resistin in human cerebrospinal fluid and expression of adiponectin receptors in the human hypothalamus. *J Clin Endocrinol Metab* **92**, 1129-1136 (2007).
39. Coope, A*., et al.* AdipoR1 mediates the anorexigenic and insulin/leptin-like actions of adiponectin in the hypothalamus. *FEBS Lett* **582**, 1471-1476 (2008).

40. Qi, Y.*, et al.* Adiponectin acts in the brain to decrease body weight. *Nature Medicine* **10**, 524-529 (2004).
41. Nishimura, M.*, et al.* Adiponectin prevents cerebral ischemic injury through endothelial nitric oxide synthase dependent mechanisms. *Circulation* **117**, 216-223 (2008).
42. Une, K.*, et al.* Adiponectin in plasma and cerebrospinal fluid in MCI and Alzheimer's disease. *European journal of neurology* **18**, 1006-1009 (2011).
43. Phielix, E. & Mensink, M. Type 2 diabetes mellitus and skeletal muscle metabolic function. *Physiology & behavior* **94**, 252-258 (2008).
44. Ceddia, R.B.*, et al.* Globular adiponectin increases GLUT4 translocation and glucose uptake but reduces glycogen synthesis in rat skeletal muscle cells. *Diabetologia* **48**, 132-139 (2005).
45. Yamauchi, T.*, et al.* Adiponectin stimulates glucose utilization and fatty-acid oxidation by activating AMP-activated protein kinase. *Nat Med* **8**, 1288-1295 (2002).
46. Ma, K.*, et al.* Increased beta -oxidation but no insulin resistance or glucose intolerance in mice lacking adiponectin. *Journal of Biological Chemistry* **277**, 34658-34661 (2002).
47. Maeda, N.*, et al.* Diet-induced insulin resistance in mice lacking adiponectin/ACRP30. *Nat Med* **8**, 731-737 (2002).
48. Yoon, M.J.*, et al.* Adiponectin Increases Fatty Acid Oxidation in Skeletal Muscle Cells by Sequential Activation of AMP-Activated Protein Kinase, p38 Mitogen-Activated Protein Kinase, and Peroxisome Proliferator–Activated Receptor α. *Diabetes* **55**, 2562-2570 (2006).
49. Civitarese, A.E.*, et al.* Role of adiponectin in human skeletal muscle bioenergetics. *Cell Metab* **4**, 75-87 (2006).
50. Qiao, L.*, et al.* Adiponectin Increases Skeletal Muscle Mitochondrial Biogenesis by Suppressing Mitogen-Activated Protein Kinase Phosphatase-1. *Diabetes* **61**, 1463-1470 (2012).
51. Austin, S. & St-Pierre, J. PGC1α and mitochondrial metabolism – emerging concepts and relevance in ageing and neurodegenerative disorders. *Journal of Cell Science* **125**, 4963-4971 (2012).
52. Iwabu, M.*, et al.* Adiponectin and AdipoR1 regulate PGC-1alpha and mitochondria by Ca(2+) and AMPK/SIRT1. *Nature* **464**, 1313-1319 (2010).
53. Felder, T.K.*, et al.* Hepatic adiponectin receptors (ADIPOR) 1 and 2 mRNA and their relation to insulin resistance in obese humans. *International Journal Of Obesity* **34**, 846 (2010).
54. Berg, A.H., Combs, T.P., Du, X., Brownlee, M. & Scherer, P.E. The adipocyte-secreted protein Acrp30 enhances hepatic insulin action. *Nat Med* **7**, 947-953 (2001).
55. Katz, E.B., Stenbit, A.E., Hatton, K., DePinho, R. & Charron, M.J. Cardiac and adipose tissue abnormalities but not diabetes in mice deficient in GLUT4. *Nature* **377**, 151-155 (1995).
56. Combs, T.P. & Marliss, E.B. Adiponectin signaling in the liver. *Reviews in Endocrine and Metabolic Disorders* **15**, 137-147 (2014).
57. Combs, T.P., Berg, A.H., Obici, S., Scherer, P.E. & Rossetti, L. Endogenous glucose production is inhibited by the adipose-derived protein Acrp30. *J Clin Invest* **108**, 1875-1881 (2001).
58. Pajvani, U.B.*, et al.* Structure-function studies of the adipocyte-secreted hormone Acrp30/adiponectin. Implications fpr metabolic regulation and bioactivity. *The Journal of biological chemistry* **278**, 9073-9085 (2003).
59. Kagawa, Y. Impact of westernization on the nutrition of Japanese: Changes in physique, cancer, longevity and centenarians. *Preventive Medicine* **7**, 205-217 (1978).
60. J., W.B.*, et al.* Caloric Restriction, the Traditional Okinawan Diet, and Healthy Aging. *Annals of the New York Academy of Sciences* **1114**, 434-455 (2007).
61. Gavrilova, N.S. & Gavrilov, L.A. Comments on Dietary Restriction, Okinawa Diet and Longevity. *Gerontology* **58**, 221-223 (2012).

62. Walford, R.L., Bechtel, R., MacCallum, T., Paglia, D. & Weber, L. " Biospheric medicine" as viewed from the two-year first closure of Biosphere 2. *Aviation, space, and environmental medicine* **67**, 609-617 (1996).
63. Walford, R.L. Biosphere 2 as voyage of discovery: The serendipity from inside. *BioScience* **52**, 259-263 (2002).
64. Walford, R.L., Mock, D., Verdery, R. & MacCallum, T. Calorie Restriction in Biosphere 2Alterations in Physiologic, Hematologic, Hormonal, and Biochemical Parameters in Humans Restricted for a 2-Year Period. *The Journals of Gerontology: Series A* **57**, B211-B224 (2002).
65. Weyer, C.*, et al.* Energy metabolism after 2 y of energy restriction: the Biosphere 2 experiment. *The American Journal of Clinical Nutrition* **72**, 946-953 (2000).
66. Verdery, R.B. & Walford, R.L. Changes in plasma lipids and lipoproteins in humans during a 2-year period of dietary restriction in biosphere 2. *Archives of Internal Medicine* **158**, 900-906 (1998).
67. Rickman, A.D.*, et al.* The CALERIE Study: Design and methods of an innovative 25% caloric restriction intervention. *Contemporary clinical trials* **32**, 874-881 (2011).
68. Most, J.*, et al.* Significant improvement in cardiometabolic health in healthy nonobese individuals during caloric restriction-induced weight loss and weight loss maintenance. *American Journal of Physiology-Endocrinology and Metabolism* **314**, E396-E405 (2018).
69. Fontana, L., Klein, S. & Holloszy, J.O. Effects of long-term calorie restriction and endurance exercise on glucose tolerance, insulin action, and adipokine production. *Age* **32**, 97-108 (2010).
70. Lin, S.-J.*, et al.* Calorie restriction extends Saccharomyces cerevisiae lifespan by increasing respiration. *Nature* **418**, 344-348 (2002).
71. Weindruch, R., Walford, R.L., Fligiel, S. & Guthrie, D. The Retardation of Aging in Mice by Dietary Restriction: Longevity, Cancer, Immunity and Lifetime Energy Intake. *The Journal of Nutrition* **116**, 641-654 (1986).
72. McCay, C.M., Crowell, M.F. & Maynard, L.A. The Effect of Retarded Growth Upon the Length of Life Span and Upon the Ultimate Body Size: One Figure. *The Journal of Nutrition* **10**, 63-79 (1935).
73. Colman, R.J.*, et al.* Caloric restriction reduces age-related and all-cause mortality in rhesus monkeys. *Nat Commun* **5**(2014).
74. Mattison, J.A.*, et al.* Impact of caloric restriction on health and survival in rhesus monkeys from the NIA study. *Nature* **489**, 318-321 (2012).
75. Mattison, J.A.*, et al.* Caloric restriction improves health and survival of rhesus monkeys. *Nature Communications* **8**, 14063 (2017).
76. Berg JM, T.J., Stryer L. *Biochemistry 5th Edition*, (W H Freeman, New York, 2002).
77. Cahill, G.F., Jr. Fuel metabolism in starvation. *Annual review of nutrition* **26**, 1-22 (2006).
78. Osborne, T.B., Mendel, L.B. & Ferry, E.L. The Effect of Retardation of Growth Upon the Breeding Period and Duration of Life of Rats. *Science (New York, N.Y.)* **45**, 294-295 (1917).
79. Berg, B.N. & Simms, H.S. Nutrition and Longevity in the Rat: II. Longevity and Onset of Disease with Different Levels of Food Intake. *The Journal of Nutrition* **71**, 255-263 (1960).
80. Masoro, E.J., Yu, B.P. & Bertrand, H.A. Action of food restriction in delaying the aging process. *Proceedings of the National Academy of Sciences* **79**, 4239-4241 (1982).
81. McCarter, R., Masoro, E.J. & Yu, B.P. Does food restriction retard aging by reducing the metabolic rate? *American Journal of Physiology-Endocrinology and Metabolism* **248**, E488-E490 (1985).
82. McCarter, R.J. & McGee, J.R. Transient reduction of metabolic rate by food restriction. *American Journal of Physiology-Endocrinology and Metabolism* **257**, E175-E179 (1989).
83. Redman, L.M.*, et al.* Metabolic Slowing and Reduced Oxidative Damage with Sustained Caloric Restriction Support the Rate of Living and Oxidative Damage Theories of Aging. *Cell Metab* **27**, 805-815.e804 (2018).

84. Gabriely, I. & Barzilai, N. The Role of Fat Depletion in the Biological Benefits of Caloric Restriction. *The Journal of Nutrition* **131**, 903S-906S (2001).
85. Habegger, K.M.*, et al.* The metabolic actions of glucagon revisited. *Nature Reviews Endocrinology* **6**, 689 (2010).
86. Greene, A.E., Todorova, M.T., McGowan, R. & Seyfried, T.N. Caloric Restriction Inhibits Seizure Susceptibility in Epileptic EL Mice by Reducing Blood Glucose. *Epilepsia* **42**, 1371-1378 (2001).
87. Masoro, E.J., McCarter, R.J.M., Katz, M.S. & McMahan, C.A. Dietary Restriction Alters Characteristics of Glucose Fuel Use. *Journal of Gerontology* **47**, B202-B208 (1992).
88. Masoro, E.J., Sabatino, F., McMahan, C.A. & Kuhn, R.W. Assessment of the Role of the Glucocorticoid System in Aging Processes and in the Action of Food Restriction. *Journal of Gerontology* **46**, B171-B179 (1991).
89. Klebanov, S., Diais, S., Stavinoha, W.B., Suh, Y. & Nelson, J.F. Hyperadrenocorticism, attenuated inflammation, and the life-prolonging action of food restriction in mice. *The Journals of Gerontology Series A: Biological Sciences and Medical Sciences* **50**, B78-B82 (1995).
90. Lee, J., Herman, J.P. & Mattson, M.P. Dietary Restriction Selectively Decreases Glucocorticoid Receptor Expression in the Hippocampus and Cerebral Cortex of Rats. *Experimental Neurology* **166**, 435-441 (2000).
91. Wrigley, S., Arafa, D. & Tropea, D. Insulin-Like Growth Factor 1: At the Crossroads of Brain Development and Aging. *Frontiers in Cellular Neuroscience* **11**(2017).
92. Mitchell, S.E.*, et al.* The effects of graded levels of calorie restriction: II. Impact of short term calorie and protein restriction on circulating hormone levels, glucose homeostasis and oxidative stress in male C57BL/6 mice. *Oncotarget* **6**, 23213-23237 (2015).
93. Dunn, S.E.*, et al.* Dietary restriction reduces insulin-like growth factor I levels, which modulates apoptosis, cell proliferation, and tumor progression in p53-deficient mice. *Cancer Res* **57**, 4667-4672 (1997).
94. Sonntag, W.E.*, et al.* Pleiotropic effects of growth hormone and insulin-like growth factor (IGF)-1 on biological aging: inferences from moderate caloric-restricted animals. *The journals of gerontology. Series A, Biological sciences and medical sciences* **54**, B521-538 (1999).
95. Bonkowski, M.S., Rocha, J.S., Masternak, M.M., Al Regaiey, K.A. & Bartke, A. Targeted disruption of growth hormone receptor interferes with the beneficial actions of calorie restriction. *Proc Natl Acad Sci U S A* **103**, 7901-7905 (2006).
96. Jacob, R., Barrett, E., Plewe, G., Fagin, K.D. & Sherwin, R.S. Acute effects of insulin-like growth factor I on glucose and amino acid metabolism in the awake fasted rat. Comparison with insulin. *J Clin Invest* **83**, 1717-1723 (1989).
97. Scheiwiller, E.*, et al.* Growth restoration of insulin-deficient diabetic rats by recombinant human insulin-like growth factor I. *Nature* **323**, 169-171 (1986).
98. Fontana, L.*, et al.* Effects of 2-year calorie restriction on circulating levels of IGF-1, IGF-binding proteins and cortisol in nonobese men and women: a randomized clinical trial. *Aging cell* (2015).
99. Higami, Y.*, et al.* Adipose tissue energy metabolism: altered gene expression profile of mice subjected to long-term caloric restriction. *FASEB journal : official publication of the Federation of American Societies for Experimental Biology* **18**, 415-417 (2004).
100. Combs, T.P.*, et al.* Sexual differentiation, pregnancy, calorie restriction, and aging affect the adipocyte-specific secretory protein adiponectin. *Diabetes* **52**, 268-276 (2003).
101. Zhu, M.*, et al.* Circulating adiponectin levels increase in rats on caloric restriction: the potential for insulin sensitization. *Experimental gerontology* **39**, 1049-1059 (2004).
102. Bruun, J.M.*, et al.* Regulation of adiponectin by adipose tissue-derived cytokines: in vivo and in vitro investigations in humans. *American journal of physiology. Endocrinology and metabolism* **285**, E527-533 (2003).
103. Nishida, M., Funahashi, T. & Shimomura, I. Pathophysiological significance of adiponectin. *Medical Molecular Morphology* **40**, 55-67 (2007).

104. Behre, C.J. Adiponectin and its role. *Scandinavian journal of clinical and laboratory investigation* **68**, 678-680 (2008).
105. Behre, C.J. Adiponectin: a defense protein in catabolism. *The Journal of allergy and clinical immunology* **122**, 1236 (2008).
106. Behre, C.J. Adiponectin: saving the starved and the overfed. *Medical hypotheses* **69**, 1290-1292 (2007).
107. Abete, P.*, et al.* Cardioprotective effect of ischemic preconditioning is preserved in food-restricted senescent rats. *American Journal of Physiology-Heart and Circulatory Physiology* **282**, H1978-H1987 (2002).
108. Shinmura, K.*, et al.* Cardioprotective effects of short-term caloric restriction are mediated by adiponectin via activation of AMP-activated protein kinase. *Circulation* **116**, 2809-2817 (2007).
109. Kondo, M.*, et al.* Caloric restriction stimulates revascularization in response to ischemia via adiponectin-mediated activation of endothelial nitric-oxide synthase. *The Journal of biological chemistry* **284**, 1718-1724 (2009).
110. Scheller, E.L., Burr, A.A., MacDougald, O.A. & Cawthorn, W.P. Inside out: Bone marrow adipose tissue as a source of circulating adiponectin. *Adipocyte* **22**, 251-269 (2016).
111. Muir, R. & Drummond, W.B. On the Structure of the Bone-Marrow in Relation to Blood-Formation. *Journal of anatomy and physiology* **28**, 125-141 (1893).
112. Tavassoli, M. & Crosby, W.H. Bone marrow histogenesis: a comparison of fatty and red marrow. *Science (New York, N.Y.)* **169**, 291-293 (1970).
113. Tavassoli, M. Ultrastructural development of bone marrow adipose cell. *Acta Anat (Basel)* **94**, 65-77 (1976).
114. Piney, A. The anatomy of the bone marrow: With special reference to the distribution of the red marrow. *British Medical Journal* **1922**, 792-795 (1922).
115. Emery, J.L. & Follett, G.F. Regression of Bone-Marrow Haemopoiesis from the Terminal Digits in the Foetus and Infant. *British journal of haematology* **10**, 485-489 (1964).
116. Kricun, M.E. Red-yellow marrow conversion: its effect on the location of some solitary bone lesions. *Skeletal radiology* **14**, 10-19 (1985).
117. Tavassoli, M., Watson, L.R. & Khademi, R. Retention of hemopoiesis in tail vertebrae of newborn rats. *Cell Tissue Res* **200**, 215-222 (1979).
118. Scheller, E.L.*, et al.* Region-specific variation in the properties of skeletal adipocytes reveals regulated and constitutive marrow adipose tissues. *Nat Commun* **6**, 7808 (2015).
119. Tavassoli, M. Marrow adipose cells. Histochemical identification of labile and stable components. *Archives of pathology & laboratory medicine* **100**, 16-18 (1976).
120. Valentin, J. Basic anatomical and physiological data for use in radiological protection: reference values: ICRP Publication 89. *Annals of the ICRP* **32**, 1-277 (2002).
121. Cawthorn, W.P.*, et al.* Bone Marrow Adipose Tissue Is an Endocrine Organ that Contributes to Increased Circulating Adiponectin during Caloric Restriction. *Cell Metabolism* **20**, 368-375 (2014).
122. Baum, T.*, et al.* Does vertebral bone marrow fat content correlate with abdominal adipose tissue, lumbar spine bone mineral density, and blood biomarkers in women with type 2 diabetes mellitus? *Journal of magnetic resonance imaging : JMRI* **35**, 117-124 (2012).
123. Wronski, T.J., Smith, J.M. & Jee, W.S. Variations in mineral apposition rate of trabecular bone within the beagle skeleton. *Calcif Tissue Int* **33**, 583-586 (1981).
124. Burkhardt, R.*, et al.* Changes in trabecular bone, hematopoiesis and bone marrow vessels in aplastic anemia, primary osteoporosis, and old age: a comparative histomorphometric study. *Bone* **8**, 157-164 (1987).
125. Shen, W.*, et al.* MRI-measured bone marrow adipose tissue is inversely related to DXA-measured bone mineral in Caucasian women. *Osteoporosis International* **18**, 641-647 (2007).
126. Griffith, J.F.*, et al.* Vertebral bone mineral density, marrow perfusion, and fat content in healthy men and men with osteoporosis: dynamic contrast-enhanced MR imaging and MR spectroscopy. *Radiology* **236**, 945-951 (2005).

127. Wren, T.A., *et al.* Bone marrow fat is inversely related to cortical bone in young and old subjects. *J Clin Endocrinol Metab* **96**, 782-786 (2011).
128. Justesen, J., *et al.* Mice deficient in 11beta-hydroxysteroid dehydrogenase type 1 lack bone marrow adipocytes, but maintain normal bone formation. *Endocrinology* **145**, 1916-1925 (2004).
129. Cawthorn, W.P., *et al.* Expansion of bone marrow adipose tissue during caloric restriction is associated with increased circulating glucocorticoids and not with hypoleptinemia. *Endocrinology* **157**, 508-521 (2016).
130. Grey, A., *et al.* Pioglitazone increases bone marrow fat in type 2 diabetes: results from a randomized controlled trial. *European Journal of Endocrinology / European Federation of Endocrine Societies* **166**, 1087-1091 (2012).
131. Wagstaff, A.J. & Goa, K.L. Rosiglitazone: a review of its use in the management of type 2 diabetes mellitus. *Drugs* **62**, 1805-1837 (2002).
132. Loke, Y.K., Singh, S. & Furberg, C.D. Long-term use of thiazolidinediones and fractures in type 2 diabetes: a meta-analysis. *Canadian Medical Association Journal* **180**, 32-39 (2009).
133. Devlin, M.J., *et al.* Caloric restriction leads to high marrow adiposity and low bone mass in growing mice. *Journal of bone and mineral research : the official journal of the American Society for Bone and Mineral Research* **25**, 2078-2088 (2010).
134. Waid, D.D. & Warren, R.J. SEASONAL VARIATIONS IN PHYSIOLOGICAL INDICES OF ADULT FEMALE WHITE-TAILED DEER IN TEXAS. *Journal of Wildlife Diseases* **20**, 212-219 (1984).
135. MURRAY, D.L., *et al.* Pathogens, Nutritional Deficiency, and Climate Influences on a Declining Moose Population. *Wildlife Monographs* **166**, 1-30 (2006).
136. Bredella, M.A., *et al.* Increased bone marrow fat in anorexia nervosa. *J Clin Endocrinol Metab* **94**, 2129-2136 (2009).
137. Ecklund, K., *et al.* Bone marrow changes in adolescent girls with anorexia nervosa. *Journal of bone and mineral research : the official journal of the American Society for Bone and Mineral Research* **25**, 298-304 (2010).
138. Tamasi, J.A., Arey, B.J., Bertolini, D.R. & Feyen, J.H. Characterization of Bone Structure in Leptin Receptor-Deficient Zucker (fa/fa) Rats. *Journal of Bone and Mineral Research* **18**, 1605-1611 (2003).
139. Hamrick, M.W. Leptin, bone mass, and the thrifty phenotype. *Journal of Bone and Mineral Research* **19**, 1607-1611 (2004).
140. Hamrick, M.W., *et al.* Leptin treatment induces loss of bone marrow adipocytes and increases bone formation in leptin-deficient ob/ob mice. *Journal of bone and mineral research : the official journal of the American Society for Bone and Mineral Research* **20**, 994-1001 (2005).
141. Menagh, P.J., *et al.* Growth hormone regulates the balance between bone formation and bone marrow adiposity. *Journal of Bone and Mineral Research* **25**, 757-768 (2010).
142. Yakar, S., *et al.* Serum complexes of insulin-like growth factor-1 modulate skeletal integrity and carbohydrate metabolism. *The FASEB Journal* **23**, 709-719 (2009).
143. Lawson, E.A. & Klibanski, A. Endocrine abnormalities in anorexia nervosa. *Nature Clinical Practice Endocrinology & Metabolism* **4**, 407-414 (2008).
144. Viallon, M., *et al.* Chemical-Shift-Encoded Magnetic Resonance Imaging and Spectroscopy to Reveal Immediate and Long-Term Multi-Organs Composition Changes of a 14-Days Periodic Fasting Intervention: A Technological and Case Report. *Frontiers in Nutrition* **6**(2019).
145. Zhang, Y., *et al.* Positional cloning of the mouse obese gene and its human homologue. *Nature* **372**, 425-432 (1994).
146. Friedman, J.M. & Halaas, J.L. Leptin and the regulation of body weight in mammals. *Nature* **395**, 763-770 (1998).
147. Lo, James C., *et al.* Adipsin Is an Adipokine that Improves β Cell Function in Diabetes. *Cell* **158**, 41-53 (2014).
148. Laharrague, P., *et al.* High expression of leptin by human bone marrow adipocytes in primary culture. *FASEB journal : official publication of the Federation of American Societies for Experimental Biology* **12**, 747-752 (1998).

149. Ryden, M., *et al.* Functional characterization of human mesenchymal stem cell-derived adipocytes. *Biochem Biophys Res Commun* **311**, 391-397 (2003).
150. Laharrague, P., *et al.* Regulation by Cytokines of Leptin Expression in Human Bone Marrow Adipocytes. *Horm Metab Res* **32**, 381-385 (2000).
151. Liu, L.F., Shen, W.J., Ueno, M., Patel, S. & Kraemer, F.B. Characterization of age-related gene expression profiling in bone marrow and epididymal adipocytes. *BMC Genomics* **12**, 212 (2011).
152. Isobe, T., *et al.* Influence of gender, age and renal function on plasma adiponectin level: the Tanno and Sobetsu study. *European journal of endocrinology* **153**, 91-98 (2005).
153. Imagawa, A., *et al.* Elevated serum concentration of adipose-derived factor, adiponectin, in patients with type 1 diabetes. *Diabetes care* **25**, 1665-1666 (2002).
154. Botolin, S. & McCabe, L.R. Bone loss and increased bone adiposity in spontaneous and pharmacologically induced diabetic mice. *Endocrinology* **148**, 198-205 (2007).
155. Iwahashi, H., *et al.* Plasma adiponectin levels in women with anorexia nervosa. *Horm Metab Res* **35**, 537-540 (2003).
156. Crossno, J.T., Jr., Majka, S.M., Grazia, T., Gill, R.G. & Klemm, D.J. Rosiglitazone promotes development of a novel adipocyte population from bone marrow-derived circulating progenitor cells. *J Clin Invest* **116**, 3220-3228 (2006).
157. Maeda, N., *et al.* PPARgamma ligands increase expression and plasma concentrations of adiponectin, an adipose-derived protein. *Diabetes* **50**, 2094-2099 (2001).
158. Bennett, C.N., *et al.* Wnt10b increases postnatal bone formation by enhancing osteoblast differentiation. *Journal of bone and mineral research : the official journal of the American Society for Bone and Mineral Research* **22**, 1924-1932 (2007).
159. Cawthorn, W.P., *et al.* Wnt6, Wnt10a and Wnt10b inhibit adipogenesis and stimulate osteoblastogenesis through a beta-catenin-dependent mechanism. *Bone* **50**, 477-489 (2012).
160. Mitchell, S.E., *et al.* The effects of graded levels of calorie restriction: I. impact of short term calorie and protein restriction on body composition in the C57BL/6 mouse. *Oncotarget* **6**, 15902-15930 (2015).
161. Bruker. Automated trabecular and cortical bone selection. (2015).
162. Folch, J., Lees, M. & Sloane Stanley, G.H. A simple method for the isolation and purification of total lipides from animal tissues. *The Journal of biological chemistry* **226**, 497-509 (1957).
163. Lehmann, J.M., *et al.* An Antidiabetic Thiazolidinedione Is a High Affinity Ligand for Peroxisome Proliferator-activated Receptor γ (PPARγ). *Journal of Biological Chemistry* **270**, 12953-12956 (1995).
164. Willson, T.M., Brown, P.J., Sternbach, D.D. & Henke, B.R. The PPARs: from orphan receptors to drug discovery. *Journal of medicinal chemistry* **43**, 527-550 (2000).
165. Tontonoz, P. & Spiegelman, B.M. Fat and beyond: the diverse biology of PPARgamma. *Annu Rev Biochem* **77**, 289-312 (2008).
166. Barak, Y., *et al.* PPAR gamma is required for placental, cardiac, and adipose tissue development. *Mol Cell* **4**, 585-595 (1999).
167. Imai, T., *et al.* Peroxisome proliferator-activated receptor gamma is required in mature white and brown adipocytes for their survival in the mouse. *Proc Natl Acad Sci U S A* **101**, 4543-4547 (2004).
168. Tomaru, T., Steger, D.J., Lefterova, M.I., Schupp, M. & Lazar, M.A. Adipocyte-specific expression of murine resistin is mediated by synergism between peroxisome proliferator-activated receptor gamma and CCAAT/enhancer-binding proteins. *The Journal of biological chemistry* **284**, 6116-6125 (2009).
169. Hollenberg, C.H. & Vost, A. Regulation of DNA synthesis in fat cells and stromal elements from rat adipose tissue. *J Clin Invest* **47**, 2485-2498 (1969).
170. Iwaki, M., *et al.* Induction of adiponectin, a fat-derived antidiabetic and antiatherogenic factor, by nuclear receptors. *Diabetes* **52**, 1655-1663 (2003).
171. Bailey, C.J. Rosiglitazone and pioglitazone: two new thiazolidinediones. *Practical Diabetes International* **17**, 135-137 (2000).

172. Kahn, S.E.*, et al.* Glycemic Durability of Rosiglitazone, Metformin, or Glyburide Monotherapy. *New England Journal of Medicine* **355**, 2427-2443 (2006).
173. Chen, X., Yang, L. & Zhai, S.D. Risk of cardiovascular disease and all-cause mortality among diabetic patients prescribed rosiglitazone or pioglitazone: a meta-analysis of retrospective cohort studies. *Chinese medical journal* **125**, 4301-4306 (2012).
174. Rzonca, S.O., Suva, L.J., Gaddy, D., Montague, D.C. & Lecka-Czernik, B. Bone Is a Target for the Antidiabetic Compound Rosiglitazone. *Endocrinology* **145**, 401-406 (2004).
175. Yu, J.G.*, et al.* The Effect of Thiazolidinediones on Plasma Adiponectin Levels in Normal, Obese, and Type 2 Diabetic Subjects. *Diabetes* **51**, 2968-2974 (2002).
176. Belfiore, A., Genua, M. & Malaguarnera, R. PPAR-γ agonists and their effects on IGF-I receptor signaling: Implications for cancer. *PPAR research* **2009**, 830501-830501 (2009).
177. Jarrar, M.H. & Baranova, A. PPARgamma activation by thiazolidinediones (TZDs) may modulate breast carcinoma outcome: the importance of interplay with TGFbeta signalling. *Journal of cellular and molecular medicine* **11**, 71-87 (2007).
178. Cabre, A.*, et al.* Fatty acid binding protein 4 is increased in metabolic syndrome and with thiazolidinedione treatment in diabetic patients. *Atherosclerosis* **195**, e150-158 (2007).
179. Kizer, J.R.*, et al.* Change in Circulating Adiponectin in Advanced Old Age: Determinants and Impact on Physical Function and Mortality. The Cardiovascular Health Study All Stars Study. *The Journals of Gerontology: Series A* **65A**, 1208-1214 (2010).
180. Justesen, J.*, et al.* Adipocyte tissue volume in bone marrow is increased with aging and in patients with osteoporosis. *Biogerontology* **2**, 165-171 (2001).
181. Ermetici, F.*, et al.* Bone marrow fat contributes to insulin sensitivity and adiponectin secretion in premenopausal women. *Endocrine* **59**, 410-418 (2018).
182. de Araujo, I.M.*, et al.* Marrow adipose tissue spectrum in obesity and type 2 diabetes mellitus. *European journal of endocrinology* **176**, 21-30 (2017).
183. Legroux-Gerot, I.*, et al.* Adipokines and bone status in a cohort of anorexic patients. *Joint, bone, spine : revue du rhumatisme* **86**, 95-101 (2019).
184. Myers, M.G., Cowley, M.A. & Munzberg, H. Mechanisms of leptin action and leptin resistance. *Annual review of physiology* **70**, 537-556 (2008).
185. Fogteloo, J., Meinders, E., Frolich, M., McCamish, M. & Pijl, H. The decline in plasma leptin in response to calorie restriction predicts the effects of adjunctive leptin treatment on body weight in humans. *European journal of internal medicine* **14**, 415-418 (2003).
186. Hamrick, M.W., Pennington, C., Newton, D., Xie, D. & Isales, C. Leptin deficiency produces contrasting phenotypes in bones of the limb and spine. *Bone* **34**, 376-383 (2004).
187. Hamrick, M.W.*, et al.* Injections of leptin into rat ventromedial hypothalamus increase adipocyte apoptosis in peripheral fat and in bone marrow. *Cell Tissue Res* **327**, 133-141 (2007).
188. Bennett, B.D.*, et al.* A role for leptin and its cognate receptor in hematopoiesis. *Current biology : CB* **6**, 1170-1180 (1996).
189. Naveiras, O.*, et al.* Bone-marrow adipocytes as negative regulators of the haematopoietic microenvironment. *Nature* **460**, 259-263 (2009).
190. Ambati, S.*, et al.* Central leptin versus ghrelin: effects on bone marrow adiposity and gene expression. *Endocrine* **37**, 115-123 (2010).
191. Jensen, L.B., Quaade, F. & Sorensen, O.H. Bone loss accompanying voluntary weight loss in obese humans. *Journal of bone and mineral research : the official journal of the American Society for Bone and Mineral Research* **9**, 459-463 (1994).
192. Villareal, D.T.*, et al.* Effect of Two-Year Caloric Restriction on Bone Metabolism and Bone Mineral Density in Non-Obese Younger Adults: A Randomized Clinical Trial. *Journal of bone and mineral research : the official journal of the American Society for Bone and Mineral Research* **31**, 40-51 (2015).
193. Young, N., Formica, C., Szmukler, G. & Seeman, E. Bone density at weight-bearing and nonweight-bearing sites in ballet dancers: the effects of exercise,

hypogonadism, and body weight. *The Journal of Clinical Endocrinology & Metabolism* **78**, 449-454 (1994).
194. Hamrick, M.W., Ding, K.H., Ponnala, S., Ferrari, S.L. & Isales, C.M. Caloric restriction decreases cortical bone mass but spares trabecular bone in the mouse skeleton: implications for the regulation of bone mass by body weight. *Journal of bone and mineral research : the official journal of the American Society for Bone and Mineral Research* **23**, 870-878 (2008).
195. Srinivasan, S.R., Myers, L. & Berenson, G.S. Temporal association between obesity and hyperinsulinemia in children, adolescents, and young adults: The Bogalusa Heart Study. *Metabolism* **48**, 928-934 (1999).
196. Larson-Meyer, D.E.*, et al.* Effect of calorie restriction with or without exercise on insulin sensitivity, beta-cell function, fat cell size, and ectopic lipid in overweight subjects. *Diabetes Care* **29**, 1337-1344 (2006).
197. McELDUFF, A. & HICKMAN, J. Insulin Promotes Growth of the Cultured Rat Osteosarcoma Cell Line UMR-106-01: An Osteoblast-Like Cell*. *Endocrinology* **124**, 701-706 (1989).
198. Cornish, J., Callon, K.E. & Reid, I.R. Insulin increases histomorphometric indices of bone formation In vivo. *Calcified Tissue International* **59**, 492-495 (1996).
199. Steppan, C.M., Crawford, D.T., Chidsey-Frink, K.L., Ke, H. & Swick, A.G. Leptin is a potent stimulator of bone growth in ob/ob mice. *Regulatory Peptides* **92**, 73-78 (2000).
200. Holloway, W.R.*, et al.* Leptin inhibits osteoclast generation. *Journal of bone and mineral research : the official journal of the American Society for Bone and Mineral Research* **17**, 200-209 (2002).
201. Canalis, E. & Delany, A.M. Mechanisms of glucocorticoid action in bone. *Ann N Y Acad Sci* **966**, 73-81 (2002).
202. Klein, G.L. THE EFFECT OF GLUCOCORTICOIDS ON BONE AND MUSCLE. *Osteoporosis and sarcopenia* **1**, 39-45 (2015).
203. Richards, J.B., Valdes, A.M., Burling, K., Perks, U.C. & Spector, T.D. Serum adiponectin and bone mineral density in women. *J Clin Endocrinol Metab* **92**, 1517-1523 (2007).
204. Mallmin, H.*, et al.* Serum Adiponectin in Elderly Men Does Not Correlate with Fracture Risk. *The Journal of Clinical Endocrinology & Metabolism* **93**, 4041-4047 (2008).
205. Ealey, K.N., Kaludjerovic, J., Archer, M.C. & Ward, W.E. Adiponectin is a negative regulator of bone mineral and bone strength in growing mice. *Experimental Biology and Medicine* **233**, 1546-1553 (2008).
206. Abbott, M.J.*, et al.* Negative Skeletal Effects of Locally Produced Adiponectin. *PLOS ONE* **10**, e0134290 (2015).
207. Scheller, E.L. & Rosen, C.J. What's the matter with MAT? Marrow adipose tissue, metabolism, and skeletal health. *Annals of the New York Academy of Sciences* **1311**, 14-30 (2014).
208. Wheater, G., Elshahaly, M., Tuck, S.P., Datta, H.K. & van Laar, J.M. The clinical utility of bone marker measurements in osteoporosis. *Journal of translational medicine* **11**, 201 (2013).
209. Bouxsein, M.L.*, et al.* Guidelines for assessment of bone microstructure in rodents using micro-computed tomography. *Journal of bone and mineral research : the official journal of the American Society for Bone and Mineral Research* **25**, 1468-1486 (2010).
210. Zoch, M.L., Clemens, T.L. & Riddle, R.C. New insights into the biology of osteocalcin. *Bone* **82**, 42-49 (2016).
211. Sulston, R.J.*, et al.* Increased Circulating Adiponectin in Response to Thiazolidinediones: Investigating the Role of Bone Marrow Adipose Tissue. *Frontiers in Endocrinology* **7**(2016).
212. Muruganandan, S., Govindarajan, R. & Sinal, C.J. Bone Marrow Adipose Tissue and Skeletal Health. *Current osteoporosis reports* **16**, 434-442 (2018).
213. Oshima, K.*, et al.* Adiponectin increases bone mass by suppressing osteoclast and activating osteoblast. *Biochem Biophys Res Commun* **331**, 520-526 (2005).
214. Fontana, L., Meyer, T.E., Klein, S. & Holloszy, J.O. Long-term calorie restriction is highly effective in reducing the risk for atherosclerosis in humans. *Proceedings*

of the National Academy of Sciences of the United States of America **101**, 6659-6663 (2004).
215. Civitarese, A.E.*, et al.* Calorie restriction increases muscle mitochondrial biogenesis in healthy humans. *PLoS medicine* **4**, e76 (2007).
216. Zhu, M.*, et al.* Adipogenic signaling in rat white adipose tissue: modulation by aging and calorie restriction. *Experimental gerontology* **42**, 733-744 (2007).
217. Otabe, S.*, et al.* Overexpression of human adiponectin in transgenic mice results in suppression of fat accumulation and prevention of premature death by high-calorie diet. *American journal of physiology. Endocrinology and metabolism* **293**, E210-218 (2007).
218. Kim, J.Y.*, et al.* Obesity-associated improvements in metabolic profile through expansion of adipose tissue. *J Clin Invest* **117**, 2621-2637 (2007).
219. Wang, Y.*, et al.* Post-translational modifications of the four conserved lysine residues within the collagenous domain of adiponectin are required for the formation of its high molecular weight oligomeric complex. *The Journal of biological chemistry* **281**, 16391-16400 (2006).
220. Holland, W.L.*, et al.* An FGF21-adiponectin-ceramide axis controls energy expenditure and insulin action in mice. *Cell Metabolism* **17**, 790-797 (2013).
221. Sohal, R.S. & Weindruch, R. Oxidative stress, caloric restriction, and aging. *Science (New York, N.Y.)* **273**, 59-63 (1996).
222. López-Lluch, G.*, et al.* Calorie restriction induces mitochondrial biogenesis and bioenergetic efficiency. *Proceedings of the National Academy of Sciences of the United States of America* **103**, 1768-1773 (2006).
223. Sparks, L.M.*, et al.* Effects of 12 Months of Caloric Restriction on Muscle Mitochondrial Function in Healthy Individuals. *The Journal of Clinical Endocrinology & Metabolism* **102**, 111-121 (2017).
224. Lanza, I.R.*, et al.* Chronic Caloric Restriction Preserves Mitochondrial Function in Senescence Without Increasing Mitochondrial Biogenesis. *Cell metabolism* **16**, 777-788 (2012).
225. Hancock, C.R., Han, D.-H., Higashida, K., Kim, S.H. & Holloszy, J.O. Does calorie restriction induce mitochondrial biogenesis? A reevaluation. *The FASEB Journal* **25**, 785-791 (2011).
226. Finley, L.W.*, et al.* Skeletal muscle transcriptional coactivator PGC-1alpha mediates mitochondrial, but not metabolic, changes during calorie restriction. *Proceedings of the National Academy of Sciences of the United States of America* **109**, 2931-2936 (2012).
227. Bevilacqua, L., Ramsey, J.J., Hagopian, K., Weindruch, R. & Harper, M.-E. Effects of short- and medium-term calorie restriction on muscle mitochondrial proton leak and reactive oxygen species production. *American Journal of Physiology-Endocrinology and Metabolism* **286**, E852-E861 (2004).
228. McShane, T.M. & Wise, P.M. Life-long moderate caloric restriction prolongs reproductive life span in rats without interrupting estrous cyclicity: effects on the gonadotropin-releasing hormone/luteinizing hormone axis. *Biology of reproduction* **54**, 70-75 (1996).
229. Knuth, U.A. & Friesen, H.G. Starvation induced anoestrus: effect of chronic food restriction on body weight, its influence on oestrous cycle and gonadotrophin secretion in rats. *Acta endocrinologica* **104**, 402-409 (1983).
230. Nelson, J.F., Karelus, K., Bergman, M.D. & Felicio, L.S. Neuroendocrine involvement in aging: evidence from studies of reproductive aging and caloric restriction. *Neurobiology of aging* **16**, 837-843; discussion 855-836 (1995).
231. Maxwell, S.R.J. Women and heart disease. *Basic Research in Cardiology* **93**, s079-s084 (1998).
232. Edwards, I.J.*, et al.* Caloric restriction lowers plasma lipoprotein (a) in male but not female rhesus monkeys. *Experimental gerontology* **36**, 1413-1418 (2001).
233. Christensen, P.*, et al.* Men and women respond differently to rapid weight loss: Metabolic outcomes of a multi-centre intervention study after a low-energy diet in 2500 overweight, individuals with pre-diabetes. *Diabetes, Obesity and Metabolism* **20**, 2840-2851 (2018).

234. Redman, L.M., *et al.* Effect of Calorie Restriction with or without Exercise on Body Composition and Fat Distribution. *The Journal of clinical endocrinology and metabolism* **92**, 865-872 (2007).
235. Wong, M.H., *et al.* Caloric restriction induces changes in insulin and body weight measurements that are inversely associated with subsequent weight regain. *PLoS One* **7**, e42858 (2012).
236. Barzilai, N., *et al.* Surgical removal of visceral fat reverses hepatic insulin resistance. *Diabetes* **48**, 94-98 (1999).
237. Thiebaud, D., *et al.* The effect of graded doses of insulin on total glucose uptake, glucose oxidation, and glucose storage in man. *Diabetes* **31**, 957-963 (1982).
238. Elsukova, E.I., Medvedev, L.N., Mizonova, O.V. & Taidonov, S.V. Effect of calorie restricted diet on brown adipose tissue in mice. *Bulletin of experimental biology and medicine* **152**, 286-288 (2012).
239. Okita, N., *et al.* Differential responses of white adipose tissue and brown adipose tissue to caloric restriction in rats. *Mechanisms of Ageing and Development* **133**, 255-266 (2012).
240. Bredella, M.A., *et al.* Young women with cold-activated brown adipose tissue have higher bone mineral density and lower Pref-1 than women without brown adipose tissue: a study in women with anorexia nervosa, women recovered from anorexia nervosa, and normal-weight women. *J Clin Endocrinol Metab* **97**, E584-590 (2012).
241. Dionne, D.A., Templeman, N.M., Skovsø, S., Clee, S.M. & Johnson, J.D. Caloric Restriction Paradoxically Increases Adiposity in Mice With Genetically Reduced Insulin. *Endocrinology* **157**, 2724-2734 (2016).
242. Ayala, J.E., *et al.* Standard operating procedures for describing and performing metabolic tests of glucose homeostasis in mice. *Disease models & mechanisms* **3**, 525-534 (2010).
243. Andrikopoulos, S., Blair, A.R., Deluca, N., Fam, B.C. & Proietto, J. Evaluating the glucose tolerance test in mice. *American journal of physiology. Endocrinology and metabolism* **295**, E1323-1332 (2008).
244. Petersen, K.F., *et al.* Mitochondrial Dysfunction in the Elderly: Possible Role in Insulin Resistance. *Science (New York, N.Y.)* **300**, 1140-1142 (2003).
245. Agnello, M., Morici, G. & Rinaldi, A.M. A method for measuring mitochondrial mass and activity. *Cytotechnology* **56**, 145-149 (2008).
246. Hong, J., Stubbins, R.E., Smith, R.R., Harvey, A.E. & Núñez, N.P. Differential susceptibility to obesity between male, female and ovariectomized female mice. *Nutrition Journal* **8**, 11-11 (2009).
247. Liao, C.Y., *et al.* Fat maintenance is a predictor of the murine lifespan response to dietary restriction. *Aging cell* **10**, 629-639 (2011).
248. Li, X., Cope, M.B., Johnson, M.S., Smith, D.L., Jr. & Nagy, T.R. Mild calorie restriction induces fat accumulation in female C57BL/6J mice. *Obesity* **18**, 456-462 (2010).
249. Colman, R.J., Nam, G., Huchthausen, L., Mulligan, J.D. & Saupe, K.W. Energy Restriction-Induced Changes in Body Composition Are Age Specific in Mice. *The Journal of Nutrition* **137**, 2247-2251 (2007).
250. Montani, J.P., *et al.* Ectopic fat storage in heart, blood vessels and kidneys in the pathogenesis of cardiovascular diseases. *International Journal Of Obesity* **28**, S58 (2004).
251. Mann, A., Thompson, A., Robbins, N. & Blomkalns, A.L. Localization, Identification, and Excision of Murine Adipose Depots. *Journal of Visualized Experiments : JoVE*, 52174 (2014).
252. DeFronzo, R.A., Ferrannini, E., Sato, Y., Felig, P. & Wahren, J. Synergistic interaction between exercise and insulin on peripheral glucose uptake. *Journal of Clinical Investigation* **68**, 1468-1474 (1981).
253. DeFronzo, R.A., *et al.* The Effect of Insulin on the Disposal of Intravenous Glucose: Results from Indirect Calorimetry and Hepatic and Femoral Venous Catheterization. *Diabetes* **30**, 1000-1007 (1981).
254. Jeffery, R.W., Thompson, P.D. & Wing, R.R. Effects on weight reduction of strong monetary contracts for calorie restriction or weight loss. *Behaviour Research and Therapy* **16**, 363-369 (1978).

255. Barzilai, N., Banerjee, S., Hawkins, M., Chen, W. & Rossetti, L. Caloric restriction reverses hepatic insulin resistance in aging rats by decreasing visceral fat. *The Journal of Clinical Investigation* **101**, 1353-1361 (1998).
256. Mattison, J.A., Lane, M.A., Roth, G.S. & Ingram, D.K. Calorie restriction in rhesus monkeys. *Experimental Gerontology* **38**, 35-46 (2003).
257. Tannenbaum, A. & Silverstone, H. The Influence of the Degree of Caloric Restriction on the Formation of Skin Tumors and Hepatomas in Mice. *Cancer Research* **9**, 724-727 (1949).
258. Sinha, M.K.*, et al.* Analytical Validation and Biological Evaluation of a High–Molecular-Weight Adiponectin ELISA. *Clinical Chemistry* **53**, 2144-2151 (2007).
259. Tanita, T., Miyakoshi, H. & Nakano, Y. Performance of ELISA for specific measurement of High-Molecular-Weight (HMW) adiponectin. *Journal of Immunological Methods* **333**, 139-146 (2008).
260. Tvarijonaviciute, A., Martínez-Subiela, S. & Ceron, J.J. Validation of 2 commercially available enzyme-linked immunosorbent assays for adiponectin determination in canine serum samples. *Canadian Journal of Veterinary Research* **74**, 279-285 (2010).
261. Gavrila, A.*, et al.* Serum Adiponectin Levels Are Inversely Associated with Overall and Central Fat Distribution but Are Not Directly Regulated by Acute Fasting or Leptin Administration in Humans: Cross-Sectional and Interventional Studies. *The Journal of Clinical Endocrinology & Metabolism* **88**, 4823-4831 (2003).
262. Enroth, S., Hallmans, G., Grankvist, K. & Gyllensten, U. Effects of Long-Term Storage Time and Original Sampling Month on Biobank Plasma Protein Concentrations. *EBioMedicine* **12**, 309-314 (2016).
263. Deng, X.*, et al.* Adiponectin in Fresh Frozen Plasma Contributes to Restoration of Vascular Barrier Function after Hemorrhagic Shock. *Shock (Augusta, Ga.)* **45**, 50-54 (2016).
264. Cederholm, J. & Wibell, L. Insulin release and peripheral sensitivity at the oral glucose tolerance test. *Diabetes Research and Clinical Practice* **10**, 167-175 (1990).
265. Cnop, M.*, et al.* Relationship of adiponectin to body fat distribution, insulin sensitivity and plasma lipoproteins: evidence for independent roles of age and sex. *Diabetologia* **46**, 459-469 (2003).
266. Spranger, J.*, et al.* Adiponectin and protection against type 2 diabetes mellitus. *The Lancet* **361**, 226-228 (2003).
267. Kubota, N.*, et al.* Disruption of adiponectin causes insulin resistance and neointimal formation. *The Journal of biological chemistry* **277**, 25863-25866 (2002).
268. Nawrocki, A.R.*, et al.* Mice Lacking Adiponectin Show Decreased Hepatic Insulin Sensitivity and Reduced Responsiveness to Peroxisome Proliferator-activated Receptor γ Agonists. *Journal of Biological Chemistry* **281**, 2654-2660 (2006).
269. Kawahara, E.I.*, et al.* Energy restriction and impact on indirect calorimetry and oxidative stress in cardiac tissue in rat. *Indian journal of biochemistry & biophysics* **51**, 365-371 (2014).
270. McCarter, R.J. & Palmer, J. Energy metabolism and aging: a lifelong study of Fischer 344 rats. *The American journal of physiology* **263**, E448-452 (1992).
271. Ferguson, M., Sohal, B.H., Forster, M.J. & Sohal, R.S. Effect of long-term caloric restriction on oxygen consumption and body temperature in two different strains of mice. *Mech Ageing Dev* **128**, 539-545 (2007).
272. Mitchell, S.E.*, et al.* The effects of graded levels of calorie restriction: V. Impact of short term calorie and protein restriction on physical activity in the C57BL/6 mouse. *Oncotarget* **7**, 19147-19170 (2016).
273. Nguyen, P.*, et al.* Liver lipid metabolism. *Journal of animal physiology and animal nutrition* **92**, 272-283 (2008).
274. Holland, W.L.*, et al.* Receptor-mediated activation of ceramidase activity initiates the pleiotropic actions of adiponectin. *Nat Med* **17**, 55-63 (2011).
275. Hannun, Y.A. & Obeid, L.M. Many ceramides. *The Journal of biological chemistry* **286**, 27855-27862 (2011).

276. Williford, J., Hardy, R.W., Meckling-Gill, K.A., Desmond, R.A. & Wei, H. Energy Restriction Reduces Long-Chain Saturated Fatty Acids Associated with Plasma Lipids in Aging Male Rats. *The Journal of Nutrition* **132**, 3172-3177 (2002).
277. Acosta-Rodríguez, V.A., de Groot, M.H.M., Rijo-Ferreira, F., Green, C.B. & Takahashi, J.S. Mice under Caloric Restriction Self-Impose a Temporal Restriction of Food Intake as Revealed by an Automated Feeder System. *Cell Metabolism* **26**, 267-277.e262 (2017).
278. Faulks, S.C., Turner, N., Else, P.L. & Hulbert, A.J. Calorie Restriction in Mice: Effects on Body Composition, Daily Activity, Metabolic Rate, Mitochondrial Reactive Oxygen Species Production, and Membrane Fatty Acid Composition. *The Journals of Gerontology: Series A* **61**, 781-794 (2006).
279. Mistlberger, R.E. Circadian food-anticipatory activity: Formal models and physiological mechanisms. *Neuroscience & Biobehavioral Reviews* **18**, 171-195 (1994).
280. Kwak, S.J.*, et al.* Drosophila adiponectin receptor in insulin producing cells regulates glucose and lipid metabolism by controlling insulin secretion. *PLoS One* **8**, e68641 (2013).
281. Ruffner, H. Metabolism of tartaric and malic acids in Vitis: A review-Part B. *Vitis* **21**, 65 (1982).
282. Fiume, Z. Final report on the safety assessment of Malic Acid and Sodium Malate. *International journal of toxicology* **20 Suppl 1**, 47-55 (2001).
283. Nakaya, Y.*, et al.* Respiratory quotient in patients with non-insulin-dependent diabetes mellitus treated with insulin and oral hypoglycemic agents. *Annals of nutrition & metabolism* **42**, 333-340 (1998).
284. Kaiyala, K.J.*, et al.* Identification of body fat mass as a major determinant of metabolic rate in mice. *Diabetes* **59**, 1657-1666 (2010).
285. Fan, Y.*, et al.* Parathyroid Hormone Directs Bone Marrow Mesenchymal Cell Fate. *Cell Metab* **25**, 661-672 (2017).
286. Yokota, T.*, et al.* Paracrine regulation of fat cell formation in bone marrow cultures via adiponectin and prostaglandins. *J Clin Invest* **109**, 1303-1310 (2002).
287. Yamashita, T.*, et al.* An orally-active adiponectin receptor agonist mitigates cutaneous fibrosis, inflammation and microvascular pathology in a murine model of systemic sclerosis. *Sci Rep* **8**, 11843-11843 (2018).